UNIVERSITY OF THESSALY

SCHOOL OF ENGINEERING

DEPARMENT OF CIVIL ENGINEERING

Diploma Thesis

Scale effects modeling in bubbles and trusses using first strain gradient elasticity

by

APOSTOLOS NASIKAS

Supervisor: Dr. Antonios. E. Giannakopoulos, Professor

Submitted in partial fulfillment

of the requirements for the

Diploma of Civil Engineering

Volos, 2015

ΠΑΝΕΠΙΣΤΗΜΙΟ ΘΕΣΣΑΛΙΑΣ

ΠΟΛΥΤΕΧΝΙΚΗ ΣΧΟΛΗ

ΤΜΗΜΑ ΠΟΛΙΤΙΚΩΝ ΜΗΧΑΝΙΚΩΝ

Διπλωματική Εργασία

Μοντελοποίηση φαινομένων κλίμακας σε φυσαλίδες και δικτυώματα μέσω βαθμωτής ελαστικότητας

υπό

ΑΠΟΣΤΟΛΟΥ ΝΑΣΙΚΑ

Επιβλέπων: Δρ. Αντώνιος. Ε. Γιαννακόπουλος, Καθηγητής

Υπεβλήθη για την εκπλήρωση μέρους των

απαιτήσεων για την απόκτηση του

Διπλώματος Πολιτικού Μηχανικού

Βόλος, 2015

Approval of this diploma thesis by the Department of Civil Engineering, School of Engineering, University of Thessaly, does not constitute in any way an acceptance of the views of the author by the said academic organization (L. 5343/32, art. 202, § 2).

Examination Committee:

Dr. Antonios E. Giannakopoulos (Supervisor),
Professor, Department of Civil Engineering, University of Thessaly

Dr. Pelekasis Nikolaos,
Professor, Department of Mechanical Engineering, University of Thessaly

Dr. Karakasidis Theodoros,
Associate Professor, Department of Civil Engineering, University of Thessaly

Εξεταστική Επιτροπή:

Δρ. Αντώνιος Ε. Γιαννακόπουλος (Επιβλέπων)
Καθηγητής, Τμήμα Πολιτικών Μηχανικών, Πανεπιστήμιο Θεσσαλίας

Δρ. Πελεκάσης Νικόλαος
Καθηγητής, Τμήμα Μηχανολόγων Μηχανικών, Πανεπιστήμιο Θεσσαλίας

Δρ. Καρακασίδης Θεόδωρος

Αναπληρωτής Καθηγητής, Τμήμα Πολιτικών Μηχανικών, Πανεπιστήμιο Θεσσαλίας

Scale effects modeling in bubbles and trusses using first strain gradient elasticity

Apostolos Nasikas

University of Thessaly, Department of Civil Engineering,2015

Supervisor: Dr. Antonios. E. Giannakopoulos, Professor

1.a. Abstract

In today's technology applications in most scientific branches, structures of micro and nano scale are often used in attempt to minimize the volume of the objects, the material use and to optimize the material's properties. Experimental studies, though, indicate that the behavior of structures of such scale cannot always be described using the classical theory of elasticity. Scale effect appear resulting to significantly stiffer behaviors in many cases. That directed research to approach small scale problems using non classical non local theories with extra length parameters in order to model scale effects. Various such theories have been developed, and one of the simplest ones is the Aifantis' ((Aifantis, 1992) (Altan & Aifantis, 1992)) modification of Mindlins ((Mindlin & Tiersen, 1964) (Mindlin, 1964)) strain gradient theory of elasticity, which is used in this work.

Several boundary condition (BC) problems have been addressed and solved the past decades using strain gradient elasticity and other non local theories. However, due to the complexity of resulting fourth order differential equations, only problems of simple geometry have been solved. This fact was the inspiration for the present thesis. This thesis is based on gradient problems already solved, especially those by (Tsepoura, et al., 2002) and (Polyzos, et al., 2003), and attempts to model the behavior of structures of more complex geometry. Such are structures consisting of multiple structural elements, possibly of different mechanical properties. Following this, a need emerged to return to the

fundamental theory and then make an extensive research in the available literature in order to investigate the continuity and boundary conditions between the different members of the composite bodies that are being studied.

The present work is divided in two main parts. First, is presented the simplified strain gradient theory for two and three dimensional (2D and 3D) problems suggested by Aifantis along with the respective classical one. Then, its form is obtained for bodies of spherical geometry, subjected to radial loads only. Such are the cases of a solid sphere and a spherical cavity in an infinite gradient elastic space under various loading cases. Although, some loading cases have already been addressed by (Tsepoura, et al., 2002), they are also presented in the present work, along with some new boundary value problems, for completeness. All results are compared to the results of respective classical elasticity problems.

Next, thin walled spherical shell problems are being studied, triggered by an experimental investigation by (Glynos & Koutsos, 2009). It suggests stiffening of microbubbles which may be attributed to scale effects. A thin walled spherical shell theory is developed that aspires to model the scale effects in microbubbles -or microspheres which is the term used in the article-. Having modeled the single gradient elastic bubble, a composite bubble is modeled. It is the case of a composite thin walled spherical shell, consisting of two gradient elastic materials that share a fully elastic interface (a double-layered microbubble). The shell's behavior is found and compared with behavior described by the respective classical problems.

In the second part of this thesis, the goal is to form an algorithm for solving gradient elastic 2D truss structures. This part begins by addressing the simplest problem in gradient elasticity. That is the case of a one dimensional bar subjected to uniaxial loading. Several boundary value problems for the bar are presented in order to obtain a good understanding of each BC's effect on the bar's behavior.

As a first step to solving 2D structures, 1D composite structures of multiple collinear bars under various load case are solved. In order to investigate the interaction of different collinear bar elements, the connecting nodes' properties needed to be determined. Two types of node

where considered; the fully elastic node, which works as an interface between the elements, has no stiffness of its own and imposes a continuous strain to the bars' ends, and the rigid node that restrains the strain at the bar's ends. The appropriate 1D stiffness matrix is obtained, and using the stiffness method, multiple bar problems of non standard loading and geometry are solved and compared to the respective analytical gradient solutions and , both analytical and numerical, classical solutions. In this way, it is show that the bar elements can be used as finite elements, too, in 1D problems and describe the bar's scale effects.

Finally, the 2D truss problem is addressed. The function of the node is discussed in the 2D case, and the case of a two bar truss is presented as a simplest example of 2D structure. Also, α simple indeterminate bar structure with classical loading is solved, in order to find how indeterminate gradient trusses behave.

Μοντελοποίηση φαινομένων κλίμακας σε φυσαλίδες και δικτυώματα μέσω βαθμωτής ελαστικότητας

Απόστολος Νασίκας

Πανεπιστήμιο Θεσσαλίας, Τμήμα Πολιτικών Μηχανικών, 2015

Επιβλέπων: Δρ. Αντώνιος. Ε. Γιαννακόπουλος, Καθηγητής

1.b. Περίληψη

Στις σύγχρονες τεχνολογικές εφαρμογές, στους περισσότερους επιστημονικούς κλάδους, συχνά χρησιμοποιούνται κατασκευές μικρό ή νάνο κλίμακας στην προσπάθεια να ελαχιστοποιηθεί ο όγκος και η μάζα των τελικών αντικειμένων, να βελτιστοποιηθούν η χρήση υλικών και οι ιδιότητες αυτών. Πειραματικές μελέτες δείχνουν ότι η συμπεριφορά μιας κατασκευής τέτοιας κλίμακας δε μπορεί πάντα να περιγραφεί μέσω της κλασσικής θεωρίας ελαστικότητας, διότι φαινόμενα κλίμακας παρουσιάζονται, προκαλώντας συχνά κράτυνση αυτών των μελών. Αυτό οδήγησε την επιστημονική έρευνα στο να προσεγγίσει μικρής κλίμακας προβλήματα μέσω μη κλασικών, μη τοπικών (non local) θεωριών ελαστικότητας με επιπλέον παραμέτρους μήκους, οι οποίες μπορούν να μοντελοποιήσουν φαινόμενα κλίμακας. Διάφορες non local θεωρίες έχουν αναπτυχθεί. Μια από τι απλούστερες, η οποία χρησιμοποιείται στην παρούσα εργασία είναι η θεωρία της βαθμωτής ελαστικότητας του Mindlin((Mindlin & Tiersen, 1964) (Mindlin, 1964)) που στην απλοποιημένη της μορφή προτάθηκε από τον Αϋφαντή ((Aifantis, 1992) (Altan & Aifantis, 1992)).

Τις τελευταίες δεκαετίες, αρκετά προβλήματα συνοριακών συνθηκών έχουν επιλυθεί αναλυτικά χρησιμοποιώντας βαθμωτή ελαστικότητα. Λόγω, όμως, της πολυπλοκότητας που επιφέρει η αύξηση της τάξης των διαφορικών εξισώσεων, και η αβεβαιότητα γύρω από την φυσική σημασία των μη κλασικών συνοριακών συνθηκών, αυτά περιορίζονται σε σώματα πολύ απλής γεωμετρίας και περιορισμένα είδη φορτίσεων. Αυτή

η παρατήρηση αποτέλεσε το έναυσμα για την παρούσα διπλωματική εργασία. Αυτή η δουλειά, βασιζόμενη σε ήδη λυμένα απλά προβλήματα, κυρίως αυτά των Τσεπούρα και συνεργάτών ((Tsepoura, et al., 2002),) και Πολύζου και συνεργατών (Polyzos, et al., 2003), στοχεύει να μοντελοποιήσει τη συμπεριφορά πιο σύνθετων κατασκευών. Τέτοιες κατασκευές αποτελούνται από περισσότερα του ενός μέλη τα οποία αλληλεπιδρούν και ενδεχομένως έχουν μεταξύ τους διαφορετικές μηχανικές ιδιότητες. Για την μελέτη της αλληλεπίδρασης των μελών, χρειάστηκε αρχικά αναδρομή στην βασική θεωρία και στη συνέχεια εκτεταμένη βιβλιογραφική έρευνα, ώστε να επιλεγούν οι κατάλληλες συνθήκες συνέχειας και ισορροπίας μεταξύ των μελών του σύνθετου σώματος.

Η παρούσα εργασία χωρίζεται σε δυο κύρια μέρη. Αρχικά, παρουσιάζεται η απλοποιημένη θεωρία βαθμωτής ελαστικότητας του Αϋφαντή, παράλληλα με την αντίστοιχη κλασική, ώστε είναι διακριτές οι ομοιότητες και οι διαφορές τους. Στην συνέχεια, βρίσκεται η μορφή που αυτή παίρνει για σώματα σφαιρικώς συμμετρικά, στα οποία ασκούνται μόνο ακτινικά φορτία. Τέτοιες περιπτώσεις είναι αυτή μίας συμπαγούς σφαίρας και αυτή μιας σφαιρικής κοιλότητας σε έναν άπειρα εκτεινόμενο βαθμωτά ελαστικό χώρο, υπό διάφορους συνδυασμούς φορτίσεων. Κάποιες φορτίσεις (συνοριακές συνθήκες) έχουν ήδη εξεταστεί από τους Πολύζο και συνεργάτες (Polyzos, et al., 2003), ωστόσο και αυτά μεταξύ άλλων προβλημάτων συνοριακών συνθηκών παρουσιάζονται, για λόγους πληρότητας. Όλα τα αποτελέσματα συγκρίνονται τελικά με τα αντίστοιχα της κλασσικής ελαστικότητας.

Στη συνέχεια, ένα λεπτότοιχο σφαιρικό κέλυφος μελετάται, με αφορμή μια πειραματική εργασία των Γλυνού και Κουτσού ((Glynos & Koutsos, 2009)). Σε αυτήν παρατηρήθηκε κράτυνση μικροφυσαλίδων, η οποία θεωρήθηκε ότι ίσως οφείλεται σε φαινόμενα κλίμακας. Μια θεωρία λεπτότοιχων σφαιρικών κελυφών αναπτύσσεται με στόχο τη μοντελοποίηση φαινομένων κλίμακας στις μικροφυσαλίδες. Έχοντας μελετήσει την απλή φυσαλίδα, ακλουθεί μια σύνθετη, αποτελούμενη από δυο διαφορετικά υλικά που μοιράζονται μια επιφάνεια (διεπιφάνεια). Η συμπεριφορά της σύνθετης φυσαλίδας, συγκρίνεται με την συμπεριφορά που περιγράφεται στο αντίστοιχο κλασικό μοντέλο, το οποίο επίσης παρουσιάζεται .

Τα παρακάτω συμπεράσματα εξάγονται από την μελέτη αυτών των προβλημάτων:

Για τη συμπαγή σφαίρα:

- Όταν δεσμεύεται η παραμόρφωση στο σύνορο της σφαίρας, αυτή κρατύνεται, οπότε προκύπτουν μικρότερες παραμορφώσεις.
- Ανεξάρτητα από το μέγεθος της σφαίρας και της μικροδομής, όταν μόνο κλασικά φορτία ασκούνται σε αυτή, τότε η απόκριση της είναι η κλασσική.
- Για την ανάπτυξη φαινομένων κλίμακας, πρέπει να ασκηθούν και διπλές τάσεις.
- Για μικρές τιμές του λόγου του εσωτερικού μήκους του υλικού (g) προς την ακτίνα, η συμπεριφορά της σφαίρας πρακτικά δεν αποκλίνει από την αντίστοιχη κλασική.

Για τη σφαιρική κοιλότητα:

- Η μικροδομή προκαλεί κράτυνση όταν δεν είναι πολύ μικρή, ανεξάρτητα από την άσκηση διπλών τάσεων, ακόμα και με την άσκηση μόνο πίεσης.
- Σημαντική είναι και η επιρροή του λόγου Poisson.
- Οι διπλές τάσεις δεν είναι αμελητέες μόνο κοντά στο όριο της κοιλότητας.
- Πάντα η λύση απλοποιείται στην κλασική όταν η ακτίνα είναι πολύ μεγαλύτερη του μήκους g της μικροδομής.

Για το σφαιρικό κέλυφος (φυσαλίδα):

- Μόνο το πρόβλημα όπου οι ασκούμενες κλασικές και μη κλασικές δυνάμεις έδωσε χρήσιμα αποτελέσματα.
- Ακόμα και όταν δεν ασκούνται διπλές τάσεις οι μετατοπίσεις είναι μικρότερες από τις κλασικές.
- Όταν η μικροδομή είναι ασήμαντη, τα πεδία των μετακινήσεων και των παραμορφώσεων απλοποιούνται στα κλασικά, όχι όμως και το πεδίο των καμπυλοτήτων.

Για το διπλό σφαιρικό κέλυφος:

- Μόνο το πρόβλημα όπου οι ασκούμενες κλασικές και μη κλασικές δυνάμεις έδωσε χρήσιμα αποτελέσματα.
- Επειδή οι παράμετροι είναι πολλές, δύσκολα εξάγονται αποτελέσματα αν δεν επιλεχθούν πιο στοχευόμενα κάποιες περιπτώσεις.
- Όταν θεωρηθεί ότι τα δυο υλικά που το αποτελούν είναι ίδια, το μοντέλο αυτό απλοποιείται στο μοντέλου του απλού σφαιρικού κελύφους
- Όταν μηδενιστεί η μικροδομή των δυο υλικών, η συμπεριφορά που το μοντέλο προβλέπει, δεν είναι ίδια με την κλασική.

Στο δεύτερο μέρος της παρούσας διπλωματικής εργασίας, στόχος είναι η εύρεση ενός αλγορίθμου για την επίλυση επίπεδων δικτυωμάτων στα πλαίσια της βαθμωτής ελαστικότητας, για κάθε είδος φόρτισης. Αυτό ξεκινά από το απλούστερο πρόβλημα που μπορεί να λυθεί μέσω βαθμωτής ελαστικότητας, αυτό της μονοδιάστατης ράβδου, σε μονοαξονική φόρτιση. Αρκετά προβλήματα συνοριακών συνθηκών για την ράβδο παρουσιάζονται αναλυτικά με στόχο την πλήρη κατανόηση της επιρροής κάθε συνοριακής συνθήκης στην συμπεριφορά της ράβδου.

Τα επόμενα γενικά συμπεράσματα μπορούν να εξαχθούν για τη συμπεριφορά της ράβδου με μικροδομή

- Ορίζοντας τις μετακινήσεις και τις τροπές των άκρων μιας ράβδου, στη γενική περίπτωση έχει σαν αποτέλεσμα την μη ομογενή απόκριση αυτής.
- Δεσμεύοντας τις τροπές στα άκρα των ράβδων, μικρότερες από τις κλασικές μετακινήσεις προκύπτουν για οποιαδήποτε φόρτιση και το πεδίο των μετακινήσεων είναι πάντα μη ομογενές, ανεξάρτητα από το μέγεθος της ράβδου και τη μικροδομή.
- Όταν αντί να δεσμευθεί η παραμόρφωση στα άκρα της ράβδου, ασκούνται μηδενικές διπλές δυνάμεις, τότε ανεξαρτήτως της μικροδομής, η συμπεριφορά της ταυτίζεται με την κλασική.
- Η παράμετρος l επηρεάζει την ράβδο σε κάθε περίπτωση με τρόπο που να τείνει να μειώσει το συνολικό μήκος αυτής.

- Οποιοδήποτε πρόβλημα συνοριακών συνθηκών μπορεί να αναχθεί στο αντίστοιχο κλασικό όταν ασκηθεί κατάλληλος συνδυασμός συνοριακών συνθηκών.
- Η συμπεριφορά της ράβδου υπό τις περισσότερες συνθήκες φόρτισης ταυτίζεται με τις αντίστοιχες κλασικές συμπεριφορές, όταν το χαρακτηριστικό μήκος της μικροδομής είναι ασήμαντο σε σχέση με το μήκος της ράβδου.

Σαν πρώτο βήμα για την επίλυση σύνθετων ραβδωτών κατασκευών, επιλύεται μια σειρά από μονοδιάστατα προβλήματα, σύνθετων κατασκευών αποτελούμενων από ομοαξονικές ράβδους που αλληλεπιδρούν, υπό διάφορους συνδυασμούς φορτίσεων. Για να περιγραφεί η αλληλεπίδραση των ράβδων, χρειάζεται πρώτα να διερευνηθούν οι ιδιότητες των κόμβων που τις συνδέουν. Δυο είδη κόμβων επιλέγονται. Ο ένας είναι πλήρως ελαστικός, λειτουργεί σαν διεπιφάνεια μεταξύ των ράβδων, και δεν έχει καμία δική του αντοχή, αλλά απαιτεί συνέχεια μετακινήσεων και των παραμορφώσεων των συνδεόμενων σε αυτόν άκρων ράβδων. Ο δεύτερος είναι πλήρως απαραμόρφωτος και δεσμεύει την παραμόρφωση κάθε συνδεδεμένου σε αυτόν άκρου ράβδου. Στην συνέχεια, ο πίνακας δυσκαμψίας της ράβδου, στα πλαίσια της βαθμωτής ελαστικότητας, εξάγεται και χρησιμοποιώντας μια γενικευμένη μέθοδο μετακινήσεων, επιλύονται διάφορα μονοαξονικά προβλήματα. Τα αποτελέσματά τους συγκρίνονται με αναλυτικές, βαθμωτές και αντίστοιχες κλασικές λύσεις. Με αυτόν τον τρόπο αποδεικνύεται ότι η ράβδος αυτή μπορεί να χρησιμοποιηθεί και σαν πεπερασμένο στοιχείο τουλάχιστον σε μονοδιάστατα προβλήματα.

Καταλήγοντας, εξετάζεται το πρόβλημα του επίπεδου δικτυώματος. Η λειτουργία του κόμβου στις δύο διαστάσεις συζητείται και εξετάζεται το απλό παράδειγμα του τριαρθρωτού τόξου συγκριτικά με την κλασική περίπτωση. Τέλος, εξετάζεται η περίπτωση ενός στατικά αόριστου δικτυώματος, με την κλασική έννοια του όρου, με στόχο να φανεί αν και πώς η μικροδομή επηρεάζει τη λειτουργία και στατικά αορίστων δικτυωμάτων.

2. Table of Contents

3. Introduction

The classical theory of elasticity is quite sufficient for most applications, mainly of macroscopic scale, since it's associated with the concepts of homogeneity and locality of stress. Experimental investigations, though, indicate that structures of micro and nano scale, such as the beams, bars, plates and shells used it modern technology applications, exhibit non homogenous behavior and significant microstructure effects. The classic theory fails to describe adequately such size dependant mechanical behaviors of small scaled, linear elastic structures due to their dependence of the materials microstructure. The classic theory also cannot describe the behavior of materials with significant microstructure effects like polymers, polycrystals, granular and textile materials. In these cases the state of stress needs to be described in a non-local manner. This can be achieved by using many different types of size dependent theories as higher order strain gradient theories, or couple stress theories.

Such theories were developed by Mindlin and co-workers ((Mindlin, 1965) (Mindlin, 1964) (Mindlin & Eshel, 1968)), Aifantis and co-workers((Aifantis, 1992) (Aifantis, 2003) (Altan, et al., 1996) (Altan & Aifantis, 1992)) and Vardoulakis and co-workers((Exadaktylos & Vardoulakis, 2001)),in connection with higher-order strain gradient theories, and Cosserat, Mindlin and Tiersen (Mindlin & Tiersten, 1962) and Toupin in connection with couple-stress theories. From the above theories, the most general and comprehensive is the one developed by Mindlin and co-workers, but the simplest one is the one by Aifantis and co-workers, according to Tsepoura []!!!!!

The past decades, these theories have been used, mostly in simplified forms, to solve many boundary value problems of both static and dynamic elasticity. One can mention static problems dealing with dislocations, fracture mechanics, the halfspace under various surface loads, a borehole under pressure, a bar under pressure and a beam in bending. It has been found that when using such non local theories, singularities and discontinuities of classical elastic theory disappear. Also, size effects are usually captured and wave dispersion effects are observed in cases where it was not possible in classical linear elasticity.

3.1. Conventions

Standard notation is used through the entire paper. Boldface symbols denote tensors whose orders are indicated by the context. All tensors components are written with respect to a fixed Cartesian coordinate system with base vectors $\hat{\boldsymbol{\varepsilon}}_i$. A superscript T after a second order tensor indicates its' transpose

Let $\mathbf{a},\mathbf{b},\mathbf{c},\mathbf{k},\mathbf{l},\mathbf{m}$ be vectors and $\tilde{\mathbf{A}}$ a second order tensor. The following products are used in the text:

Inner: $\mathbf{a}\cdot\mathbf{b}=a_i b_i$

Outer: $\mathbf{a}\times\mathbf{b}=\varepsilon_{ijk}a_i b_i\hat{\boldsymbol{\varepsilon}}_k$

where ε_{ijk} is the alternator, e.i. $\varepsilon_{ijk}=\begin{cases}1, & \text{if } (i,j,k) \text{ are cyclic}\\ -1, & \text{if } (i,j,k) \text{ are anticyclic}\\ 0, & \text{if any two of } (i,j,k) \text{ are equal}\end{cases}$

Dyad: $\mathbf{a}\otimes\mathbf{b}=\mathbf{ab}=\mathbf{a}\cdot\mathbf{b}^{\mathrm{T}}=a_i b_j\hat{\boldsymbol{\varepsilon}}_i\hat{\boldsymbol{\varepsilon}}_j=a_i b_j\hat{\boldsymbol{\varepsilon}}_i\otimes\hat{\boldsymbol{\varepsilon}}_j$

Dyad inner: $(\mathbf{a}\otimes\mathbf{b}):(\mathbf{c}\otimes\mathbf{d})=(\mathbf{b}\cdot\mathbf{c})(\mathbf{a}\cdot\mathbf{d})$

Triad inner: $(\mathbf{a}\otimes\mathbf{b}\otimes\mathbf{c})\vdots(\mathbf{k}\otimes\mathbf{l}\otimes\mathbf{m})=(\mathbf{c}\cdot\mathbf{k})(\mathbf{b}\cdot\mathbf{l})(\mathbf{a}\cdot\mathbf{m})$

Also $(\mathbf{a}\otimes\mathbf{b}\otimes\mathbf{c})^{321}=(\mathbf{c}\otimes\mathbf{b}\otimes\mathbf{a})$

the gradient operator: $\nabla=\hat{\boldsymbol{\varepsilon}}_i\dfrac{\partial}{\partial x_i}=\hat{\boldsymbol{\varepsilon}}_i\partial_i$

the Laplacian operator: $\nabla^2=\nabla\cdot\nabla=\partial_{ii}$

Let S be a surface and $\hat{\mathbf{n}}$ the unit normal vector on S,

$\nabla_S=(\tilde{\mathbf{I}}-\hat{\mathbf{n}}\otimes\hat{\mathbf{n}})\cdot\nabla$

$\dfrac{\partial\tilde{\mathbf{A}}}{\partial\mathbf{a}}=\mathbf{a}\cdot(\nabla\otimes\tilde{\mathbf{A}})$

When the elements of a row vector are presented, they are either separated by spaces or comas. The elements of a column vector are separated by semicolons, i.e. $\mathbf{a}=[a_1,a_2]=[a_1\ \ a_2]$ and $\mathbf{a}^{\mathrm{T}}=[a_1;a_2]$

3.2. Equilibrium equation and boundary conditions

In this section, the equilibrium equation and the corresponding boundary conditions that should be satisfied by any linear elastic material are derived. First, the case of a classical elastic material is investigated and the classical theory of elasticity for 2D and 3D bodies is presented. It is followed by the case of the linear elastic material with microstructure (gradient elastic material), investigated in the framework of Mindlin's first strain gradient elasticity theory, using the constitutive equation proposed by Aifantis. The latter as a special case of Mindlin's strain gradient theory, allows the derivation of both, the equilibrium equation and the boundary conditions by first taking the variation of the strain energy defined by Mindlin and then inserting the given constitutive equation.

3.2.1. Classical Theory of Elasticity

Consider a linear elastic body of volume V surrounded by surface S. Let $\hat{\mathbf{n}}$ be the unit normal vector on S, and a Cartesian coordinate system with its origin located interior to V. According to the classical theory of elasticity the strain energy depends upon the strain, as follows:

$$U = \int_V [\tilde{\boldsymbol{\tau}} : \tilde{\mathbf{e}}] dV = \int_V (\tau_{ij} e_{ij}) dV ,$$

where $\tilde{\boldsymbol{\tau}}$ and $\tilde{\mathbf{e}}$ are the second order stress and strain tensors respectively**.** Since $\tilde{\mathbf{e}} = \frac{1}{2}(\nabla \mathbf{u} + \mathbf{u} \nabla)$, the variation of the bodies strain energy can be written in terms of the displacement $\mathbf{u}$ as,

$$\delta U = \int_V [\tilde{\boldsymbol{\tau}} : \nabla \delta \mathbf{u}] dV$$

After some differential calculus, using the divergence theorem, the equation above takes the form:

$$\delta U = -\int_V [\nabla \cdot \tilde{\boldsymbol{\tau}}] \cdot \delta \mathbf{u} dV + \int_S (\hat{\mathbf{n}} \cdot \tilde{\boldsymbol{\tau}}) \cdot \delta \mathbf{u} dS$$

Meanwhile, the variation done by external forces to V is:

$$\delta W = \int_V \mathbf{f} \cdot \delta \mathbf{u} dV + \int_S \mathbf{P} \cdot \delta \mathbf{u} dS$$

, $\mathbf{f}, \mathbf{P}$ being respectively body forces acting to the body and external surface tractions.

Since $\delta U = \delta W$ the equations above imply that the equilibrium equation for a classical elastic body is:

$$\nabla \cdot \tilde{\boldsymbol{\tau}} + \mathbf{f} = \mathbf{0}$$

and the corresponding classical boundary conditions (BCs) are: $\mathbf{P}(\mathbf{x}) = \hat{\mathbf{n}} \cdot \tilde{\boldsymbol{\tau}} = \overline{\mathbf{P}}$ and/or $\mathbf{u} = \overline{\mathbf{u}},$ where $\overline{\mathbf{P}}, \overline{\mathbf{u}}$ denote prescribed values.

In Hooke's Law the stress and strain have the following relation $\tilde{\boldsymbol{\tau}} = 2\mu\tilde{\mathbf{e}} + \lambda(\nabla \cdot \mathbf{u})\tilde{\mathbf{I}}$. So, the equilibrium equation for an elastic continuum can be obtained in terms of the displacement field $\mathbf{u}$:

$$\mu\nabla^2\mathbf{u} + (\lambda + \mu)\nabla\nabla \cdot \mathbf{u} + \mathbf{f} = \mathbf{0}$$

3.2.2. Gradient Theory of Elasticity

Consider a linear elastic body of volume V surrounded by surface S, which is characterized by a microstructure modeled macroscopically by the gradient of the deformation. Let $\hat{\mathbf{n}}$ be the unit normal vector on S, and a Cartesian coordinate system with its origin located interior to V. According to Mindlin's strain gradient theory the strain energy depends upon both the strain and the strain's gradient:

$$U = \int_V \left[\tilde{\boldsymbol{\tau}} : \tilde{\mathbf{e}} + (\tilde{\boldsymbol{\mu}})^{321} \vdots \nabla\tilde{\mathbf{e}} \right] dV = \int_V (\tau_{ij} e_{ij} + \mu_{ijk} \partial_i e_{jk}) dV$$

,where $\tilde{\boldsymbol{\tau}}$ and $\tilde{\mathbf{e}}$ are the classical second order stress and strain tensors respectively, $\tilde{\boldsymbol{\mu}}$ is the third order tensor with 27 components μ_{ijk} representing double forces per unit area. The first subscript indicates the normal vector of the surface the second of the forces lever and the third the direction of the forces. It should be noted that the double stresses contribute only to the potential energy and to the boundary conditions of

the problem, without giving any resultant stress of couple vector at any surface of the studied body. Since $\tilde{\mathbf{e}} = \frac{1}{2}(\nabla\mathbf{u} + \mathbf{u}\nabla)$, the variation of the bodies strain energy can be written in terms of the displacement $\mathbf{u}$ as,

$$\delta U = \int_V \left[\tilde{\boldsymbol{\tau}} : \nabla\delta\mathbf{u} + (\tilde{\boldsymbol{\mu}})^{321} \vdots \nabla\nabla\delta\mathbf{u} \right] dV$$

Using the symmetry relation $(\tilde{\boldsymbol{\mu}})^{132} = \tilde{\boldsymbol{\mu}}$, and after some linear algebra and differential calculus, which are presented in detail in tsepoura[], the variation of the strain energy takes the following form:

$$\begin{aligned}\delta U = & -\int_V [\nabla \cdot (\tilde{\boldsymbol{\tau}} - \nabla \cdot \tilde{\boldsymbol{\mu}})] \cdot \delta\mathbf{u} dV + \int_S (\hat{\mathbf{n}} \cdot \tilde{\boldsymbol{\mu}} \cdot \hat{\mathbf{n}}) \cdot [\hat{\mathbf{n}} \cdot \nabla(\delta\mathbf{u})] dS \\ & + \int_S \left(\hat{\mathbf{n}} \cdot \tilde{\boldsymbol{\tau}} - (\hat{\mathbf{n}} \otimes \hat{\mathbf{n}}) : \frac{\partial \tilde{\boldsymbol{\mu}}}{\partial \hat{\mathbf{n}}} - \hat{\mathbf{n}} \cdot (\nabla_S \cdot \tilde{\boldsymbol{\mu}}) - \hat{\mathbf{n}} \cdot \left[\nabla S \cdot (\tilde{\boldsymbol{\mu}})^{213} \right] \right) \cdot \delta\mathbf{u} dS \\ & + \int_S ((\nabla_S \cdot \hat{\mathbf{n}})(\hat{\mathbf{n}} \otimes \hat{\mathbf{n}}) : \tilde{\boldsymbol{\mu}} - (\nabla_S \hat{\mathbf{n}}) : \tilde{\boldsymbol{\mu}}) \cdot \delta\mathbf{u} dS + \sum_{C_a} \oint_{C_a} \{ \| (\hat{\mathbf{m}} \otimes \hat{\mathbf{n}}) : \tilde{\boldsymbol{\mu}} \| \cdot \delta\mathbf{u} \} dC\end{aligned}$$

where for non-smooth boundaries C_a are the edge lines formed by the intersection of two surface portions S_i and S_j of S, $\hat{\mathbf{m}} = \hat{\mathbf{s}} \otimes \hat{\mathbf{n}}$, with $\hat{\mathbf{s}}$ being the tangential vector to C_a, and the brackets $\|\cdot\|$ indicate that the enclosed quantity is the difference between the values on the surface portions S_i and S_j . For smooth 3D boundaries and both smooth and non-smooth 2D boundaries the last term is always equal to zero.

Meanwhile, the variation done by external forces to V is:

$$\delta W = \int_V \mathbf{f} \cdot \delta\mathbf{u} dV + \int_S \mathbf{R} \cdot [\hat{\mathbf{n}} \cdot \nabla(\delta\mathbf{u})] dS + \int_S \mathbf{P} \cdot \delta\mathbf{u} dS + \sum_{C_a} \oint_{C_a} \{ \mathbf{E} \cdot \delta\mathbf{u} \} dC$$

, $\mathbf{f}, \mathbf{P}, \mathbf{R}, \mathbf{E}$ being respectively the classical body forces acting to the body, the classical external surface tractions, non classical traction-like vector of surface double stresses and non classical surface jump stresses acting on the non smooth bodies surface.

Since $\delta U = \delta W$ the equations above imply that the equilibrium equation for a 2D or a 3D gradient elastic body is

$$\nabla \cdot (\tilde{\boldsymbol{\tau}} - \nabla \cdot \tilde{\boldsymbol{\mu}}) + \mathbf{f} = \mathbf{0}$$

And the corresponding classical boundary conditions are

$$\mathbf{P}(\mathbf{x}) = \hat{\mathbf{n}}\cdot\tilde{\boldsymbol{\tau}} - (\hat{\mathbf{n}}\otimes\hat{\mathbf{n}}) : \frac{\partial\tilde{\boldsymbol{\mu}}}{\partial\hat{\mathbf{n}}} - \hat{\mathbf{n}}\cdot(\nabla_S\cdot\tilde{\boldsymbol{\mu}}) - \hat{\mathbf{n}}\cdot\left[\nabla_S\cdot(\tilde{\boldsymbol{\mu}})^{213}\right] + (\nabla_S\cdot\hat{\mathbf{n}})(\hat{\mathbf{n}}\otimes\hat{\mathbf{n}}) : \tilde{\boldsymbol{\mu}} - (\nabla_S\otimes\hat{\mathbf{n}}) : \tilde{\boldsymbol{\mu}} = \mathbf{P}_0 \quad \text{and/or} \quad \mathbf{u} = \mathbf{u}_0,$$

And the non-classical ones

$$\mathbf{R} = \hat{\mathbf{n}}\cdot\tilde{\boldsymbol{\mu}}\cdot\hat{\mathbf{n}} = \mathbf{R}_0 \text{ and/or } \frac{\partial\mathbf{u}}{\partial\hat{\mathbf{n}}} = \mathbf{q}_0,$$

$\mathbf{E} = \left\|(\hat{\mathbf{m}}\otimes\hat{\mathbf{n}}) : \tilde{\boldsymbol{\mu}}\right\| = \mathbf{E}_0$, where $\mathbf{P}_0, \mathbf{R}_0, \mathbf{q}_0, \mathbf{E}_0$ denote prescribed values.

Mindin (Mindlin, 1965) proposed a modification of Hooke's Law expressed by the following relations:

$$\tilde{\boldsymbol{\sigma}} = \tilde{\boldsymbol{\tau}} + \tilde{\mathbf{s}}$$
$$\tilde{\boldsymbol{\tau}} = 2\mu\tilde{\mathbf{e}} + \lambda(\nabla\cdot\mathbf{u})\tilde{\mathbf{I}}$$
$$\tilde{\mathbf{e}} = \tfrac{1}{2}(\nabla\mathbf{u} + \mathbf{u}\nabla)$$

$$\tilde{\mathbf{s}} = -[2\mu c_3\tilde{\mathbf{e}} + \lambda c_1\tilde{\mathbf{I}}\nabla^2(\nabla\cdot\mathbf{u}) + \lambda c_2\nabla\nabla(\nabla\cdot\mathbf{u})]$$

$\tilde{\boldsymbol{\sigma}}$ being the total stress tensor, correlated to the strains and their gradients through five independent material constants, $\mu, \lambda, c_1, c_2, c_3$ the first two being the Lame constants.

Aifantis (Aifantis, 1992) proposed the following modification:

$$\tilde{\boldsymbol{\mu}} = g^2\nabla\tilde{\boldsymbol{\tau}}$$
$$\tilde{\mathbf{s}} = -\nabla\cdot\tilde{\boldsymbol{\mu}} = -g^2\nabla^2\tilde{\boldsymbol{\tau}}$$

g^2 being the volumetric strain gradient energy coefficient, the unique constant related to the material's microstructure.

The equilibrium equation for a gradient elastic continuum in terms of the displacement field $\mathbf{u}$ takes the form:

$$\mu\nabla^2\mathbf{u} + (\lambda+\mu)\nabla\nabla\cdot\mathbf{u} - g^2\nabla^2(\mu\nabla^2\mathbf{u} + (\lambda+\mu)\nabla\nabla\cdot\mathbf{u}) + \mathbf{f} = \mathbf{0}$$

4.I. PART I: SPHERICAL GEOMETRY PROBLEMS

4.I.1. Spherical body applications

The simplest three dimensional bodies that can be considered in terms of geometry are those of spherical symmetry. However, perfectly spherical bodies rarely appear in everyday's life normal scaled applications. Especially in cases of only radial loading and no body forces, which are addressed in this work, spherical bodies do not have many macro scale applications.

However, when small scaled bodies are considered, the assumption of only radial loads is not as arbitrary, while the body forces might be very small compared to the radial loads. So, as far as small scaled application can be considered, spherical bodies can be found and in several cases or be used as an approximation to the true geometry of the body.

The most common spherical symmetrical body used in small scale applications is the spherical shell. That is the case of microbubbles used in medicine. Two primary applications of microbubbles are considered to be in the contrast enhanced ultrasound(CEUS), which is the application of an ultrasound contrast medium to traditional medical sonography, and targeted drug delivery. There are several advantages to using microbubbles instead of using alternative methods, since their use is considered to be cost effective and safer for the patients, since no radiation is applied and smaller drug amounts are used.

These advantages make their use very attractive, and thus their behavior needs to be modeled and studied. Since their dimensions are very small, scale effects should not be ignored, since they might be significant, and that is the reason that it is attempted to medl them using gradient elasticity.

Of course, in these applications the loading and the geometry of the bubbles is much more complex than the ones studied in this work. However, in order to understand the bubbles behavior, one must start from the basics, so both geometry and loading simplifications are made.

4.I.2. Spherical Symmetry Problems Equilibrium

In the previous section, a general theory has been presented for bodies of any geometry, subjected to various load combinations. In order to study spherically symmetric bodies, the equilibrium and the boundary conditions need to be obtained, using spherical coordinates. In the following paragraphs the equilibrium and the BCs for spherical bodies are obtained in spherical coordinates, in both the classical and the gradient theory of elasticity

4.I.2.i. Classical Theory

Consider any body characterized by spherical symmetry, for example a solid sphere, a spherical cavity, a spherical shell, any number of spherical shells the one inside the other and any combination of the above.

In spherical coordinates the displacement vector takes the form $\mathbf{u} = \mathrm{u_r}(\mathrm{r},\theta,\phi)\hat{\mathbf{r}} + \mathrm{u_\theta}(\mathrm{r},\theta,\phi)\hat{\boldsymbol{\theta}} + \mathrm{u_\phi}(\rho,\theta,\phi)\hat{\boldsymbol{\varphi}}$

The body is subjected only to radial loads and displacements of spherical symmetry and zero body forces are assumed. Under these assumptions, the bodies displacement vector is simplified to $\mathbf{u} = \mathrm{u_r}\hat{\mathbf{r}}$, $u_r = u_r(r) = \rho(r)$, $\mathrm{u_\theta}(\mathrm{r},\theta,\phi) = 0$, $\mathrm{u_\phi}(\mathrm{r},\theta,\phi) = 0$ where $\mathrm{u_r}$ is the radial displacement and r the distance of the center of the body.

The classical equilibrium equation takes the following form:

$$\mu\nabla^2\mathbf{u} + (\lambda+\mu)\nabla\nabla\cdot\mathbf{u} = \mathbf{0} \Rightarrow$$

$$(2\mu+\lambda)\nabla^2\mathbf{u} = \mathbf{0} \quad \Leftrightarrow \quad \nabla^2\mathbf{u} = \mathbf{0} \quad \Rightarrow \quad \nabla^2\mathrm{u_r} = 0,$$

, since $2\mu+\lambda$ is a non-zero material constant.

Even though a 3D problem is addressed, the loading chosen reduced the equilibrium equation to an ordinary differential equation. It's general solution is:

$$\mathbf{u} = \sum_{\mathrm{i}=1,2} \mathrm{C_i}\rho_\mathrm{i}\hat{\mathbf{r}} = \{\mathrm{C_1}\rho_1 + \mathrm{C_2}\rho_2\}\hat{\mathbf{r}} = \left\{\mathrm{C_1 r} + \mathrm{C_2}\frac{1}{\mathrm{r}^2}\right\}\hat{\mathrm{r}}$$

i.e, the O.D.'s fundamental solutions are: $\rho_1(r) = r$ and $\rho_2(r) = 1/r^2$

In the following classical problems, the pseudo vectors $\boldsymbol{\rho}(r) \neq \mathbf{u}(r)$ and $\mathbf{C}$ are used. The first one is a vector whose elements are the O.D.s fundamental solutions. The second is the vector of the solution's constants. They are used in order to optimize the display of the results. For example, the displacement field can be written as $\mathbf{u}(r) = \left(\mathbf{C} \cdot \boldsymbol{\rho}(r)^T\right)\hat{\mathbf{r}} = C_i \rho_i(r)\hat{\mathbf{r}}$.In the same way are define the pseudo vectors of the fundamental solutions' ν^{th} derivative $\boldsymbol{\rho}^{(\nu)}(r)$ and the stress functions pseudo vector $\mathbf{P}(r) \neq \mathbf{P}(\hat{\mathbf{n}})$.

$$\boldsymbol{\rho}(r) = [\rho_1(r), \rho_3(r)] = \left[r, \frac{1}{r^2} \right] \text{ and}$$

$$\mathbf{P}(r) = [P_1(r), P_3(r)] = \left[(2\mu + 3\lambda), -\frac{4\mu}{r^3} \right], P_i = \left[(2\mu + \lambda)\rho_i' + \lambda \frac{2\rho_i}{r} \right]$$

$$\rho_i' = \frac{\partial}{\partial r}(\rho_i) \text{etc.}$$

Due to spherical symmetry the surface normal vector $\hat{\mathbf{n}}$ can be either $\hat{\mathbf{r}}$ or $-\hat{\mathbf{r}}$ thus the boundary conditions take the following form

$$\mathbf{P}(\hat{\mathbf{n}}) = \hat{\mathbf{n}} \cdot \tilde{\boldsymbol{\tau}} = \left[\mathbf{C} \cdot \mathbf{P}(r)\right]\hat{\mathbf{n}} = C_i P_i(r)\hat{\mathbf{n}}, \ \hat{\mathbf{n}} = \pm\hat{\mathbf{r}}, \text{ thus } \mathbf{P}(-\hat{\mathbf{r}}) = -\mathbf{P}(\hat{\mathbf{r}})$$

4.I.2.ii. Non – Classical / Gradient Theory

Consider any body characterized by spherical symmetry with considerable microstructure that can be modeled by adding an additional length parameter g. In spherical coordinates the displacement vector takes the form $\mathbf{u} = \mathrm{u_r}(\mathrm{r},\theta,\phi)\hat{\mathbf{r}} + \mathrm{u_\theta}(\mathrm{r},\theta,\phi)\hat{\boldsymbol{\theta}} + \mathrm{u_\phi}(\rho,\theta,\phi)\hat{\boldsymbol{\varphi}}$

Once again, the body is subjected only to radial loads and displacements of spherical symmetry and by the assumption of zero body forces the displacement vector is simplified to $\mathbf{u} = \mathrm{u_r}\hat{\mathbf{r}}$, $\mathrm{u_r} = \mathrm{u_r}(\mathrm{r}) = \rho(\mathrm{r})$ while $u_\theta(r,\theta,\phi) = 0$ and $u_\phi(r,\theta,\phi) = 0$, $\mathrm{u_r}$ being the radial displacement and r the distance of the center of the body.

The equilibrium equation can be simplified to:

$$\mu\nabla^2\mathbf{u} + (\lambda+\mu)\nabla\nabla\cdot\mathbf{u} - g^2\nabla^2(\mu\nabla^2\mathbf{u} + (\lambda+\mu)\nabla\nabla\cdot\mathbf{u}) + \mathbf{f} = \mathbf{0} \quad \Rightarrow$$
$$(2\mu+\lambda)\left(1-g^2\nabla^2\right)\nabla^2\mathbf{u} = \mathbf{0} \quad \Leftrightarrow \quad \left(1-g^2\nabla^2\right)\nabla^2\mathbf{u} = \mathbf{0}$$

The general solution for the displacement field is:

$$\mathbf{u} = \sum_{i=1}^{4} C_i \rho_i \hat{\mathbf{r}} = \{C_1\,\rho_1 + C_2\,\rho_2 + C_3\,\rho_3 + C_4\,\rho_4\}$$

$$\mathbf{u} = \left\{ C_1\, r + C_2\,\frac{1}{r^2} + C_3\left(-g^2\,\frac{\sinh(r/g)}{r^2} + g\,\frac{\cosh(r/g)}{r}\right) + C_4\,\sqrt{\frac{\pi}{2(r/g)}}\mathrm{K}_{3/2}(r/g)\right\}\hat{\mathbf{r}}$$

i.e., the O.D.'s fundamental solutions are:

$\rho_1(\mathrm{r}) = \mathrm{r}$,

$$\rho_2(r) = -g^2\,\frac{\sinh(r/g)}{r^2} + g\,\frac{\cosh(r/g)}{r} = \frac{1}{2}\left[e^{r/g}\left(\frac{1}{r/g} - \frac{1}{(r/g)^2}\right) + e^{-r/g}\left(\frac{1}{r/g} + \frac{1}{(r/g)^2}\right)\right]$$

$$\rho_3(r) = \frac{1}{r^2},$$

$$\rho_4(r) = \sqrt{\frac{\pi}{2(r/g)}}\mathrm{K}_{3/2}(r/g) = \frac{\pi}{2}e^{-r/g}\left(\frac{1}{r/g} + \frac{1}{(r/g)^2}\right),$$

$\mathrm{K}_{3/2}$ being the modified Bessel Function $\mathrm{K_n}$ with n=3/2. The $\mathrm{C_i}$ constants are determined by the BCs.

Due to spherical symmetry of the body the surface normal vector $\hat{\mathbf{n}}$ can be either $\hat{\mathbf{r}}$ or $-\hat{\mathbf{r}}$ thus the boundary conditions take the following form

The traction vector:

$$\mathbf{P}(\hat{\mathbf{n}}) = \hat{\mathbf{n}} \cdot \tilde{\boldsymbol{\tau}} - (\hat{\mathbf{n}} \otimes \hat{\mathbf{n}}) : \frac{\partial \tilde{\boldsymbol{\mu}}}{\partial \hat{\mathbf{n}}} - \hat{\mathbf{n}} \cdot (\nabla_S \cdot \tilde{\boldsymbol{\mu}}) - \hat{\mathbf{n}} \cdot \left[\nabla_S \cdot (\tilde{\boldsymbol{\mu}})^{213}\right] + (\nabla_S \cdot \hat{\mathbf{n}})(\hat{\mathbf{n}} \otimes \hat{\mathbf{n}}) : \tilde{\boldsymbol{\mu}} - (\nabla_S \otimes \hat{\mathbf{n}}) : \tilde{\boldsymbol{\mu}}$$

$$= \left[\sum_{i=1,4} C_i P_i\right] \hat{\mathbf{n}},$$

$$P_i = 2\mu\left[\rho_i' - g^2\left(\rho_i''' + 2\frac{\rho_i''}{r} - 6\frac{\rho_i'}{r^2} + 6\frac{\rho_i}{r^3}\right)\right]$$

$$+ \lambda\left[\rho_i' + \frac{2\rho_i}{r} - g^2\left(\rho_i''' + 2\frac{\rho_i''}{r} - 4\frac{\rho_i'}{r^2} + 4\frac{\rho_i}{r^3}\right)\right], \qquad \rho_i' = \frac{\partial}{\partial r}(\rho_i) \text{etc.}$$

thus $\mathbf{P}(-\hat{\mathbf{r}}) = -\mathbf{P}(\hat{\mathbf{r}})$

The surface double traction vector:

$$\mathbf{R}(\hat{\mathbf{n}}) = \hat{\mathbf{n}} \cdot \tilde{\boldsymbol{\mu}} \cdot \hat{\mathbf{n}} = \left[\sum_{i=1,4} C_i R_i\right] \hat{\mathbf{r}}, \text{ for both } \hat{\mathbf{n}} = \pm\hat{\mathbf{r}},$$

$$R_i = g^2\left\{2\mu[\rho_i''] + \lambda\left[\rho_i'' + \frac{2\rho'_i}{r} - \frac{2\rho_i}{r^2}\right]\right\}$$

And the normal displacement gradient

$$\mathbf{q}(\hat{\mathbf{n}}) = \frac{\partial \mathbf{u}}{\partial \hat{\mathbf{n}}} = \left[\sum_{i=1,4} C_i q_i\right] \hat{\mathbf{n}}, \text{ where } q_i = \rho_i'. \text{ Thus, the normal displacement gradient vector } \mathbf{q}(-\hat{\mathbf{r}}) = -\mathbf{q}(\hat{\mathbf{r}})$$

In the following non-classical problems the pseudo vectors $\boldsymbol{\rho}(r) \neq \bar{\mathbf{u}}(r)$, $\mathbf{q}(r) \neq \mathbf{q}(\hat{\mathbf{n}})$, $\mathbf{P}(r) \neq \mathbf{P}(\hat{\mathbf{n}})$ and $\mathbf{R}(r) \neq \mathbf{R}(\hat{\mathbf{n}})$ are used to indicate respectively the row vectors of the O.D.s fundamental solutions, their derivatives, the functions of the traction and double traction term of each fundamental solution. i.e.

$$\boldsymbol{\rho}(r) = \rho_i(r)\hat{\boldsymbol{\varepsilon}}_i = [\rho_1(r), \rho_2(r), \rho_3(r), \rho_4(r)],$$

$$\mathbf{q}(r) = \rho_i'(r)\hat{\boldsymbol{\varepsilon}}_i = [\rho_1'(r), \rho_2'(r), \rho_3'(r), \rho_4'(r)],$$

$$\mathbf{P}(r) = P_i\hat{\boldsymbol{\varepsilon}}_i = [P_1(r), P_2(r), P_3(r), P_4(r)]$$

$$= \left[\begin{array}{c} 2\mu + 3\lambda \\ \frac{2\mu}{g}\left[6\frac{\sinh(r/g)}{(r/g)^5} - 6\frac{\cosh(r/g)}{(r/g)^4} + 2\frac{\sinh(r/g)}{(r/g)^3} \right] + \frac{\lambda}{g}\left[-2\frac{\sinh(r/g)}{(r/g)^3} + 2\frac{\cosh(r/g)}{(r/g)^2} \right] \\ -\frac{4\mu}{r^3}\left[1 + \frac{3}{(r/g)^2} \right] \\ -\frac{\pi}{g}e^{-r/g}\left\{ 2\mu\left[\frac{3}{(r/g)^5} + \frac{3}{(r/g)^4} + \frac{1}{(r/g)^3} \right] - \lambda\left[\frac{1}{(r/g)^3} + \frac{1}{(r/g)^2} \right] \right\} \end{array} \right]^T$$

$$\mathbf{R}(r) = R_i\hat{\boldsymbol{\varepsilon}}_i = [R_1(r), R_2(r), R_3(r), R_4(r)]$$

$$= \left[\begin{array}{c} 0 \\ 2\mu\left[-6\frac{\sinh(r/g)}{(r/g)^4} + 6\frac{\cosh(r/g)}{(r/g)^4} - 3\frac{\sinh(r/g)}{(r/g)^3} + \frac{\cosh(r/g)}{(r/g)^2} \right] + \lambda\left[-\frac{\sinh(r/g)}{(r/g)^2} + \frac{\cosh(r/g)}{(r/g)} \right] \\ \frac{12\mu}{g^2}\frac{1}{(r/g)^4} \\ \frac{\pi}{2}e^{-r/g}\left\{ 2\mu\left[\frac{6}{(r/g)^4} + \frac{6}{(r/g)^3} + \frac{3}{(r/g)^2} + \frac{1}{(r/g)^1} \right] + \lambda\left[\frac{1}{(r/g)^2} + \frac{1}{(r/g)} \right] \right\} \end{array} \right]^T$$

4.I.3. Boundary Condition Problems

In the following pages numerous problems will be addressed using both the classical and the non -classical gradient linear elasticity, all characterized by spherical symmetry. The first two problems have originally been partly solved by (Polyzos, et al., 2003), but for completeness those problems are also presented here.

4.I.3.1. The solid sphere

Consider a solid sphere of radius a, whose center O coincides with the origin of both the Cartesian and the spherical coordinate system. The point 0 is a material point and thermodynamics dictate that its displacement cannot be infinite. In the classical problem the displacement field takes the form $\mathbf{u} = \{C_1 \rho_1 + C_2 \rho_2\}\hat{\mathbf{r}}$, r being the radial coordinate. Since $\lim_{r\to 0^+} \rho_2 = \lim_{r\to 0^+} \frac{1}{r^2} \to \infty$, the C_2 term needs to be zero in order to maintain a finite displacement at the center of the sphere. In the gradient problem, the displacement field takes the form $\mathbf{u} = u_r\hat{\mathbf{r}} = \{C_1 \rho_1 + C_2 \rho_2 + C_3 \rho_3 + C_4 \rho_4\}\hat{\mathbf{r}}$.

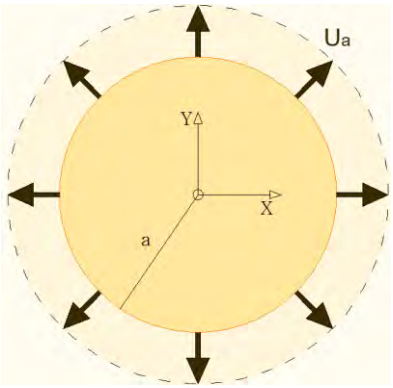

Fig. 1 x-y plane section of a solid sphere of radius a. subjected to a radial displacement Ua

Since both $\lim_{r\to 0^+} \rho_2 \to \infty$ and $\lim_{r\to 0^+} \rho_4 = \lim_{r\to 0^+} \frac{\pi}{2} e^{-r/g}\left(\frac{1}{r/g} + \frac{1}{(r/g)^2}\right) \to \infty$, for $g \neq 0$, both terms C_2 and C_4 are zero due to the thermodynamics, and the constants to be determined are two .

1a)Classical theory

In this first problem, the sphere boundary is subjected to a radial displacement Ua, i.e the BC is $\mathbf{u}(r = a) = U_a\hat{\mathbf{r}} \Rightarrow$

$$C_1\, a\, \hat{\mathbf{r}} = U_a\hat{\mathbf{r}} \Rightarrow C_1 = \frac{U_a}{a} \Rightarrow \mathbf{u}(r) = \left\{\frac{U_a}{a} r\right\}\hat{\mathbf{r}} \Rightarrow u_r(r) = \left\{\frac{U_a}{a} r\right\}$$

1b)Gradient theory

In the respective gradient problem, the sphere is made of a material with microstructure and being subjected to a radial displacement Ua (classical BC), while the normal displacement gradient at the boundary is qa (non-classical BC). The BCs and the displacement field are given below in vector forms.

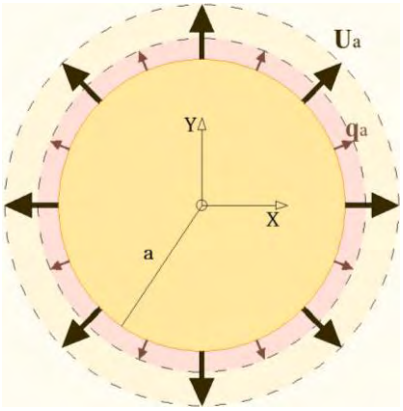

Fig. 2 x-y plane section of a solid sphere of radius a. subjected to prescribed radial displacement $\mathbf{u}(a) = U_a\hat{\mathbf{r}}$ and normal displacement gradient $\mathbf{q}(a) = q_a\hat{\mathbf{r}}$

$$\mathbf{u}(r=a) = U_a\hat{\mathbf{r}},$$

$$\mathbf{q}(r=a) = \left.\frac{\partial \mathbf{u}}{\partial \hat{\mathbf{r}}}\right|_{r=a} = q_a\hat{\mathbf{r}}$$

$$\mathbf{u} = u_r\hat{\mathbf{r}} = \{C_1\rho_1 + C_3\rho_3\}\hat{\mathbf{r}}$$

Carrying through with the linear algebra, the unique exact solution of this problem is obtained.

It order to optimize the results display, the parameter $c = a/g$ (radius to internal length parameter ratio) is used.

$$C_1 = \frac{c^2\sinh c - 2c\cosh c + 2\sinh c}{c^2\sinh c - 3c\cosh c + 3\sinh c}\frac{U_a}{a} + \frac{-c\cosh c + \sinh c}{c^2\sinh c - 3c\cosh c + 3\sinh c}q_a$$

$$C_3 = \frac{-c^2}{c^2\sinh c - 3c\cosh c + 3\sinh c}U_a + \frac{c^2}{c^2\sinh c - 3c\cosh c + 3\sinh c}aq_a$$

This solution can be divided into two simpler ones. In the first, the normal displacement gradient is restrained and so it vanishes at the boundary (q_a=0) while the sphere is subjected to a radial displacement U_a. In the second boundary's displacement is restrained (U_a=0) while the normal displacement gradient on the boundary is prescribed q_a. Obviously, any other problem can be addressed as a linear combination of the two problems above, as a result of the superposition principle. Hereupon, the solutions of these two problems are presented

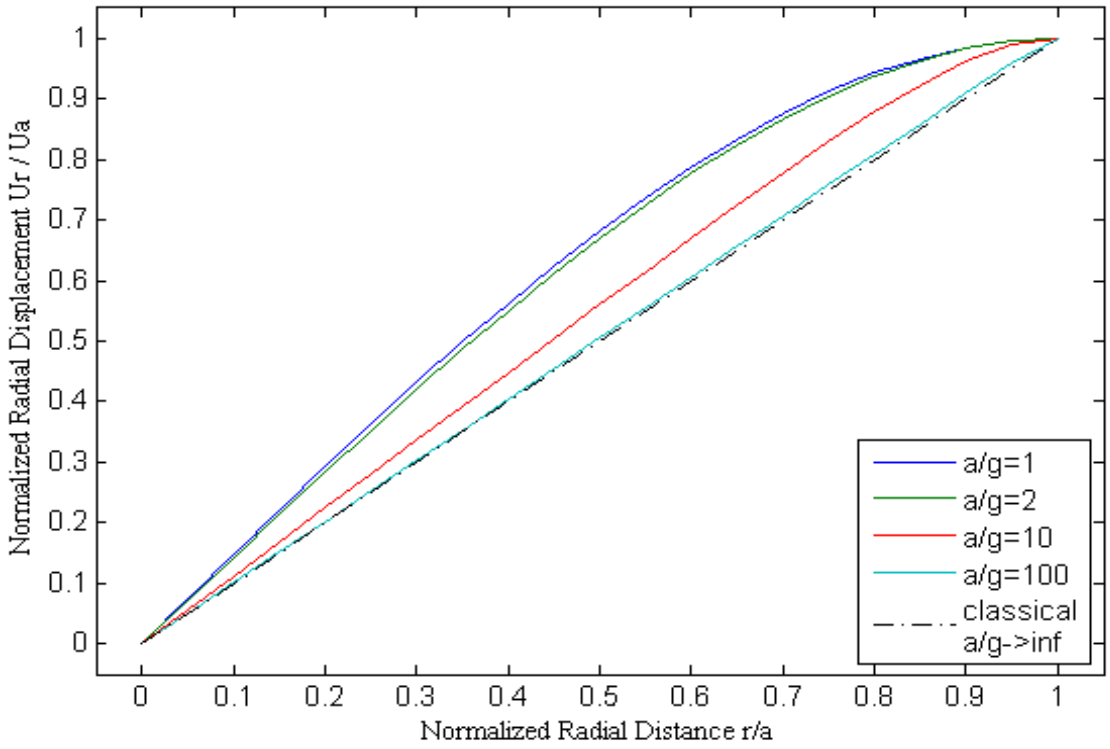

Fig. 3 Normalized radial displacement u_r/U_a versus normalized radial distance r/a of the solid sphere of radius a, for various a/g ratios. The classical boundary condition is $\mathbf{u}(\mathrm{a}) = \mathrm{U_a}\hat{\mathbf{r}}$ and the non-classical one $\mathbf{q}(a) = \mathbf{0}$

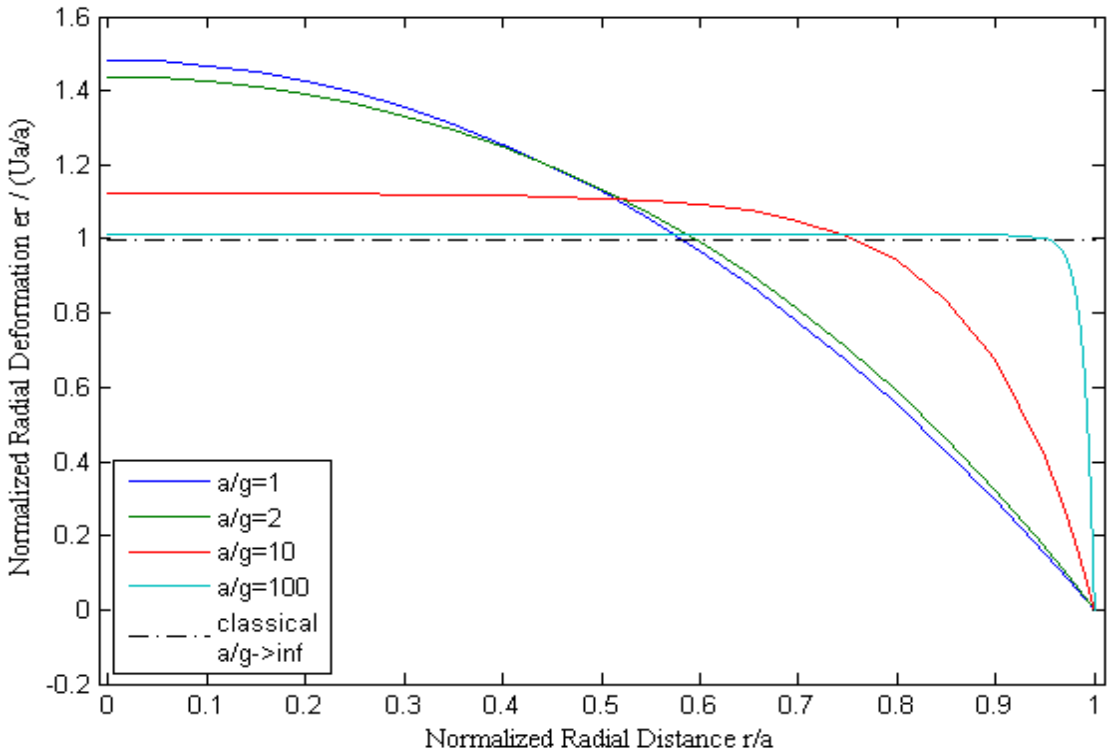

Fig. 4 Normalized radial deformation $e_r/(U_a/a)$ versus normalized radial distance r/a of the solid sphere of radius a, for various a/g ratios. The classical boundary condition is $\bar{\mathbf{u}}(a) = U_a\hat{\mathbf{r}}$ and the non-classical one $\mathbf{q}(a) = \mathbf{0}$

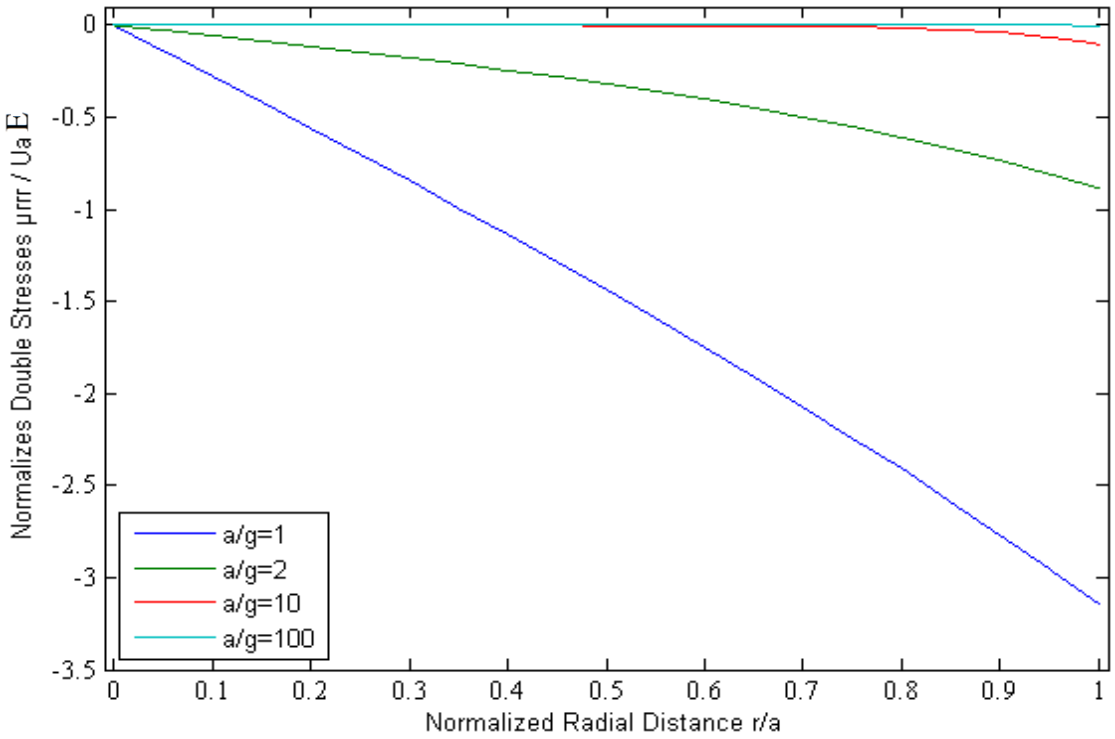

Fig. 3 Normalized double stresses μ_{rr}/EU_a **versus normalized radial distance** r/a **of the solid sphere of radius a, for various** a/g **ratios. The classical boundary condition is** $\bar{\mathbf{u}}(a) = U_a\hat{\mathbf{r}}$ **and the non-classical one** $\mathbf{q}(a) = \mathbf{0}$

Some preliminary conclusions can be drawn at this point. By restraining the spheres radial deformation at it's boundary, a non classical behavior is obtained, where the spheres displacement field along it's radius is greater than the one of the classical theory. Even in the cases that the c=L/g ratio is great (c=10, c=100), the divergence from the classical solution is discernible. Also, the deformation field approaches the classical deformation field as the c ratio increases. For great c ratio values, only close to the sphere's boundary the strain diverges from the classical, while along the rest of it's radius, the strains are practically those described by the classical theory. The radial double stresses distribution along the bars radius takes greater values for small c ratios, with it's maximum always being at the spheres surface, and zero double stresses at it's center. For great c values, the double stresses are significant only in a small part of the spheres radius, close to its surface.

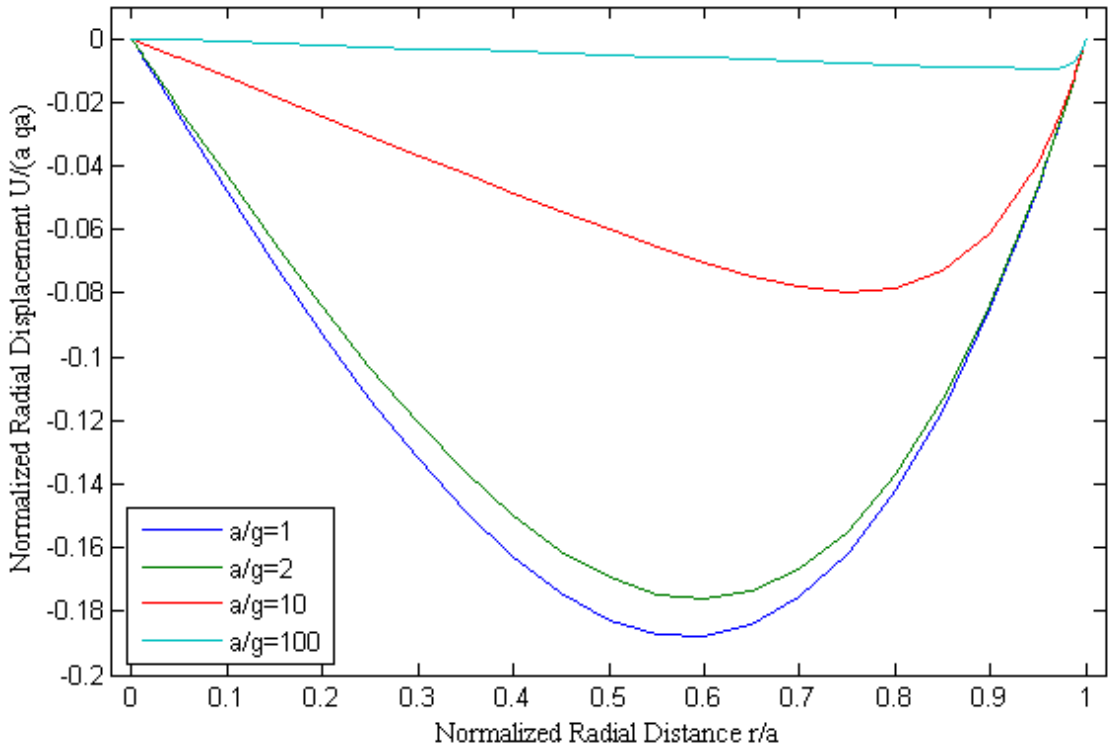

Fig. 5 Normalized radial displacement $u_r/(\,a\,q_a)$ **versus normalized radial distance** r/a **of the solid sphere of radius a, for various** a/g **ratios. The classical boundary condition is** $\bar{\mathbf{u}}(a)=\mathbf{0}$ **and the non-classical one** $\mathbf{q}(a)=q_a\hat{\mathbf{r}}$

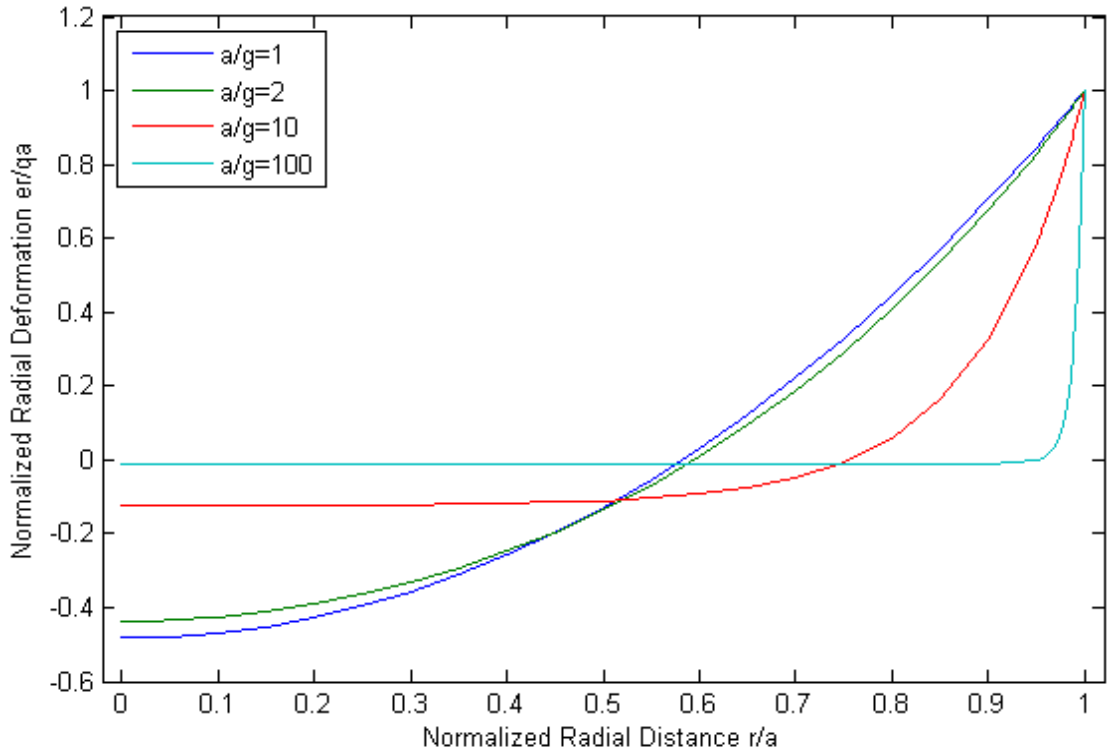

Fig. 4 Normalized radial deformation $e_r/(q_a)$ **versus normalized radial distance** r/a **of the solid sphere of radius a, for various** a/g **ratios. The classical boundary condition is** $\bar{\mathbf{u}}(a)=\mathbf{0}$ **and the non-classical one** $\mathbf{q}(a)=q_a\hat{\mathbf{r}}$

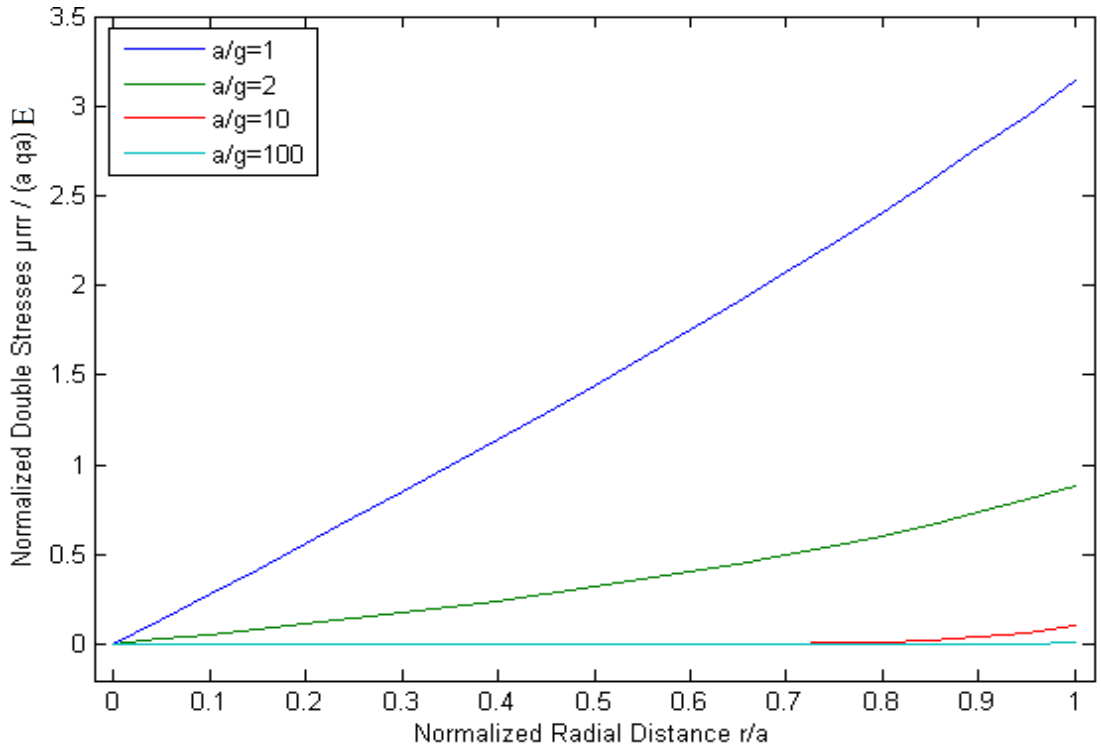

Fig. 6 Normalized double stresses μ_{rr}/Eaq_a versus normalized radial distance r/a of the solid sphere of radius a, for various a/g ratios. The classical boundary condition is $\bar{\mathbf{u}}(a)=\mathbf{0}$ and the non-classical one $\mathbf{q}(a)=q_a\hat{\mathbf{r}}$

In the figures above is clearly depicted the fact that the effect of the non classical BC decreases for great c ratio values, and it is limited only close to the spheres boundary.

It is noted that applying certain combinations of Ua and qa the classical or the gradient fundamental solution can be eliminated. Hence, every sphere even one with significant microstructure subjected to the right combination of loads (qa=Ua/a) behaves exactly as the classical theory of elasticity dictates. Furthermore, by applying a different set of Ua, qa,($q_a=\frac{U_a}{a}\left[\frac{c^2}{c\coth c-1}-2\right]$) the classical term from the spheres displacement field is eliminated and a completely non-classical field is acquired.

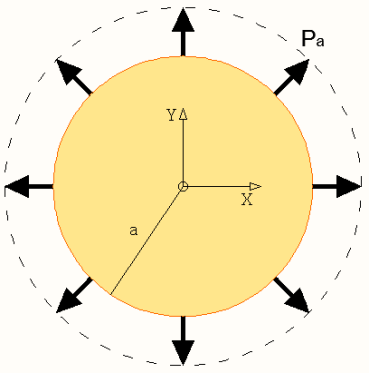

Fig. 7 x-y plane section of a solid sphere of radius a subjecter to radial stress $\mathbf{P}(a) = P_a\hat{\mathbf{r}}$

2a)Classical theory

In this second problem a non holonomic kind of loading is discussed, so the sphere is subjected to radial tensile stress Pa (in the common case of a compressive pressure Pa<0). The boundary condition is $\mathbf{P}(\mathrm{r}=\mathrm{a}) = \mathrm{P_a}\hat{\mathbf{r}}$ and the displacement field is obtained as follows

$$\{C_1(2\mu+3\lambda)\}\hat{\mathbf{r}} = P_a\hat{\mathbf{r}} \Rightarrow C_1 = \frac{P_a}{2\mu+3\lambda} \Rightarrow$$

$$\mathbf{u}(\mathrm{r}) = \left\{\frac{\mathrm{P_a}}{2\mu+3\lambda}\mathrm{r}\right\}\hat{\mathbf{r}}$$

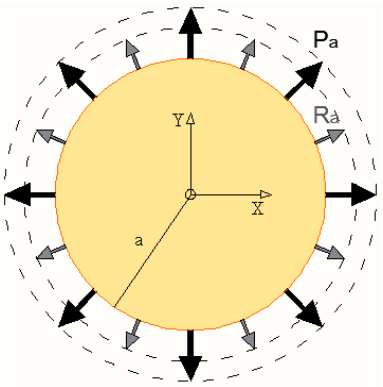

Fig. 8 x-y plane section of a solid sphere of radius a, subjected to a tesile stress $\mathbf{P}(a) = P_a\hat{\mathbf{r}}$ **and surface double stresses** $\mathbf{R}(a) = R_a\hat{\mathbf{r}}$

2b)Gradient theory

In the case of the gradient elastic sphere under a radial tensile stress Pa (classical BC), while the surface double stresses at the boundary read Ra (non-classical BC) , i.e. $\mathbf{P}(\mathrm{r}=\mathrm{a}) = \mathrm{P_a}\hat{\mathbf{r}}$ and $\mathbf{R}(\mathrm{r}=\mathrm{a}) = \mathrm{R_a}\hat{\mathbf{r}}$, the unique solution obtained is the following

$$\mathbf{u} = \mathrm{u_r}\hat{\mathbf{r}} = \{C_1\rho_1 + C_3\rho_3\}\hat{\mathbf{r}} \underset{\text{Conditions}}{\overset{\text{Boundary}}{\Rightarrow}}$$

$$C_1 = \frac{1}{2\mu+3\lambda}\mathrm{P_a}$$

$$+\frac{-2}{(2\mu+3\lambda)\mathrm{a}}\left\{\frac{[c^3\lambda - c\,6\mu]\cosh c + [c^2(2\mu-\lambda)+6\mu]\sinh c}{[c^3(2\mu+\lambda)+c12\mu]\cosh c - [c^2(6\mu+\lambda)+2\mu]\sinh c}\right\}\mathrm{R_a}$$

$$C_3 = 0\mathrm{P_a}$$

$$+\left\{\frac{c^4}{[c^3(2\mu+\lambda)+c12\mu]\cosh c - [c^2(6\mu+\lambda)+2\mu]\sinh c}\right\}\mathrm{R_a}$$

The solution above denotes that when no double stresses are applied at the spheres surface (R_a=0), while a P_a stress is applied, the sphere behaves exactly as the classical theory describes, no matter how small it might be or how significant it's microstructure (g length). The following figures present the sphere's displacement, strain and double stress radial distribution. In order to normalize this solution the Lame constants have be substituted with their equivalents in terms of the Young's modulus E and the Poisson ratio ν, i.e. $\lambda = \frac{E\nu}{(1+\nu)(1-2\nu)}$ and $\mu = \frac{E}{2(1+\nu)}$.

In the pressure problem the length g is eliminated from this solution, and the parameters left in its normalized form are the r/a ratio and the Poisson constant. Thus the next figures are plotted it terms of these parameters.

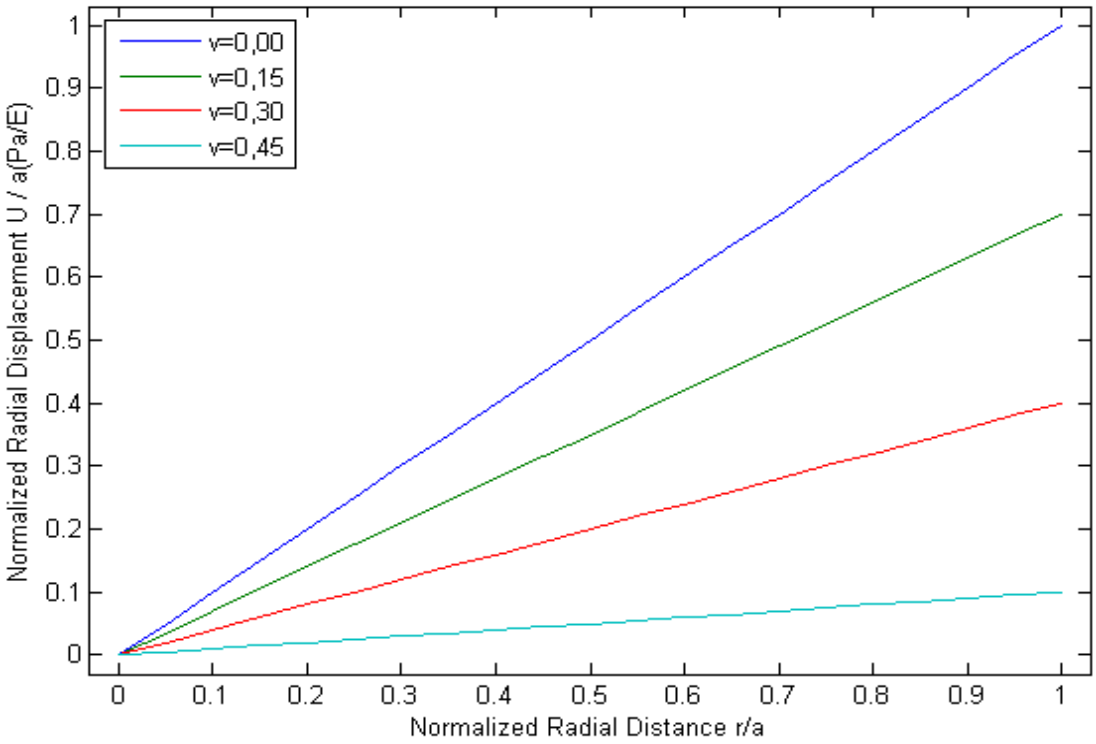

Fig. 9 Normalized radial displacement $u_r/(a\,P_a/E)$ versus normalized radial distance r/a of the solid sphere of radius a, for various a/g ratios. The classical boundary condition is $\mathbf{P}(a) = P_a\hat{\mathbf{r}}$ and the non-classical one $\mathbf{R}(a) = \mathbf{0}$

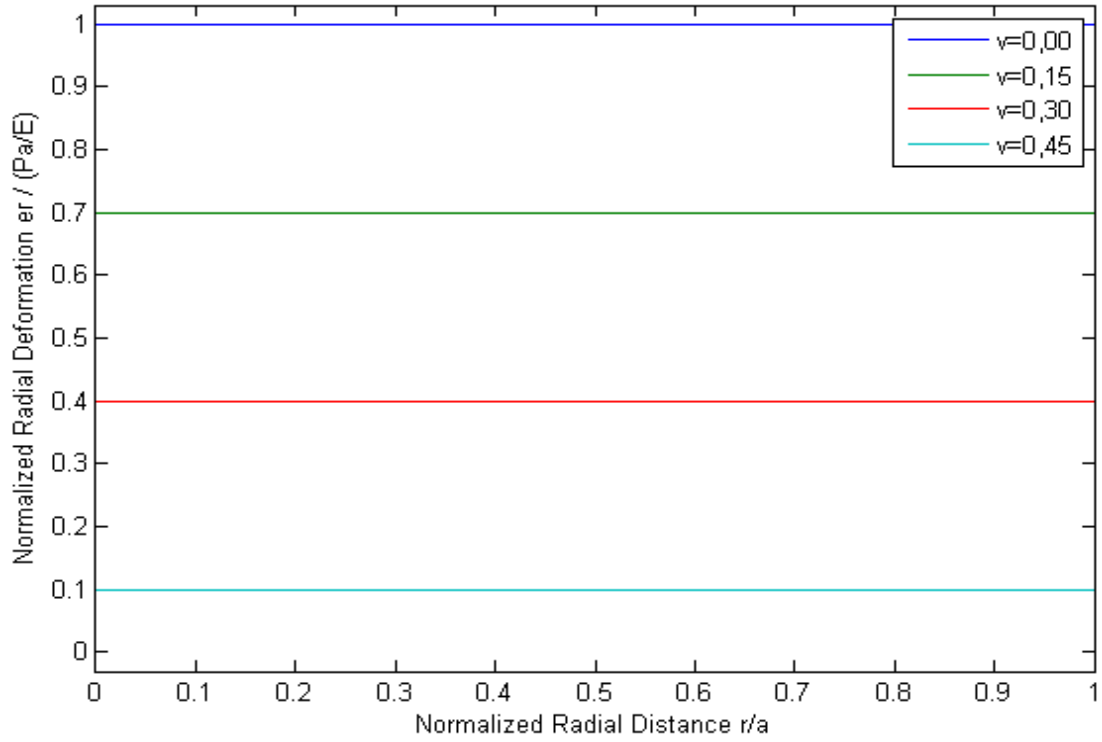

Fig. 10 Normalized radial deformation $e_r/(P_a/E)$ versus normalized radial distance r/a of the solid sphere of radius a, for various a/g ratios. The classical boundary condition is $\mathbf{P}(a)=P_a\hat{\mathbf{r}}$ and the non-classical one $\mathbf{R}(a)=\mathbf{0}$

When only double stresses are applied the sphere's behavior is size dependent, i.e. the g parameter is not eliminated – as expected - and after the normalization of the solution, three parameters are left, the ratios r/a, a/g and ν. The displacement, strain and double forces fields are plotted with respect to the r/a and a/g ratios, for the values of the Poisson ratio ν=0.00 and ν=0.30, which are considered to be typical.

It should be noticed that the radial double stresses affect both the displacement and the strain field so when restraining of prescribing either of them (the first problem) double stresses need to be applied. Also, in the case that the poisons ratio is ν=0.00, for great c=L/g values, these fields tend to be reduced to the classical ones (zero fields, since this BC is not takes into account it the classical elasticity). However, for other ν values the solution is not reduced to zero field for great c values, meaning that even large scale spheres will behave non classically when properly loaded.

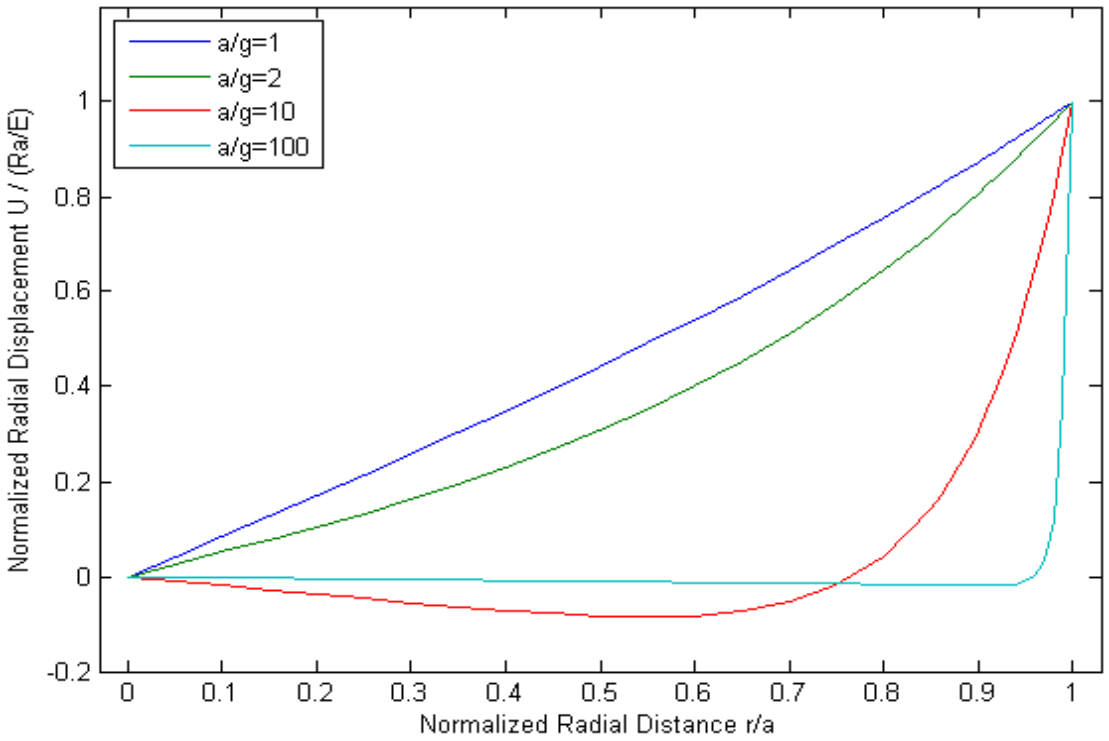

Fig. 11 Normalized radial displacement $u_r/(R_a/E)$ versus normalized radial distance r/a of the solid sphere of radius a, for various a/g ratios for Poisson ratio v=0.00. The classical boundary condition is $\mathbf{P}(a)=\mathbf{0}$ and the non-classical one $\mathbf{R}(a)=R_a\hat{\mathbf{r}}$

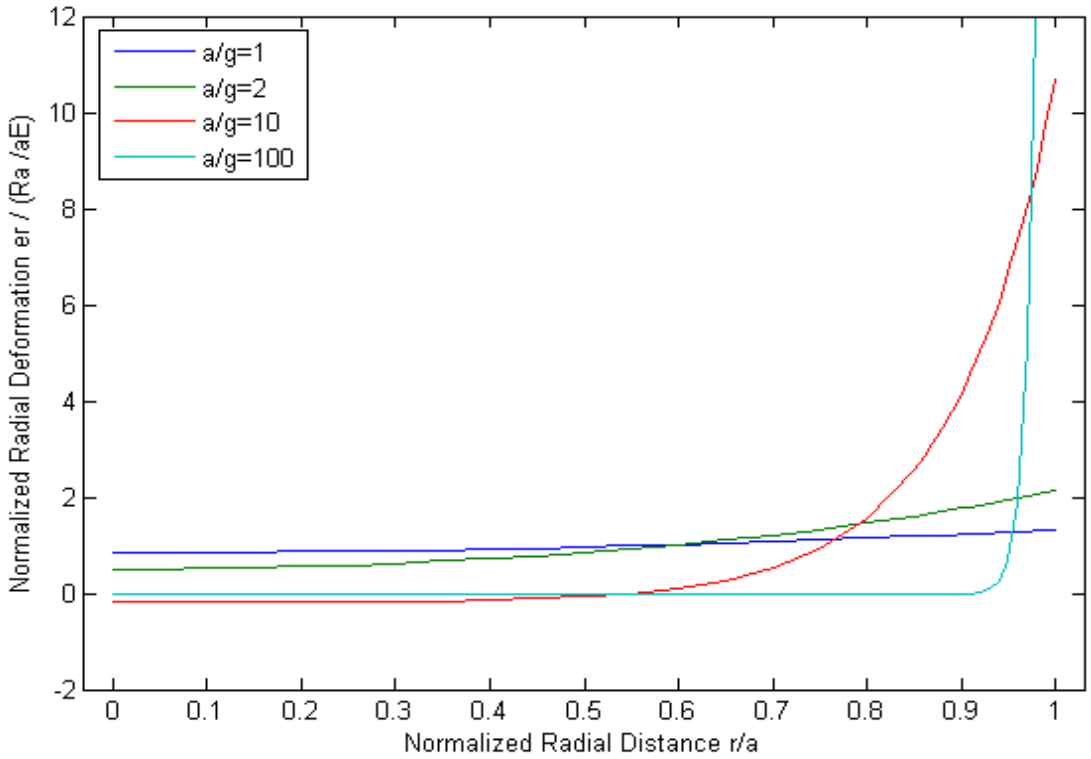

Fig. 12 Normalized radial deformation $e_r/(R_a/aE)$ versus normalized radial distance r/a of the solid sphere of radius a, for various a/g ratios for Poisson ratio v=0.00. The classical boundary condition is $\mathbf{P}(a)=\mathbf{0}$ and the non-classical one $\mathbf{R}(a)=R_a\hat{\mathbf{r}}$

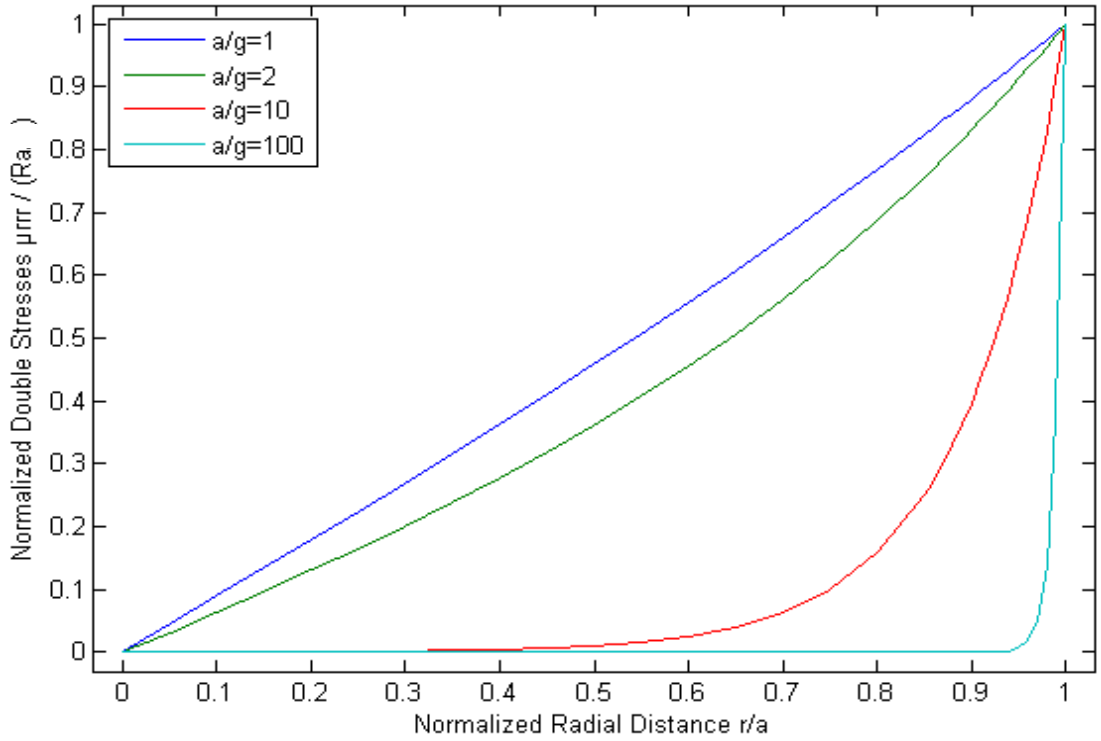

Fig. 13 Normalized double stresses $\mu_{rrr}/(\mathrm{R_a})$ versus normalized radial distance r/a of the solid sphere of radius a, for various a/g ratios for Poisson ratio v=0.00. The classical boundary condition is $\mathbf{P}(a)=\mathbf{0}$ and the non-classical one $\mathbf{R}(a)=R_a\hat{\mathbf{r}}$

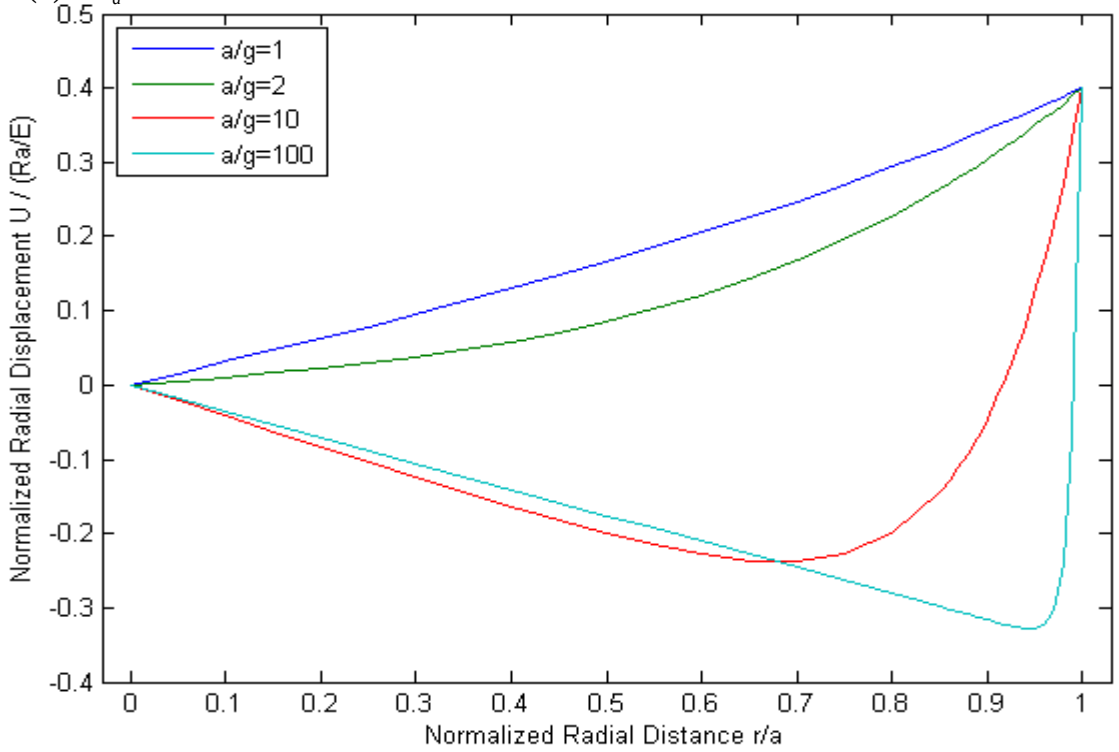

Fig. 14 Normalized radial displacement $u_r/(R_a/E)$ versus normalized radial distance r/a of the solid sphere of radius a, for various a/g ratios for Poisson ratio v=0.30. The classical boundary condition is $\mathbf{P}(a)=\mathbf{0}$ and the non-classical one $\mathbf{R}(a)=R_a\hat{\mathbf{r}}$

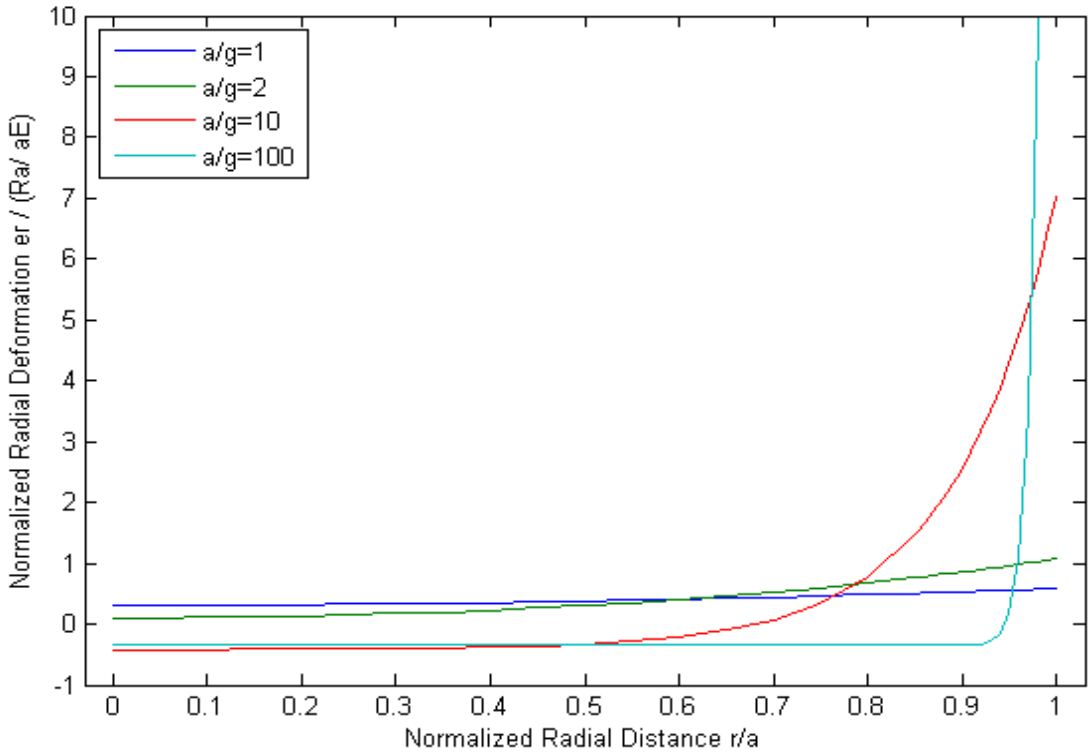

Fig. 15 Normalized radial deformation $e_r/(R_a/E)$ versus normalized radial distance r/a of the solid sphere of radius a, for various a/g ratios for Poisson ratio v=0.30. The classical boundary condition is $\mathbf{P}(a)=\mathbf{0}$ and the non-classical one $\mathbf{R}(a)=R_a\hat{\mathbf{r}}$

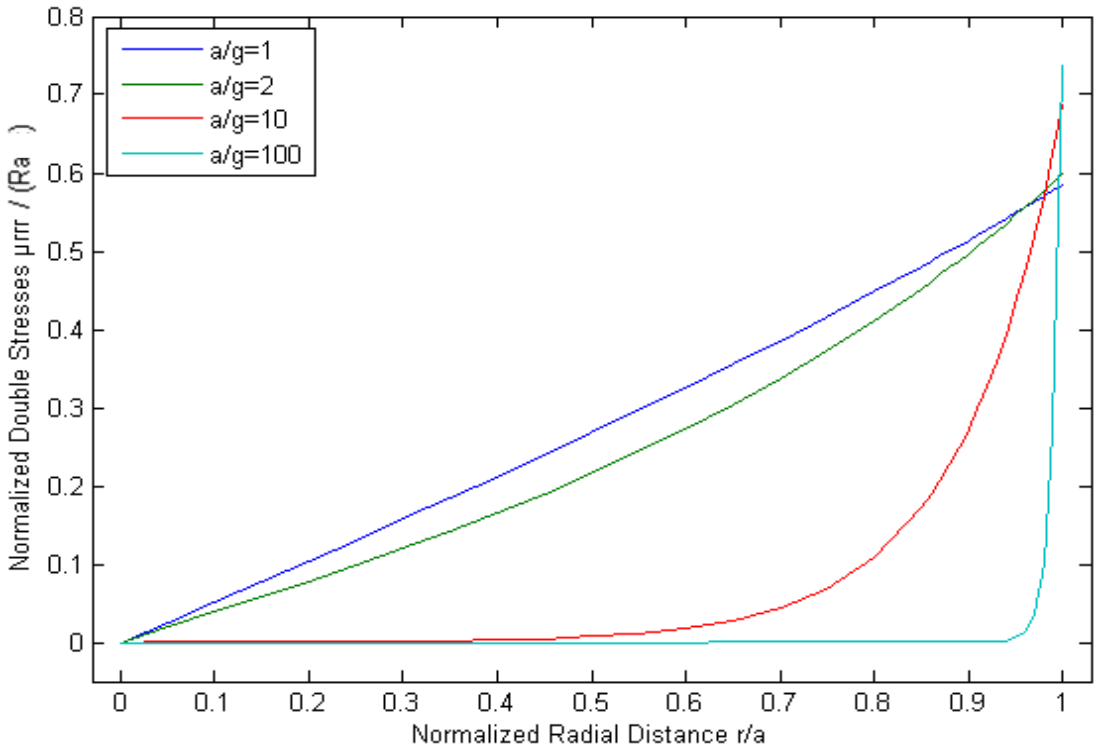

Fig. 16 Normalized double stresses $\mu_{rrr}/(R_a)$ versus normalized radial distance r/a of the solid sphere of radius a, for various a/g ratios for Poisson ratio v=0.30. The classical boundary condition is $\mathbf{P}(a)=\mathbf{0}$ and the non-classical one $\mathbf{R}(a)=R_a\hat{\mathbf{r}}$

There are two more possible cases of loading combinations. The first is the one that the displacement and the double stresses at the spheres surface are prescribed, i.e. the BCs are $\mathbf{u}(\mathrm{r}=\mathrm{a})=\mathrm{U_a}\hat{\mathbf{r}}$ and $\mathbf{R}(\mathrm{r}=\mathrm{a})=\mathrm{R_a}\hat{\mathbf{r}}$, while the second one, is the case in which the stress and the strain at the sphere's boundary is prescribed, i.e. $\mathbf{P}(\mathrm{r}=\mathrm{a})=\mathrm{P_a}\hat{\mathbf{r}}$ and , $\mathbf{q}(\mathrm{r}=\mathrm{a})=\partial\mathbf{u}/\partial\hat{\mathbf{r}}\big|_{\mathrm{r=a}}=\mathrm{q_a}\hat{\mathbf{r}}$. These cases can be addressed through the ones already presented by substituting either the degree of freedom BC with its work conjugate, or the generalized stress BC with its respective degree of freedom BC, using the following relations:

$$\begin{bmatrix}\mathrm{U_a}\\ \mathrm{q_a}\end{bmatrix}=\frac{1}{2\mu+3\lambda}\begin{bmatrix}\mathrm{a} & 1\\ 1 & \mathrm{K}\end{bmatrix}\begin{bmatrix}\mathrm{P_a}\\ \mathrm{R_a}\end{bmatrix}\leftrightarrow\begin{bmatrix}\mathrm{P_a}\\ \mathrm{R_a}\end{bmatrix}=\frac{(2\mu+3\lambda)}{\mathrm{aK}-1}\begin{bmatrix}\mathrm{K} & -1\\ -1 & \mathrm{a}\end{bmatrix}\begin{bmatrix}\mathrm{U_a}\\ \mathrm{q_a}\end{bmatrix}$$

$$\mathrm{K}=\frac{\left(-4\mathrm{c}^2(\mu+2\lambda)+12\mu\right)\mathrm{c}\cosh(\mathrm{c})-\left(\mathrm{c}^4(2\mu+3\lambda)+\mathrm{c}^2 8\lambda-12\mu\right)\sinh(\mathrm{c})}{\left(\mathrm{c}^2(2\mu+\lambda)+12\mu\right)\mathrm{c}\cosh(\mathrm{c})-\left(\mathrm{c}^2(6\mu+\lambda)+12\mu\right)\sinh(\mathrm{c})}$$

4.I.3.ii. The spherical cavity

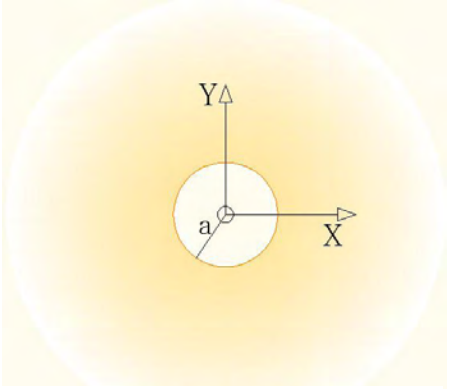

Fig. 17 Schematic representation of a spherical cavity – x-y section

Consider an infinite elastic 3D space with a spherical cavity embedded in it at point 0 which is the origin of both the spherical and the Cartesian coordinate system used. Since the space exceeds infinitely due to thermodynamics the displacement of the material point at infinity needs to be finite. . In the classical problem the displacement field takes the form $\mathbf{u} = \{C_1 \rho_1 + C_2 \rho_2\}\hat{\mathbf{r}}$. Since $\lim_{r\to\infty} \rho_1 = \lim_{r\to\infty} r \to \infty$, the C_1 term needs to be zero. In the gradient problem, the displacement field is $\mathbf{u} = u_r\hat{\mathbf{r}} = \{C_1 \rho_1 + C_2 \rho_2 + C_3 \rho_3 + C_4 \rho_4\}\hat{\mathbf{r}}$. Both limits $\lim_{r\to\infty} \rho_1 \to \infty$ and $\lim_{r\to\infty} \rho_3 \to \infty$, thus the terms C_1 and C_3 are both zero in this case, for a finite displacement at infinity.

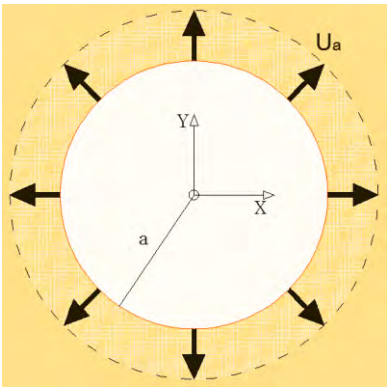

Fig. 18 x-y plane section of the spherical cavitysubjected to radial displacement U_a

1a)Classical theory

The spherical cavity is subjected to a radial displacement U_a. The BC is $\mathbf{u}(r = a) = U_a\hat{\mathbf{r}} \Rightarrow$

$$\left\{C_2 \frac{1}{a^2}\right\}\hat{\mathbf{r}} = U_a\hat{\mathbf{r}} \Rightarrow C_2 = a^2 U_a \Rightarrow \mathbf{u}(r) = \left\{U_a \frac{a^2}{r^2}\right\}\hat{\mathbf{r}}$$

$$\Rightarrow u_r(r) = \left\{U_a \frac{a^2}{r^2}\right\}$$

1b)Gradient theory

In this case, the infinite space is made of a material with microstructure and the cavity is subjected to a radial displacement U_a (classical BC), while the normal displacement gradient at the boundary is q_a (non-classical BC), i.e.

$$\mathbf{u}(r = a) = U_a\hat{\mathbf{r}}, \qquad \mathbf{q}(r = a) = \left.\frac{\partial \mathbf{u}}{\partial \hat{\mathbf{r}}}\right|_{r=a} = q_a\hat{\mathbf{r}}$$

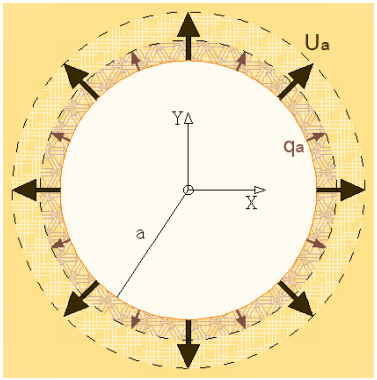

Fig. 19 x-y plane section of the spherical cavity subjected to prescribed radial displacement $\bar{\mathbf{u}}(a) = U_a\hat{\mathbf{r}}$ and deformation $\mathbf{q}(a) = q_a\hat{\mathbf{r}}$

This problems exact and unique solution is found: $\mathbf{u} = \{C_2 \rho_2 + C_4 \rho_4\}\hat{\mathbf{r}}$,

$$C_2 = a^2\left(\frac{2}{c^2}+\frac{2}{c}+1\right)U_a + a^2\left(\frac{1}{c^2}+\frac{1}{c}\right)aq_a$$

$$C_4 = -\frac{4}{\pi}e^c U_a + \frac{2}{\pi}e^c aq_a$$

where c is the ratio of the spherical cavity radius a to the characteristic material length g. Dividing this problem into two simpler ones, one that the normal displacement gradient vanishes on the boundary (q_a=0) while the sphere is subjected to a radial displacement Ua, and one that one that the boundaries' displacement is zero (U_a=0) while the normal displacement gradient on the boundary is determined q_a, a better understanding of the cavities behavior can be obtained. The following figures present this behavior normalized appropriately in each case, for various values of the problems parameters. Any other problem can be addressed as a linear combination of the two problems above, based on the superposition principle.

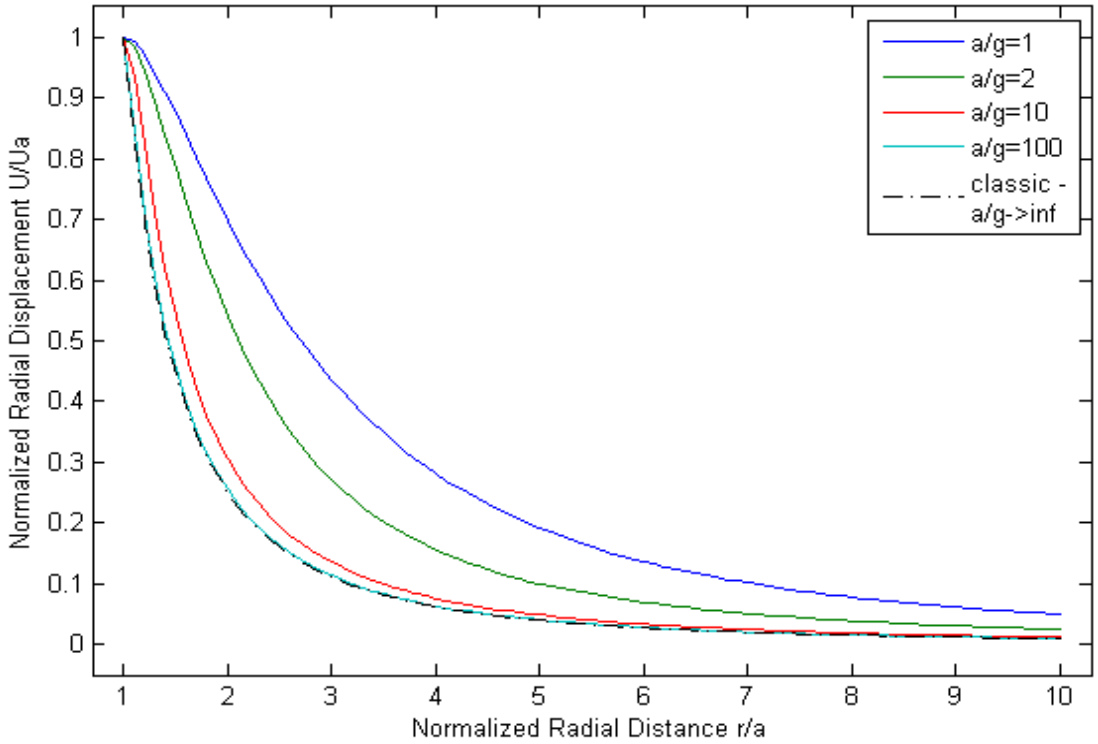

Fig. 20 Normalized radial displacement u_r/U_a versus normalized radial distance r/a of a spherical cavity of radius a, for various ratios a/g, for any radius a. The classical boundary condition is $\mathbf{u}(a) = U_a\hat{\mathbf{r}}$ and the non classical boundary condition is $\mathbf{q}(a) = \mathbf{0}$

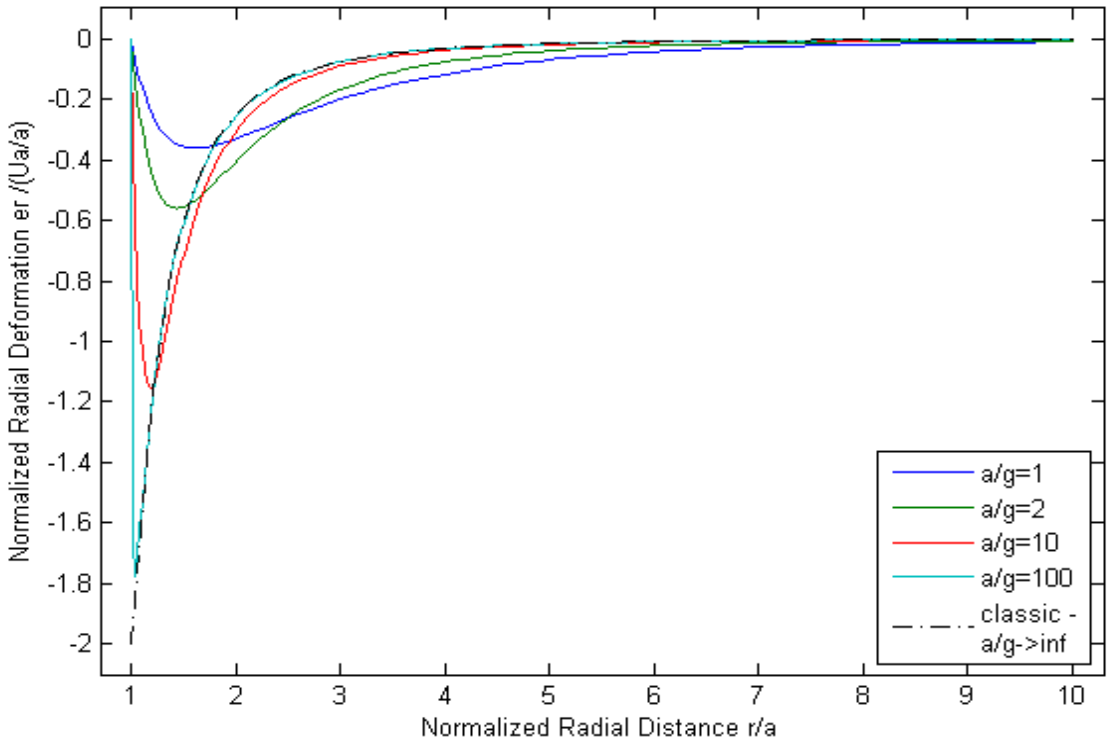

Fig. 21 Normalized radial deformation $e_r/(U_a/a)$ versus normalized radial distance r/a of spherical cavity of radius a, for various ratios a/g, for any radius a. The classical boundary condition is $\mathbf{u}(a)=U_a\hat{\mathbf{r}}$ and the non classical boundary condition is $\mathbf{q}(a)=\mathbf{0}$

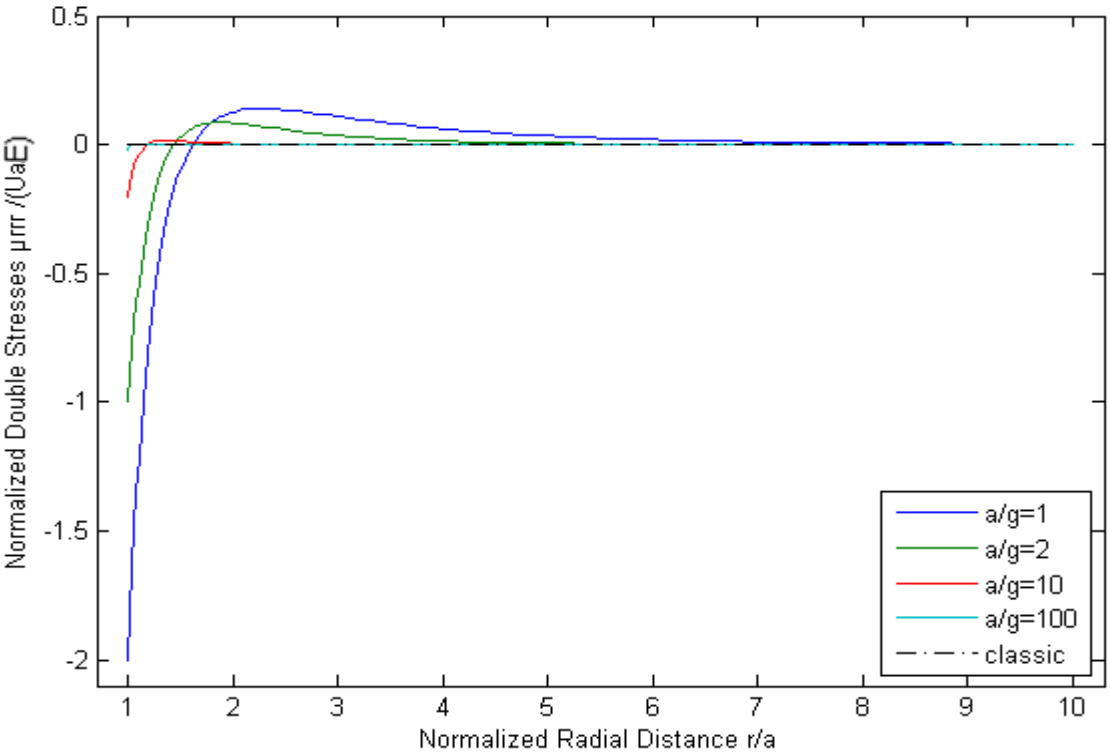

Fig. 22 Normalized double stresses $\mu_{rr}/(U_a E)$ versus normalized radial distance r/a of a solid sphere of radius a, for various ratios a/g, for any radius a. The classical boundary condition is $\mathbf{u}(a)=Ua\hat{\mathbf{r}}$ and the non classical boundary condition is $\mathbf{q}(a)=\mathbf{0}$

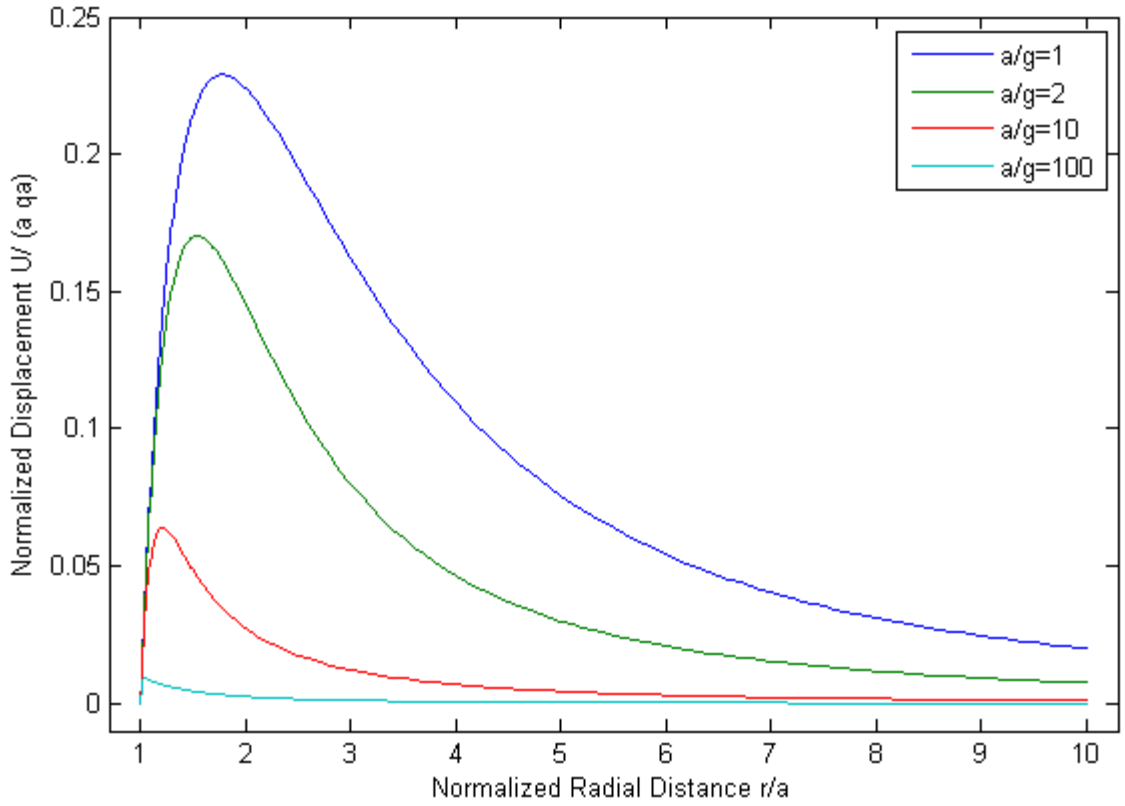

Fig. 23 Normalized radial displacement $u_r/(a\ q_a)$ versus normalized radial distance r/a of a spherical cavity of radius a, for various ratios a/g, for any radius a. The classical boundary condition is $\mathbf{u}(a)=\mathbf{0}$ and the non classical boundary condition is $\mathbf{q}(a)=q_a\hat{\mathbf{r}}$

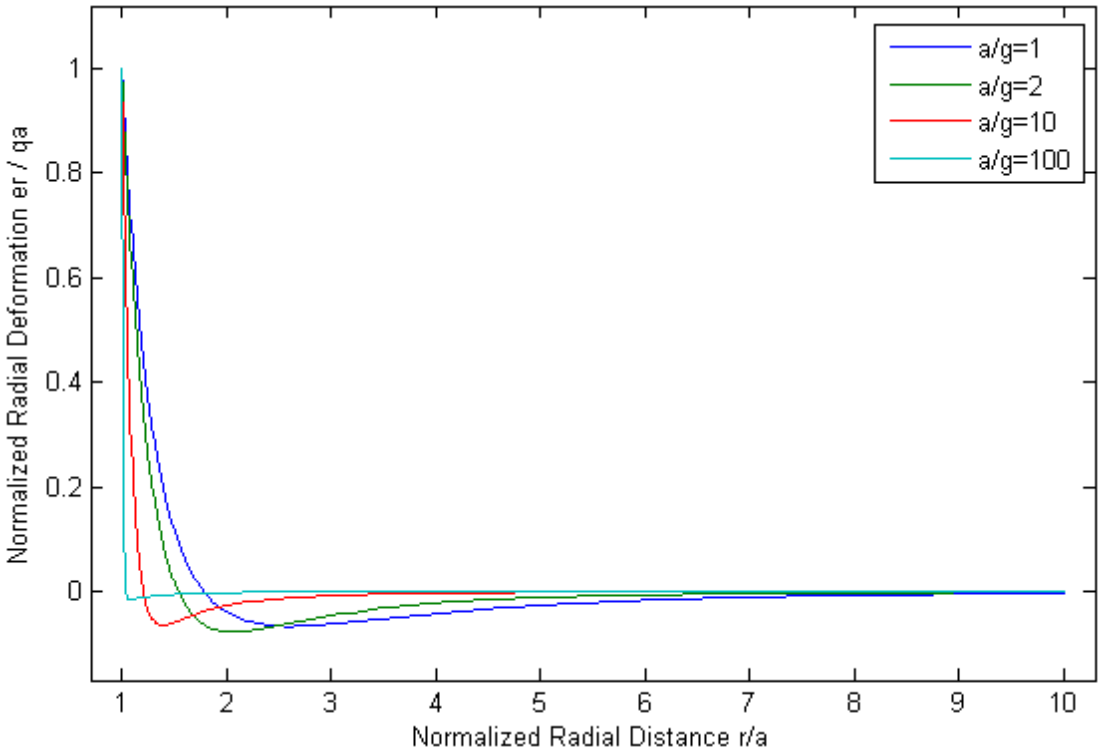

Fig. 24 Normalized radial deformation $e_r/(\ q_a)$ versus normalized radial distance r/a of a spherical cavity of radius a, for various ratios a/g, for any radius a. The classical boundary condition is $\mathbf{u}(a)=\mathbf{0}$ and the non classical boundary condition is $\mathbf{q}(a)=q_a\hat{\mathbf{r}}$

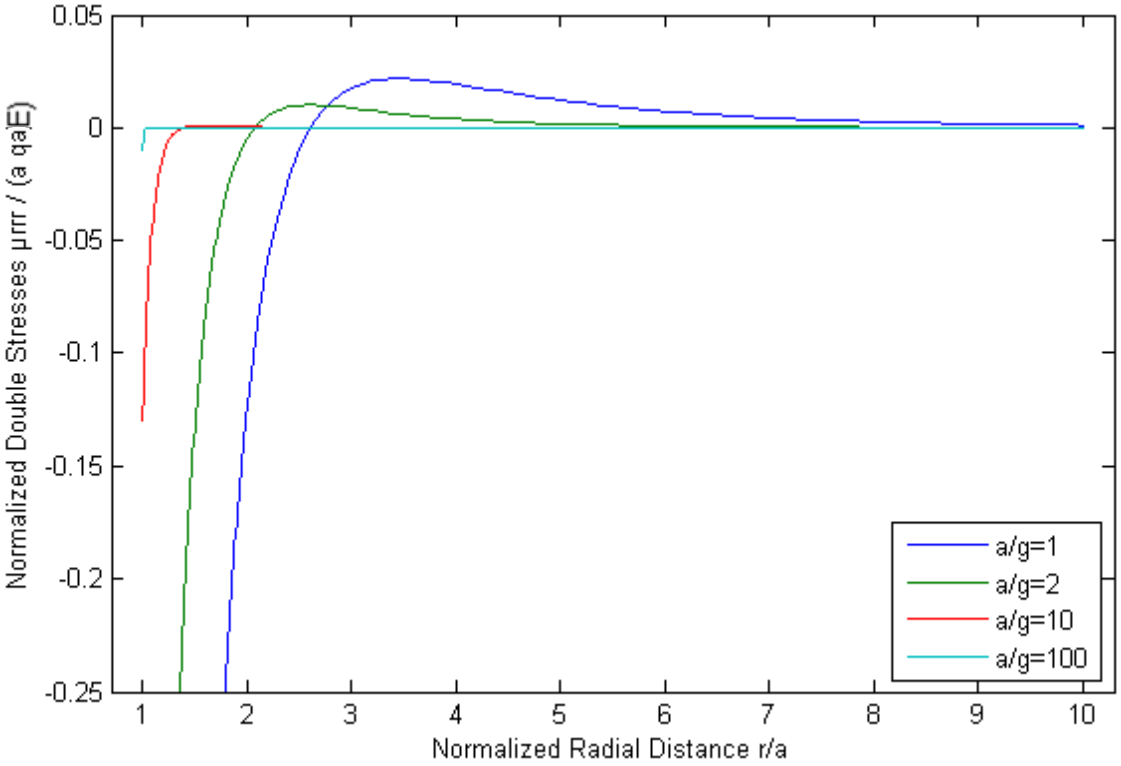

Fig. 25 Normalized double stresses $\mu_{rrr}/(\,aq_aE)$ versus normalized radial distance r/a of a spherical cavity of radius a, for various ratios a/g, for any radius a. The classical boundary condition is $\mathbf{u}(a)=\mathbf{0}$ and the non classical boundary condition is $\mathbf{q}(a)=q_a\hat{\mathbf{r}}$

When the deformation at the cavity's boundary is determined, the displacement distribution in the material is greater than the one described by the classical theory. The double forces are significant only near the boundary, and as the c ratio increases their range decreases, while the strain at the boundary approaches the classical one. Also, the application of certain combinations of BCs either the classical or the gradient part of the solution can be eliminated, exactly like the case of the solid sphere. Hence, a spherical cavity, too, may behave exactly like the classical theory predicts even one with significant microstructure, when subjected to the right combination of loads (qa=-2Ua/a). If the strain is prescribed as $q_a=\frac{U_a}{a}\left[\frac{c^2}{c\coth c-1}-2\right]$ the classical part of the solution is eliminated and a completely non-classical behavior is described for the spherical cavity.

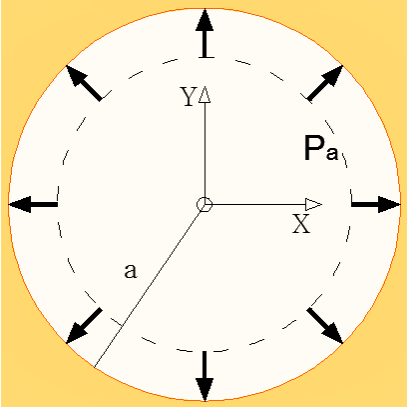

Fig. 26 x-y plane section of the spherical cavity with radial pressure applied at the boundary $\mathbf{P}(a) = P_a\hat{\mathbf{r}}$

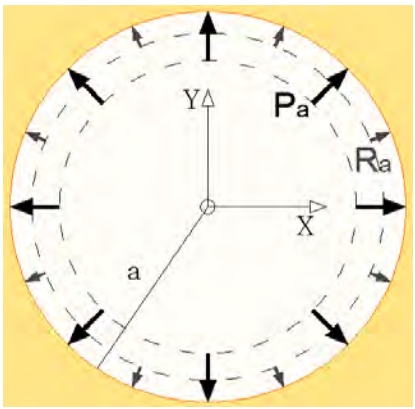

Fig. 27 x-y plane section of the spherical cavity. The boundary conditions are $\mathbf{P}(a) = P_a\hat{\mathbf{r}}$ and $\mathbf{R}(a) = R_a\hat{\mathbf{r}}$

2a)Classical theory

When the spherical cavity is subjected to radial compressive stress - pressure Pa, i.e. the BC is $\mathbf{P}(r=a) = P_a\hat{\mathbf{r}}$, the analytical displacement field acquired is:

$$\mathbf{u}(r) = \left\{\frac{P_a}{4\mu}\frac{a^3}{r^2}\right\}\hat{\mathbf{r}}$$

2b)Gradient theory

When a gradient elastic spherical cavity is subjected to a radial compressive stress Pa (classical BC), while the surface double stresses at the boundary are Ra (non-classical BC) ,i.e. $\mathbf{P}(r=a) = P_a\hat{\mathbf{r}}$ and $\mathbf{R}(r=a) = R_a\hat{\mathbf{r}}$, the displacement field takes the following form:

$$\mathbf{u} = u_r\hat{\mathbf{r}} = \{C_2\rho_2 + C_4\rho_4\}\hat{\mathbf{r}}$$

Where c=a/g the spherical cavity radius to g length ratio and C_2 and C_4 expressions are given below:

$$C_2 = \frac{a^3}{4\mu}\left\{\frac{(2\mu+\lambda)\cdot c^3 + (6\mu+\lambda)\cdot c^2 + 12\mu\cdot c + 12\mu}{(2\mu+\lambda)\cdot c^3 + (6\mu+\lambda)\cdot c^2 + 9\cdot(2\mu+\lambda)\cdot c + 9\cdot(2\mu+\lambda)}\right\}P_a$$
$$-\frac{a^2}{2\mu}\left\{\frac{-\lambda\cdot c^3 + (2\mu-\lambda)\cdot c^2 + 6\mu\cdot c + 6\mu}{(2\mu+\lambda)\cdot c^3 + (6\mu+\lambda)\cdot c^2 + 9\cdot(2\mu+\lambda)\cdot c + 9\cdot(2\mu+\lambda)}\right\}R_a$$

$$C_4 = -\frac{a}{\pi}\left\{\frac{6\cdot c^2\cdot e^c}{(2\mu+\lambda)\cdot c^3 + (6\mu+\lambda)\cdot c^2 + 9\cdot(2\mu+\lambda)\cdot c + 9\cdot(2\mu+\lambda)}\right\}P_a$$
$$+\frac{1}{\pi}\left\{\frac{(2\cdot c^4 + 6\cdot c^2)\cdot e^c}{(2\mu+\lambda)\cdot c^3 + (6\mu+\lambda)\cdot c^2 + 9\cdot(2\mu+\lambda)\cdot c + 9\cdot(2\mu+\lambda)}\right\}R_a$$

First, the case where pressure Pa is applied and no double stresses(Ra=0).

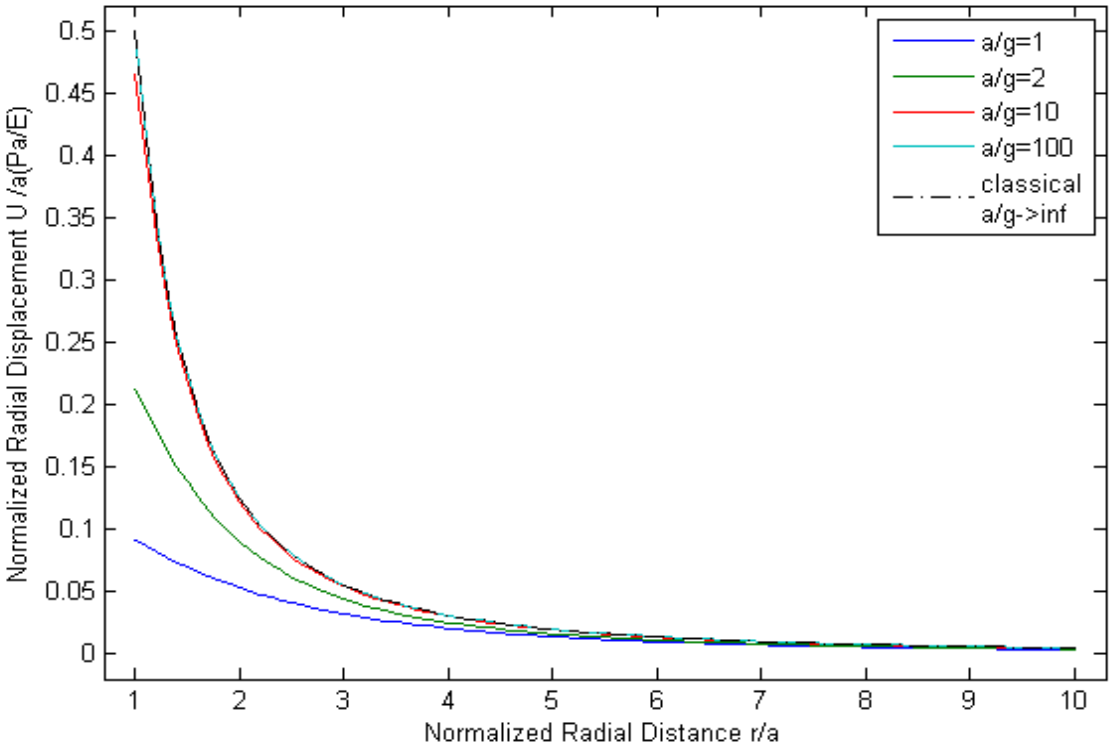

Fig. 28 Normalized radial displacement $u_r/a(P_a/E)$ versus normalized radial distance r/a of a spherical cavity of radius a, for various ratios a/g, for any radius a.,for o poissons ratio v=0.00 The classical boundary condition is $\mathbf{P}(a) = P_a\hat{\mathbf{r}}$ and the non classical boundary condition is $\mathbf{R}(a) = \mathbf{0}$

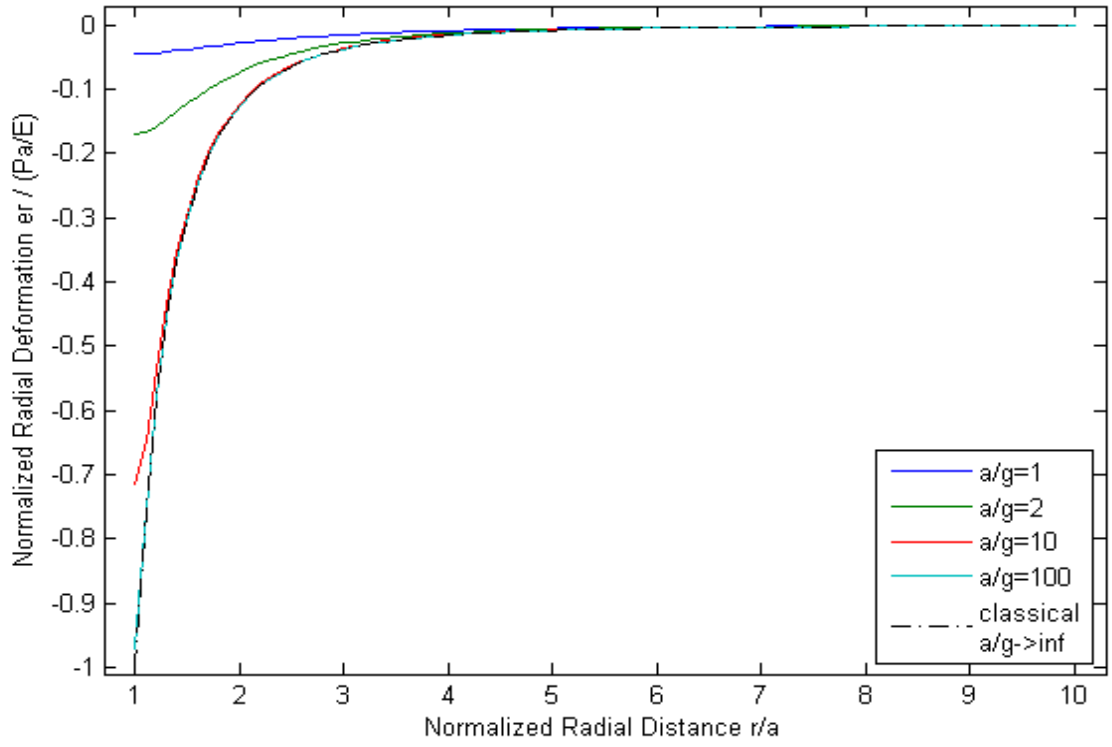

Fig. 29 Normalized radial deformation $e_r/(P_a/E)$ versus normalized radial distance r/a of a spherical cavity of radius a, for various ratios a/g, for any radius a, for a materials poisson ratio v=0.00. The classical boundary condition is $\mathbf{P}(a) = P_a\hat{\mathbf{r}}$ and the non classical boundary condition is $\mathbf{R}(a) = \mathbf{0}$

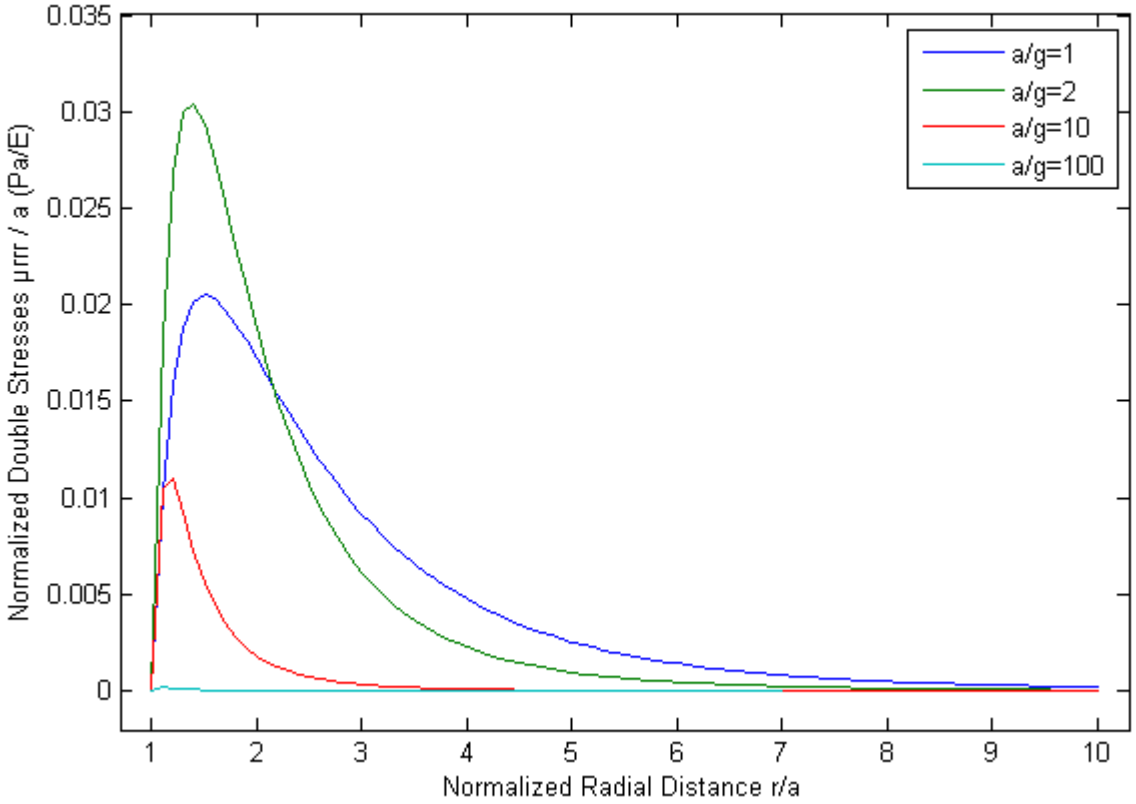

Fig. 30 Normalized double stresses $\mu_{rrr}/a(P_a/E)$ versus normalized radial distance r/a of a spherical cavity of radius a, for various ratios a/g, for any radius a, for a materials poisson ratio ν=0.00. The classical boundary condition is $\mathbf{P}(a) = P_a\hat{\mathbf{r}}$ and the non classical boundary condition is $\mathbf{R}(a) = \mathbf{0}$

When normalizing the fields in this problem, exactly like in the case of the solid sphere, the Poisson's ratio could not be eliminated, so different plots are been given for typical poisson ratio values. Above the cavities behavior is presented in the case that ν=0, and the case that ν=0,3 is presented next.

It should be noted that the cavilty's behavior is stiffer, when the material is gradient elastic, meaning that smaller displacements and deformations are anticipated, than the ones the classical theory describes. In the case that the c=a/g ratio is relatively small, especially when it is close to unity, this behavior is considerably stiffer. Furthermore, double stresses appear to the material even when no doublestresses are applied at the cavitys surface, which are smaller in range as the c ratio increases.

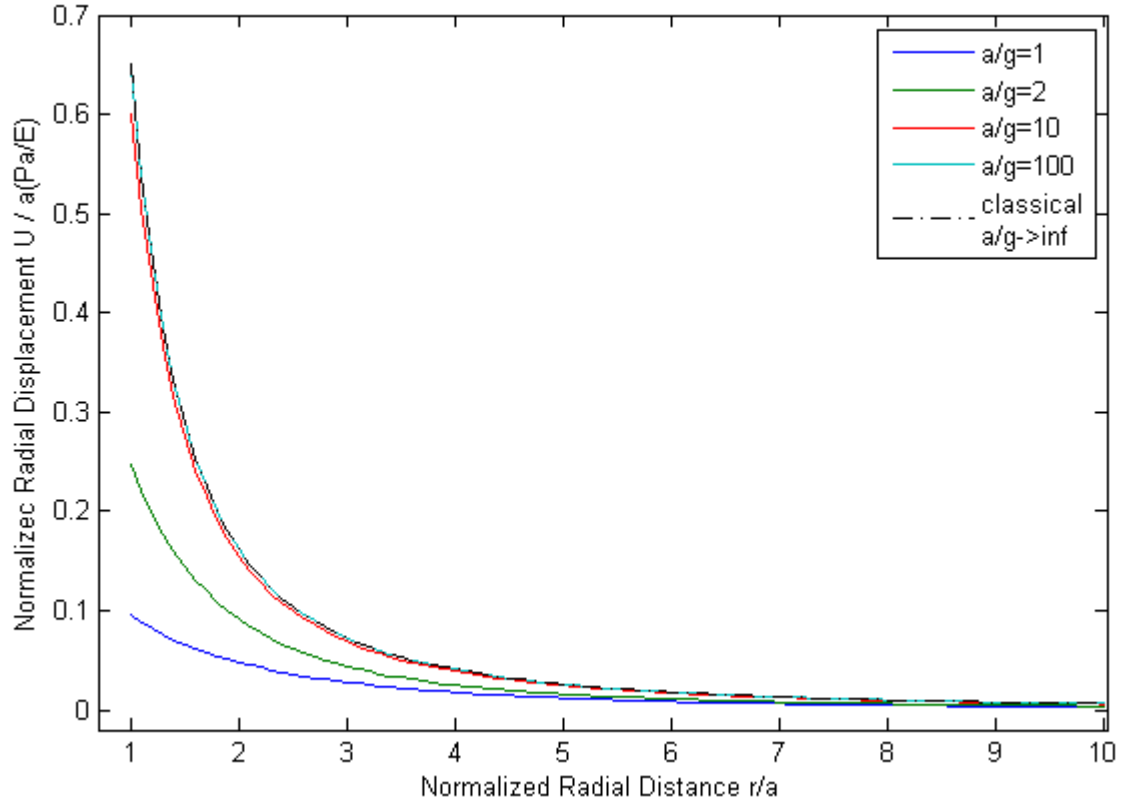

Fig. 31 Normalized radial displacement $u_r/a(P_a/E)$ versus normalized radial distance r/a of a spherical cavity of radius a, for various ratios a/g, for any radius a, for a materials poisson ratio n=0.30. The classical boundary condition is $\mathbf{P}(a) = P_a\hat{\mathbf{r}}$ and the non classical boundary condition is $\mathbf{R}(a) = \mathbf{0}$

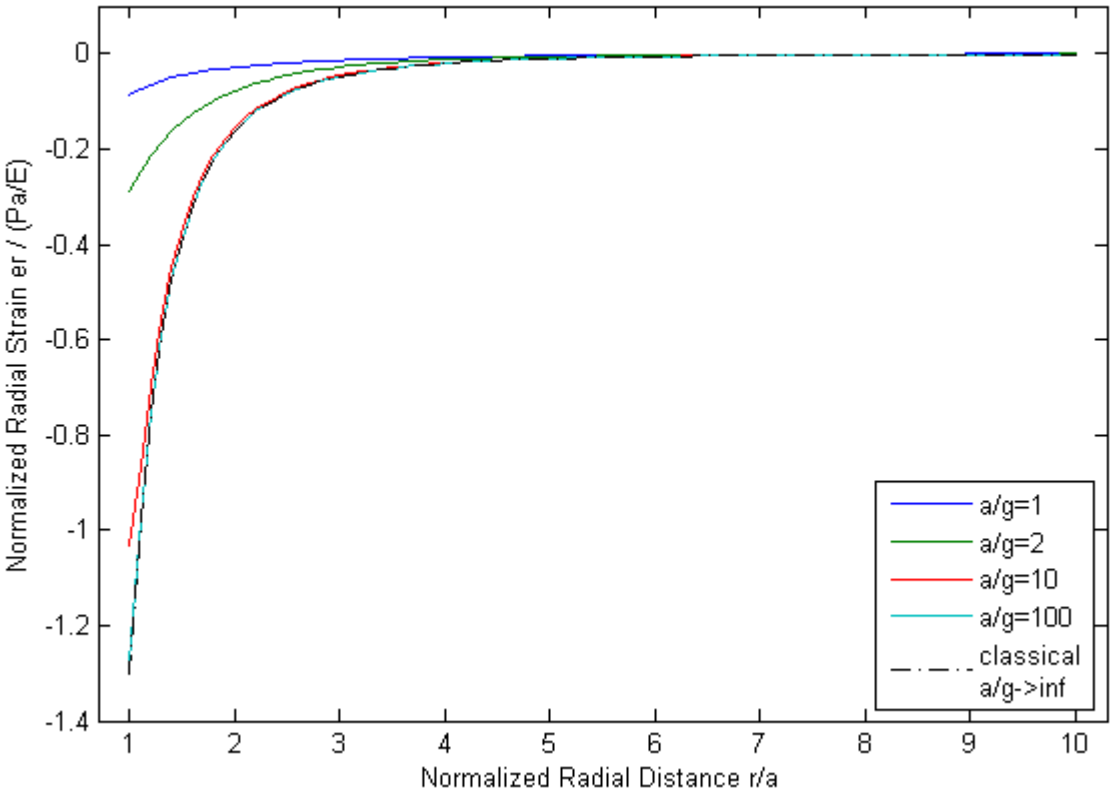

Fig. 32 Normalized radial strain $e_r/(P_a/E)$ versus normalized radial distance r/a of a spherical cavity of radius a, for various ratios a/g, for any radius a, for a materials poisson ratio v=0.30. The classical boundary condition is $\mathbf{P}(a) = P_a\hat{\mathbf{r}}$ and the non classical boundary condition is $\mathbf{R}(a) = \mathbf{0}$

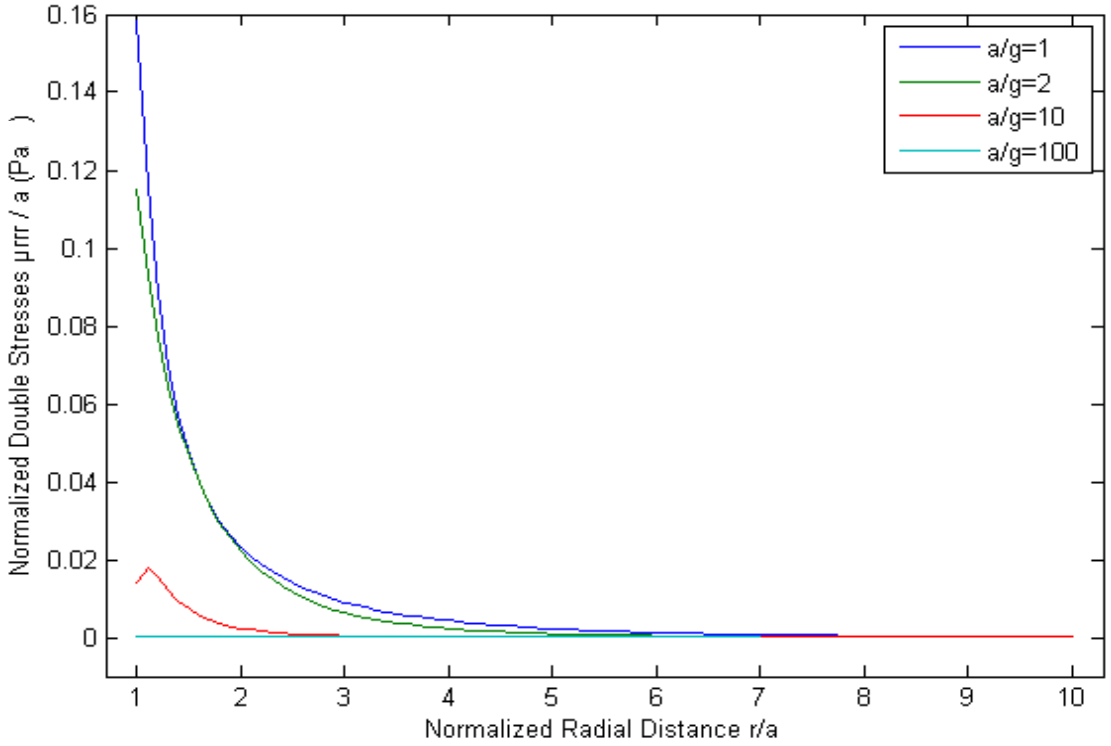

Fig. 33 Normalized double stresses μ_{rrr}/aP_a versus normalized radial distance r/a of a spherical cavity of radius a, for various ratios a/g, for any radius a, for a materials poisson ratio v=0.30. The classical boundary condition is $\mathbf{P}(a) = P_a\hat{\mathbf{r}}$ and the non classical boundary condition is $\mathbf{R}(a) = \mathbf{0}$

A very interesting remark on the double stresses is that in the case in which the poisson ratio is not zero the radial double stresses at the cavities surface are not zero, no matter the fact that the total double stresses R are zero. This can be attributed to the fact that due to the poisson ratio the non radial deformation and its work conjugate non radial double stresses contribute to the total double stress, so imposing the surface double stresses are zero does not mean that the radial ones that are plotted above are imposed to be zero. About the diplacement and deformation fields, the same observation as in the case can be made.

The following figures depict the cavity's behavior when only double stresses are applied to its surface and no pressure.

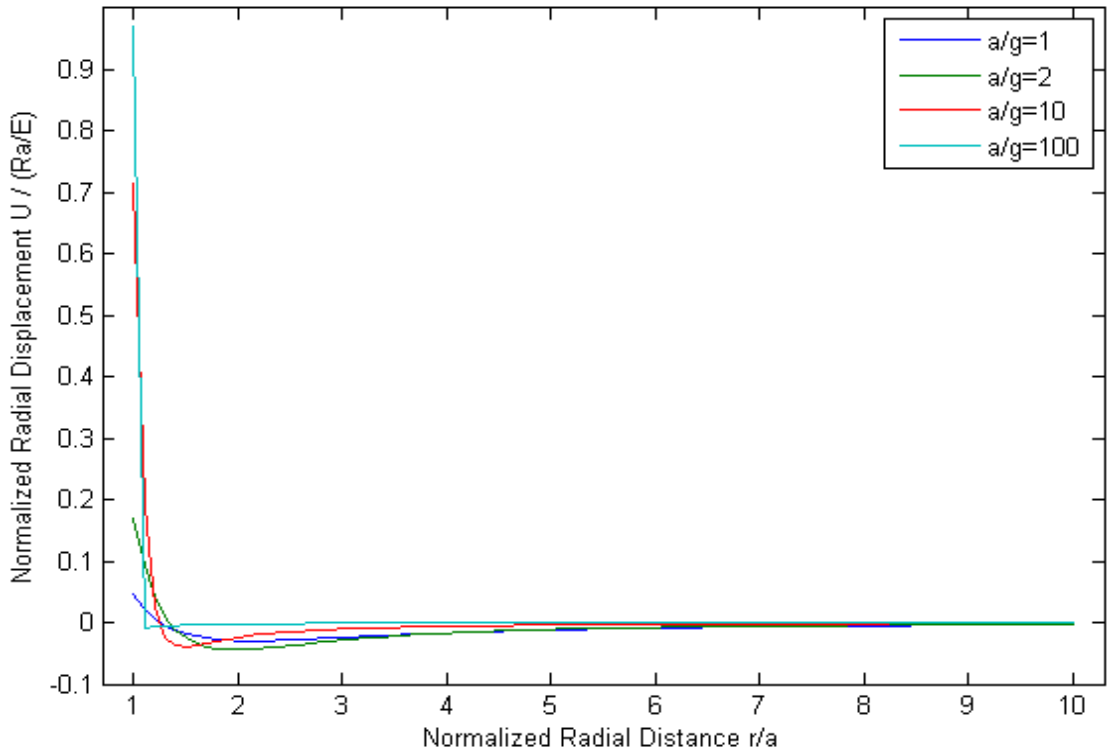

Fig. 34 Normalized radial displacement $u_r/(R_a/E)$ versus normalized radial distance r/a of a spherical cavity of radius a, for various ratios a/g, for any radius a, for a materials poisson ratio n=0.00. The classical boundary condition is $\mathbf{P}(a)=\mathbf{0}$ and the non classical boundary condition is $\mathbf{R}(a)=R_a\hat{\mathbf{r}}$

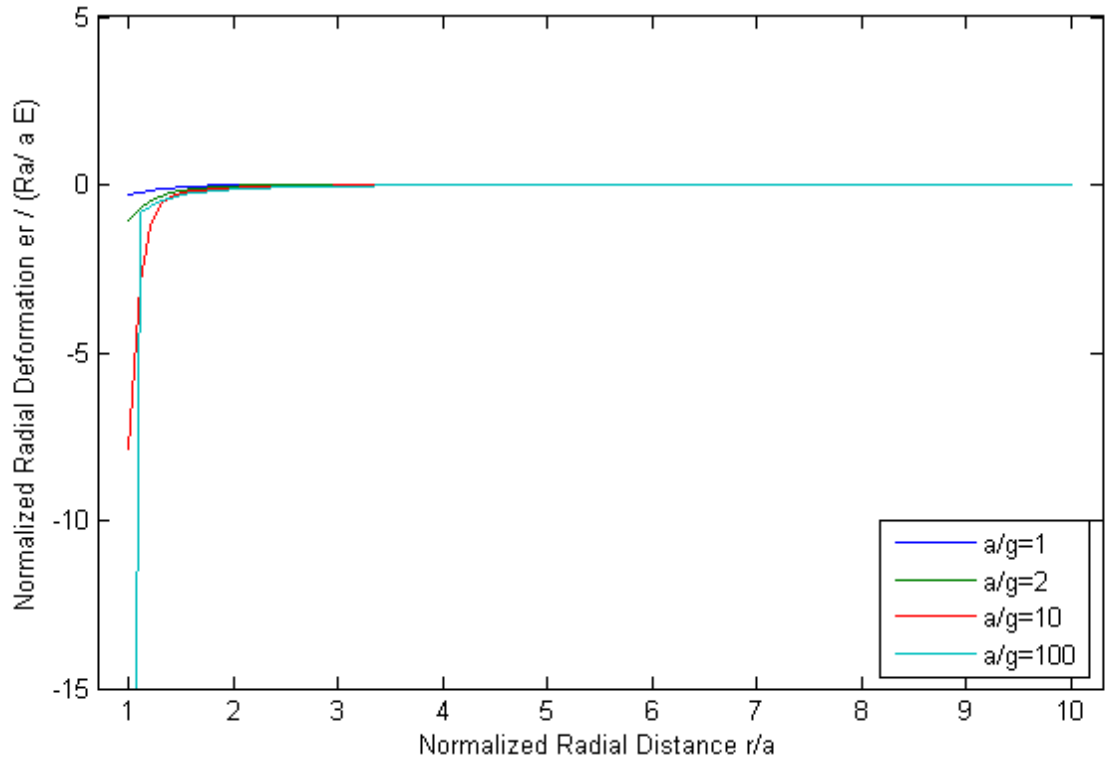

Fig. 35 Normalized radial deformation $u_r/(R_a/aE)$ versus normalized radial distance r/a of a spherical cavity of radius a, for various ratios a/g, for any radius a, for a materials poisson ratio n=0.00. The classical boundary condition is $\mathbf{P}(a)=\mathbf{0}$ and the non classical boundary condition is $\mathbf{R}(a)=R_a\hat{\mathbf{r}}$

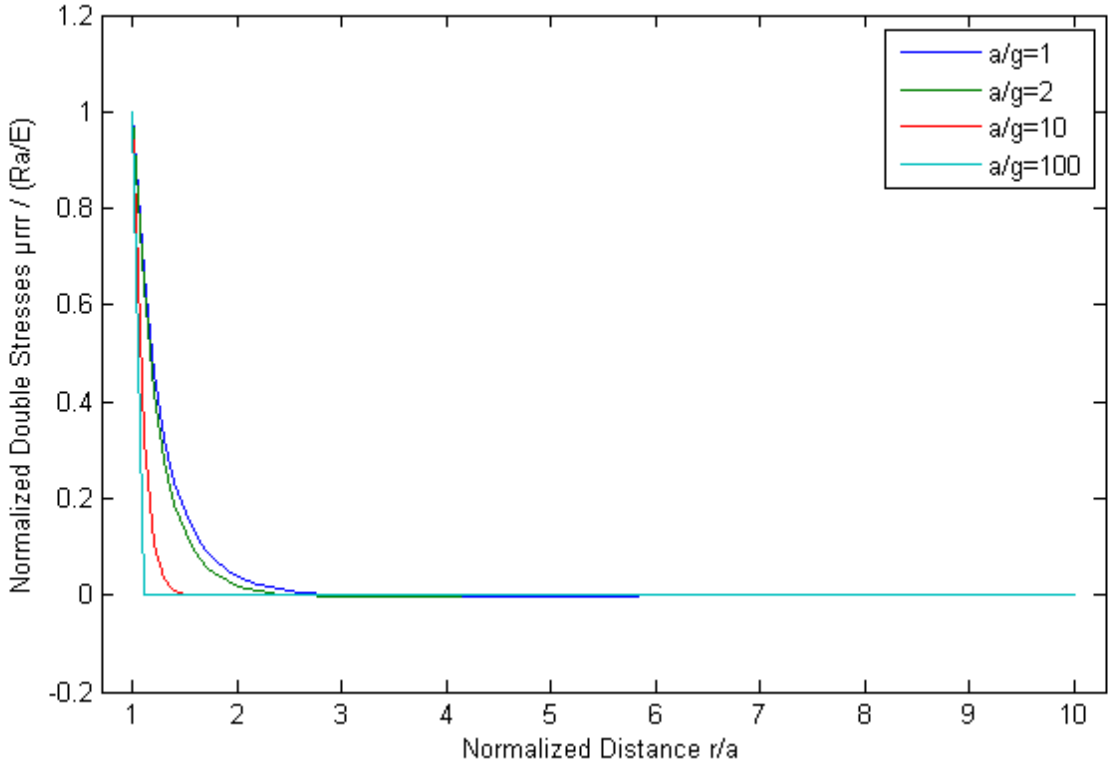

Fig. 36 Normalized double stresses $\mu_{rrr}/(R_a / E)$ versus normalized radial distance r/a of a spherical cavity of radius a, for various ratios a/g, for any radius a, for a materials poisson ratio n=0.00. The classical boundary condition is $\mathbf{P}(a) = \mathbf{0}$ and the non classical boundary condition is $\mathbf{R}(a) = R_a \hat{\mathbf{r}}$

As pictured above, even to this non classical BC, the materials behavior is stiffer when the c=a/g ratio gets smaller, and when it approaches unity, this difference is significant. Also, in the graph above, the local character of the double stresses is depicted. It is shown that the double stresses are present and significant only near the body's boundary and vanish gradually when moving away from it.

Next, the cavity's behavior is displayed when the poisson ratio is ν=0,30, in which case the same conclusion can be drawn.

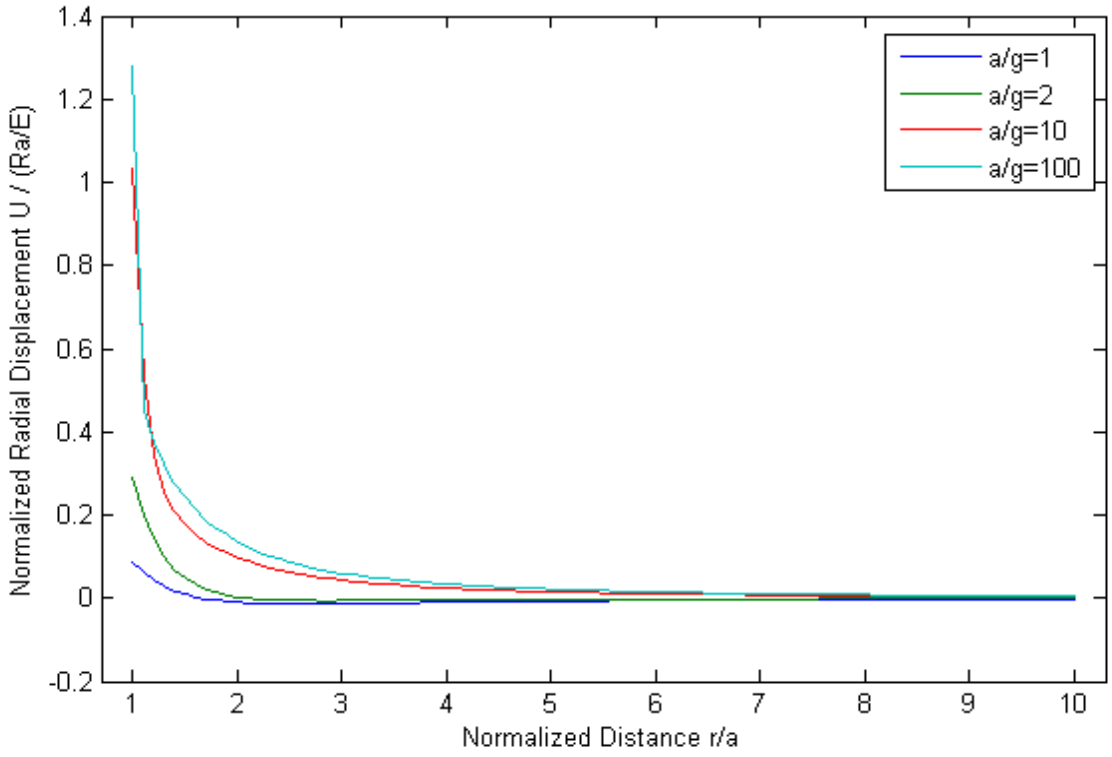

Fig. 37 Normalized radial displacement $u_r/(R_a/E)$ versus normalized radial distance r/a of a spherical cavity of radius a, for various ratios a/g, for any radius a, for a materials poisson ratio n=0.30. The classical boundary condition is $\mathbf{P}(a)=\mathbf{0}$ and the non classical boundary condition is $\mathbf{R}(a)=R_a\hat{\mathbf{r}}$

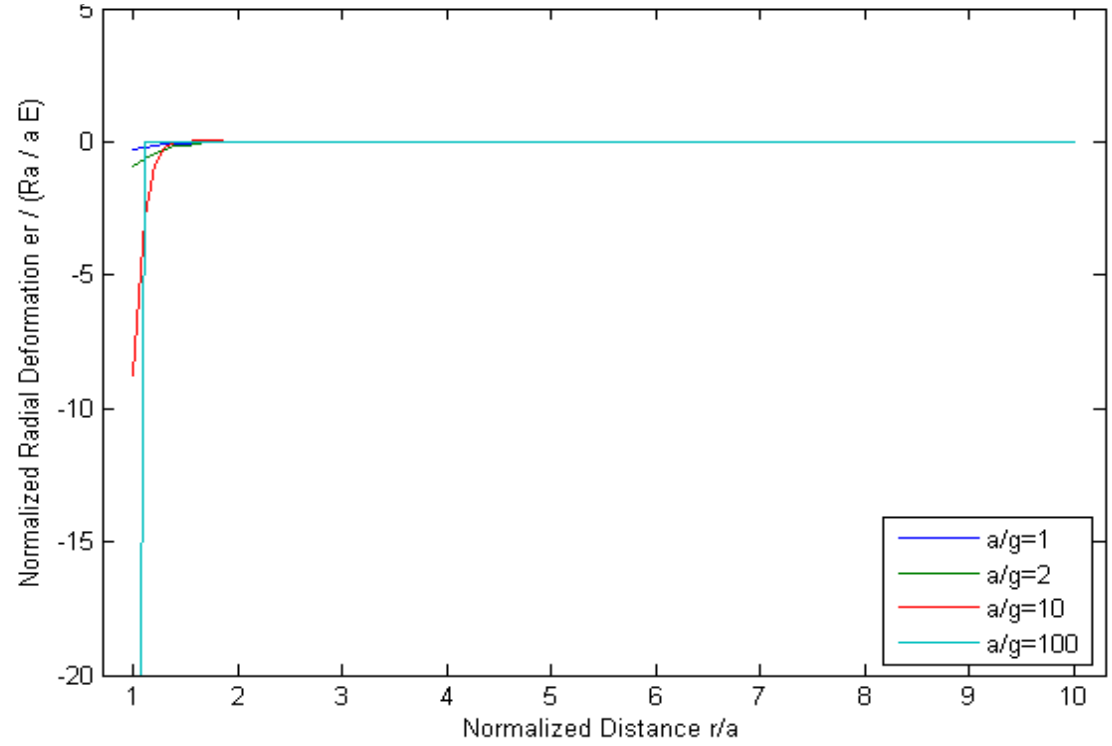

Fig. 38 Normalized radial deformation $\mathrm{e_r}/(\mathrm{R_a}/\mathrm{aE})$ versus normalized radial distance r/a of a spherical cavity of radius a, for various ratios a/g, for any radius a, for a materials poisson ratio n=0.30. The classical boundary condition is $\mathbf{P}(a)=\mathbf{0}$ and the non classical boundary condition is $\mathbf{R}(a)=R_a\hat{\mathbf{r}}$

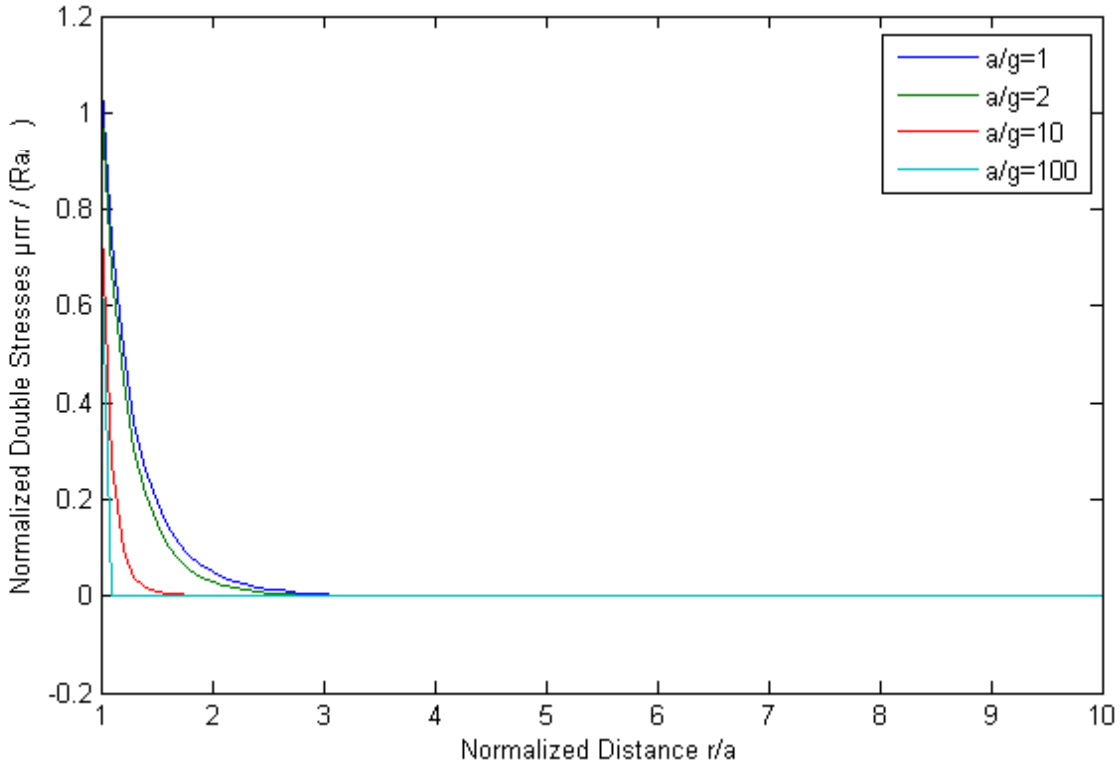

Fig. 39 Normalized radial double stresses μ_{rr}/R_a versus normalized radial distance r/a of a spherical cavity of radius a, for various ratios a/g, for any radius a, for a materials poisson ratio n=0.30. The classical boundary condition is $\mathbf{P}(a)=\mathbf{0}$ and the non classical boundary condition is $\mathbf{R}(a)=R_a\hat{\mathbf{r}}$

Any other case of loading, i.e. the cases that at the boundary one degree of freedom and one generalized force are prescribed can be addressed by converting the one BC to the other kind using the relations that follow. The new problem will be one of the cases above, and has already been studied.

$$\begin{bmatrix} U_a \\ q_a \end{bmatrix} = \frac{1}{4\mu T}\begin{bmatrix} aT_{11} & T_{12} \\ T_{21} & T_{22}/a \end{bmatrix}.\begin{bmatrix} P_a \\ R_a \end{bmatrix}$$

$$T = (2\mu+\lambda)c^3 + (6\mu+\lambda)c^2 + 9(2\mu+\lambda)c + 9(2\mu+\lambda)$$

$$T_{11} = (2\mu+\lambda)c^3 + (6\mu+\lambda)c^2$$

$$T_{12} = 2(2\mu+\lambda)c^3 + 2\lambda c^2$$

$$T_{21} = -2(2\mu+\lambda)c^3 - 2\lambda c^2 = -T_{12}$$

$$T_{22} = -4\mu c^4 - 4(2\mu+\lambda)c^3 - 4(3\mu+\lambda)c^2$$

4.I.3.iii. The Spherical Shell

Consider a spherical shell consisting of a solid sphere of radius b and a concentric spherical cavity of radius a. Let S_a be the internal and S_b the outer surface of the shell.

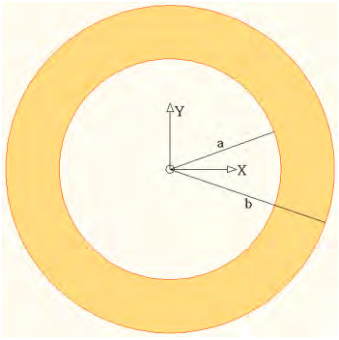

Fig. 40 Schematic representation of a spherical shell x-y section

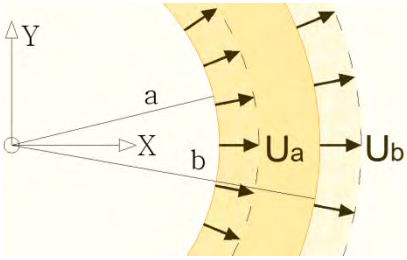

Fig. 41 x-y plane section of the shell. The boundary conditions are $\mathbf{u}(a) = U_a\hat{\mathbf{r}}$ **and** $\mathbf{u}(b) = U_b\hat{\mathbf{r}}$

1a)Classical theory

In the first problem both surfaces are subjected to radial displacements U_a and U_b on S_a and S_b respectively (classical BCs), i.e

$$\mathbf{u}(r)\big|_{r=a} = U_a\hat{\mathbf{r}}, \qquad \mathbf{u}(r)\big|_{r=b} = U_b\hat{\mathbf{r}}$$

$$\begin{bmatrix}\rho(a)\\ \rho(b)\end{bmatrix}\cdot\begin{bmatrix}C_1\\ C_2\end{bmatrix} = \begin{bmatrix}U_a\\ U_b\end{bmatrix} \Leftrightarrow \begin{bmatrix}C_1\\ C_2\end{bmatrix} = \begin{bmatrix}\rho(a)\\ \rho(b)\end{bmatrix}^{-1}\cdot\begin{bmatrix}U_a\\ U_b\end{bmatrix} \Leftrightarrow \mathbf{C} = \mathbf{M}^{-1}\cdot\mathbf{D}$$

$$u_r(r) = [\rho(r)]\cdot\mathbf{C} = \begin{bmatrix}\rho_1(r)\\ \rho_3(r)\end{bmatrix}^T\begin{bmatrix}C_1\\ C_2\end{bmatrix} = \left\{\frac{\begin{vmatrix}\rho(r)\\ \rho(b)\end{vmatrix}U_a - \begin{vmatrix}\rho(r)\\ \rho(a)\end{vmatrix}U_b}{\begin{vmatrix}\rho(a)\\ \rho(b)\end{vmatrix}}\right\}$$

$$= \left\{\left[\frac{a^2U_a - b^2U_b}{a^3 - b^3}\right]r + \left[\frac{-a^2b^3U_a + a^3b^2U_b}{a^3 - b^3}\right]\frac{1}{r^2}\right\}$$

Note that in the equations above, the $[\rho(r)]$ function denotes a horizontal vector, with elements the two fundamental solutions of classical elasticity spherical problem. This symbolism is used in order to optimize the presentation of the results.

The matrix $\mathbf{M}$ is singular only when the two boundaries coincide, i.e. the inner and the outer radius of the shell tend to be the same b→a, which is the case of the thin walled spherical shell. In this case the singularity can be eliminated by using a first order Taylor expansions of the displacement functions, i.e. $\rho_i(b) = \rho_i(a) + T\rho'_i(a)$, $T = b - a$. Since b→a =>r→a, so the displacement takes the form $u_r(a) = 0$, which means that the solution collapses/crushes.

1b)Gradient Theory

In this problem both surfaces are subjected to radial displacements U_a and U_b on S_a and S_b respectively (classical BCs) while the normal displacement gradient at each boundary is prescribed, respectively q_a and q_b (non-classical BCs), i.e.

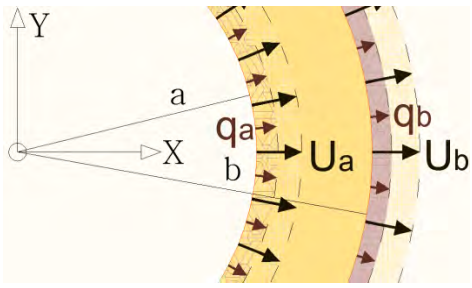

Fig. 42 x-y plane section of the shell. The boundary conditions are $\mathbf{u}(a) = U_a\hat{\mathbf{r}}$ $\mathbf{q}(a) = q_a\hat{\mathbf{r}}$, $\mathbf{u}(b) = U_b\hat{\mathbf{r}}$ **and** $\mathbf{q}(b) = q_b\hat{\mathbf{r}}$

$$\mathbf{u}(r)\big|_{r=a} = U_a\hat{\mathbf{r}}\ , \qquad \mathbf{u}(r)\big|_{r=b} = U_b\hat{\mathbf{r}}$$

$$\mathbf{q}(r)\big|_{r=a} = \frac{\partial \mathbf{u}(r)}{\partial \mathbf{n}}\bigg|_{r=a} = \frac{\partial \mathbf{u}(r)}{\partial -\hat{\mathbf{r}}}\bigg|_{r=a} = q_a\hat{\mathbf{r}}\,, \qquad \mathbf{q}(r)\big|_{r=b} = \frac{\partial \mathbf{u}(r)}{\partial \mathbf{n}}\bigg|_{r=b} = \frac{\partial \mathbf{u}(r)}{\partial \hat{\mathbf{r}}}\bigg|_{r=b} = q_b\hat{\mathbf{r}}$$

These BCs are translated to the following equation:

$$\begin{bmatrix} \rho(a) \\ -\rho'(a) \\ \rho(b) \\ \rho'(b) \end{bmatrix} \cdot \begin{bmatrix} C_1 \\ C_2 \\ C_3 \\ C_4 \end{bmatrix} = \begin{bmatrix} U_a \\ q_a \\ U_b \\ q_b \end{bmatrix} \Leftrightarrow \begin{bmatrix} C_1 \\ C_2 \\ C_3 \\ C_4 \end{bmatrix} = \begin{bmatrix} \rho(a) \\ -\rho'(a) \\ \rho(b) \\ \rho'(b) \end{bmatrix}^{-1} \cdot \begin{bmatrix} U_a \\ q_a \\ U_b \\ q_b \end{bmatrix} \Leftrightarrow \mathbf{C} = \mathbf{M}^{-1} \cdot \mathbf{D}$$

$$u_r(r) = \begin{bmatrix} \rho_1(r) \\ \rho_2(r) \\ \rho_3(r) \\ \rho_4(r) \end{bmatrix}^T \begin{bmatrix} C_1 \\ C_2 \\ C_3 \\ C_4 \end{bmatrix} \Leftrightarrow u_r = \left\{ \frac{\begin{vmatrix} \rho(r) \\ \rho'(a) \\ \rho(b) \\ \rho'(b) \end{vmatrix} U_a + \begin{vmatrix} \rho(r) \\ \rho(a) \\ \rho'(a) \\ \rho'(b) \end{vmatrix} U_b + \begin{vmatrix} \rho(r) \\ \rho(a) \\ \rho(b) \\ \rho'(b) \end{vmatrix} q_a - \begin{vmatrix} \rho(r) \\ \rho(a) \\ \rho'(a) \\ \rho(b) \end{vmatrix} q_b}{\begin{vmatrix} \rho(a) \\ \rho'(a) \\ \rho(b) \\ \rho'(b) \end{vmatrix}} \right\}$$

This time, the $[\rho(r)]$ function denotes a horizontal vector, with elements the four fundamental solutions of the spherical gradient problem.

It can be proved that this solution is reduced to the classical one when the microstructure is insignificant compared to the shells dimensions i.e. $a/g \to \infty$ or $b/g \to \infty$, hence, the solutions ability of being reduced to the classical one when the scales are great is not lost in this more complex problem.

The matrix **M** is singular only when the inner and the outer radius of the shell are very close to one another, i.e. the case of a thin walled spherical shell.

Let T=b-a be the shells thickness. The singularity can be eliminated using second order Taylor expansions of the displacement functions $\rho_i(b) = \rho_i(a) + T\rho_{i'}(a) + T^2\rho''_i(a)/2$ and its derivative $\rho'_i(b) = \rho'_i(a) + T\rho''_{i'}(a) + T^2\rho'''_i(a)/2$.

The displacement field then takes the following form:

$$u_r = \left\{ \frac{T\begin{vmatrix}\rho(r)\\ \rho'(a)\\ \rho(a)\\ \rho''(a)\end{vmatrix} U_a + T\begin{vmatrix}\rho(r)\\ \rho(a)\\ \rho'(a)\\ \rho'(b)\end{vmatrix} U_b + \frac{T^2}{2}\begin{vmatrix}\rho(r)\\ \rho(a)\\ \rho(b)\\ \rho'(b)\end{vmatrix} q_a - \frac{T^2}{2}\begin{vmatrix}\rho(r)\\ \rho(a)\\ \rho'(a)\\ \rho(b)\end{vmatrix} q_b}{\frac{T^4}{12}\begin{vmatrix}\rho(a)\\ \rho'(a)\\ \rho''(a)\\ \rho'''(a)\end{vmatrix}} \right\},$$

$$r \in [a, a+T] \cong a \Rightarrow ur = u_r = 0$$

So the gradient solution crushes, too, exactly the classical one does. This may be interpreted physically as: on a thin walled spherical shell both boundaries are practically one thus different displacement cannot be imposed on them without the body getting destroyed/failing.

2a) Classical Theory

In this problem the surface Sa is subjected to radial displacements U_a while on the surface S_b a tensile stress P_b is applied, i.e.

$$\mathbf{u}(r)\big|_{r=a} = U_a\hat{\mathbf{r}}, \qquad \mathbf{P}(r)\big|_{r=b} = P_b\hat{\mathbf{r}}$$

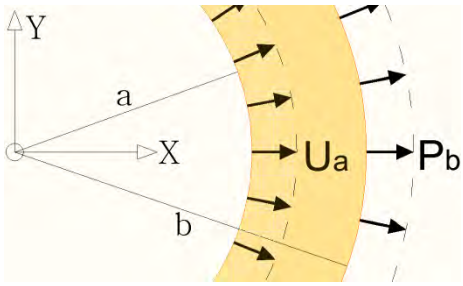

Fig. 43 x-y plane section of the shell. The boundary conditions are $\mathbf{u}(a) = U_a\hat{\mathbf{r}}$ and $\mathbf{P}(b) = P_b\hat{\mathbf{r}}$

$$u_r(r) = \left\{ \frac{\begin{vmatrix} \rho(r) & U_a \\ P(b) & \end{vmatrix} - \begin{vmatrix} \rho(r) & P_b \\ \rho(a) & \end{vmatrix}}{\begin{vmatrix} \rho(a) & \\ P(b) & \end{vmatrix}} \right\}$$

$$= \left\{ \left[\frac{4\mu a^2 U_a + b^3 P_b}{4\mu a^3 + (2\mu+3\lambda)b^3} \right] r + \left[\frac{(2\mu+3\lambda)a^2 b^3 U_a - a^3 b^3 P_b}{4\mu a^3 + (2\mu+3\lambda)b^3} \right] \frac{1}{r^2} \right\}$$

In the case of a thin walled spherical shell, of thickness T=b-a the problem doesn't become singular and the solution gets very simple, $\mathbf{u} = u_r\hat{\mathbf{r}} = U_a\hat{\mathbf{r}}$, $\mathbf{P} = P_b\hat{\mathbf{r}}$, this thought doesn't mean that any displacement U_a can be subjected by applying any stress P_a. The relation between them must be prefixed and it is obtained through problem 4. Thus, this is not a problem of great practical interest.

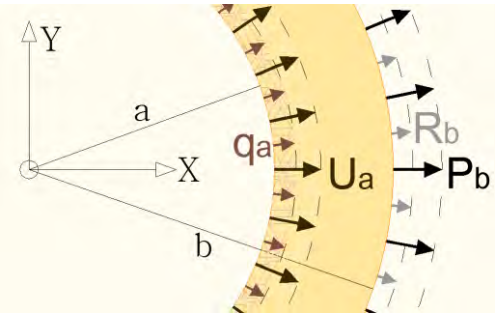

Fig. 44 x-y plane section of the shell. The boundary conditions are $\mathbf{u}(a) = U_a\hat{\mathbf{r}}$ $\mathbf{q}(a) = q_a\hat{\mathbf{r}}$, $\mathbf{P}(b) = P_b\hat{\mathbf{r}}$ and $\mathbf{R}(b) = R_b\hat{\mathbf{r}}$

2b)Gradient Theory

In the respective gradient elasticity problem the surface Sa is subjected to radial displacements U_a (classical BC) while the normal displacement gradient on boundary is predetermined q_a (non-classical BC) and on the surface S_b a tensile stress P_b (classical BC) and surface double stresses R_b (non-classical BC) are applied, i.e.

$$\mathbf{u}(r)\big|_{r=a} = U_a\hat{\mathbf{r}}, \qquad \mathbf{P}(r)\big|_{r=b} = P_b\hat{\mathbf{r}}$$

$$\mathbf{q}(r)\big|_{r=a} = \frac{\partial \mathbf{u}(r)}{\partial -\hat{\mathbf{r}}}\bigg|_{r=a} = q_a\hat{\mathbf{r}}, \qquad \mathbf{R}(r)\big|_{r=b} = R_b\hat{\mathbf{r}}$$

The displacement field takes the following form:

$$u_r(r)=\begin{bmatrix}\rho_1(r)\\ \rho_2(r)\\ \rho_3(r)\\ \rho_4(r)\end{bmatrix}^T\begin{bmatrix}C_1\\ C_2\\ C_3\\ C_4\end{bmatrix}\Leftrightarrow u_r=\left\{\frac{\begin{vmatrix}\rho(r)\\ \rho'(a)\\ P(b)\\ R(b)\end{vmatrix}U_a+\begin{vmatrix}\rho(r)\\ \rho(a)\\ \rho'(a)\\ R(b)\end{vmatrix}P_b+\begin{vmatrix}\rho(r)\\ \rho(a)\\ \rho(b)\\ R(b)\end{vmatrix}q_a-\begin{vmatrix}\rho(r)\\ \rho(a)\\ \rho'(a)\\ P(b)\end{vmatrix}R_b}{\begin{vmatrix}\rho(a)\\ \rho'(a)\\ P(b)\\ R(b)\end{vmatrix}}\right\}$$

When the microstructure becomes insignificant i.e a/g$\rightarrow\infty$ the solution is reduced to the one obtained using the classical theory. This solution is never singular not even in the case that b$\rightarrow$a, the case of a thin walled spherical shell. In that case the solution is simplified to:

$$\mathbf{u}=u_r\hat{\mathbf{r}}=U_a\hat{\mathbf{r}},\mathbf{q}=q_a\hat{\mathbf{r}},\mathbf{P}=P_b\hat{\mathbf{r}},\mathbf{R}=R_b\hat{\mathbf{r}}$$

This, too, is a solution of no practical interest, thought, one can deduce that the displacement and its normal surface gradient of a thin walled spherical shell are approximately uniform throughout its body. Also the external load Pa needs to be the total external load from both surfaces, and this is a result of the small shell's thickness, due to which we cannot be precise about where exactly the external loads are applied. The same remark applies on the surface double stresses. Once again, the displacement and its normal gradient cannot be independent of the external loads Pa and Ra, so this solution isn't very useful, since it doesn't present this relation.

The next problem to be studied is the symmetrical of this one, meaning that the BCs applied at each boundary of the shell are applied in the other one in that problem.

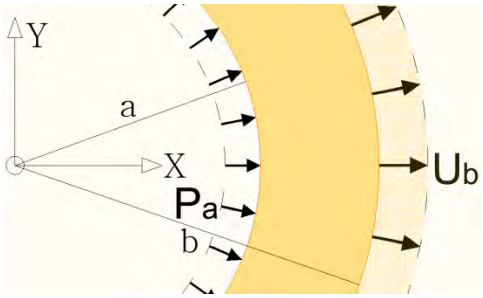

Fig. 45 x-y plane section of the shell. The boundary conditions are $\mathbf{P}(a)=P_a\hat{\mathbf{r}}$ **and** $\mathbf{u}(b)=U_b\hat{\mathbf{r}}$

3a) Classical Theory

In this problem on the surface S_a a compressive stress-pressure P_a is applied, while the surface S_b is subjected to radial displacement U_b, i.e.

$$\mathbf{P}(r)\big|_{r=a}=P_a\hat{\mathbf{r}} \text{ and}$$

$$\mathbf{u}(r)\big|_{r=b}=U_b\hat{\mathbf{r}},$$

$$u_r(r)=\left\{\frac{\begin{vmatrix}\rho(r)\\ \rho(b)\end{vmatrix}P_a-\begin{vmatrix}\rho(r)\\ P(a)\end{vmatrix}U_b}{\begin{vmatrix}P(a)\\ \rho(b)\end{vmatrix}}\right\}=\left\{\left[\frac{-a^3P_a+4\mu b^2U_b}{4\mu b^3+(2\mu+3\lambda)a^3}\right]r+\left[\frac{a^3b^3P_a+(2\mu+3\lambda)a^3b^2U_b}{4\mu b^3+(2\mu+3\lambda)a^3}\right]\frac{1}{r^2}\right\}$$

In the case of a thin walled spherical shell, of thickness T=b-a the problem doesn't become singular and the solution gets very simple exactly like in problem 2. No new interesting conclusion about this solution can be drawn. $\mathbf{u}=u_r\hat{\mathbf{r}}=U_b\hat{\mathbf{r}}$, $\mathbf{P}=P_a\hat{\mathbf{r}}$

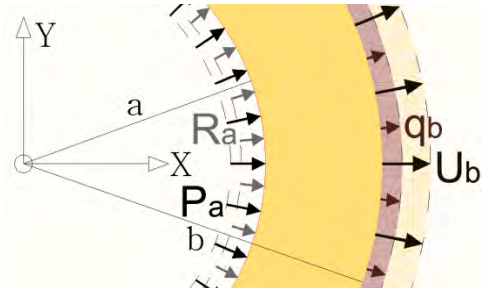

Fig. 46 x-y plane section of the shell. The boundary conditions are $\mathbf{P}(a)=P_a\hat{\mathbf{r}}$, $\mathbf{R}(a)=R_a\hat{\mathbf{r}}$, $\mathbf{u}(b)=U_b\hat{\mathbf{r}}$ **and** $\mathbf{q}(b)=q_b\hat{\mathbf{r}}$

3b) Gradient theory

In this gradient problem on the surface S_a a compressive stress/pressure P_a (classical BC) and surface double stresses R_a (non-classical BC) are applied, while the surface S_b is subjected to radial displacement U_b (classical BC) and the normal displacement gradient on boundary is q_b (BC) , i.e.

$$\mathbf{P}(r)\big|_{r=a}=P_a\hat{\mathbf{r}} \quad , \quad \mathbf{u}(r)\big|_{r=b}=U_b\hat{\mathbf{r}}$$

$$\mathbf{R}(r)\big|_{r=a}=R_a\hat{\mathbf{r}} \quad , \quad \mathbf{q}(r)\big|_{r=b}=\frac{\partial\mathbf{u}(r)}{\partial\mathbf{n}}\bigg|_{r=b}=\frac{\partial\mathbf{u}(r)}{\partial\hat{\mathbf{r}}}\bigg|_{r=b}=q_b\hat{\mathbf{r}} \quad ,$$

Thus the displacement field is:

$$u_r(r)=\begin{bmatrix}\rho_1(r)\\ \rho_2(r)\\ \rho_3(r)\\ \rho_4(r)\end{bmatrix}^T\begin{bmatrix}C_1\\ C_2\\ C_3\\ C_4\end{bmatrix}\Leftrightarrow u_r=\left\{\frac{-\begin{vmatrix}\rho(r)\\ R(a)\\ \rho(b)\\ \rho'(b)\end{vmatrix}P_a+\begin{vmatrix}\rho(r)\\ P(a)\\ R(a)\\ \rho'(b)\end{vmatrix}U_b-\begin{vmatrix}\rho(r)\\ P(a)\\ R(a)\\ \rho(b)\end{vmatrix}q_b-\begin{vmatrix}\rho(r)\\ P(a)\\ \rho(b)\\ \rho'(b)\end{vmatrix}R_a}{\begin{vmatrix}P(a)\\ R(a)\\ \rho(b)\\ \rho'(b)\end{vmatrix}}\right\}$$

and when the microstructure is insignificant i.e. $a/g\to\infty$, it is reduced to the field obtained using the classical theory.

In the case of a thin walled spherical shell, of thickness T=b-a the problem doesn't become singular and the solution gets very simple, but isn't very useful, i.e. $\mathbf{u}=u_r\hat{\mathbf{r}}=U_b\hat{\mathbf{r}}$, $\mathbf{q}=q_b\hat{\mathbf{r}}$, $\mathbf{P}=P_a\hat{\mathbf{r}}$, $\mathbf{R}=R_a\hat{\mathbf{r}}$, exactly like the previous problem. This solution is very similar to the solution of the second problem and the previous conclusions about the shell can be drawn from this case too.

The following problem is the one of the most interest and practical application.

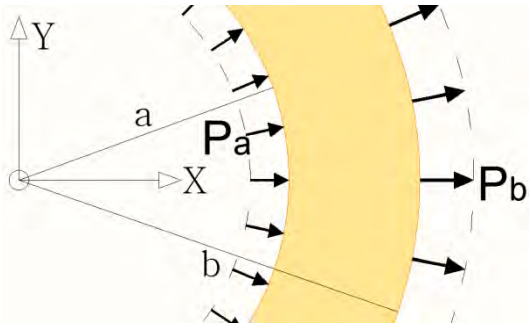

Fig. 47 x-y plane section of the shell. The boundary conditions are $\mathbf{P}(a)=P_a\hat{\mathbf{r}}$ and $\mathbf{P}(b)=P_b\hat{\mathbf{r}}$

4a)Classical theory

In this problem on the surfaces S_a to a compressive stress-pressure P_a is applied, while the surface S_b is subjected to a tensile stress, i.e.

$$\mathbf{P}(r)\big|_{r=a}=P_a\hat{\mathbf{r}},\qquad \mathbf{P}(r)\big|_{r=b}=P_b\hat{\mathbf{r}}$$

The displacement field is found to be the following:

$$u_r(r)=\left\{\frac{-\begin{vmatrix}\rho(r)\\ P(b)\end{vmatrix}P_a-\begin{vmatrix}\rho(r)\\ P(a)\end{vmatrix}P_b}{\begin{vmatrix}P(a)\\ P(b)\end{vmatrix}}\right\}=\left\{\left[\frac{-a^3P_a-b^3P_b}{(2\mu+3\lambda)(a^3-b^3)}\right]r+\left[\frac{-a^3b^3P_a-a^3b^3P_b}{4\mu(a^3-b^3)}\right]\frac{1}{r^2}\right\}$$

In the case of a thin walled spherical shell, of thickness T=b-a, the system becomes singular. Any singularity can be eliminated using first order Taylor expansions of the functions of the external radius, i.e. $P_i(b) = P_i(a) + TP'_{i'}(a)$. The displacement, deformation and curvature are:

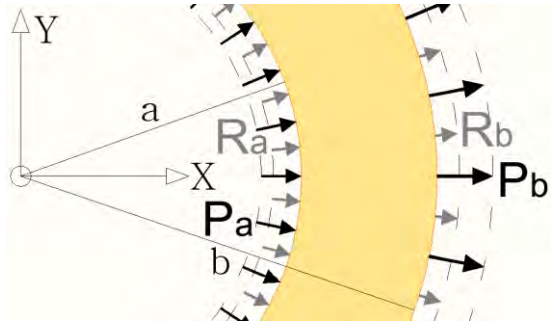

Fig. 48 x-y plane section of the shell. The boundary conditions are $\mathbf{P}(a) = P_a\hat{\mathbf{r}}$, $\mathbf{R}(a) = R_a\hat{\mathbf{r}}$, $\mathbf{P}(b) = P_b\hat{\mathbf{r}}$ **and** $\mathbf{R}(b) = R_b\hat{\mathbf{r}}$

$$u_r = \left\{ \frac{a^2}{T} \frac{(2\mu+\lambda)}{4\mu(2\mu+3\lambda)} (P_a + P_b) \right\}$$

$$u_r' = \left\{ -\frac{a}{T} \frac{\lambda}{2\mu(2\mu+3\lambda)} (P_a + P_b) \right\}$$

$$u_r'' = \left\{ \frac{1}{T} \frac{1}{2\mu} (P_a + P_b) \right\}$$

4b) Gradient theory

On the surfaces S_a of the shell a compressive stress-pressure P_a (classical BC) is applied and surface double stresses R_a (non-classical BC), while the surface S_b is subjected a tensile stress P_b (classical BC) and surface double stresses R_b (non-classical BC), i.e.

$$\mathbf{P}(\mathrm{r})\big|_{\mathrm{r=a}} = \mathrm{P_a}\hat{\mathbf{r}}\ , \qquad \mathbf{P}(\mathrm{r})\big|_{\mathrm{r=b}} = \mathrm{P_b}\hat{\mathbf{r}}$$

$$\mathbf{R}(\mathrm{r})\big|_{\mathrm{r=a}} = \mathrm{R_a}\hat{\mathbf{r}}, \qquad \mathbf{R}(\mathrm{r})\big|_{\mathrm{r=b}} = \mathrm{R_b}\hat{\mathbf{r}}$$

The solution takes the following form.

$$\mathrm{u_r(r)} = \begin{bmatrix} \rho_1(\mathrm{r}) \\ \rho_2(\mathrm{r}) \\ \rho_3(\mathrm{r}) \\ \rho_4(\mathrm{r}) \end{bmatrix}^{\mathrm{T}} \begin{bmatrix} \mathrm{C_1} \\ \mathrm{C_2} \\ \mathrm{C_3} \\ \mathrm{C_4} \end{bmatrix} \Leftrightarrow \mathrm{u_r} = \left\{ \frac{+\begin{vmatrix} \rho(\mathrm{r}) \\ \mathrm{R(a)} \\ \mathrm{P(b)} \\ \mathrm{R(b)} \end{vmatrix} \mathrm{P_a} - \begin{vmatrix} \rho(\mathrm{r}) \\ \mathrm{P(a)} \\ \mathrm{R(a)} \\ \mathrm{R(b)} \end{vmatrix} \mathrm{P_b} + \begin{vmatrix} \rho(\mathrm{r}) \\ \mathrm{P(a)} \\ \mathrm{P(b)} \\ \mathrm{R(b)} \end{vmatrix} \mathrm{R_a} + \begin{vmatrix} \rho(\mathrm{r}) \\ \mathrm{P(a)} \\ \mathrm{R(a)} \\ \mathrm{P(b)} \end{vmatrix} \mathrm{R_b}}{\begin{vmatrix} \mathrm{P(a)} \\ \mathrm{R(a)} \\ \mathrm{P(b)} \\ \mathrm{R(b)} \end{vmatrix}} \right\}$$

Note that this solution too, when the microstructure is insignificant, i.e. $a/g \to \infty$ is reduced to the classical one.

In the case of the thin walled spherical shell b→a, of thickness T=b-a, this solution becomes singular. The singularity is eliminated using first order Taylor expansions of the functions of the external radius, i.e. $P_i(b) = P_i(a) + TP'_{i'}(a)$, $R_i(b) = R_i(a) + TR'_{i'}(a)$

So the solution finally takes the following form:

$$u_r(r) = \begin{bmatrix} \rho_1(r) \\ \rho_2(r) \\ \rho_3(r) \\ \rho_4(r) \end{bmatrix}^T \begin{bmatrix} A \\ C \\ B \\ D \end{bmatrix} \Leftrightarrow u_r = \left\{ \frac{\begin{vmatrix} \rho(r) \\ P(a) \\ R(a) \\ R'(a) \end{vmatrix} (P_a + P_b) + \begin{vmatrix} \rho(r) \\ P(a) \\ P'(a) \\ R(a) \end{vmatrix} (R_b - R_a)}{T \begin{vmatrix} P(a) \\ P'(a) \\ R(a) \\ R'(a) \end{vmatrix}} \right\}, r \in [a, a+T] \cong a$$

This form of the solution can be derivated and any combination of the derivatives of u_r can be easily be obtained. That isn't the case with the following simplified forms of it, which thought are more lucid.

$$u_r = \frac{1}{4T} \frac{a^2}{(2\mu+3\lambda)} \left[\frac{4\mu(g/a)^2(6\mu+5\lambda) + (2\mu+\lambda)^2}{3\mu(g/a)^2(6\mu+5\lambda) + \mu(2\mu+\lambda)} \right] (P_a + P_b)$$

$$- \frac{1}{2T} \frac{a}{(2\mu+3\lambda)} \left[\frac{-2\mu(g/a)^2(6\mu+5\lambda) + \lambda(2\mu+\lambda)}{3\mu(g/a)^2(6\mu+5\lambda) + \mu(2\mu+\lambda)} \right] (R_b - R_a)$$

$$u_r' = -\frac{1}{2T} \frac{a}{(2\mu+3\lambda)} \left[\frac{-2\mu(g/a)^2(6\mu+5\lambda) + \lambda(2\mu+\lambda)}{3\mu(g/a)^2(6\mu+5\lambda) + \mu(2\mu+\lambda)} \right] (P_a + P_b)$$

$$+ \frac{1}{T} \frac{1}{(2\mu+3\lambda)} \left[\frac{\mu(g/a)^2(6\mu+5\lambda) + (2\mu+\lambda)(\mu+\lambda)}{3\mu(g/a)^2(6\mu+5\lambda) + \mu(2\mu+\lambda)} \right] (R_b - R_a)$$

$$u_r'' = \frac{1}{2T} \left[\frac{\lambda}{3\mu(g/a)^2(6\mu+5\lambda) + \mu(2\mu+\lambda)} \right] (P_a + P_b)$$

$$- \frac{1}{T} \frac{1}{a} \left[\frac{\lambda}{3\mu(g/a)^2(6\mu+5\lambda) + \mu(2\mu+\lambda)} \right] (R_b - R_a)$$

It comes with a surprise that when the ratio a/g→∞, both the displacement and the deformation functions are reduced to the respective

classical functions, while the higher order derivatives of the displacement don't.

In order to examine the effect of each BC to the displacement and deformation fields of this solution, the same procedure as before is followed. The problem is divided into two simpler, (i) one that the total applied stress is non zero while the surface double stresses at both surfaces are equal (i.e. $P_a + P_b \neq 0$ and $R_b - R_a = 0$) and (ii) one that the total applied stress is zero while the surface double stresses at both surfaces aren't equal (i.e. $P_a + P_b = 0$ while $R_b - R_a \neq 0$). Any problem can be addressed as a superposition of these two problems.

It is noted that for small c=a/g values, the displacement of the shell is considerably smaller than the respective classical one and great radial double stresses are anticipated for such values, with the greatest ones appearing in the materials that Poisson's ratio is the greatest. For great c values, both the displacement and deformation fields are reduced to the classical ones, while the double stresses tend to disappear.

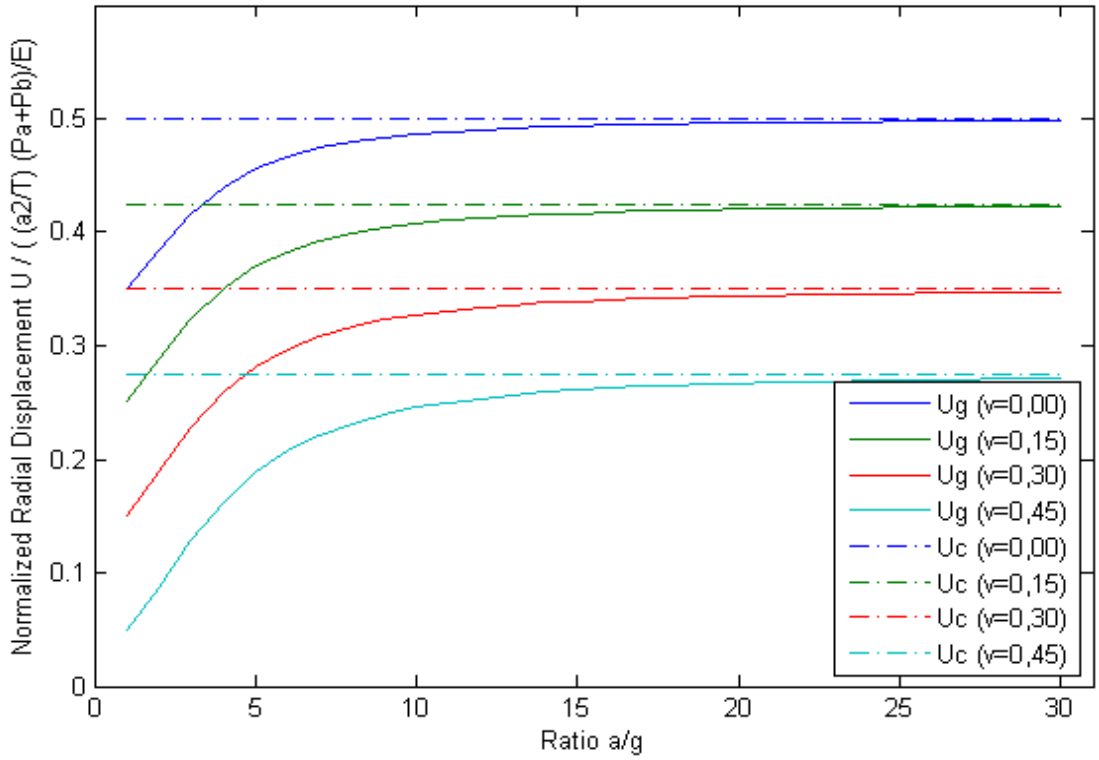

Fig. 49 Normalized radial displacement $u_r / \left(\left(a^2 / T \right) \left((P_a + P_b) / E \right) \right)$ **versus the ratio a/g for different values of the poisons ratio v. The classical boundary conditions are** $\mathbf{P}(a^-) = P_a \hat{\mathbf{r}}$ **and** $\mathbf{P}(a^+) = P_b \hat{\mathbf{r}}$ **and the non classical ones** $\mathbf{R}(a^-) = R_a \hat{\mathbf{r}}$ **and** $\mathbf{R}(a^+) = R_b \hat{\mathbf{r}}$ **with** $R_b - R_a = 0$

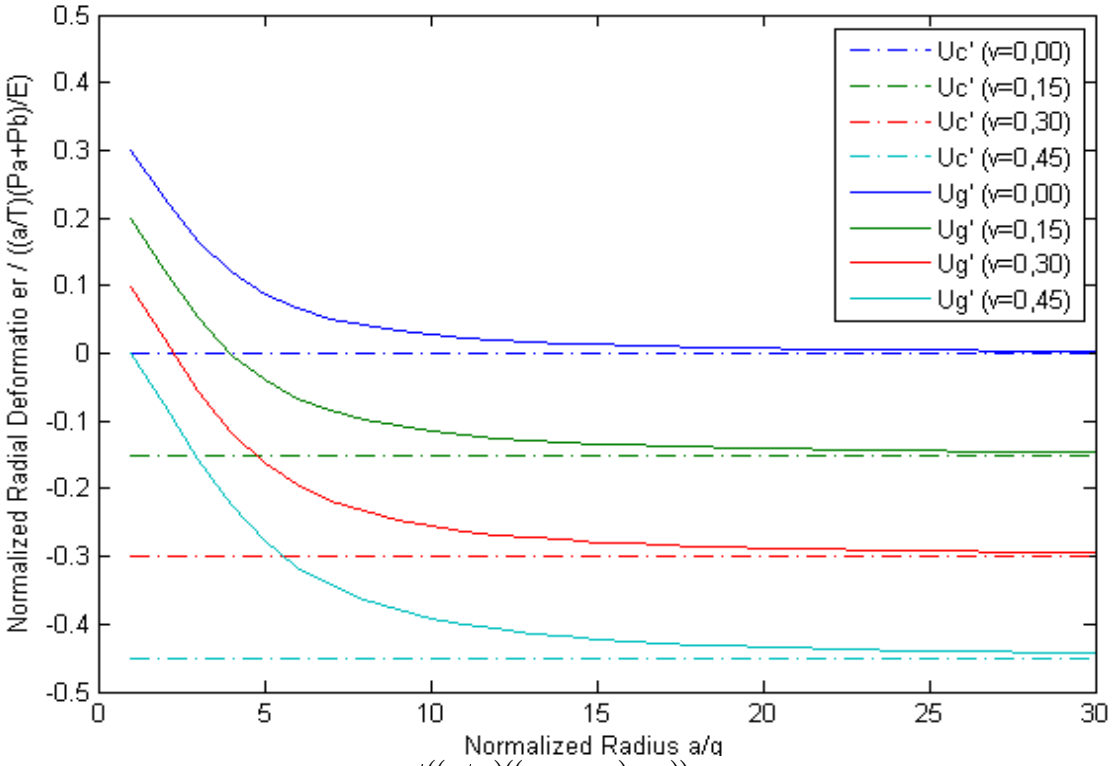

Fig. 50 Normalized radial deformation $e_r/\left((a/T)\left((P_a+P_b)/E\right)\right)$ **versus the ratio a/g for different values of the poisons ratio v. The classical boundary conditions are** $\mathbf{P}(a^-)=P_a\hat{\mathbf{r}}$ **and** $\mathbf{P}(a^+)=P_b\hat{\mathbf{r}}$ **and the non classical ones** $\mathbf{R}(a^-)=R_a\hat{\mathbf{r}}$ **and** $\mathbf{R}(a^+)=R_b\hat{\mathbf{r}}$ **with** $R_b-R_a=0$

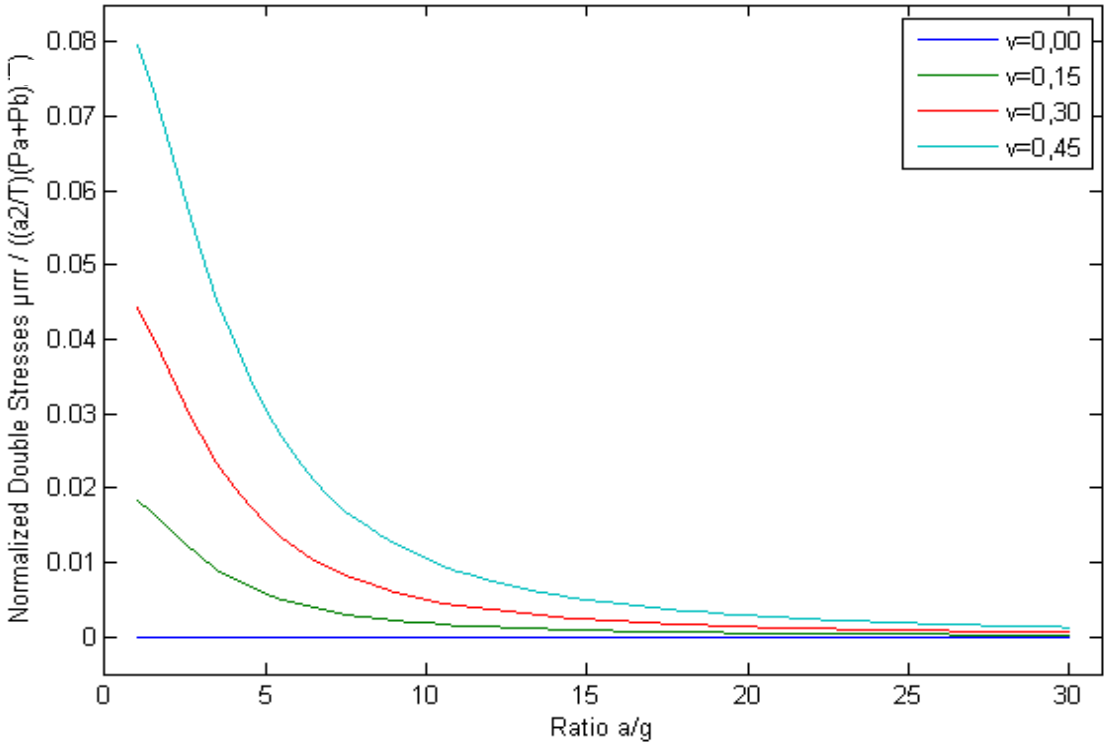

Fig. 51 Normalized double stresses $\mu_{rr}/\left(\left(a^2/T\right)\left(P_a+P_b\right)\right)$ **versus the ratio a/g for different values of the poisons ratio v. The classical boundary conditions are** $\mathbf{P}(a^-)=P_a\hat{\mathbf{r}}$ **and** $\mathbf{P}(a^+)=P_b\hat{\mathbf{r}}$ **and the non classical ones** $\mathbf{R}(a^-)=R_a\hat{\mathbf{r}}$ **and** $\mathbf{R}(a^+)=R_b\hat{\mathbf{r}}$ **with** $R_b-R_a=0$

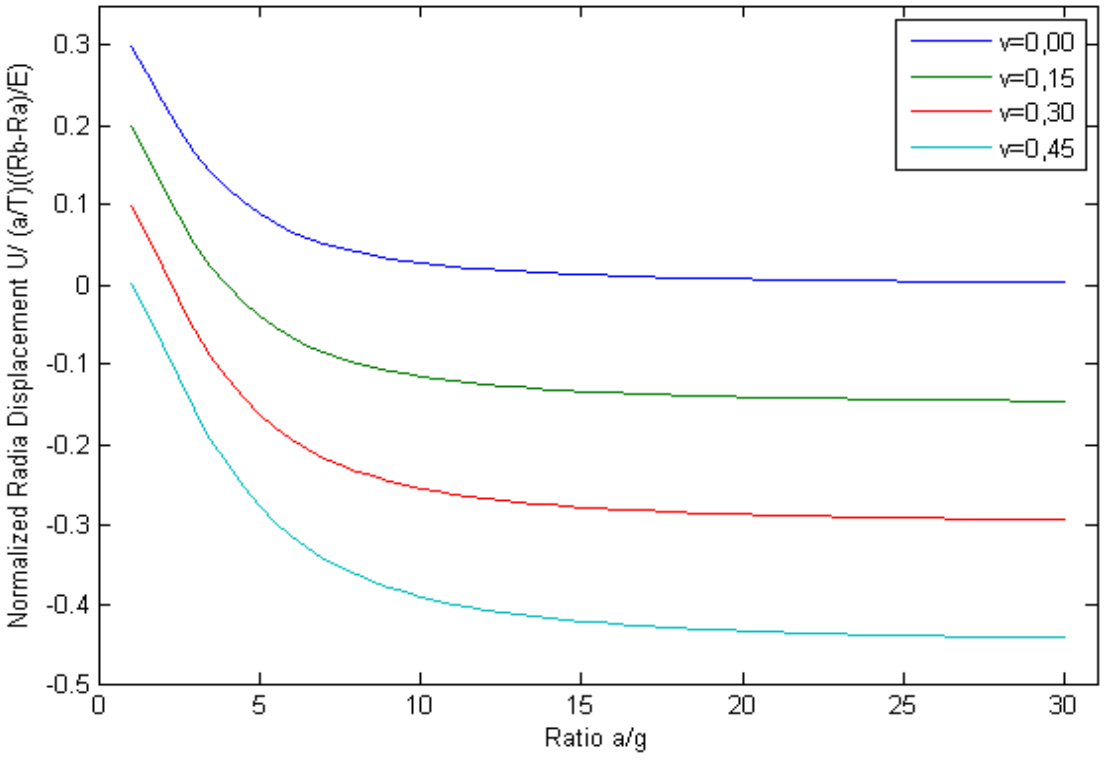

Fig. 52 Normalized radial displacement $u_r/\left(\left(a/T\right)\left(\left(R_a+R_b\right)/E\right)\right)$ **versus the ratio a/g for different values of the poisons ratio v. The classical boundary conditions are** $\mathbf{P}(a^-)=P_a\hat{\mathbf{r}}$ **and** $\mathbf{P}(a^+)=P_b\hat{\mathbf{r}}$ **and the non classical ones** $\mathbf{R}(a^-)=R_a\hat{\mathbf{r}}$ **and** $\mathbf{R}(a^+)=R_b\hat{\mathbf{r}}$ **with** $P_a+P_b=0$

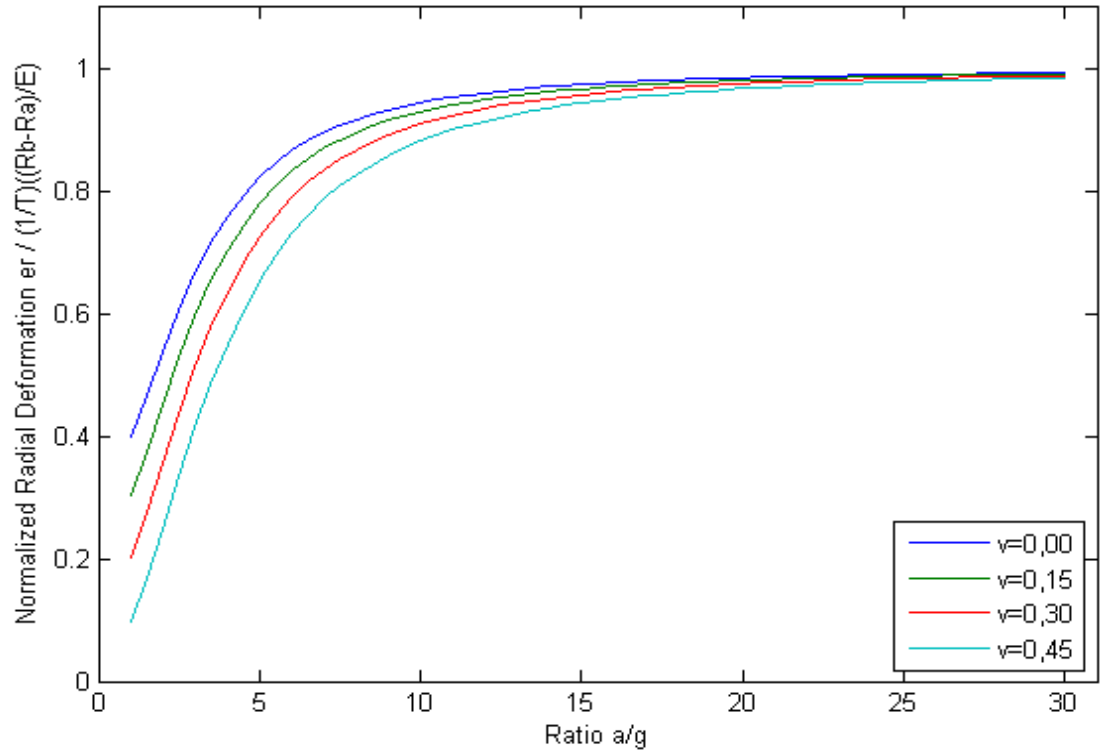

Fig. 53 Normalized radial deformation $e_r/\left(\left(1/T\right)\left(\left(R_a+R_b\right)/E\right)\right)$ **versus the ratio a/g for different values of the poisons ratio v. The classical boundary conditions are** $\mathbf{P}(a^-)=P_a\hat{\mathbf{r}}$ **and** $\mathbf{P}(a^+)=P_b\hat{\mathbf{r}}$ **and the non classical ones** $\mathbf{R}(a^-)=R_a\hat{\mathbf{r}}$ **and** $\mathbf{R}(a^+)=R_b\hat{\mathbf{r}}$ **with** $P_a+P_b=0$

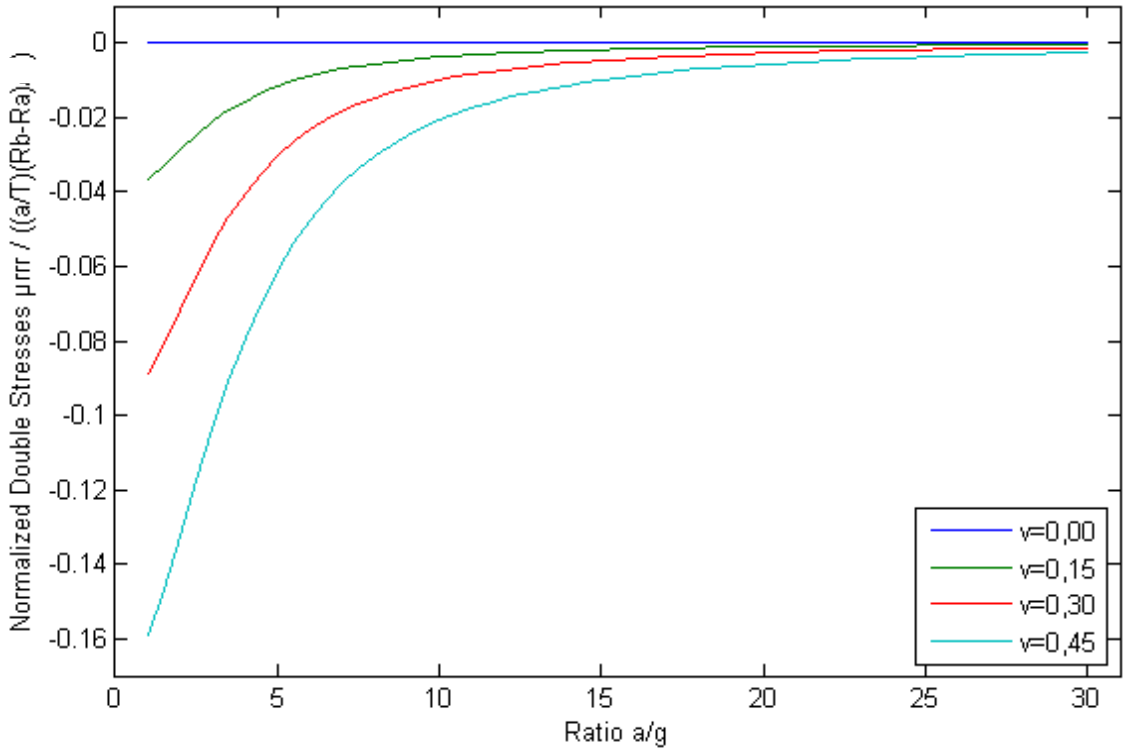

Fig. 54 Normalized double stresses $\mu_{rr}/((a/T)((R_a+R_b)))$ versus the ratio a/g for different values of the poisons ratio v. The classical boundary conditions are $\mathbf{P}(a^-)=P_a\hat{\mathbf{r}}$ and $\mathbf{P}(a^+)=P_b\hat{\mathbf{r}}$ and the non classical ones $\mathbf{R}(a^-)=R_a\hat{\mathbf{r}}$ and $\mathbf{R}(a^+)=R_b\hat{\mathbf{r}}$ with $P_a+P_b=0$

When radial double stresses are applied to the shell's boundary, additional displacements and deformations and double stresses are imposed.

In this case too, it should be noted, the classical behavior from the bubble under pressure $(P_b+P_a)_{classical}$ can be obtained then the right BCs are applied, i.e. $(P_b+P_a)_{gradient}=\frac{2\mu+\lambda}{\lambda}(P_b+P_a)_{classical}$ and $(R_b-R_a)=\frac{2\mu+\lambda}{4\mu}a\cdot(P_a+P_b)_{classical}$. Hence, independent of the microstructure, in order to obtain the classical behavior, both a greater than the classical pressure needs to be applied, and certain double stresses. Consequently, the gradient elastic bubble is considerably stiffer.

4.I.3.iv. The double-layer shell

Having already considered the case of a thin walled spherical shell, the next step of this study is to consider the case of a composite thin walled spherical shell.

The composite thin walled spherical shell is considered to be of radius d consisting of two tangent spherical shells of thicknesses T_1 and T_2 respectively, each one made of materials, with Lame's constants μ_1,λ_1 and μ_2,λ_2 and characteristic lengths g_1 and g_2 respectively. Let S_a be the internal and S_b the outer surface of the shell.

In the classical theory displacement continuity and equilibrium of the interface (r=d) dictate that at both its' ends displacement and the stress must be equal. In the gradient theory, these conditions are not sufficient. Two more need to be chosen. Following the works of Weitsman (Weitsman, 1965) (who addresses the problem of the interface through a couple-stress theory) and Yueqiu Li (Li, et al., 2015) who considers a gradient elastic interface, besides the two classical boundary conditions, the non classical ones are chosen to be the continuity of the displacement's normal gradient and the surface double stresses at the interface. These BCs represent the continuity of the second degree of freedom of the gradient elastic shell and its work conjugate. These are considered to be the BC that allow strain energy to be freely transmitted through the interface, as Wetsman (Weitsman, 1965) notes in the respective theory used in that paper.

Classical theory $\quad \mathbf{u}(\mathrm{r})\big|_{\mathrm{r=d}^-} = \mathbf{u}(\mathrm{r})\big|_{\mathrm{r=d}^+}$, $\mathbf{P}(r)\big|_{r=c^-} = \mathbf{P}(r)\big|_{r=c^+}$

Gradient theory $\quad \mathbf{u}(\mathrm{r})\big|_{\mathrm{r=d}^-} = \mathbf{u}(\mathrm{r})\big|_{\mathrm{r=d}^+}$, $\mathbf{P}(\mathrm{r})\big|_{\mathrm{r=d}^-} = \mathbf{P}(\mathrm{r})\big|_{\mathrm{r=d}^+}$

$\mathbf{q}(\mathrm{r})\big|_{\mathrm{r=d}^-} = \mathbf{q}(\mathrm{r})\big|_{\mathrm{r=d}^+}$, $\mathbf{R}(\mathrm{r})\big|_{\mathrm{r=d}^-} = \mathbf{R}(\mathrm{r})\big|_{\mathrm{r=d}^+}$

Also, the row vectors depicted in the first and the second column of the following expressions are functions of the first and the second material's parameters (μ_1,λ_1, g_1) and (μ_2,λ_2, g_2) respectively. Note that in the classical problems, $\rho(a) = [\rho_1, \rho_3]\big|_{r=a}$ etc while in the gradient ones $\rho(a) = [\rho_1, \rho_2, \rho_3, \rho_4]\big|_{r=a}$ etc. while O is the zero vector with 2 and 4 in each theory elements respectively. In order to obtain the solution to any

classical double layered shell BC problem four constants need to be determined two for each layer of the shell. These constants are named using the following convention: C_{ij}, i=a,b for the first and second material respectively, j=1,2 and are multiplied with the j^{th} fundamental classical solution, $\rho_1 = r, \rho_2 = 1/r^2$. In the gradient problems, four constants are necessary for each layer, so the total unknowns are eight. The same convention is used for naming them: C_{ij}, i=a,b for the first and second layer respectively, j=1,2,3,4 and are multiplied with the j^{th} gradient fundamental solution

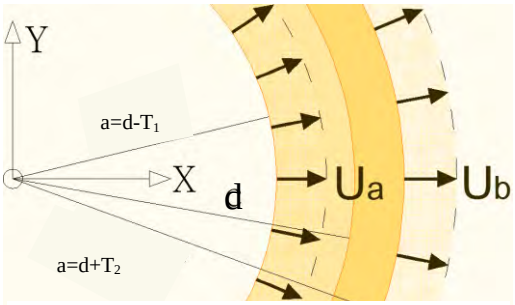

Fig. 55 x-y plane section of the double-layer shell. The boundary conditions are $\mathbf{u}(a) = U_a\hat{\mathbf{r}}$ **and** $\mathbf{u}(b) = U_b\hat{\mathbf{r}}$

1a)Classical theory

In this problem both surfaces are subjected to radial displacements U_a and U_b on S_a and S_b respectively, i.e. the BCs are:

$$\mathbf{u}(r)\big|_{r=a} = U_a\hat{\mathbf{r}}, \quad \mathbf{u}(r)\big|_{r=b} = U_b\hat{\mathbf{r}} \overset{\text{Thin walled}}{\Rightarrow}$$

$$\begin{bmatrix} \rho(d) - T_1\rho'(d) & 0 \\ 0 & \rho(d) + T_2\rho'(d) \\ \rho(d) & -\rho(d) \\ P(d) & -P(d) \end{bmatrix} \cdot \begin{bmatrix} C_{a1} \\ C_{a2} \\ C_{b1} \\ C_{b2} \end{bmatrix} = \begin{bmatrix} U_a \\ U_b \\ 0 \\ 0 \end{bmatrix} \Rightarrow u_r = [\rho(d)] \cdot \begin{bmatrix} C_{a1} \\ C_{a2} \end{bmatrix} = [\rho(d)] \cdot \begin{bmatrix} C_{b1} \\ C_{b2} \end{bmatrix}$$

$$u_r = u_r(d) = \left\{ \frac{(2\mu_1 + \lambda_1)U_a T_2 + (2\mu_2 + \lambda_2)U_b T_1}{(2\mu_1 + \lambda_1)T_2 + (2\mu_2 + \lambda_2)T_1} \right\}$$

In the case of a bi layered shell, the solution does not crush, as it happens into the single layered one. The displacement field obtained is practically a weighted mean value of the displacements of the two boundaries. The reason for such a difference is that in this case the interface is mathematically modeled as two different surfaces.

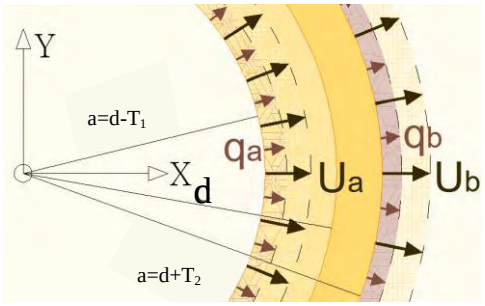

Fig. 56 x-y plane section of the double-layer shell. The boundary conditions are $\mathbf{u}(a)=U_a\hat{\mathbf{r}}$, $\mathbf{q}(a)=q_a\hat{\mathbf{r}}$, $\mathbf{u}(b)=U_b\hat{\mathbf{r}}$ **and** $\mathbf{q}(b)=q_b\hat{\mathbf{r}}$

1b)Gradient theory

In the respective gradient problem, both surfaces are subjected to radial displacements U_a and U_b on S_a and S_b respectively (classical BCs) while the normal displacement gradient at each boundary are prescribed, respectively q_a and q_b (non-classical BC), i.e.

$$\begin{bmatrix} \rho(a) & O \\ -\rho'(a) & O \\ O & \rho(b) \\ O & \rho'(b) \\ \rho(d) & -\rho(d) \\ \rho'(d) & -\rho'(d) \\ P(d) & -P(d) \\ R(d) & -R(d) \end{bmatrix} \cdot \begin{bmatrix} C_{a1} \\ C_{a2} \\ C_{a3} \\ C_{a4} \\ C_{b1} \\ C_{b2} \\ C_{b3} \\ C_{b4} \end{bmatrix} = \begin{bmatrix} U_a \\ q_a \\ U_b \\ q_b \\ 0 \\ 0 \\ 0 \\ 0 \end{bmatrix}$$

$$\mathbf{u}(r)\big|_{r=a}=U_a\hat{\mathbf{r}}\ , \qquad \mathbf{u}(r)\big|_{r=b}=U_b\hat{\mathbf{r}}$$

$$\mathbf{q}(r)\big|_{r=a}=\frac{\partial\mathbf{u}(r)}{\partial\mathbf{n}}\bigg|_{r=a}=\frac{\partial\mathbf{u}(r)}{\partial-\hat{\mathbf{r}}}\bigg|_{r=a}=q_a\hat{\mathbf{r}}$$

$$\mathbf{q}(r)\big|_{r=b}=\frac{\partial\mathbf{u}(r)}{\partial\mathbf{n}}\bigg|_{r=b}=\frac{\partial\mathbf{u}(r)}{\partial\hat{\mathbf{r}}}\bigg|_{r=b}=q_b\hat{\mathbf{r}}$$

The boundary value problem takes the adjacent matrix equation form.

Using second order Taylor expansions around the radius d for the functions of a and b, i.e.

$\rho_i(a)=\rho_i(d)-T_1\rho_i'(d)+T_1^2\rho''_i(d)/2$, T_1= d-a

$\rho_i(b)=\rho_i(d)+T_2\rho_i'(d)+T_2^2\rho''_i(d)/2$, T_2= b-d, the following solution for the shell's displacement is obtained.

$$u_r=\frac{\left\{\begin{array}{c}+\left[g_1^2(2\mu_1+\lambda_1)T_2^2+g_2^2(2\mu_2+\lambda_2)T_1^2\right]\cdot\left\{\left[g_1^2(2\mu_1+\lambda_1)T_2^2\right]U_a+\left[g_2^2(2\mu_2+\lambda_2)T_1^2\right]U_b\right\}\\ +2T_1T_2(2\mu_1+\lambda_1)(2\mu_2+\lambda_2)g_1^2g_2^2\left\{T_2^2U_a+T_1^2U_b\right\}\end{array}\right\}}{\left\{\begin{array}{c}g_1^4(2\mu_1+\lambda_1)^2T_2^4+g_2^4(2\mu_2+\lambda_2)^2T_1^4\\ +2T_1T_2g_1^2g_2^2(2\mu_1+\lambda_1)(2\mu_2+\lambda_2)[T_1^3T_2+T_1^2T_2^2+T_1T_2^3]\end{array}\right\}}$$

$$-\frac{T_1T_2\left[g_1^2(2\mu_1+\lambda_1)T_1+g_2^2(2\mu_2+\lambda_2)T_2\right]\cdot\left\{-\left[g_1^2(2\mu_1+\lambda_1)T_2^2\right]q_a+\left[g_2^2(2\mu_2+\lambda_2)T_1^2\right]q_b\right\}}{\left\{\begin{array}{c}g_1^4(2\mu_1+\lambda_1)^2T_2^4+g_2^4(2\mu_2+\lambda_2)^2T_1^4\\ +2T_1T_2g_1^2g_2^2(2\mu_1+\lambda_1)(2\mu_2+\lambda_2)[T_1^2T_2+T_1T_2+T_1T_2^2]\end{array}\right\}}$$

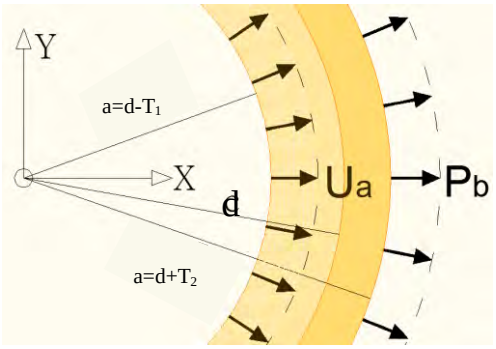

Fig. 57 x-y plane section of the double-layer shell. The boundary conditions are $\mathbf{u}(a) = U_a\hat{\mathbf{r}}$ **and** $\mathbf{P}(b) = P_b\hat{\mathbf{r}}$

2a)Classical problem

In this problem the surface S_a is subjected to radial displacements U_a while on the surface S_b a tensile stress P_b is applied, i.e.

$$\mathbf{u}(r)\big|_{r=a} = U_a\hat{\mathbf{r}}, \qquad \mathbf{P}(r)\big|_{r=b} = P_b\hat{\mathbf{r}}$$

$$\begin{bmatrix} \rho(a) & O \\ O & P(b) \\ \rho(d) & -\rho(d) \\ P(d) & -P(d) \end{bmatrix} \cdot \begin{bmatrix} C_{a1} \\ C_{a2} \\ C_{b1} \\ C_{b2} \end{bmatrix} = \begin{bmatrix} U_a \\ P_b \\ 0 \\ 0 \end{bmatrix} \overset{\text{Thin}}{\underset{\text{walled}}{\Rightarrow}}$$

$$\begin{bmatrix} \rho(d) & 0 \\ 0 & P(d) \\ \rho(d) & -\rho(d) \\ P(d) & -P(d) \end{bmatrix} \cdot \begin{bmatrix} C_{a1} \\ C_{a2} \\ C_{b1} \\ C_{b2} \end{bmatrix} = \begin{bmatrix} U_a \\ P_b \\ 0 \\ 0 \end{bmatrix}$$

Since the problem doesn't become singular for a=b=c, and its solution is

$$\mathbf{u} = u_r\hat{\mathbf{r}} = U_a\hat{\mathbf{r}},$$

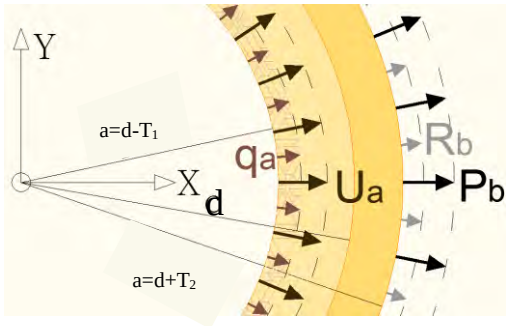

Fig. 58 x-y plane section of the double-layer shell. The boundary conditions are $\mathbf{u}(a) = U_a\hat{\mathbf{r}}$, $\mathbf{q}(a) = q_a\hat{\mathbf{r}}$, $\mathbf{P}(b) = P_b\hat{\mathbf{r}}$ **and** $\mathbf{R}(b) = R_b\hat{\mathbf{r}}$

2b)Gradient theory

In the gradient problem, the surface S_a is subjected to radial displacements U_a while the normal displacement gradient on boundary is q_a and on the surface S_b a tensile stress P_b (classical boundary conditions) and surface double stresses R_b (non-classical boundary conditions) are applied, i.e.

$$\mathbf{u}(r)\big|_{r=a} = U_a\hat{\mathbf{r}}\ , \qquad \mathbf{P}(r)\big|_{r=b} = P_b\hat{\mathbf{r}}$$

$$\begin{bmatrix} \rho(a) & O \\ -\rho'(a) & O \\ O & P(b) \\ O & R(b) \\ \rho(d) & -\rho(d) \\ \rho'(d) & -\rho'(d) \\ P(d) & -P(d) \\ R(d) & -R(d) \end{bmatrix} \cdot \begin{bmatrix} C_{a1} \\ C_{a2} \\ C_{a3} \\ C_{a4} \\ C_{b1} \\ C_{b2} \\ C_{b3} \\ C_{b4} \end{bmatrix} = \begin{bmatrix} U_a \\ q_a \\ P_b \\ R_b \\ 0 \\ 0 \\ 0 \\ 0 \end{bmatrix}$$

$$\mathbf{q}(r)\big|_{r=a} = \frac{\partial \mathbf{u}}{\partial \mathbf{n}}\bigg|_{r=a} = q_a\hat{\mathbf{r}}, \qquad \mathbf{R}(r)\big|_{r=b} = R_b\hat{\mathbf{r}}$$

Consequently, the boundary condition problem takes the following form:

Now, once again, this problem even with a=b=d doesn't become singular, thus the

solution one obtains is exactly the same obtained for the single layer shell, i.e. $\mathbf{u} = u_r\hat{\mathbf{r}} = U_a\hat{\mathbf{r}}$, and also $\mathbf{q} = q_a\hat{\mathbf{r}}$, $\mathbf{P} = P_b\hat{\mathbf{r}}$ and $\mathbf{R} = R_b\hat{\mathbf{r}}$

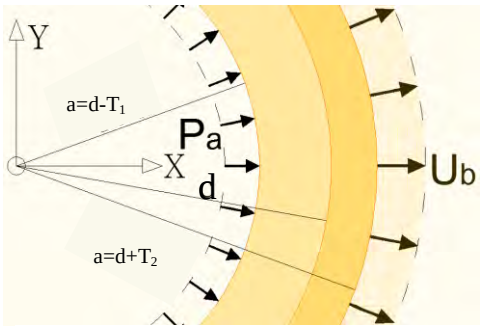

Fig. 59 x-y plane section of the double-layer shell. The boundary conditions are $\mathbf{P}(a) = P_a\hat{\mathbf{r}}$ **and** $\mathbf{u}(b) = U_b\hat{\mathbf{r}}$

The problem doesn't become singular for a=b=d, and its solution is

$\bar{\mathbf{u}} = u_r\hat{\mathbf{r}} = U_a\hat{\mathbf{r}}$, while $\mathbf{P} = P_b\hat{\mathbf{r}}$

3a)Classical theory

In this problem on the surface S_a is applied to a compressive stress-pressure P_a while on the surface S_b is subjected to a displacement U_b, i.e.

$$\mathbf{P}(r)\big|_{r=a} = P_a\hat{\mathbf{r}}, \qquad \mathbf{u}(r)\big|_{r=b} = U_b\hat{\mathbf{r}} \Rightarrow$$

$$\begin{bmatrix} -P(a) & O \\ O & \rho(b) \\ \rho(d) & -\rho(d) \\ P(d) & -P(d) \end{bmatrix} \cdot \begin{bmatrix} C_{a1} \\ C_{a2} \\ C_{b1} \\ C_{b2} \end{bmatrix} = \begin{bmatrix} P_a \\ U_b \\ 0 \\ 0 \end{bmatrix}$$

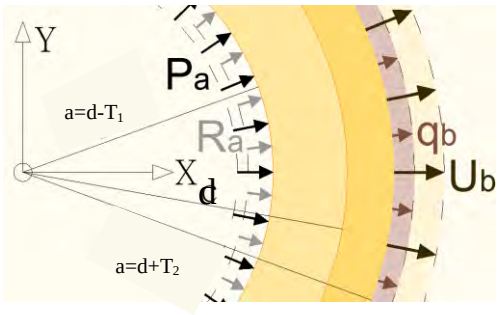

Fig. 60 x-y plane section of the double-layer shell. The boundary conditions are $\mathbf{P}(a) = P_a\hat{\mathbf{r}}$, $\mathbf{R}(a) = R_a\hat{\mathbf{r}}$, $\mathbf{u}(b) = U_b\hat{\mathbf{r}}$

3b)Gradient theory

In this problem on the surface S_a a compressive stress-pressure P_a (classical BC) and surface double stresses R_a (non-classical BC) are applied, while the surface S_b is subjected to radial displacement U_b (classical BC) while the normal displacement gradient on boundary is q_b (Non-classical BC) , i.e.

$$\begin{bmatrix} -P(a) & O \\ R(a) & O \\ O & \rho(b) \\ O & \rho'(b) \\ \rho(d) & -\rho(d) \\ \rho'(d) & -\rho'(d) \\ P(d) & -P(d) \\ R(d) & -R(d) \end{bmatrix} \cdot \begin{bmatrix} C_{a1} \\ C_{a2} \\ C_{a3} \\ C_{a4} \\ C_{b1} \\ C_{b2} \\ C_{b3} \\ C_{b4} \end{bmatrix} = \begin{bmatrix} P_a \\ R_a \\ U_b \\ q_b \\ 0 \\ 0 \\ 0 \\ 0 \end{bmatrix}$$

$$\mathbf{P}(r)\big|_{r=a} = P_a\hat{\mathbf{r}}, \qquad \mathbf{u}(r)\big|_{r=b} = U_b\hat{\mathbf{r}}$$

$$\mathbf{R}(r)\big|_{r=a} = R_a\hat{\mathbf{r}}, \qquad \mathbf{q}(r)\big|_{r=b} = \frac{\partial \mathbf{u}(r)}{\partial \hat{\mathbf{r}}}\bigg|_{r=b} = q_b\hat{\mathbf{r}}$$

Consequently, the boundary condition problem takes the adjacent form:

This solution even in the case of a thin walled

spherical shell (a=b=d) is not singular and the solution obtained is exactly the same obtained by the single layer shell, i.e.

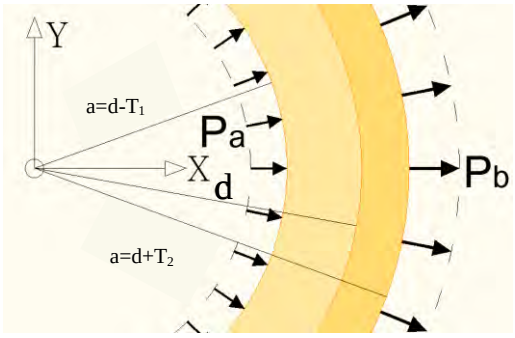

Fig. 61 x-y plane section of the double-layer shell. The boundary conditions are $\mathbf{P}(a)=P_a\hat{\mathbf{r}}$ **and** $\mathbf{P}(b)=P_b\hat{\mathbf{r}}$

$\mathbf{u}=\mathrm{u_r}\hat{\mathbf{r}}=\mathrm{U_b}\hat{\mathbf{r}}$, and also $\mathbf{q}=q_b\hat{\mathbf{r}}$, $\mathbf{P}=P_a\hat{\mathbf{r}}$ and $\mathbf{R}=R_a\hat{\mathbf{r}}$.

4a)Classical theory

In this problem on the surfaces S_a is subjected to a compressive stress-pressure P_a and the surface S_b is subjected a tensile stress P_b, i.e.

$$\mathbf{P}(r)\big|_{r=a}=P_a\hat{\mathbf{r}} \quad , \quad \mathbf{u}(r)\big|_{r=b}=P_b\hat{\mathbf{r}}$$

$$\begin{bmatrix} \mathrm{P(d)}-\mathrm{T_1P'(d)} & 0 \\ 0 & \mathrm{R(d)}+\mathrm{T_2R'(d)} \\ \rho(\mathrm{d}) & -\rho(\mathrm{d}) \\ \mathrm{P(d)} & -\mathrm{P(d)} \end{bmatrix} \cdot \begin{bmatrix} \mathrm{C_{a1}} \\ \mathrm{C_{a2}} \\ \mathrm{C_{b1}} \\ \mathrm{C_{b2}} \end{bmatrix} = \begin{bmatrix} \mathrm{P_a} \\ \mathrm{P_b} \\ 0 \\ 0 \end{bmatrix},$$

$$\mathrm{u_r}=[\rho(\mathrm{d})]\cdot\begin{bmatrix}\mathrm{C_{a1}}\\ \mathrm{C_{a2}}\end{bmatrix}=[\rho(\mathrm{d})]\cdot\begin{bmatrix}\mathrm{C_{b1}}\\ \mathrm{C_{b2}}\end{bmatrix}\Rightarrow$$

$$u_r=u_r(c)=\frac{c^2}{4}(P_a+P_b)\frac{(2\mu_1+\lambda_1)(2\mu_2+\lambda_2)}{T_1\mu_1(2\mu_1+3\lambda_1)(2\mu_2+\lambda_2)+T_2\mu_2(2\mu_2+3\lambda_2)(2\mu_1+\lambda_1)}$$

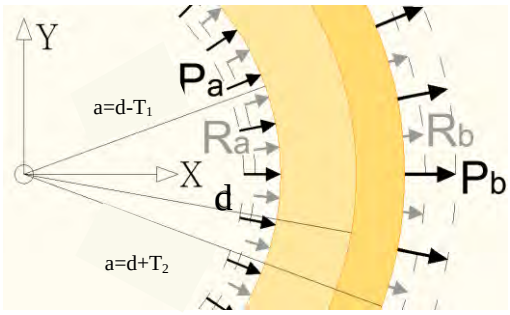

Fig. 62 x-y plane section of the shell. The boundary conditions are $\mathbf{P}(a)=P_a\hat{\mathbf{r}}$, $\mathbf{R}(a)=R_a\hat{\mathbf{r}}$, $\mathbf{P}(b)=P_b\hat{\mathbf{r}}$ **and** $\mathbf{R}(b)=R_b\hat{\mathbf{r}}$

$$\mathbf{P}(r)\big|_{r=a}=P_a\hat{\mathbf{r}} \quad , \quad \mathbf{P}(r)\big|_{r=b}=P_b\hat{\mathbf{r}}$$

$$\mathbf{R}(r)\big|_{r=a}=R_a\hat{\mathbf{r}} \quad , \quad \mathbf{R}(r)\big|_{r=b}=R_b\hat{\mathbf{r}}$$

4d)Gradient theory

On the gradient elastic bilayer shell's surfaces S_a is applied a compressive stress-pressure P_a (classical BC) and surface double stresses R_a (non-classical BC), while the surface S_b is subjected to a tensile stress P_b (classical BC) and surface double stresses R_b (non-classical BC) , i.e.

$$\begin{bmatrix} -P(d)+T_1P'(d) & O \\ R(d)-T_1R'(d) & O \\ O & P(d)+T_1P'(d) \\ O & R(d)+T_1R'(d) \\ \rho(d) & -\rho(d) \\ \rho'(d) & -\rho'(d) \\ P(d) & -P(d) \\ R(d) & -R(d) \end{bmatrix} \cdot \begin{bmatrix} C_{a1} \\ C_{a2} \\ C_{a3} \\ C_{a4} \\ C_{b1} \\ C_{b2} \\ C_{b3} \\ C_{b4} \end{bmatrix} = \begin{bmatrix} P_a \\ R_a \\ P_b \\ R_b \\ 0 \\ 0 \\ 0 \\ 0 \end{bmatrix}$$

For a thin walled double-layer shell, using first order Taylor expansions around d, this BC problem takes the form above, which finally leads to the next solution

$$u_r = \frac{d_2}{4}(P_b + P_a)\frac{\left\{\begin{array}{l} +T_1(2\mu_2+\lambda_2)\cdot\left[4(g_1/d)^2\mu_1(6\mu_1+5\lambda_1)+(2\mu_1+\lambda_1)^2\right] \\ +T_2(2\mu_1+\lambda_1)\cdot\left[4(g_2/d)^2\mu_2(6\mu_2+5\lambda_2)+(2\mu_2+\lambda_2)^2\right] \end{array}\right\}}{\left\{\begin{array}{l} +{T_1}^2(2\mu_1+3\lambda_1)(2\mu_2+\lambda_2)\cdot\left[3(g_1/d)^2\mu_1(6\mu_1+5\lambda_1)+\mu_1(2\mu_1+\lambda_1)\right] \\ +{T_2}^2(2\mu_2+3\lambda_2)(2\mu_1+\lambda_1)\cdot\left[3(g_2/d)^2\mu_2(6\mu_2+5\lambda_2)+\mu_2(2\mu_2+\lambda_2)\right] \\ +T_1T_2\left\{\begin{array}{c} 3(g_1/d)^2\mu_1(6\mu_1+5\lambda_1)(2\mu_2+\lambda_2)(2\mu_2+3\lambda_2) \\ 3(g_2/d)^2\mu_2(6\mu_2+5\lambda_2)(2\mu_1+\lambda_1)(2\mu_1+3\lambda_1) \\ (2\mu_1+\lambda_1)(2\mu_2+\lambda_2)\left[(2\mu_1+3\lambda_1)\mu_2+(2\mu_2+3\lambda_2)\mu_1\right] \end{array}\right\} \end{array}\right\}}$$

$$-\frac{d}{2}(R_b - R_a)\frac{\left\{\begin{array}{l} +T_1(2\mu_2+\lambda_2)\cdot\left[-2(g_1/d)^2\mu_1(6\mu_1+5\lambda_1)+\lambda_1(2\mu_1+\lambda_1)\right] \\ +T_2(2\mu_1+\lambda_1)\cdot\left[-2(g_2/d)^2\mu_2(6\mu_2+5\lambda_2)+\lambda_2(2\mu_2+\lambda_2)\right] \end{array}\right\}}{\left\{\begin{array}{l} +{T_1}^2(2\mu_1+3\lambda_1)(2\mu_2+\lambda_2)\cdot\left[3(g_1/d)^2\mu_1(6\mu_1+5\lambda_1)+\mu_1(2\mu_1+\lambda_1)\right] \\ +{T_2}^2(2\mu_2+3\lambda_2)(2\mu_1+\lambda_1)\cdot\left[3(g_2/d)^2\mu_2(6\mu_2+5\lambda_2)+\mu_2(2\mu_2+\lambda_2)\right] \\ +T_1T_2\left\{\begin{array}{c} 3(g_1/d)^2\mu_1(6\mu_1+5\lambda_1)(2\mu_2+\lambda_2)(2\mu_2+3\lambda_2) \\ 3(g_2/d)^2\mu_2(6\mu_2+5\lambda_2)(2\mu_1+\lambda_1)(2\mu_1+3\lambda_1) \\ (2\mu_1+\lambda_1)(2\mu_2+\lambda_2)\left[(2\mu_1+3\lambda_1)\mu_2+(2\mu_2+3\lambda_2)\mu_1\right] \end{array}\right\} \end{array}\right\}}$$

$$u_r' = -\frac{d}{2}(P_a + P_b)\frac{\left\{\begin{array}{c} +T_1(2\mu_2+\lambda_2)\cdot\left[-2(g_1/c)^2\mu_1(6\mu_1+5\lambda_1)+\lambda_1(2\mu_1+\lambda_1)\right] \\ +T_2(2\mu_1+\lambda_1)\cdot\left[-2(g_2/c)^2\mu_2(6\mu_2+5\lambda_2)+\lambda_2(2\mu_2+\lambda_2)\right] \end{array}\right\}}{\left\{\begin{array}{c} +T_1^{\,2}(2\mu_1+3\lambda_1)(2\mu_2+\lambda_2)\cdot\left[3(g_1/d)^2\mu_1(6\mu_1+5\lambda_1)+\mu_1(2\mu_1+\lambda_1)\right] \\ +T_2^{\,2}(2\mu_2+3\lambda_2)(2\mu_1+\lambda_1)\cdot\left[3(g_2/d)^2\mu_2(6\mu_2+5\lambda_2)+\mu_2(2\mu_2+\lambda_2)\right] \\ +T_1T_2\left\{\begin{array}{c} 3(g_1/d)^2\mu_1(6\mu_1+5\lambda_1)(2\mu_2+\lambda_2)(2\mu_2+3\lambda_2) \\ 3(g_2/d)^2\mu_2(6\mu_2+5\lambda_2)(2\mu_1+\lambda_1)(2\mu_1+3\lambda_1) \\ (2\mu_1+\lambda_1)(2\mu_2+\lambda_2)\left[(2\mu_1+3\lambda_1)\mu_2+(2\mu_2+3\lambda_2)\mu_1\right] \end{array}\right\} \end{array}\right\}}$$

$$+\frac{d}{2}(R_b - R_a)\frac{\left\{\begin{array}{c} +T_1(2\mu_2+\lambda_2)\cdot\left[-2(g_1/d)^2\mu_1(6\mu_1+5\lambda_1)+\lambda_1(2\mu_1+\lambda_1)\right] \\ +T_2(2\mu_1+\lambda_1)\cdot\left[-2(g_2/d)^2\mu_2(6\mu_2+5\lambda_2)+\lambda_2(2\mu_2+\lambda_2)\right] \end{array}\right\}}{\left\{\begin{array}{c} +T_1^{\,2}(2\mu_1+3\lambda_1)(2\mu_2+\lambda_2)\cdot\left[3(g_1/d)^2\mu_1(6\mu_1+5\lambda_1)+\mu_1(2\mu_1+\lambda_1)\right] \\ +T_2^{\,2}(2\mu_2+3\lambda_2)(2\mu_1+\lambda_1)\cdot\left[3(g_2/d)^2\mu_2(6\mu_2+5\lambda_2)+\mu_2(2\mu_2+\lambda_2)\right] \\ +T_1T_2\left\{\begin{array}{c} 3(g_1/d)^2\mu_1(6\mu_1+5\lambda_1)(2\mu_2+\lambda_2)(2\mu_2+3\lambda_2)+ \\ 3(g_2/d)^2\mu_2(6\mu_2+5\lambda_2)(2\mu_1+\lambda_1)(2\mu_1+3\lambda_1)+ \\ (2\mu_1+\lambda_1)(2\mu_2+\lambda_2)\left[(2\mu_1+3\lambda_1)\mu_2+(2\mu_2+3\lambda_2)\mu_1\right] \end{array}\right\} \end{array}\right\}}$$

Interesting property of this solution is that if any of the of $T_1$and T_2 is zero or the material is the same in both layers, thus the shell isn't composite, then the solution degenerates is reduced to the one obtain for a single layer shell.

If both materials' microstructures are assumed to be insignificant $\Leftrightarrow$ $g_1 \to 0^+$and $g_2 \to 0^+$, this solution doesn't take the form of the classical solution. However, this does not mean that it is wrong. In the literature, cases can be found that the solutions obtained, when the length parameter g is assumed zero, are not reduced to the classical respective problem solutions. In this particular case this result might also be attributed to the fact that only the lowest order thickness orders of the solution are kept, and the others are assumed to be insignificant combined with the assumption that was made that $T/d << g/d,\ \forall T, g$, which is the case of the microspheres studied by (Glynos & Koutsos, 2009)

4.I.4. Experimental data treatment

Glynos,E. and Koutsos,V. (Glynos & Koutsos, 2009) investigated experimentally the mechanical behavior of micro scale spherical shells, they used the term MS (Micro Sphere), using nanocompression testing with tipless cantilevers. The MSs used consisted of a thin shell of stiff structural polymer polylactide, surrounded by a cross linked albium outer layer and incapsulated nitrogen gas at atmospheric pressure.

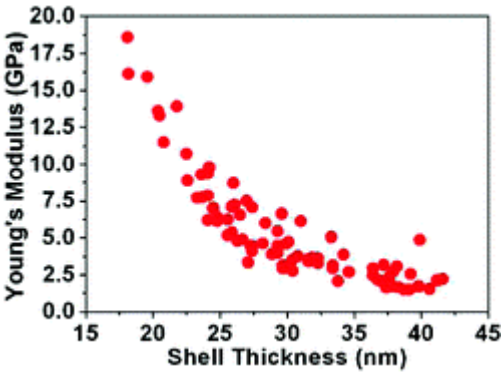

Fig. 63 Young's modulus of MS structural shell versus MS shell thickness (Glynos & Koutsos, 2009)

The MS's thickness to radius ratio was considered to be constant $T/a=1.5x10^{-2}$ and the polymer's Poisson's ratio was assumed to be 0.42. The classical theory of elasticity calculates the MS's stiffness, k, under this type of loading using the following equation.

$$k = \frac{4}{\sqrt{3(1-\nu^2)}}\frac{T^2}{a}E = 5.73x10^{-4}aE$$

That indicates that bigger MS have are stiffer than smaller ones, then the thickness to radius ratio is constant. The experiment's findings, though, indicate that small MSs are stiffer than larger, which comes in contradiction with the classical theory. Relaxing the assumption for a constant Young's modulus , Glynos obtained the figure 63 presenting the relation for the Young's modulus to the MS's thickness.

Using the spherical shell model that was developed, it is attempted to interpret those results. There isn't enough data available to address the problem as a multiple layer shell as it is, so it will be treated as a single layered one. Also the MSs' loading is not the one studied in the model. However, in hope that the same stiffening effects might be observed in both loading cases, this attempt of fitting the model to the experimental results is being made.

The following relation can be obtained for its materials Young's modulus as a function of the shell's radius a, it's materials characteristic length g and Poisson ratio ν:

$$E = E_0 \frac{(1-\nu)\cdot\left[3(3-\nu)\cdot(g/a)^2+(1-\nu)\right]}{\left[2(1-2\nu)\cdot(3-\nu)\cdot(g/a)^2+(1-\nu)^2\right]} = E_0\left\{1+\frac{(1+\nu)\cdot(3-\nu)}{\left[2(1-2\nu)\cdot(3-\nu)+\cdot(a/g)^2\cdot(1-\nu)^2\right]}\right\}$$

,E_o being the Young's modulus computed using the classical theory for the MS in the case that it is loaded only by pressure.

Substituting the Poisson ratio(ν=0.42) and the thickness to radius ratio ($T/a=1.5x10^{-2}$,), the following equation is obtained

$$E = E_0\left\{1+\frac{4.4375}{0.4075\cdot(a/g)^2+1}\right\} = E_0\left\{1+\frac{4.4375}{1811.1\cdot(T/g)^2+1}\right\}$$

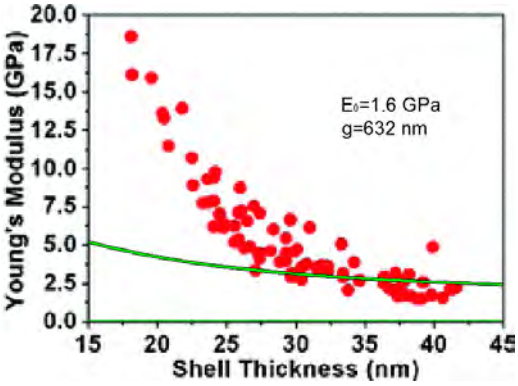

Fig. 64 Experimental data compared to the Eo=1.6GPa, g=632nm stiffness curve described by the model of a thin walled spherical shell

This does indicate that for smaller shells the Young's modulus does increase. However, in the model, sole the reduction of the shells size cannot induce such a dramatic increase of its stiffness, as the one described by the experiment's result.

This does not mean necessarily that the model fails to capture these stiffening effects. The general stiffening trend is captured, and there can be a better fitting of the model to the experimental results if the double stresses taken into account. However, many assumptions have already been made, so it was chosen not to proceed to this attempt without more data.

In figure 66 is depicted, besides the experiments result, a curve for. E_0=1.6 while the characteristic length g is 632 nm, which is one of the curves that predict the greatest increase for the Young's modulus

4.I.5. Conclusions

Solid Sphere

- The gradient theory does capture size effects in the spheres behavior.
- When the surface normal displacement gradient is restrained, the sphere has a stiffer behavior.
- When only classical loads are applied to the sphere, its response is classical, no matter how significant the microstructure might be.
- Double stresses need to be applied for size effects to appear and stiffer responses to be obtained.
- When the microstructure is small compared to the spheres radius, the effect of the non classical BCs is very small and the spheres behavior is reduced to the classical one.

Spherical Cavity

- Significantly stiffer than classical behavior even when no double stresses are applied, for great g length to radius ratios.
- Significant effect of the poisson's ratio to its behavior
- The double stresses are significant only close to the boundary
- The solution is always reduced to the classical one when the microstructure is small.

Spherical Shell

- Only the problem that the external loads are known provides useful results.
- Its behavior is always stiffer than the classical, even when no double stresses are applied.
- When the microstructure is small, the displacement and strain fields are reduced to the classical ones, while the curvature field is not.
- The Poisson's ratio affects the bars behavior, as it does in the classical case

Double Layer Spherical Shell

- Only the problem that the external loads are known provides useful results.
- In this case too many parameters are considered, which makes the extraction of conclusions difficult.
- Generally, a stiffer than classical behavior is obtained for the shell
- When the two material parameters are the same, the solution is reduced to the simple spherical shell gradient solution
- When both materials length parameters are small compared to the shell's radius, the solution obtained is not the classical one

4.II. PART II: 1D PROBLEMS & TRUSSES

4.II.1. Truss modeling through gradient elasticity.

Trusses are a very common and useful and common kind of structure. There are several real life applications for trusses. For starters, in structural mechanics, they are commonly used for bridges and roofs. In vascular surgery, the STENTs used to increase blood flow in areas blocked by plaque are three dimensional trusses. In material science, in research for very light materials, a microscale 3D lattice was developed, with the intent to be possibly used as a structural material. Trusses, also, have more theoretical use. For example, they are a very simple way of modeling complex bodies under various kinds of loading, by discretizing a continuum in a network of truss elements in order to solve many elasticity problems.

From a geometrical perspective, the simplest finite elements is the one dimensional bar element, which, in the classical elasticity framework, can be subjected only to axial loads, either tensile or compressive. These bar elements, though, can be used not only in one but also in two or three spatial dimensions by transforming their local coordinate system to a global one.

A truss elements can model satisfactorily even complex geometries and give good stress and displacement results, using very few and simple equations, especially when used in appropriate problems, they give a very cost effective solution.

Truss problems are mostly solved the stiffness method. This method starts by obtaining the truss elements' stiffness matrices, assembling them in a global coordinate system and obtaining the global stiffness matrix of the structure. Then, the global load vector is defined and it's relation to the displacement vector is obtained for the whole structure and the chosen boundary conditions (BCs) are imposed.

The following part of this work addresses the behavior of a gradient elastic bar, as a start, in order to conclude about the overall behavior of a composite gradient bar structure- truss. First, the equilibrium equation and the corresponding boundary conditions of a gradient elastic bar under static loading are derived using the variation principle. Second, various BC problems of the bar are addressed in order to obtain a good understanding of the effect that each BC has on the bars displacement, strain and double stresses fields, and the effect of the surface energy parameter l, which is not considered a parameter in the general strain gradient elasticity theory by Aifantis and is not taken into consideration in the general 3D problem presented in the first part of this work. Third, the function- behavior of elastic and a holonomic node is discussed in the framework of gradient elasticity in 1D problems and the non classical BCs that should be applied are found. The 1D stiffness matrix of the bar element is obtained and a series of 1D problems are solved in both their gradient and classical cases using the stiffness method and compared to their respective analytical solutions, in order to certify that the gradient elements can be used as 1D FEMs.

Finally, the 2D truss problem is addressed directly. The function of a node in 2 dimensions is discussed. The Global 2D element stiffness matrix is obtained and some 2 D examples are presented. Last, another model for a 2D node behavior is proposed, and an example of its application is given.

4.II.2. The single bar behavior

4.II.2.i. Equilibrium equation and boundary conditions in 1D problems

The problem of the gradient elastic bar in uniaxial loading is the simplest one dimensional problem that can be addressed through first strain gradient elasticity. It has been addressed several times in the past years, not only as a static problem, as it will be here, but also as a dynamic one. This is the case of the works by Aifantis (Altan, et al., 1996), Tsepoyra (Tsepoura, et al., 2002), Polizzotto (Polizzotto, 2003), Mustapha (Mustapha & Ruan, 2015). This problem has also been addressed though other non local elasticity theories, as shown in Aurora Angela Pisano and E. Benvenuti.

Following, assuming a material that obeys the linear gradient elasticity theory of Aifantis, the equilibrium equation and the corresponding boundary conditions are presented as obtained by Tsepoyra by application of the variation principle.

Consider a straight prismatic slender bar, with constant cross sectional and elastic properties along its axis subjected to uniaxial tensile stress $\sigma_x(x)$ resulting to an axial displacement $u=u_x(x)$, along its longitudinal axis x. The displacements u_y and u_z are assumed to be zero, thus the strain field $e = e_{11} = \frac{du_x}{dx}$

Following the one dimensional gradient elasticity theory with surface energy by Aifantis the strain energy U of the bar in axial loading is defined as

$$U = \frac{1}{2}\int_V [\tau \cdot e + \mu \cdot \nabla e] dV = \frac{1}{2} A \int_0^L [\tau \cdot e + \mu \cdot \nabla e] dx$$

Where A is the area of a cross section, $\nabla e = \frac{de}{dx}$ is the strains gradient, and τ, μ denote the Cauchy stresses and double stresses, respectively and are given by the following constitutive relations

$$\tau = Eu' + lEu''$$

$$\mu = lEu' + g^2 Eu''$$

Where the constants l, g represent ,material lengths related to the surface and volumetric elastic strain energy respectively with $0 < l < g$, E is the Young modulus and $(\bullet)' = d(\bullet)/dx$,

The bars strain energy and its variation are given below

$$U = \frac{1}{2}\int_0^L EA\left[(u')^2 + g^2(u'')^2 + 2lu'u''\right]dx$$

$$\delta U = -\int_0^L EA\,(u''-g^2u^{iv})\delta u\,dx + \left[EA\,(u'-g^2u''')\,\delta u\right]_0^L + \left[EA\,(g^2u''+lu')\,\delta u'\right]_0^L$$

The variation of the work done by external classical forces q and P and non-classical double forces R read

$$\delta W = \int_0^L q\delta u\,dx + \left[P\delta u\right]_0^L + \left[R\delta u'\right]_0^L$$

The variation equation $\delta(U - W) = 0$ takes the following form

$$\delta U = -\int_0^L \left[EA\,(u''-g^2u^{iv}) + q\right]\delta u\,dx$$
$$+ \left[\left(P - EA\,(u'-g^2u''')\right)\delta u\right]_0^L + \left[\left(R - EA\,(g^2u''+lu')\right)\delta u'\right]_0^L$$

The equation above implies that each term must be equal to zero, thus the governing equation of the bar and its boundary conditions (BCs) are extracted.

$$u''(x) - g^2u^{iv}(x) + \frac{q(x)}{EA} = 0$$

And at each end

i. Either the displacement is known $u = \bar{u}$

or the applied axial force is known $u'-g^2u''' = \dfrac{\bar{P}}{EA}$

ii. Either the strain at each end is known $u' = \bar{u}'$

or the applied axial double forces are known $lu' + g^2 u'' = \frac{\bar{R}}{EA}$

Where the dashed superscript denotes prescribed values.

The O.D.s general solution is $u = u_{hom} + u_{partial} = C_i \rho_i + u_{partial}$

$$u = C_1 x + C_2 + C_3 \cosh(x/g) + C_4 \sinh(x/g) + \frac{g}{EA} \int_0^x \left[\sinh\left(\frac{x-t}{g} \right) - \frac{x-t}{g} \right] q(t)\, dt$$

The force vector is: $\mathbf{P} = C_i P_i \hat{\mathbf{x}}$, $P = [1 \quad 0 \quad 0 \quad 0]$

And the double force vector is $\mathbf{R} = C_i R_i \hat{\mathbf{x}}$,

$$R = [1 \quad 0 \quad \cosh(x/g) + \frac{l}{g}\sinh(x/g) \quad \sinh(x/g) + \frac{l}{g}\cosh(x/g)]$$

4.II.2.ii. Boundary Condition Problems

In the following section the effect in the behavior of a gradient elastic bar of several boundary conditions will be presented in extend. The behavior predicted will be compared to the one predicted by the respective classical elastic bar. The effect of the extra surface energy parameter l will be discussed separately.

Consider a bar of length L, modulus of elasticity E and cross-sectional area A. Besides the original coordinate system $x \in [0, L]$, two more coordinates systems are introduced in order to simplify the results and optimize their display. The first is the normalized axial coordinate system $\xi = x/L \in [0,1]$, and the second one is a normalized coordinate system with origin at the end of the bar i.e. $x = L \Leftrightarrow \xi^* = 0$ and direction opposite to previous systems, $\xi^* = (L - x)/L = 1 - \xi, \quad \xi^* \in [0,1]$. In the following gradient problems the non dimensional parameters $c = L/g$ and $\lambda = l/g$ are used for the same reason.

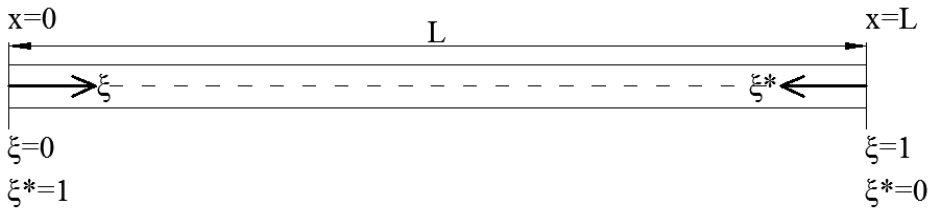

Fig. 65 Representation of the coordinate systems x, ξ, ξ* that are being used it order to simplify the following problems and used the symmetry of the solutions

The fixed-fixed bar

Fig. 68 Fixed-Fixed bar subjected to displacements $\mathbf{u}(\xi = 0) = U_0\hat{\mathbf{x}}$ and $\mathbf{u}(\xi = 1) = U_1\hat{\mathbf{x}}$

Classical theory

In fixed-fixed bars ends are subjected to axial displacements U_0 and U_1 respectively, the BCs are $u(\xi = 0) = U_0$ and $u(\xi = 1) = U_1$. The following displacement field is very simple, well known and easily obtained.

$$u(\xi) = U_0 + (U_1 - U_0)\xi = U_0\xi^* + U_1\xi$$

Obviously the case in which the displacement of one end of the bar is restrained and the other end is subjected to an axial displacement is obtained by zeroing the respective displacement.

Gradient theory

For the gradient problem the bar is made of a material with microstructure. The classical BCs are the same as in the classical theory. Two sets of non-classical BCs need to be studied next.

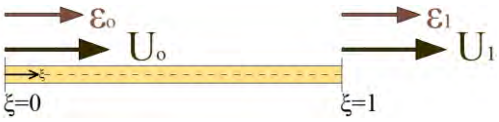

Fig. 69 Fixed-Fixed bar. The bar's ends displacements and strains are prescribed $\mathbf{u}(\xi=0)=U_0\hat{\mathbf{x}}$, $\mathbf{u}(\xi=1)=U_1\hat{\mathbf{x}}$ **and** $u'(\xi=0)=\varepsilon_0$, $u'(\xi=1)=\varepsilon_1$

In the first sub case the strain at both ends is prescribed, ε_0 and ε_1 respectively, i.e. the BCs are $u(\xi=0)=U_0$, $u(\xi=1)=U_1$, $u'(\xi=0)=\varepsilon_0$ and $u'(\xi=1)=\varepsilon_1$. This is a symmetrical problem, meaning that the BCs at both sides are of the same type. Thus the displacement field is expected to be symmetrical too. This means that the effect of each BC on the field must be symmetrical to the effect of its symmetrical BC, or more mathematically, the displacement field due to one BC – while the others are zero – can be obtained by substituting the ξ parameter with $\xi^*=1-\xi$ and the BC_i with $BC_i^{symm,}$ i.e

If $u,_{BCi}(\xi)=u_i(t=\xi)BC_i \quad\rightarrow\quad u,_{BCi^{symm}}(\xi)=u_i(t=\xi^*)BC_i^{symm}$

The displacement field of this problem takes the following form

$$u(\xi)=U_1\left\{\xi-\tanh(c/2)\frac{[1-2\xi]-\frac{\sinh\left[\frac{c}{2}(1-2\xi)\right]}{\sinh(c/2)}}{c-2\tanh(c/2)}\right\}+U_0\left\{\xi^*-\tanh(c/2)\frac{[1-2\xi^*]-\frac{\sinh\left[\frac{c}{2}(1-2\xi^*)\right]}{\sinh(c/2)}}{c-2\tanh(c/2)}\right\}$$

$$+\varepsilon_1 L\left\{\frac{\cosh(c\xi)-\xi\cosh(c)-\xi^*}{\sinh(c)\left[c-2\tanh(c/2)\right]}+\frac{1-\frac{\cosh\left[\frac{c}{2}(1-2\xi)\right]}{\cosh(c/2)}}{c\left[c-2\tanh(c/2)\right]}\right\}+\varepsilon_0 L\left\{\frac{\cosh(c\xi^*)-\xi^*\cosh(c)-\xi}{\sinh(c)\left[c-2\tanh(c/2)\right]}+\frac{1-\frac{\cosh\left[\frac{c}{2}(1-2\xi^*)\right]}{\cosh(c/2)}}{c\left[c-2\tanh(c/2)\right]}\right\}$$

It is reminded that the parameter c is non dimentional, and defined as c=L/g in the bar problems. As expected the solution is symmetrical thus the effect of only one of the symmetrical BCs - solutions will be discussed. The λ parameter does not effect the bars displacement or strain in this case. This fact can be attributed to the use of only 'holonomic' BCs, no dynamic ones.

In order to fully adress every problem possible, the solution is divided in two simpler ones, as done in the previous part of this work. In the first, the bar is fixed at one end while the other is subjected to an axial displacement U_1 and the strain at both ends is restrained, i.e. $u(\xi=0)=0$, $u(\xi=1)=U_1$ and $u'(\xi=0)=u'(\xi=1)=0$. The normalized displacement and the strain versus the normalized axial distance of the bar are given below. Also, the normalized double stresses distributions, for λ=0 and in the case that c=4, for different λ values are presented.

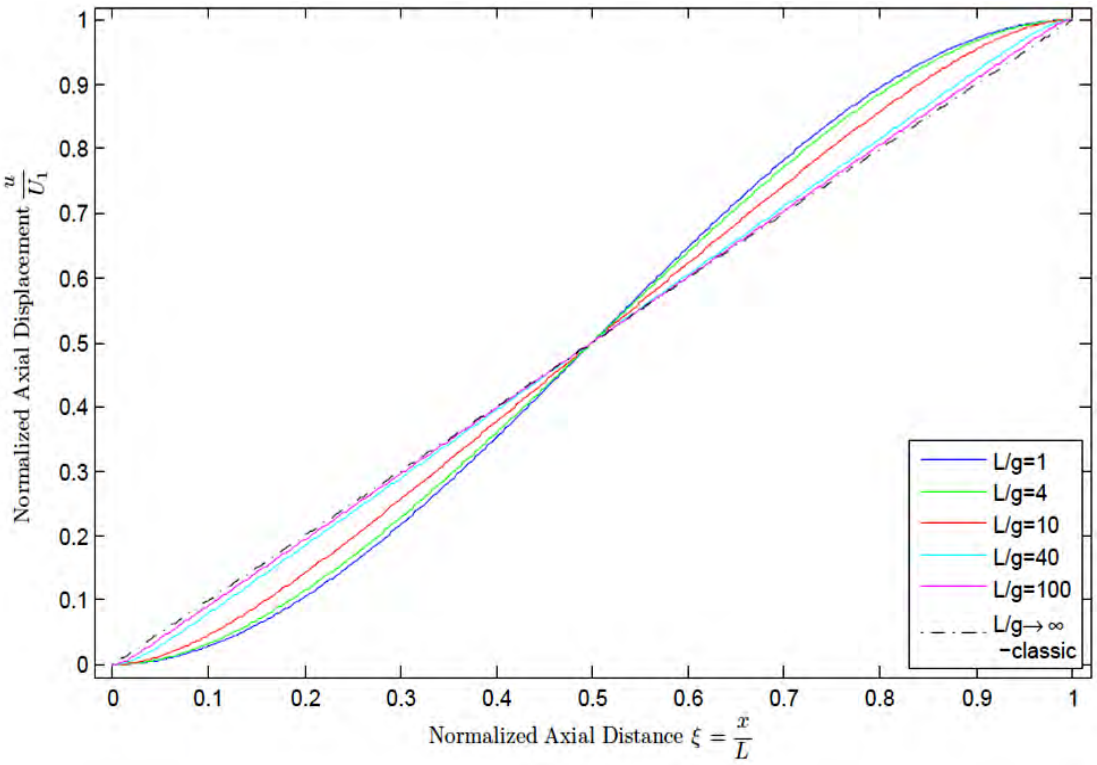

Fig. 70 Normalized axial displacement u/U_1 versus normalized axial distance $\xi = x/L$ of a Fixed-Fixed bar. The classical BCs are $u(\xi=0)=0$, $u(\xi=1)=U_1$, and the non classical ones $u'(\xi=0)=0$, $u'(\xi=1)=0$

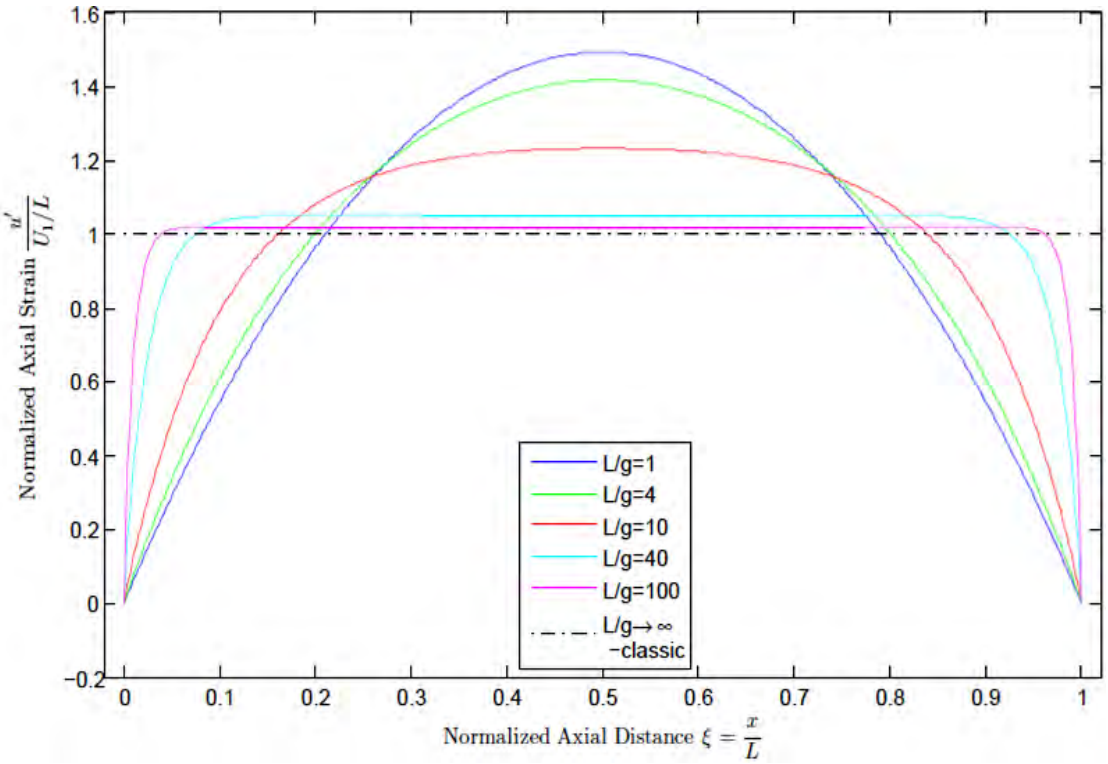

Fig. 71 Normalized axial strain $u'/(U_1/L)$ **versus normalized axial distance** $\xi = x/L$ **of a Fixed-Fixed bar. The classical BCs are** $u(\xi = 0) = 0$, $u(\xi = 1) = U_1$, **and the non classical ones** $u'(\xi = 0) = 0$, $u'(\xi = 1) = 0$

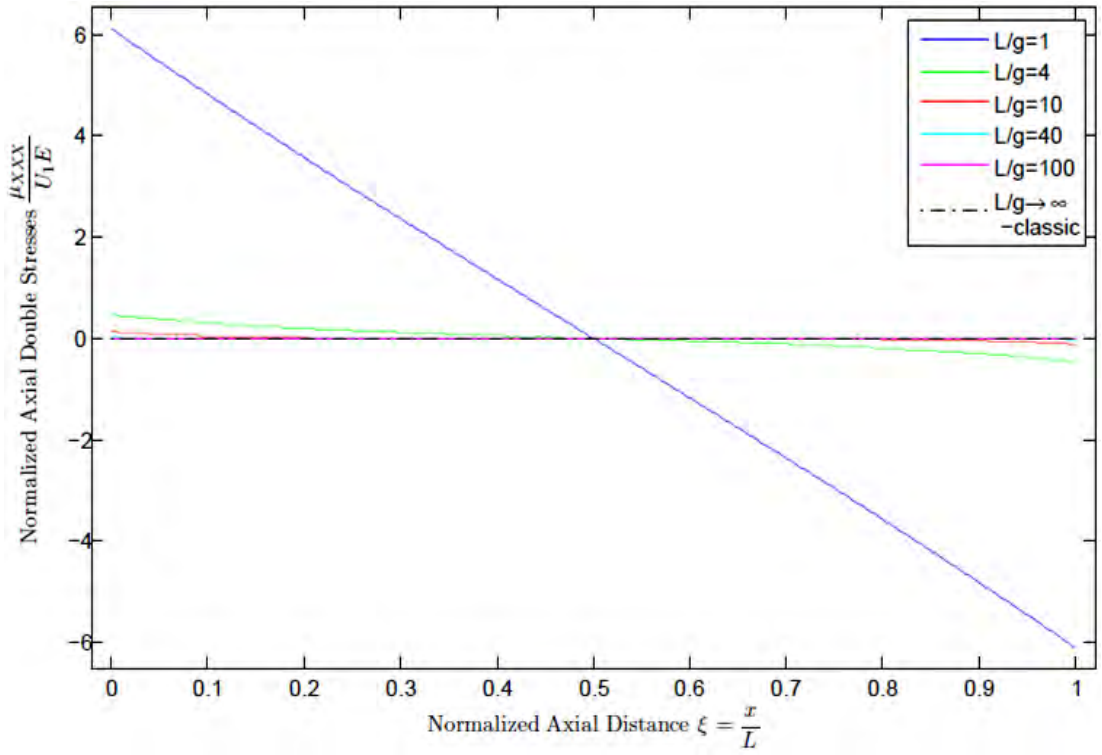

Fig. 72 Normalized axial double stresses $\mu_{xxx}/(U_1 E)$ **versus normalized axial distance** $\xi = x/L$ **of a Fixed-Fixed bar. The classical BCs are** $u(\xi = 0) = 0$, $u(\xi = 1) = U_1$, **and the non classical ones** $u'(\xi = 0) = 0$, $u'(\xi = 1) = 0$

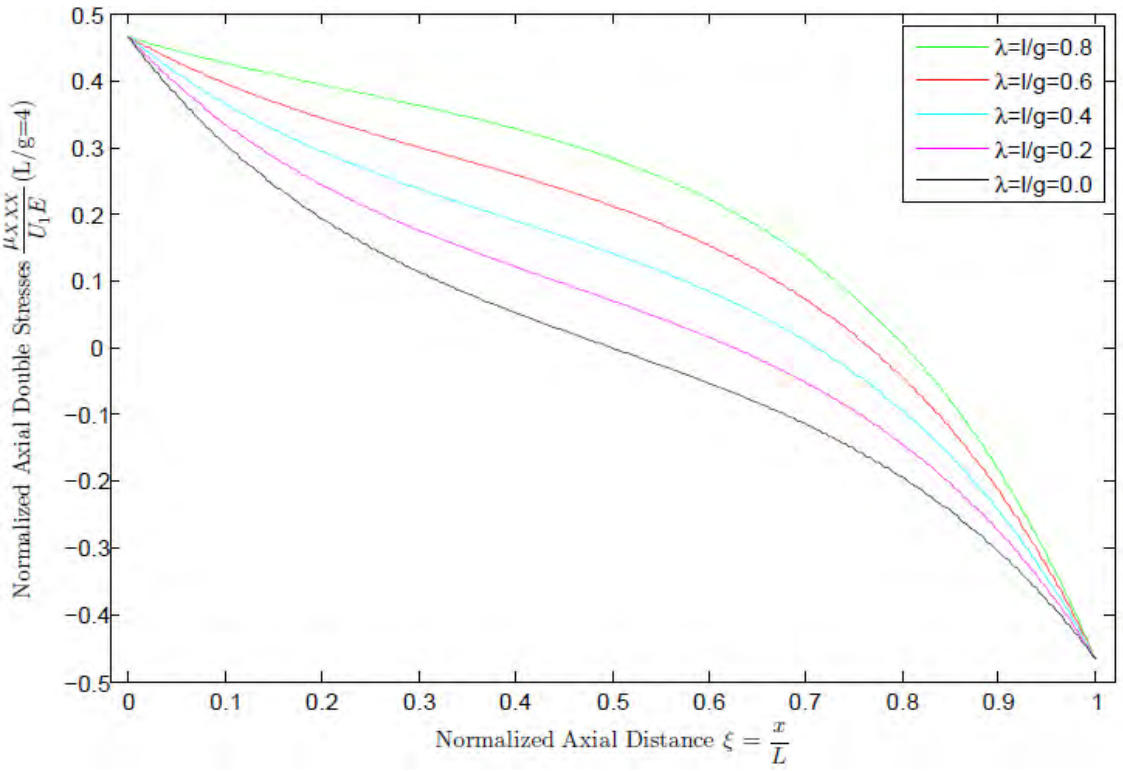

Fig. 73 Normalized axial double stresses $\mu_{xxx}/(U_1 E)$ **versus normalized axial distance** $\xi = x/L$ **of a Fixed-Fixed bar, for various λ values, and c=L/g=4. The classical BCs are** $u(\xi = 0) = 0$, $u(\xi = 1) = U_1$, **and the non classical ones** $u'(\xi = 0) = 0$, $u'(\xi = 1) = 0$

The following conclusions can be drawn.

Both the displacement and the strain fields depend on the L/g ratio, and as this ratio increases the bars behavior is reduced to the classical one. Due to the holonomic non-classical BC's, the strain at the bars ends is zero regardless of how great the c parameter might be, but the deviation from the classical solution decreases significantly as the c parameter takes great values and only close to the bars ends the deviation from the classical solution is significant. In other words, as a bar gets smaller, a greater part of its body is affected by the end effects/non classical BCs and its behavior deviates from the classical one, both displacement-wise and strain-wise.

The double stresses μ_{xxx} are strongly dependent to both the c and λ ratios. Increasing the c ratio induces a great reduction to both the greatest double-stress value, and the range of the bars length that these stresses are significant. Greater λ values (surface strain energy) result to greater

double stresses in the greater part of the bar, and at the same time eliminate the antisymmetry from the μ_{xx} distribution. The λ parameter does not affect the displacement or the strain field in this problem, since all degrees of freedom are confined.

It should be underlined though that the applied BCs - u'=0 - are very invasive in order to obtain a very non homogenous behavior from the bar. However, mathematically, by applying other strains at the bars ends, i.e $u'=(U_1-U_0)/L$, the solution obtained coincides with the classical one no matter the value of the c parameter.

The last conclusion is validated when studying the bars response to an applied strain when both its' ends are fixed, thus the BCs being $u(\xi=0)=0$, $u(\xi=1)=0$, $u'(\xi=0)=0$ and $u'(\xi=1)=\varepsilon_1$. The following figures describe this behavior for various L/g ratios and various λ parameter values in the case that c=4, since, when the λ parameter is inserted to the solution, too many parameter are present and it is impossible to plot one single normalized solution for every c and λ value.

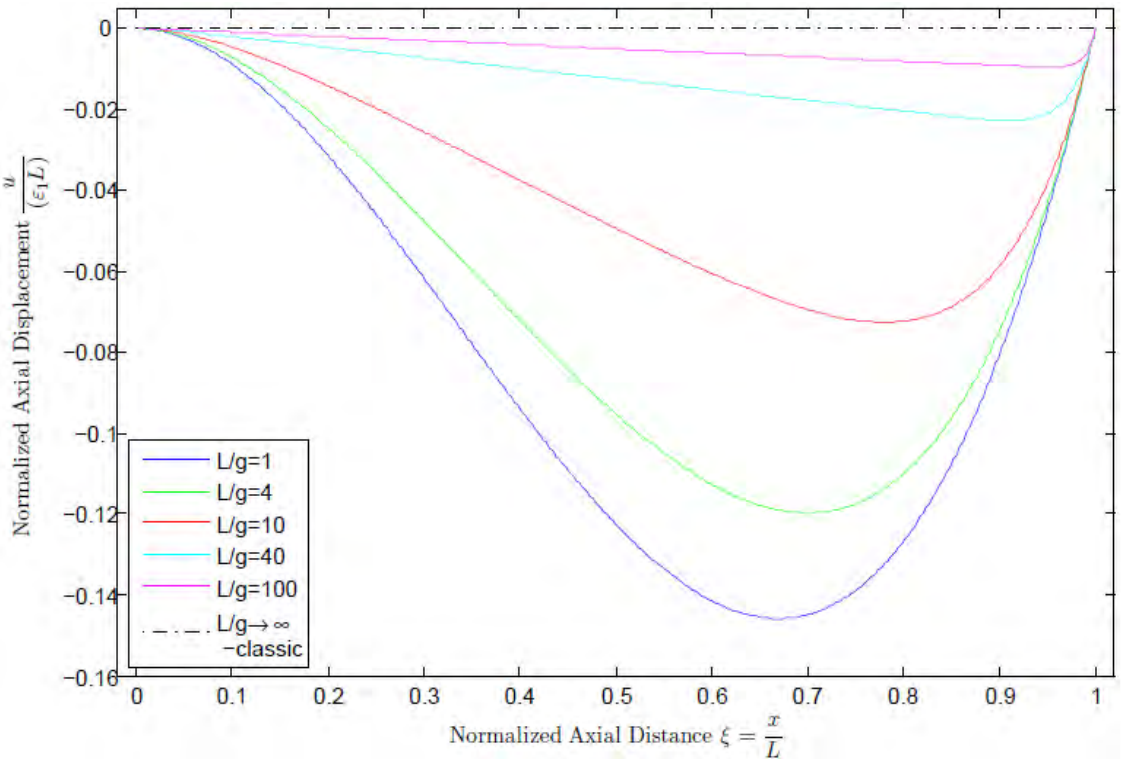

Fig. 74 Normalized axial displacement $u/(\varepsilon_1 L)$ versus normalized axial distance $\xi = x/L$ for a Fixed-Fixed bar. The classical BCs are $u(\xi=0)=0$, $u(\xi=1)=0$ and the non classical ones $u'(\xi=0)=0$, $u'(\xi=1)=\varepsilon_1$

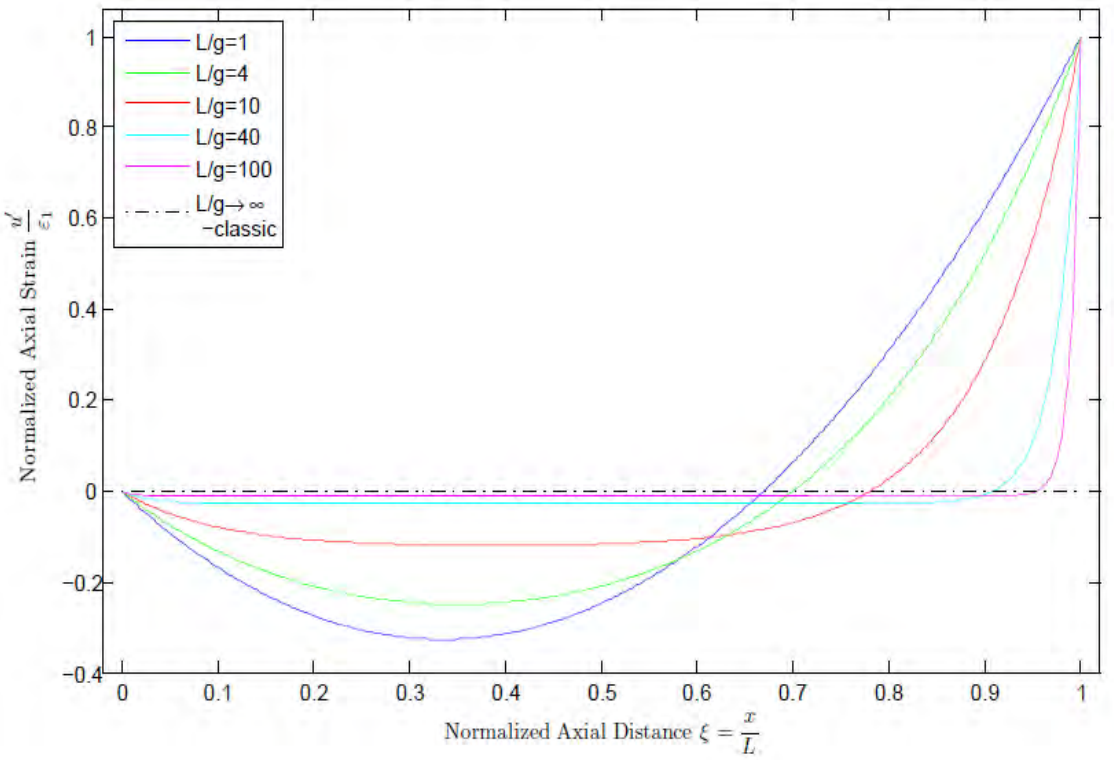

Fig. 75 Normalized axial strain u'/ε_1 **versus normalized axial distance** $\xi = x/L$ **of a Fixed-Fixed bar. The classical BCs are** $u(\xi = 0) = 0$, $u(\xi = 1) = 0$, **and the non classical ones** $u'(\xi = 0) = 0$, $u'(\xi = 1) = \varepsilon_1$

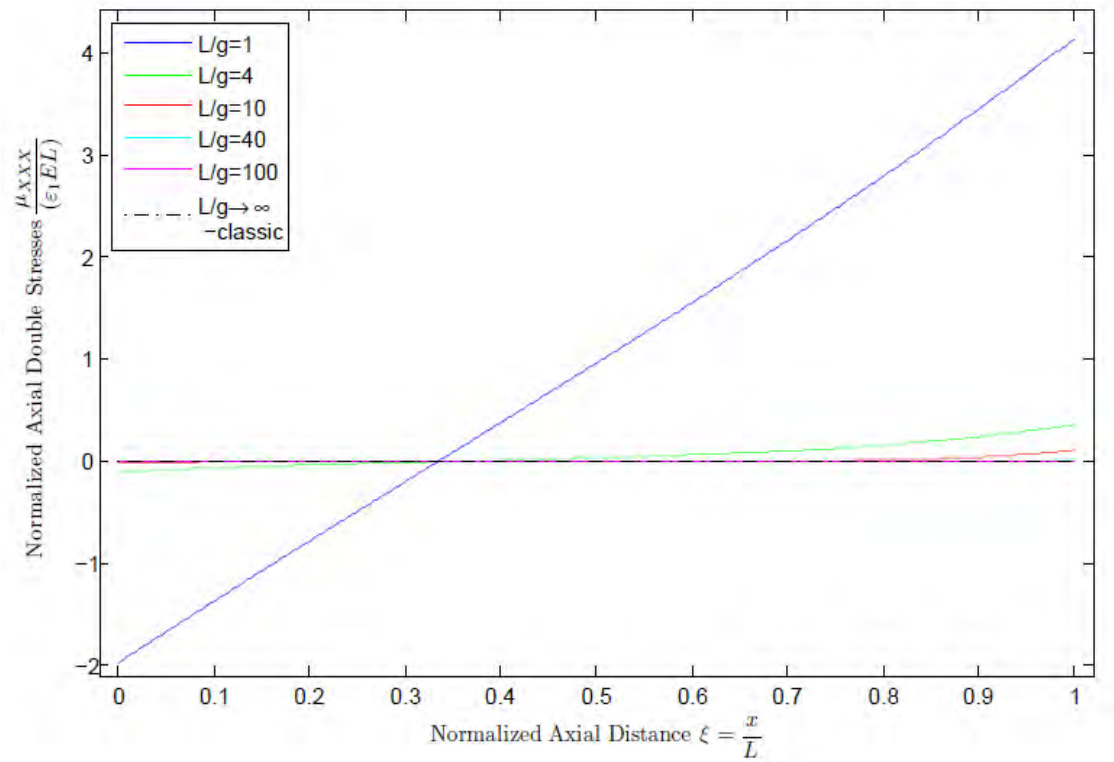

Fig. 76 Normalized axial double stresses $\mu_{xxx}/(\varepsilon_1 EL)$ **versus normalized axial distance** $\xi = x/L$ **Fixed-Fixed bar. The classical BCs are** $u(\xi = 0) = 0$, $u(\xi = 1) = 0$, **and the non classical ones** $u'(\xi = 0) = 0$, $u'(\xi = 1) = \varepsilon_1$

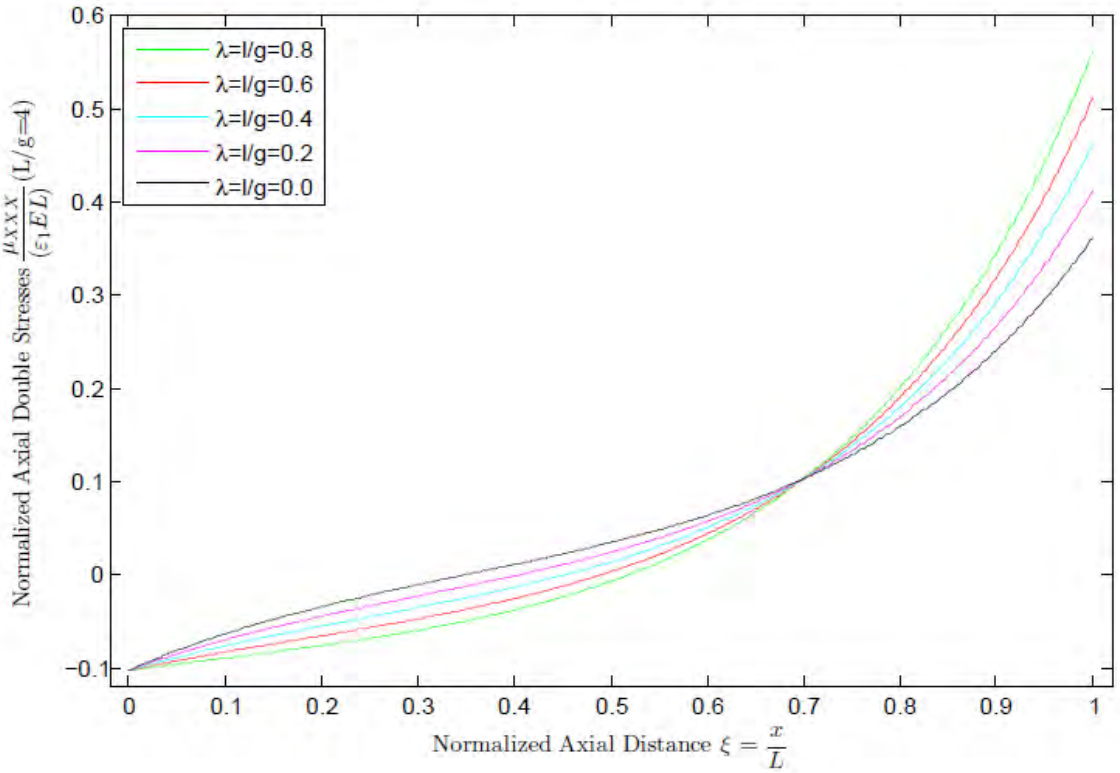

Fig. 77 Normalized axial double stresses $\mu_{xxx}/(\varepsilon_1 EL)$ versus normalized axial distance $\xi = x/L$, for c=4 and various λ values. The classical BCs are $u(\xi = 0) = 0$, $u(\xi = 1) = 0$, and the non classical ones $u'(\xi = 0) = 0$, $u'(\xi = 1) = \varepsilon_1$

Prescribing the strain at one end of the bar, while both ends displacements are restrained results to non uniform, non symmetrical displacement, strain and double forces fields. For great c values these fields tend to get zeroed in the better part of the bar, and differ only at its ends, so the effect of the non classical BC to the bar is reduced.

In order to apply these BCs, when the surface elastic strain energy is significant ($\lambda \neq 0$) greater double forces need to be applied, but always their maximum values appear at the bars ends.

Fig. 66 Fixed-Fixed bar. Subjected to axial displacaments $\mathbf{u}(\xi = 0) = U_0\hat{\mathbf{x}}$ and $\mathbf{u}(\xi = 1) = U_1\hat{\mathbf{x}}$ while the double forces at its ends are prescribed $R(\xi = 0) = R_0$ and $R(\xi = 1) = R_1$

Next, is investigated the behavior of a fixed-fixed bar, whose ends' strain is not directly prescribed, but type R BCs are applied i.e. the double forces at the ends of the bar are prescribed. The BCs are $u(\xi = 0) = U_0$ and $u(\xi = 1) = U_1$ and $R(\xi = 0) = R_0$ and $R(\xi = 1) = R_1$. This, too, is a symmetrical problem. The displacement field takes the following form in the case where the l parameter is zero

$$u(\xi) = U_1\xi + U_0\xi^* + \frac{R_1}{EA}\left[\frac{\sinh(c\xi)}{\sinh(c)} - \xi\right] + \frac{R_0}{EA}\left[\frac{\sinh(c\xi^*)}{\sinh(c)} - \xi^*\right]$$

The first part of this solution is the same as the classical one. This means that the bars behavior differs to its' classical behavior only if double forces R are applied at its ends. In other case, its response is classical regardless of how small the bar or how significant (how great the c=L/g ratio) the microstructure may be.

Hence, for a non-classical behavior from the bar, either double forces R are applied at its' ends, or their deformation is prescribed and different to the strain of the respective classical solution. Prescribed end strain, of course, means that double forces being applied, whose value depend on the prescribed end displacements and strains, as well as on material parameters as will be discussed.

Polizzoto (Polizzotto, 2003) made that observation too, and concluded that the way to obtain a classical behavior from a gradient elastic bar the non-classical BCs need to be u´´(ξ=0)=u´´(ξ=1)=0. This is not exactly accurate since it appears to be an arbitrary BC, more of a mathematical trick in order to obtain a linear solution. However, a posteriori can be said that this BC describes the condition of zeroing the double forces at the ends of the bar, in a case of a material of no surface strain energy (λ=0), which is the model Polizzoto used.

Since the first part of the solution is the same as the classical one, following, only the effect of double forces at the bars ends will be presented.

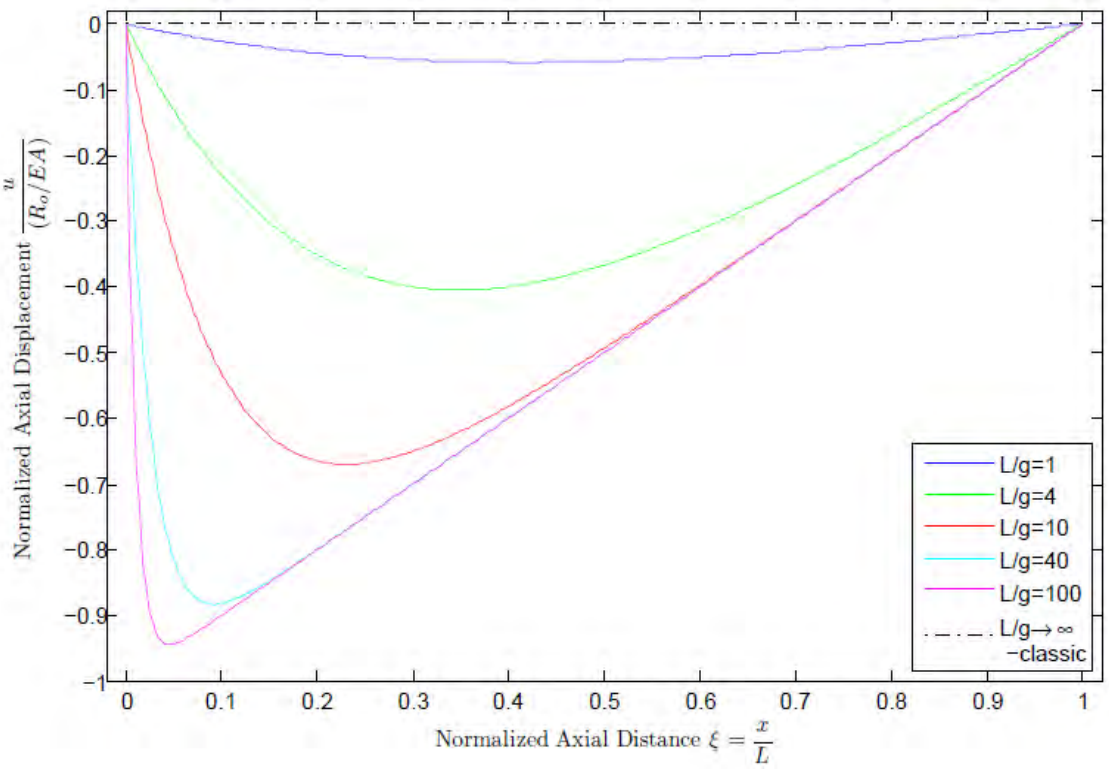

Fig. 79 Normalized axial displacement $u/(R_0/EA)$ **versus normalized axial distance** $\xi = x/L$ **of a Fixed-Fixed bar.. The classical BCs are** $u(\xi = 0) = 0$, $u(\xi = 1) = 0$, **and the non classical ones** $R(\xi = 0) = R_0$, $R(\xi = 1) = 0$

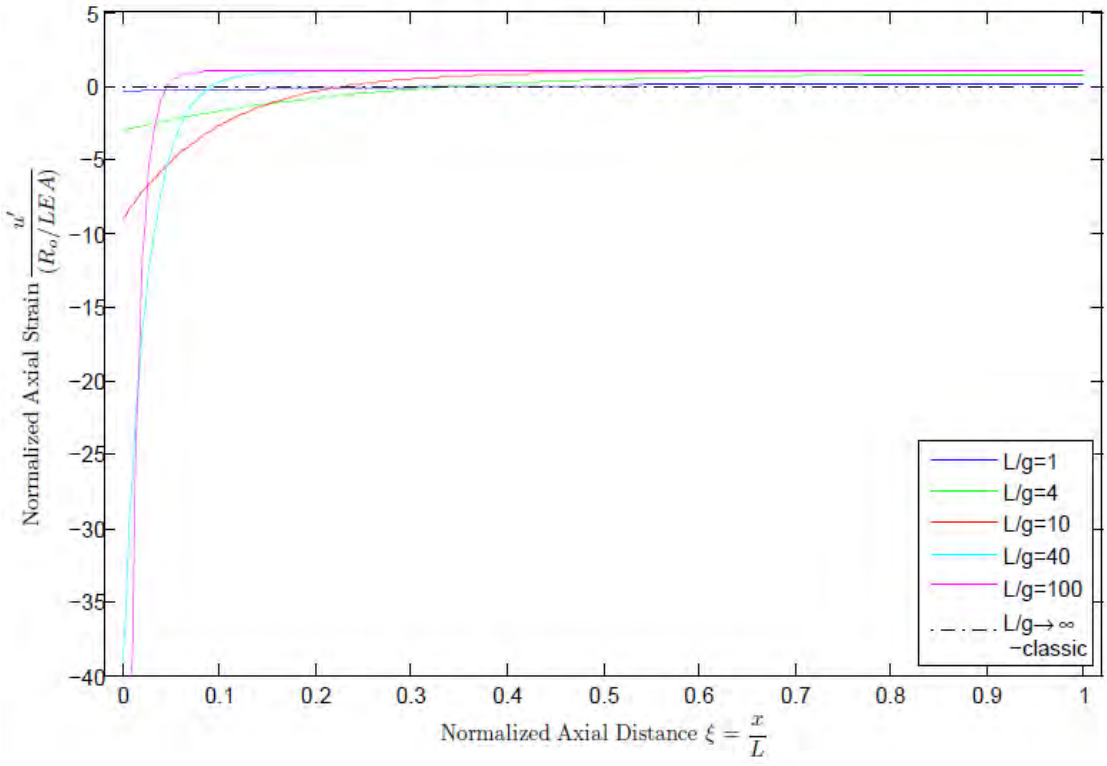

Fig. 80 Normalized axial strain $u'/(R_0/LEA)$ **versus normalized axial distance** $\xi = x/L$ **of a Fixed-Fixed bar. The classical BCs are** $u(\xi = 0) = 0$, $u(\xi = 1) = 0$, **and the non classical ones** $R(\xi = 0) = R_0$, $R(\xi = 1) = 0$

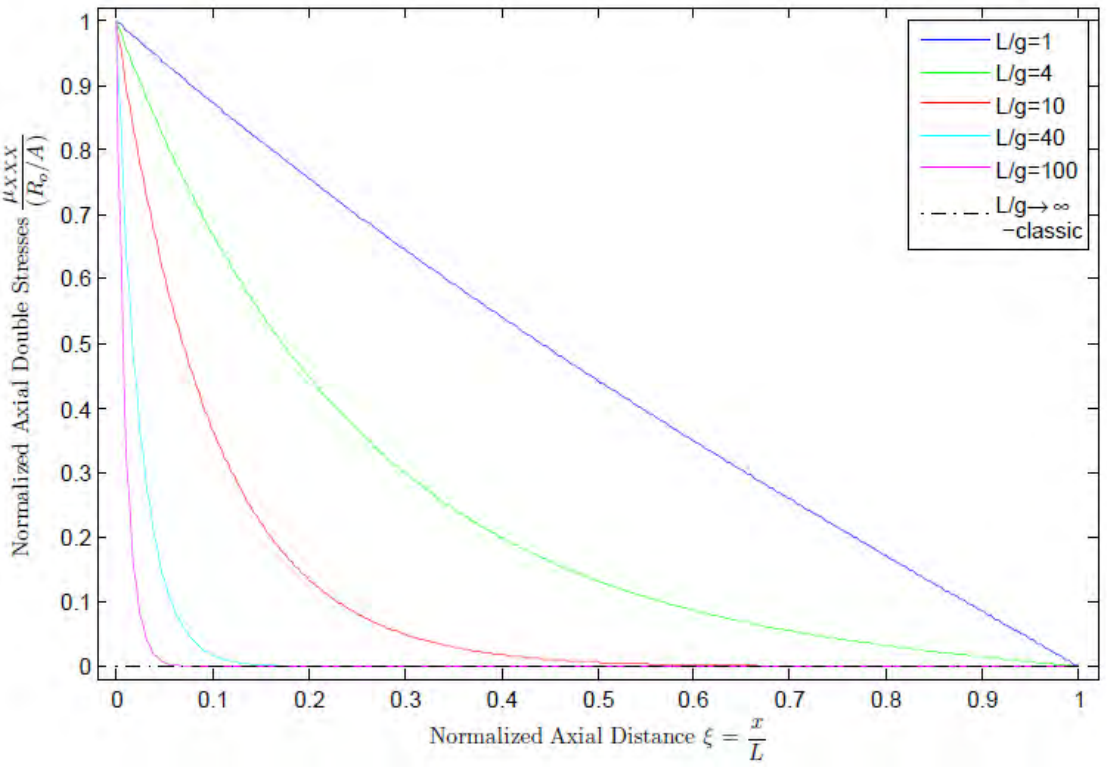

Fig. 81 Normalized axial double stresses $\mu_{xxx}/(R_0/A)$ versus normalized axial distance $\xi = x/L$ of a Fixed-Fixed bar. The classical BCs are $u(\xi=0)=0$, $u(\xi=1)=0$, and the non classical ones $R(\xi=0)=R_0$, $R(\xi=1)=0$

In the graphs above the displacements do not approach the classical solution as the c=L/g parameter increases. This behavior is attributed the restriction the bar's ends displacement. As will be shown further on, the application of double forces at a free bars end affects its length. The bar elongates when the double forces direction is away from the bars center, and it shortens in the opposite case. The R_0 double forces' direction is towards the center of the bar so the bar tends to get shorter. By restraining the bars' ends movement, practically an opposite displacement to the one that resulted from the application of the double forces, is applied, which is a hidden classical kind of load, responsible for this seemingly odd, non classical behavior.

In the case of R_1 whose direction is outwards of the bar, the double forces effect elongates the bar, and the confined displacement of its ends imposes a hidden classical set of BCs, too. As a result, for great c parameter values, the displacement field is not reduced to a zero field, which was originally thought to be the respective classical problem's solution.

When the λ parameter is significant the behavior of the bar deviates drastically from the classical one, even in the case where only classical BCs are applied. The displacement field takes the following form:

$$u(\xi) = u_{\lambda=0}(\xi) + \Lambda_1 u_{\Lambda_1}(\xi) + \Lambda_2 u_{\Lambda_2}(\xi),$$

$u_{\lambda=0}(\xi)$ being the displacement field in the case that λ=0, described above,

$$\Lambda_1 = \frac{\lambda}{c - \lambda^2\left(c - 2\tanh(c/2)\right)}, \qquad \Lambda_2 = \frac{\lambda^2}{c - \lambda^2\left(c - 2\tanh(c/2)\right)} = \lambda\Lambda_1 \text{ and}$$

$$u_{\Lambda_1}(\xi) = \left[1 - \frac{\cosh\left((1-2\xi)c/2\right)}{\cosh(c/2)}\right]\left\{U_1 - U_0 - \frac{R_1}{EA} + \frac{R_0}{EA}\right\}$$
$$+ c\tanh(c/2)\left[\xi - \frac{\cosh(c\xi) - 1}{\cosh(c) - 1} - \right]\frac{R_1}{EA} \qquad - c\tanh(c/2)\left[\xi^* - \frac{\cosh(c\xi^*) - 1}{\cosh(c) - 1} - \right]\frac{R_0}{EA}$$

$$u_{\Lambda_2}(\xi) = \tanh(c/2)\left[1 - 2\xi - \frac{\sinh\left((1-2\xi)c/2\right)}{\sinh(c/2)}\right]U_1 + \tanh(c/2)\left[1 - 2\xi^* - \frac{\sinh\left((1-2\xi^*)c/2\right)}{\sinh(c/2)}\right]U_0$$
$$+ \left(c - 2\tanh(c/2)\right)\left[\frac{\sinh(c\xi)}{\sinh(c)} - \xi\right]\frac{R_1}{EA} \qquad + \left(c - 2\tanh(c/2)\right)\left[\frac{\sinh(c\xi^*)}{\sinh(c)} - \xi^*\right]\frac{R_0}{EA}$$

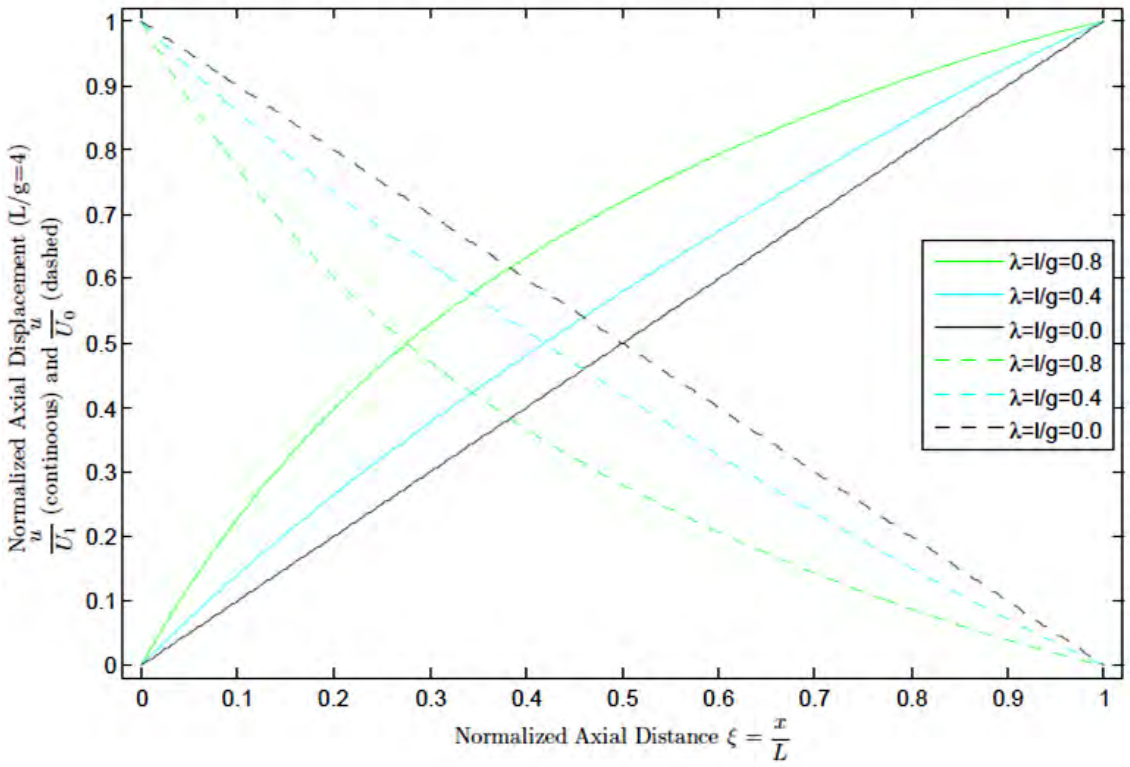

Fig. 82 Normalized axial displasement u/U_1 (cont), u/U_0 dashed, $L/(g=4)$ **versus normalized axial distance** $\xi = x/L$ **of a. Fixed-Fixed bar, for various λ values when c=L/g=4.**

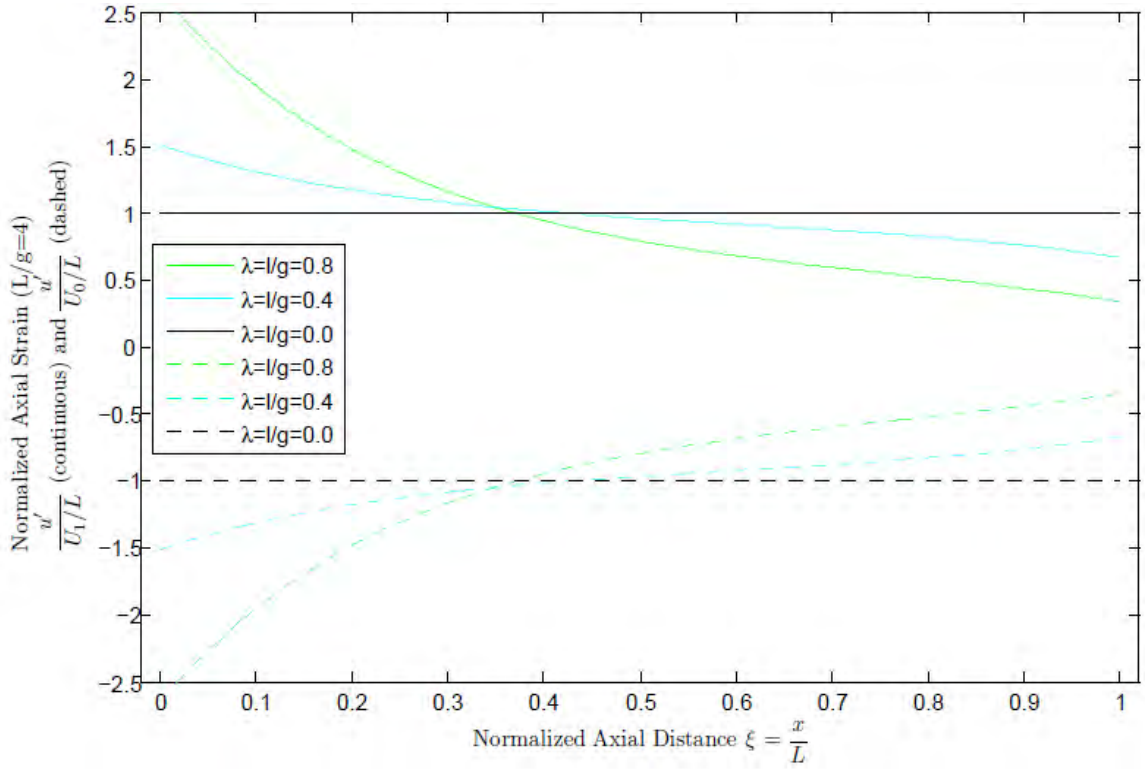

Fig. 83 Normalized axial strain $u'/(U_1/L)$ **(continuous),** $u'/(U_0/L)$ **(dashed) versus normalized axial distance** $\xi = x/L$ **of a Fixed-Fixed bar, for c=L/g=4 and various λ values**

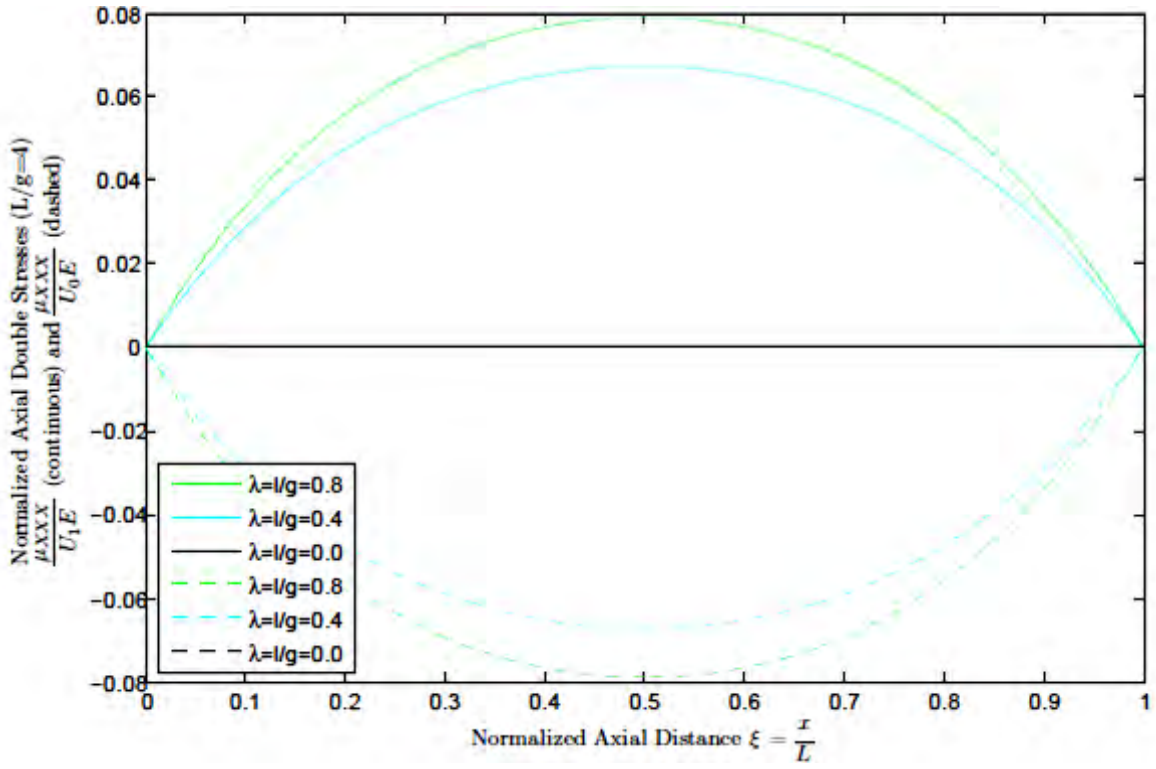

Fig. 867 Normalized axial double stresses $\mu_{xxx}/U_1 E$ **(continuous),** $\mu_{xxx}/U_0 E$ **(dashed) versus normalized axial distance** $\xi = x/L$ **of a Fixed-Fixed bar, for c=L/g=4 and various λ values**

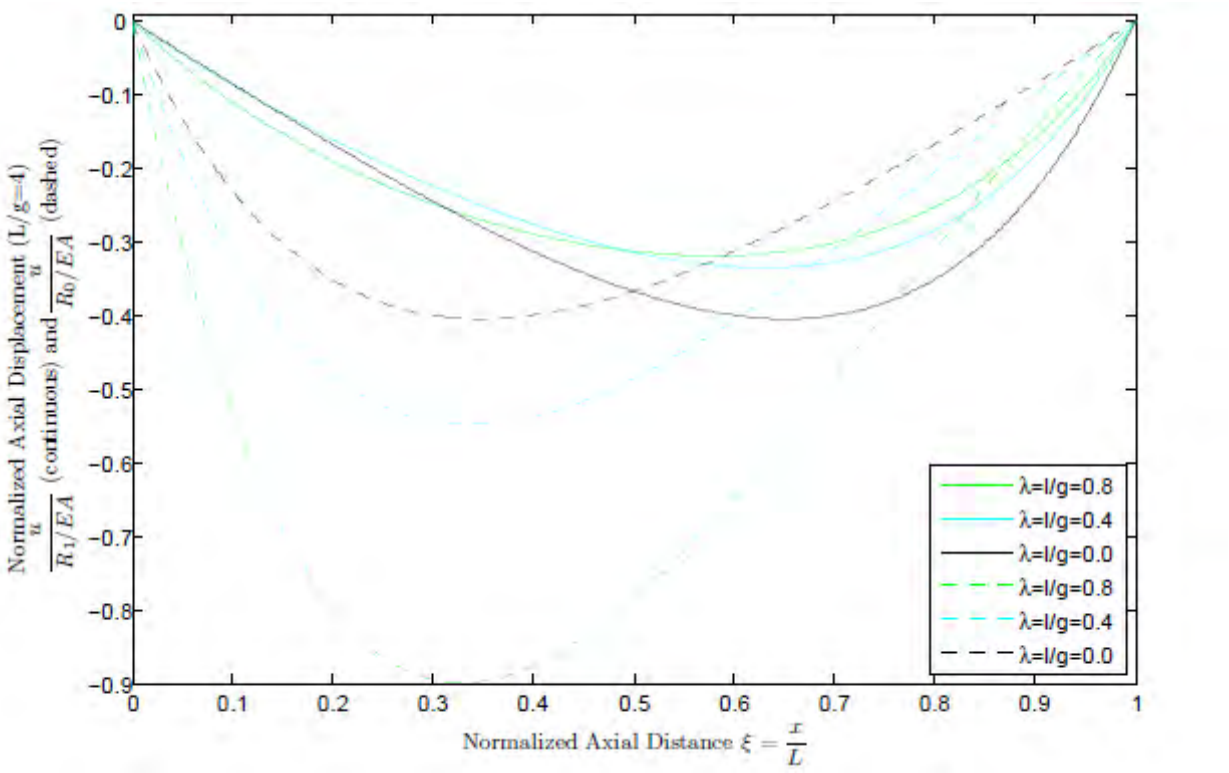

Fig. 85 Normalized axial displacement $u/(R_1/EA)$ **(continuous),** $u/(R_0/EA)$ **(dashed) versus normalized axial distance** $\xi = x/L$ **of a Fixed-Fixed bar, for c=L/g=4 and various λ values**

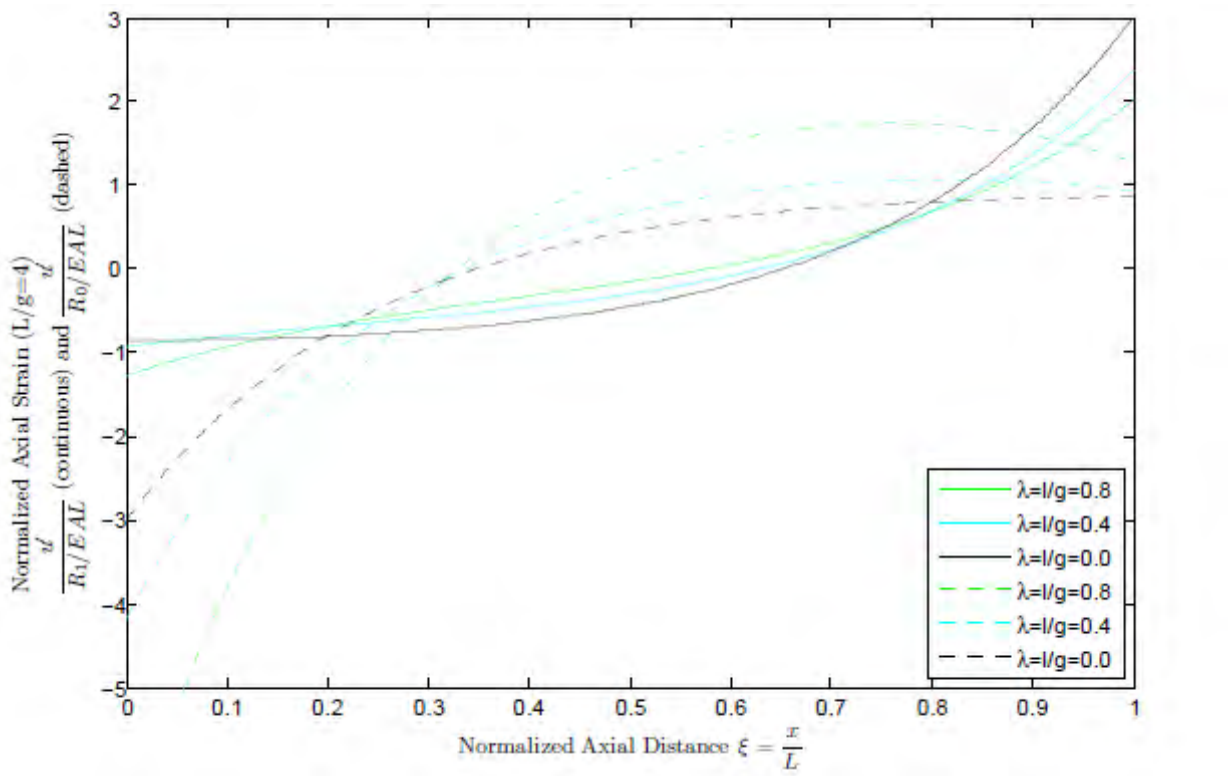

Fig. 86 Normalized axial strain $u'/(R_1/EAL)$ **(continuous),** $u'/(R_0/EAL)$ **(dashed) versus normalized axial distance** $\xi = x/L$ **of a Fixed-Fixed bar, for c=L/g=4 and various λ values**

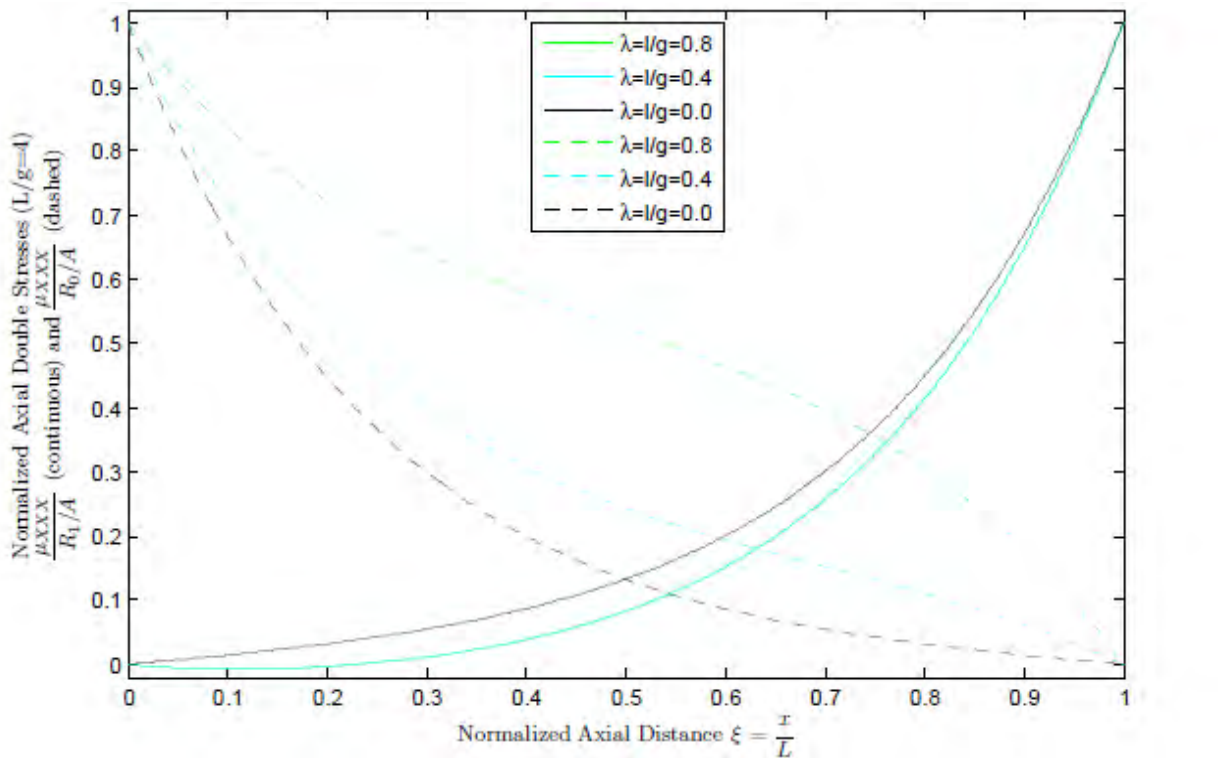

Fig. 87 Normalized axial double stresses $\mu_{xxx}/(R_1/EAL)$ (continuous), $\mu_{xxx}/(R_0/EAL)$ (dashed) versus normalized axial distance $\xi = x/L$ of a Fixed-Fixed bar, for c=L/g=4 and various λ values

The effect of the λ parameter on the bars behavior is displayed in the graphs above, for a bar of c value of four (c=4). Since, the λ parameter eliminates any symmetry from the solution, the effect of a BC is different on each end of the bar. In each of the graphs above, two cases are addressed. In the first three, the effect of an imposed displacement to each bar's end presented. In the last three, the effect of applied double forces at each bars end while no double forces are applied to the other is presented.

The λ parameter, i.e. the presence of surface energy affects strongly the displacement and deformation fields of a bar. When only classical BCs are applied, the surface energy effect on these fields has a level of symmetry. However, when non classical BCs are applied, their effect is very strong and all symmetry is eliminated from those fields. The presence of surface energy in this form, though, is rarely taken into account since it rarely is observed, and, also, following the Kordolemis (Kordolemis, et al., 2013) analogy, seems to be linked with anti symmetric properties and behaviors that until recently were not commonly used. In this case, too, in which surface energy is present and the bars behavior gets very complicated, a classical behavior can be anticipated when the double forces applied are $R_0 = R_1 = EA\ l\ (U_1-U_0) / L$.

Fig. 88 Fixed-Free bar. The BCs are $\mathbf{u}(\xi=0)=U_0\hat{\mathbf{x}}$, $\mathbf{P}(\xi=1)=P_1\hat{\mathbf{x}}$

Classical theory

In the case of a fixed-free bar, one end of the bar is subjected to an axial displacement U_0 while the other one is free and subjected to a tensile force P, thus the BCs can be expressed as $u(\xi=0)=U_0$ and $P(\xi=1)=P_1$. The solution to this problem that follows solution is very simple, well known and easily obtained.

Fig. 89 Fixed-Fixed bar. The BCs are $\mathbf{u}(\xi=0)=U_0\hat{\mathbf{x}}$, $\mathbf{u}(\xi=1)=U_1\hat{\mathbf{x}}$

$$u(\xi)=U_0+P_1\xi$$

Gradient theory

In the gradient case, the bar is made of a material with microstructure . The classical BCs are the same as before. Two sets of non-classical BCs are studied next.

In the first sub case, the strain of the both ends of the bar is prescribed, ε_0 and ε_1 respectively. The BCs are $u(\xi=0)=U_0$ and $P(\xi=1)=P_1$ and $u'(\xi=0)=\varepsilon_0$ and $u'(\xi=1)=\varepsilon_1$. This is not a symmetrical problem in respect to the BCs, so the displacement field is also not expected to be symmetrical. The displacement field takes the following form:

$$u(\xi)=Uo+\frac{P_1}{EA}\left\{\xi-\frac{\tanh(c/2)}{c}\left[1-\frac{\sinh\left(\frac{c}{2}(1-2\xi)\right)}{\sinh(c/2)}\right]\right\}$$

$$+\varepsilon_1 L\left[\frac{\cosh(c\xi)-1}{c\sinh(c)}\right]+\varepsilon_0 L\left[\frac{\cosh(c)-\cosh(c\xi^*)}{c\sinh(c)}\right]$$

The field indeed is not a symmetric one, so the effect of each BC will be presented separately. First, a bar under tension with restrained ends strain is considered. As shown in the following figures, the behavior of the bar is stiffer than the classical bar behavior. However, for great c values, the solution approaches the classical one, and only at the ends of the bar the fields deviate from their classical form. The double stresses are localized only near the ends and their values are smaller, for greater c values.

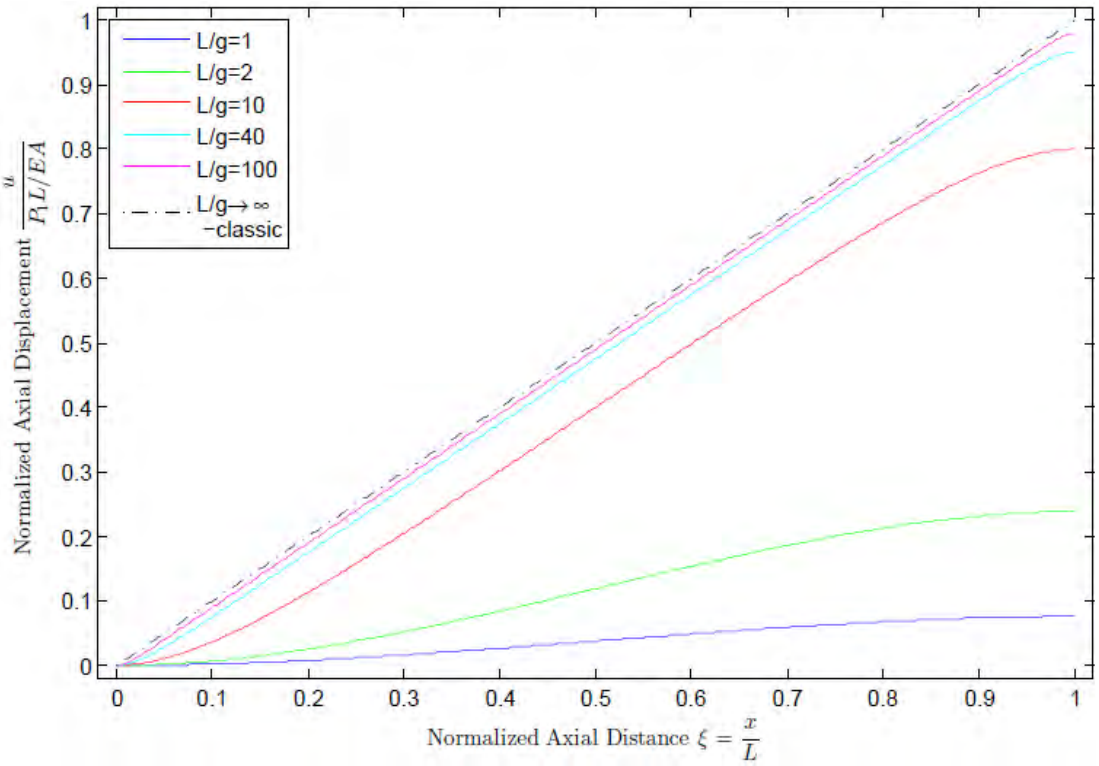

Fig. 90 Normalized axial displacement $u / P_1 L / EA$ **versus normalized axial distance** $\xi = x / L$ **of a Fixed-Free bar. The classical BCs are** $u(\xi = 0) = 0$, $P(\xi = 1) = P_1$, **and the non classical ones** $u'(\xi = 0) = 0$, $u'(\xi = 1) = 0$

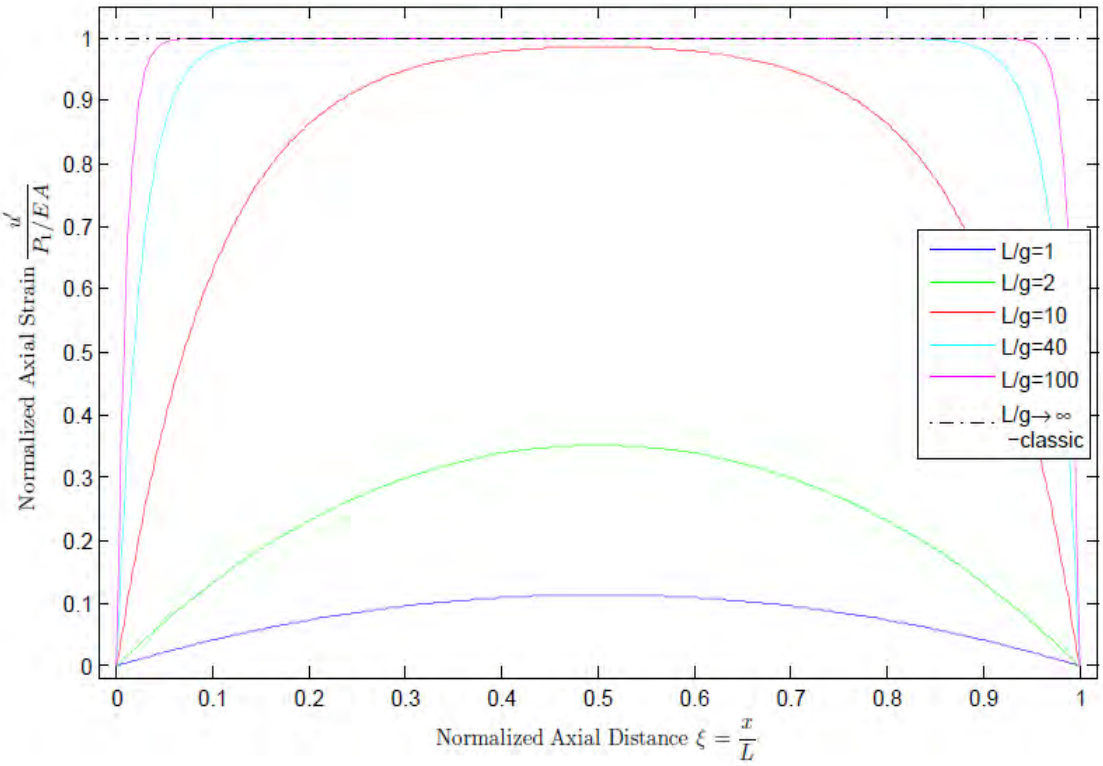

Fig. 91 Normalized axial strain $u' / P_1 EA$ **versus normalized axial distance** $\xi = x / L$ **of a Fixed-Free bar. The classical BCs are** $u(\xi = 0) = 0$, $P(\xi = 1) = P_1$, **and the non classical ones** $u'(\xi = 0) = 0$, $u'(\xi = 1) = 0$

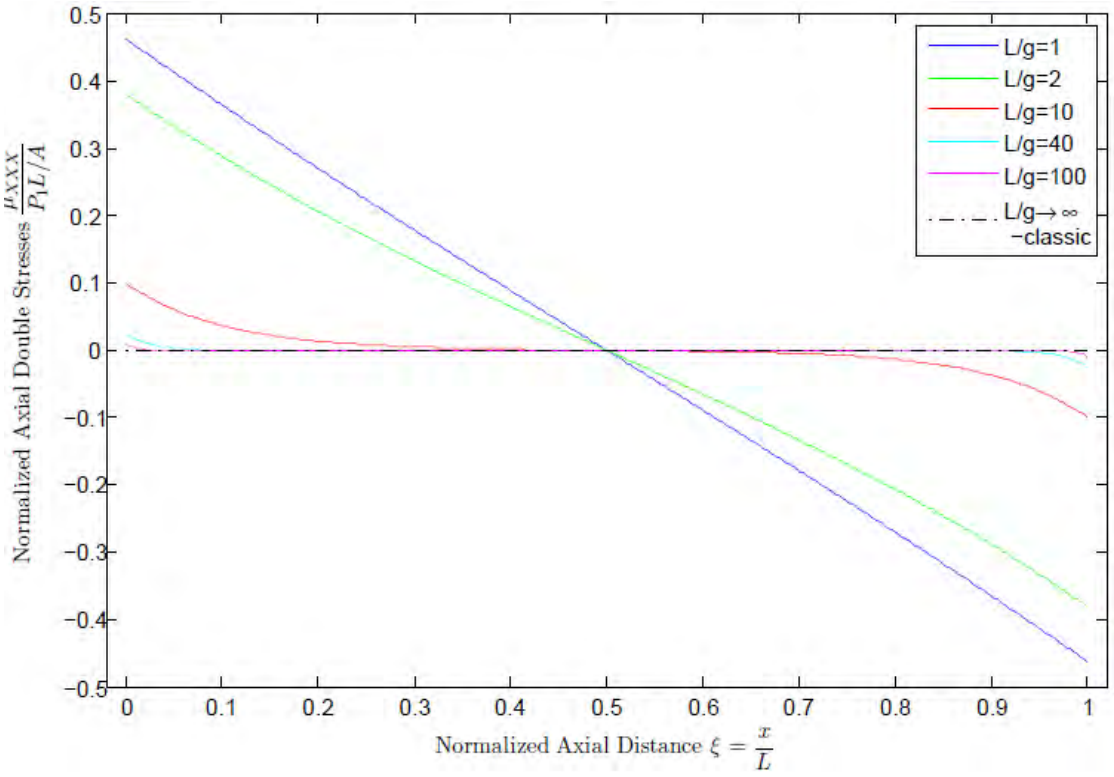

Fig. 92 Normalized axial double stresses $\mu_{xxx}/(P_1 L/A)$ **versus normalized axial distance** $\xi = x/L$ **of Fixed-Free bar. The classical BCs are** $u(\xi=0)=0$, $P(\xi=1)=P_1$, **and the non classical ones** $u'(\xi=0)=0$, $u'(\xi=1)=0$

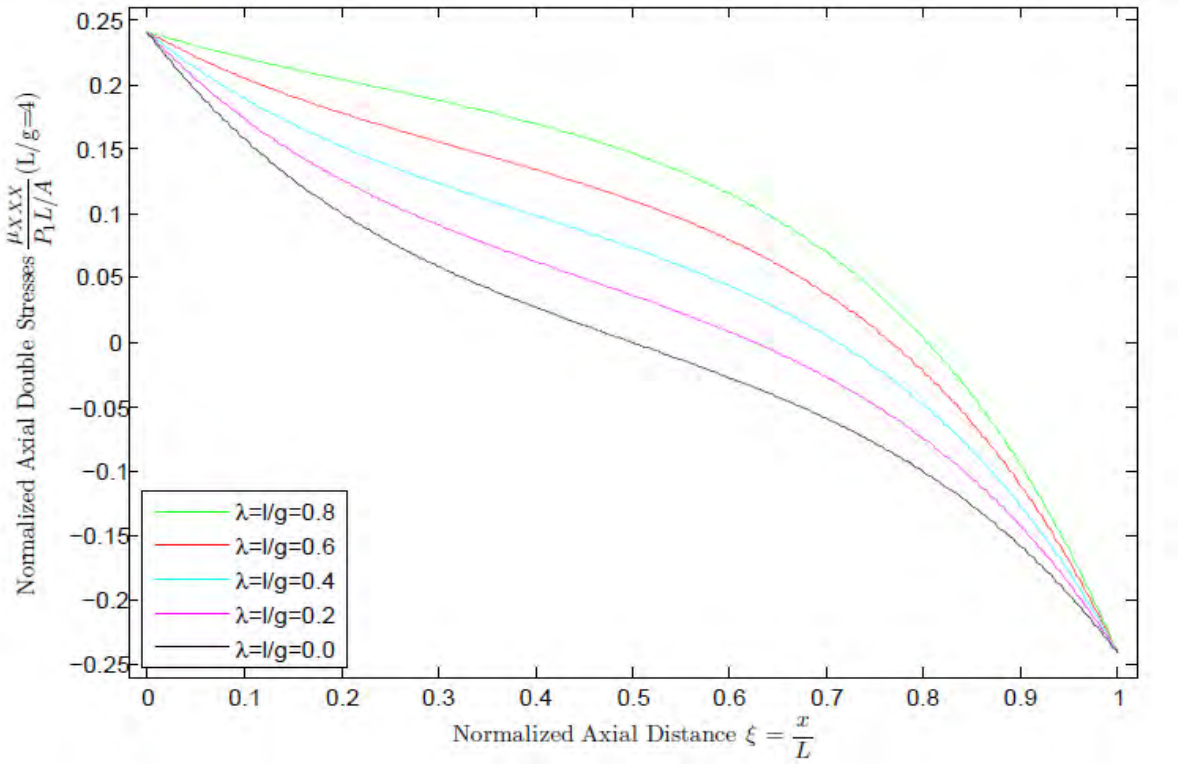

Fig. 93 Normalized double stresses $\mu_{xxx}/(P_1 L/A)$ **versus normalized axial distance** $\xi = x/L$ **of a Fixed-Free bar, for c=4 and varius λ values. The classical BCs are** $u(\xi=0)=0$, $P(\xi=1)=P_1$, **and the non classical ones** $u'(\xi=0)=0$, $u'(\xi=1)=0$

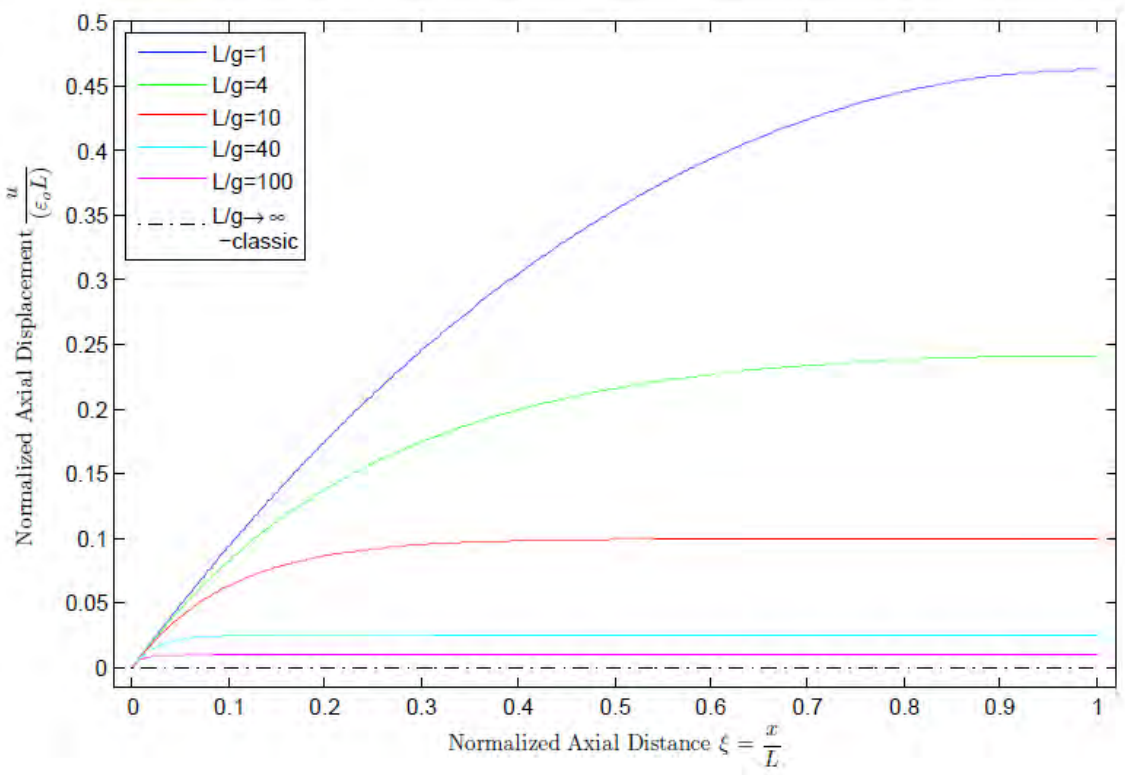

Fig. 94 Normalized axial displacement $u/\varepsilon_1 L$ **versus normalized axial distance** $\xi = x/L$ **of a Fixed-Free bar. The classical BCs are** $u(\xi = 0) = 0$, $u(\xi = 1) = 0$, **and the non classical ones** $u'(\xi = 0) = \varepsilon_0$, $u'(\xi = 1) = 0$

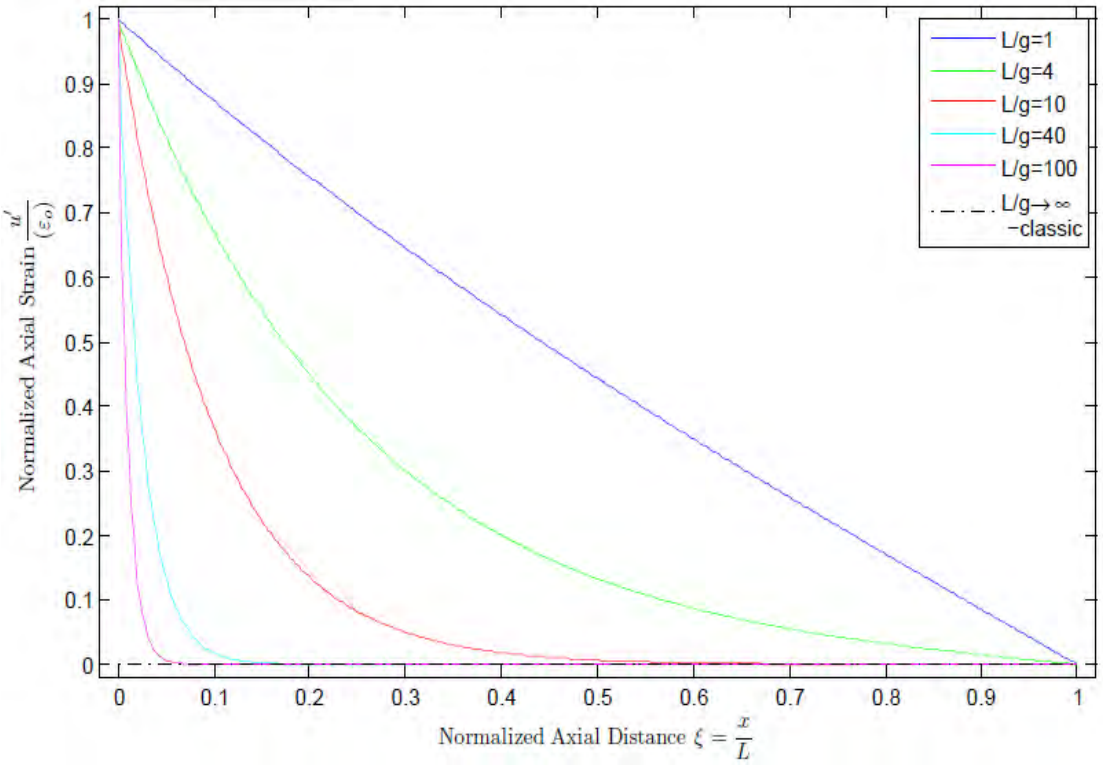

Fig. 95 Normalized axial displacement u'/ε_0 **versus normalized axial distance** $\xi = x/L$ **of a Fixed-Free bar. The classical BCs are** $u(\xi = 0) = 0$, $u(\xi = 1) = 0$, **and the non classical ones** $u'(\xi = 0) = \varepsilon_0$, $u'(\xi = 1) = 0$

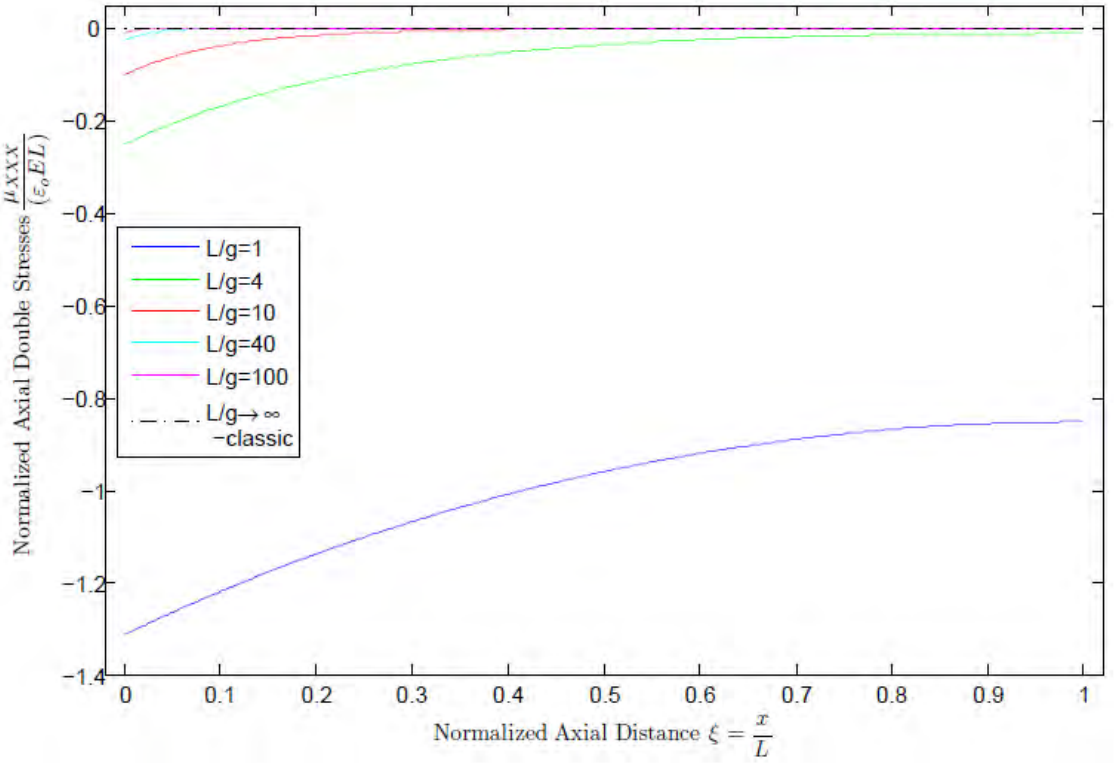

Fig. 96 Normalized axial double stresses $\mu_{xxx}/(\varepsilon_0 EL)$ **versus normalized axial distance** $\xi = x/L$ **of a Fixed-Free bar. The classical BCs are** $u(\xi=0)=0$, $u(\xi=1)=0$, **and the non classical ones** $u'(\xi=0)=\varepsilon_0$, $u'(\xi=1)=0$

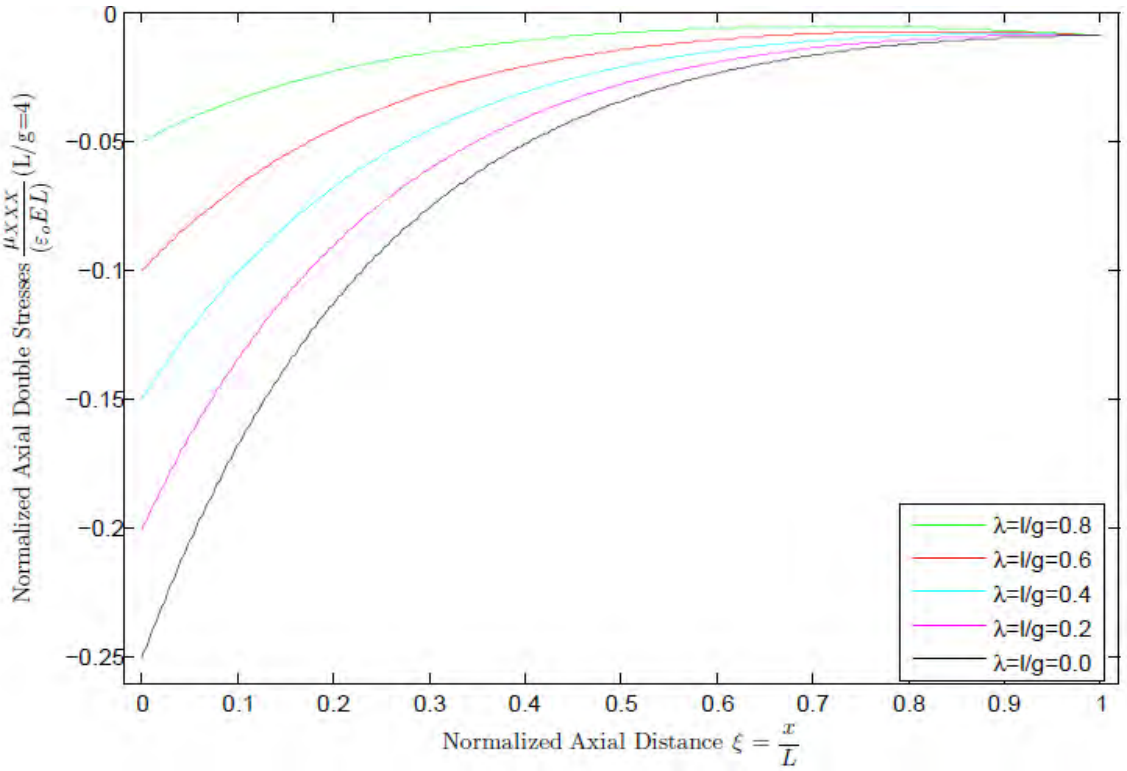

Fig. 97 Normalized axial double stresses $\mu_{xxx}/(\varepsilon_0 EL)$ **versus normalized axial distance** $\xi = x/L$ **of a Fixed-Free bar, for c=L/g=4 and various λ values**

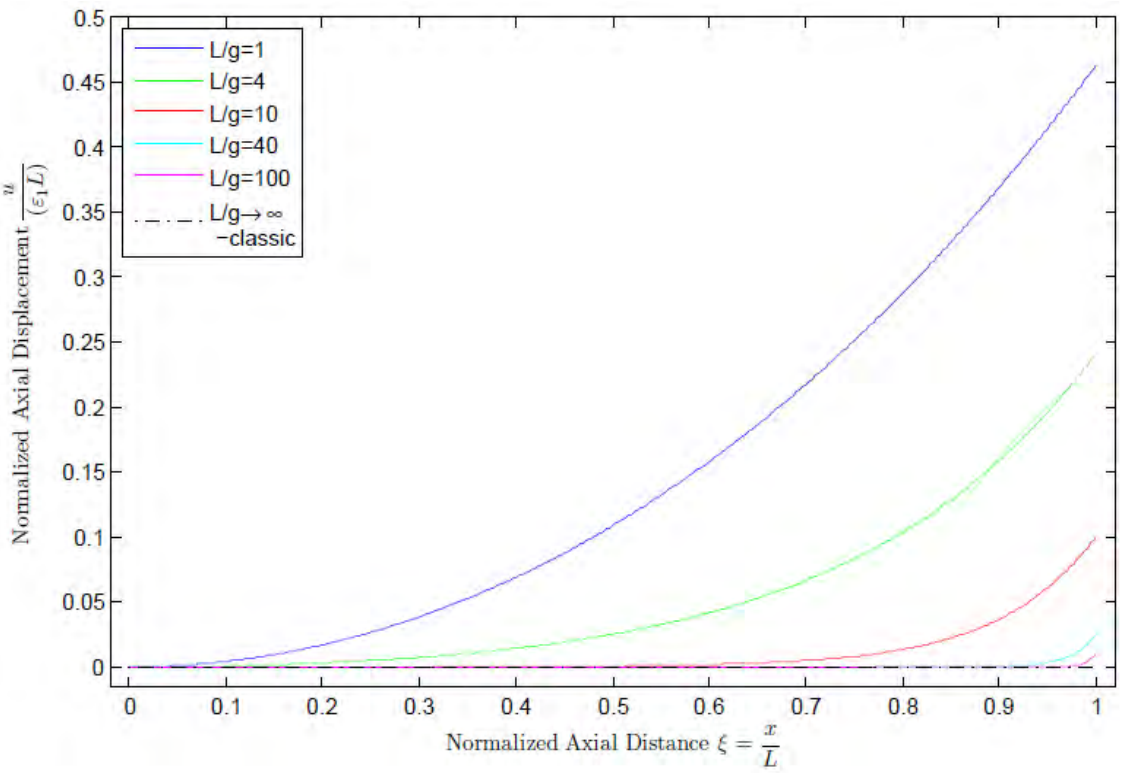

Fig. 98 Normalized axial displacement $u/\varepsilon_1 L$ **versus normalized axial distance** $\xi = x/L$ **of a Fixed-Free bar. The classical BCs are** $u(\xi = 0) = 0$, $u(\xi = 1) = 0$, **and the non classical ones** $u'(\xi = 0) = 0$, $u'(\xi = 1) = \varepsilon_1$

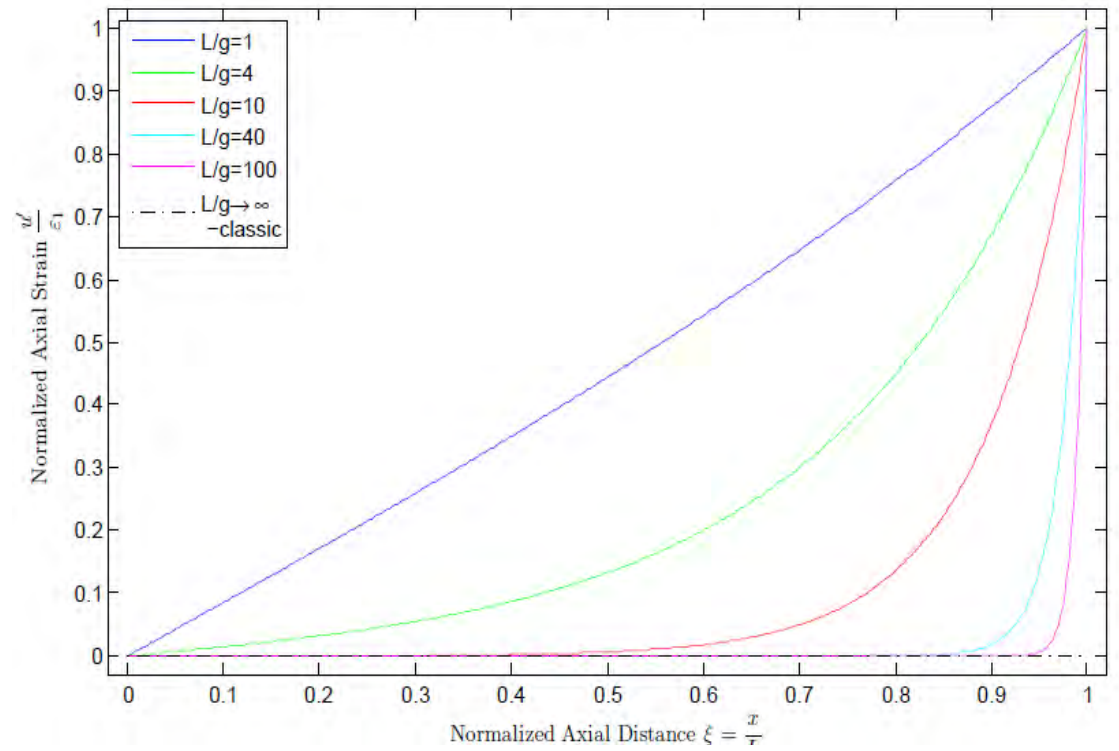

Fig. 99 Normalized axial strain u'/ε_1 **versus normalized axial distance** $\xi = x/L$ **of a Fixed-Free bar. The classical BCs are** $u(\xi = 0) = 0$, $u(\xi = 1) = 0$, **and the non classical ones** $u'(\xi = 0) = 0$, $u'(\xi = 1) = \varepsilon_1$

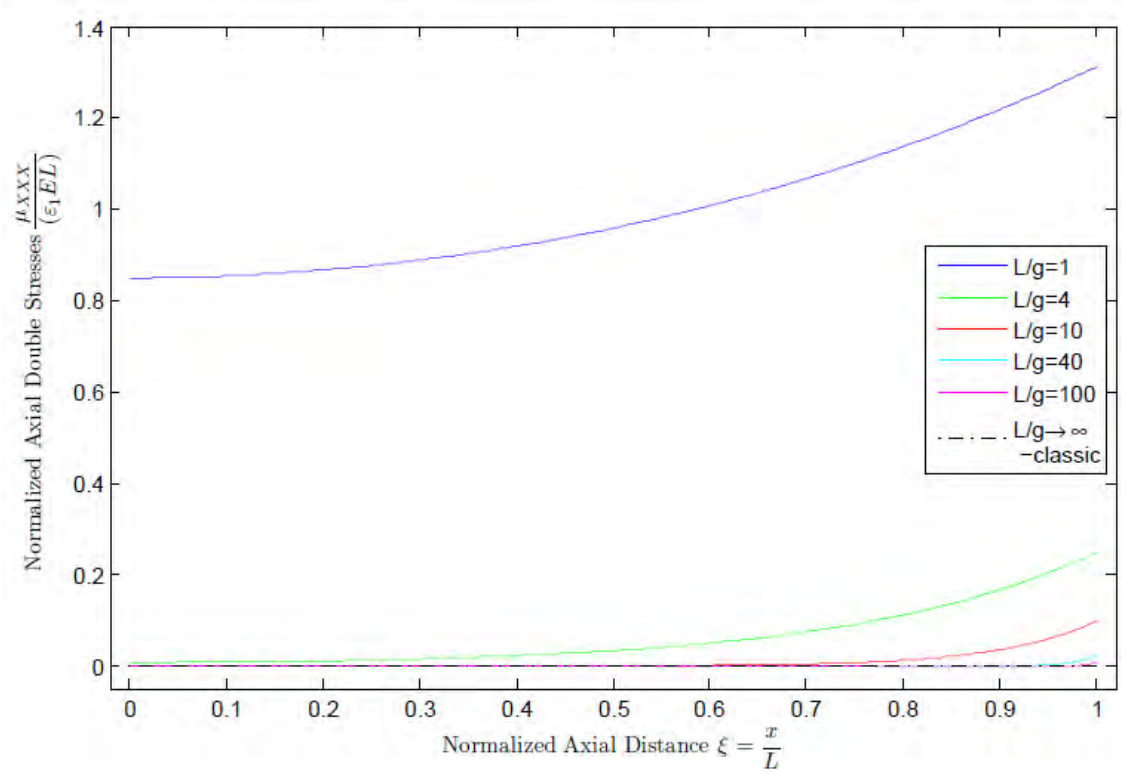

Fig. 100 Normalized axial double stresses $\mu_{xxx}/(\varepsilon_1 EL)$ **versus normalized axial distance** $\xi = x/L$ **of a Fixed-Free bar. The classical BCs are** $u(\xi=0)=0$, $u(\xi=1)=0$, **and the non classical ones** $u'(\xi=0)=0$, $u'(\xi=1)=\varepsilon_1$

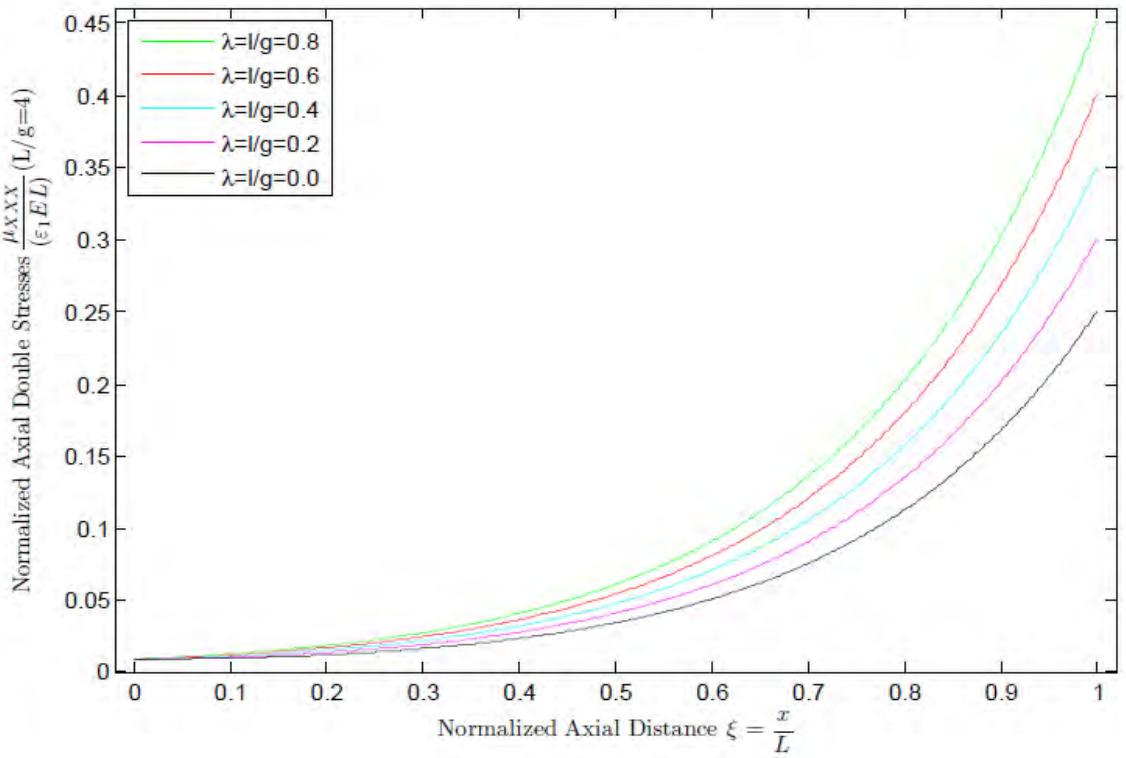

Fig. 101 Normalized axial double stresses $\mu_{xxx}/(\varepsilon_1 EL)$ **versus normalized axial distance** $\xi = x/L$ **of a Fixed-Free bar,for c=L/g=4 and various λ values**

As shown in the figures above, in order to restrain the strains at the bars ends double stresses, directly related to the applied force P, are applied at the bars ends and their value is independent of the λ parameter, which though, modifies the double stress distribution along the bar.

In the case where the strain at the ends is determined as P/EA -the value of the bars ends in the classical problem- the solution is reduced to the classical one, independent of the c ratio. Thus, the bars' behavior isn't always stiffer than the one predicted in classical theory, it can be the same as the classical one, or ever less stiff provided that the right BCs are applied.

Widely in the literature the assumption of restrained end strains is used as non classical BC. That indeed dictates a stiffer behavior for the bar as it is shown in the graphs above. This isn't the case thought if u'>P/EA, in which the bars' displacement is greater than the one of the classical case.

Another fixed-free bar is studied. It is the case that one end of the bar is subjected to an axial displacement U_o, while a tensile force P is applied to its other end and the double forces R_0 and R_1 at both ends of the bar are known, i.e. the BCs are $u(\xi=0)=U_0$ and $P(\xi=1)=P_1$ and $R(\xi=0)=R_0$ and $R(\xi=1)=R_1$. First, the case where the surface strain energy is insignificant/parameter λ=0, will be discussed and later the way the λ parameter affects the displacement field will be presented.

The displacement field takes the following form, when λ=0:

$$u(\xi)=U_0+\frac{P_1 L}{EA}\xi+\frac{R_0}{EA}\left[\frac{\sinh(c\xi^*)}{\sinh(c)}-1\right]+\frac{R_1}{EA}\left[\frac{\sinh(c\xi)}{\sinh(c)}\right]$$

The function above shows that when no double forces are applied at the ends of the bar, the bars behavior is independent for the g parameter, i.e. no scale effects are present. Next, is displayed the effect of the double forces to the bars' behavior, a division of the solution that can be done due to the superposition principle. It should be noted that the double forces on each end of the bar affect in a different way its behavior, i.e. they are not symmetric.

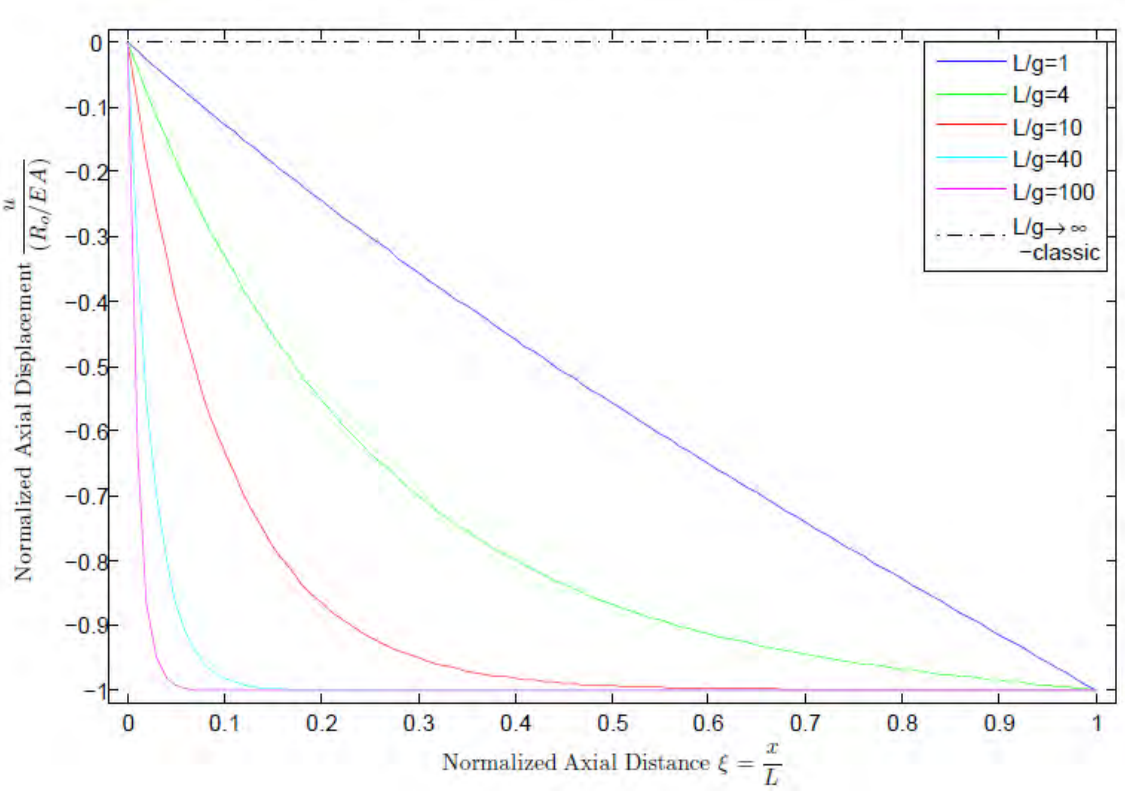

Fig. 102 Normalized axial displacement $u/(R_0/EA)$ versus normalized axial distance $\xi=x/L$ of a Fixed-free bar. The classical BCs are $u(\xi=0)=0$, $P(\xi=1)=0$, and the non classical ones $R(\xi=0)=R_0$, $R(\xi=1)=0$

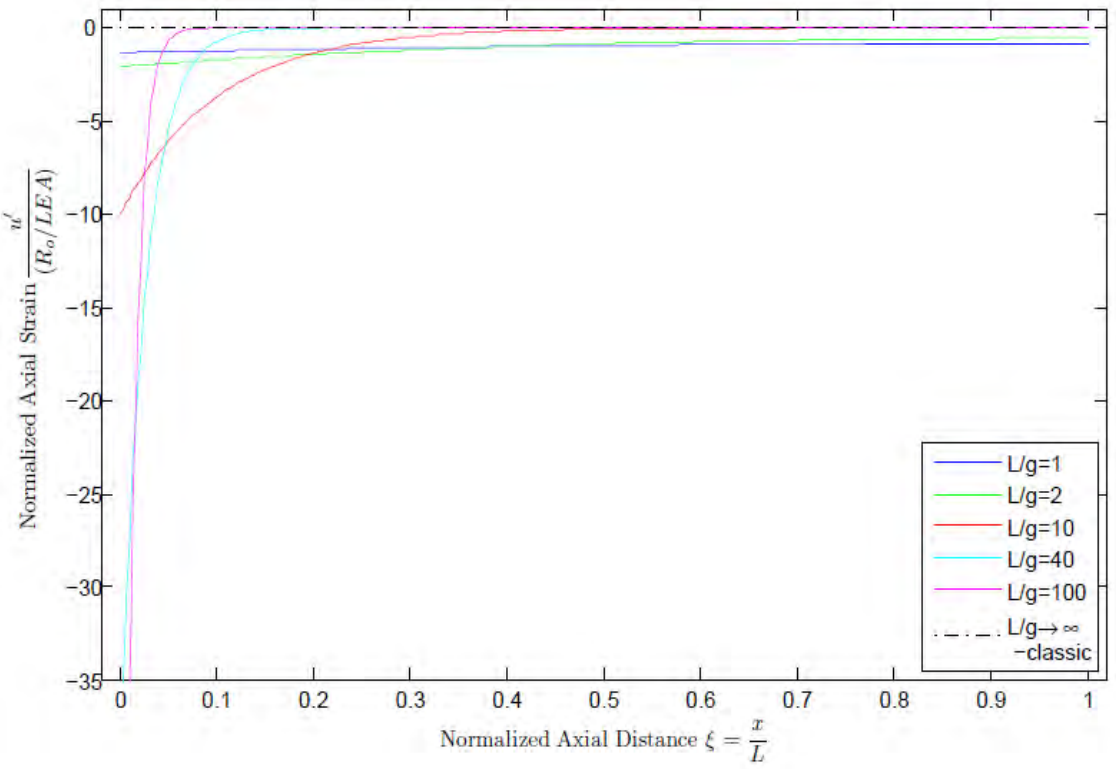

Fig. 103 Normalized axial strain $u'/(R_0/LEA)$ **versus normalized axial distance** $\xi = x/L$ **of a Fixed-free bar. The classical BCs are** $u(\xi = 0) = 0$, $P(\xi = 1) = 0$, **and the non classical ones** $R(\xi = 0) = R_0$, $R(\xi = 1) = 0$

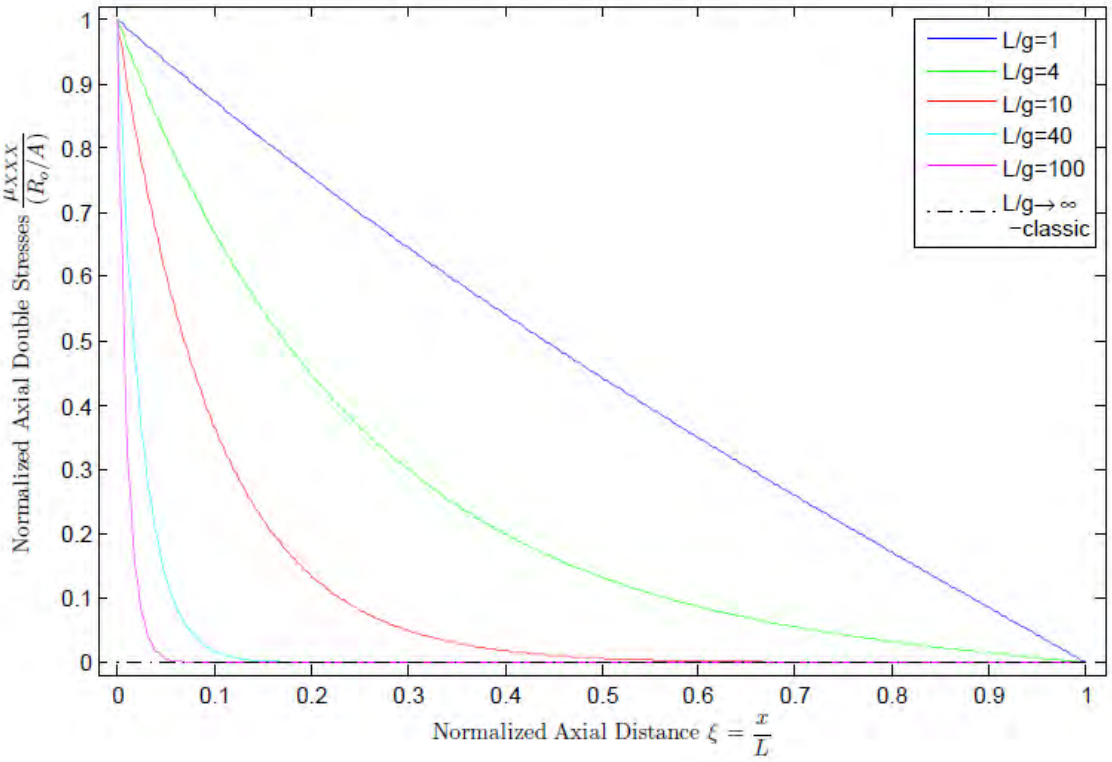

Fig. 104 Normalized axial double stresses $\mu_{xxx}/(R_0/A)$ **versus normalized axial distance** $\xi = x/L$ **of a Fixed-free bar. The classical BCs are** $u(\xi = 0) = 0$, $P(\xi = 1) = 0$, **and the non classical ones** $R(\xi = 0) = R_0$, $R(\xi = 1) = 0$

As in the case of a confined ends displacements, in this case too when double forces are applied to an end of the bar its displacement field cannot be reduced to the classical one when the L/g ration increases. Thus if able to apply such double forces to the fixed bars end, its length changes, even when no axial force is applied.

Note, though, that only the part of the bar which is near the end is affected by the double forces. The rest of the bar may be displaced, but no significant strain is anticipated. Hence, the variation of the bar's length is attributed only to the deformation of the affected by the double forces part of the bar.

Next, the double forces effect on the free end of the bar is presented. The main difference of this case to the one above is that the displacement and strain fields are reduced to the classical ones for great c values. The behavior of the bar, though, is very similar in the two cases. They differ due to a hidden imposed displacement in the first case.

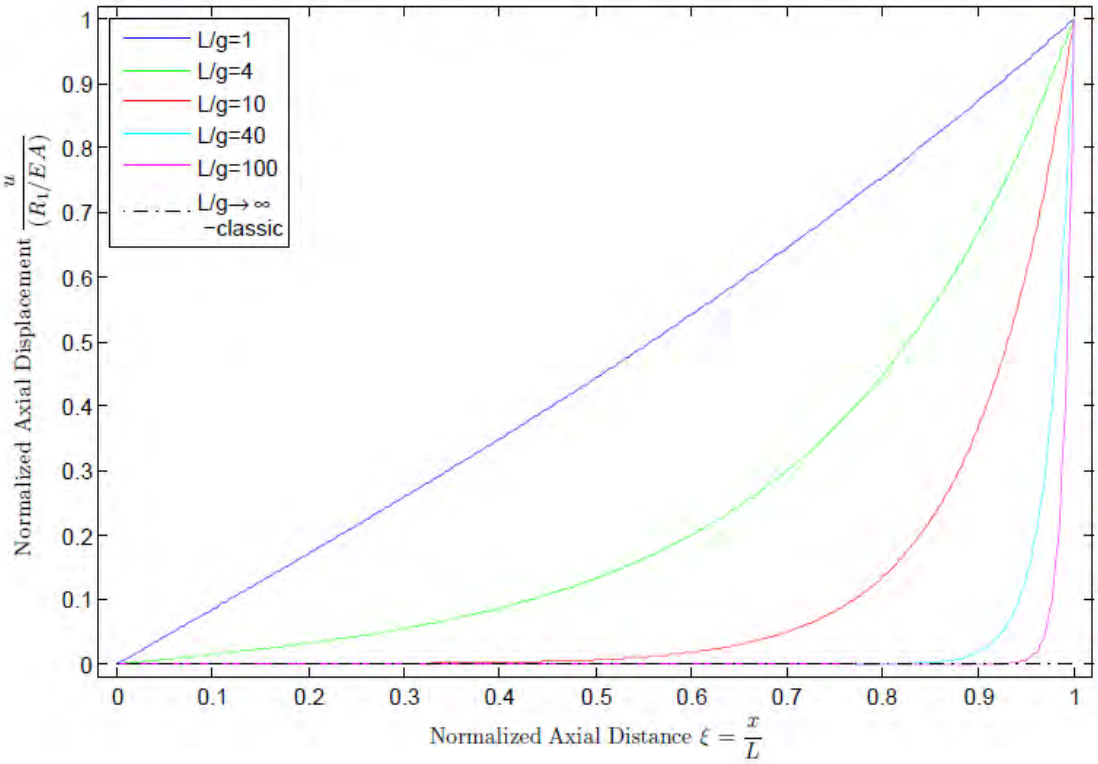

Fig. 105 Normalized axial displacement $u/(R_1/EA)$ **versus normalized axial distance** $\xi = x/L$ **of a Fixed-free bar. The classical BCs are** $u(\xi = 0) = 0$, $P(\xi = 1) = 0$, **and the non classical ones** $R(\xi = 0) = 0$, $R(\xi = 1) = R_1$

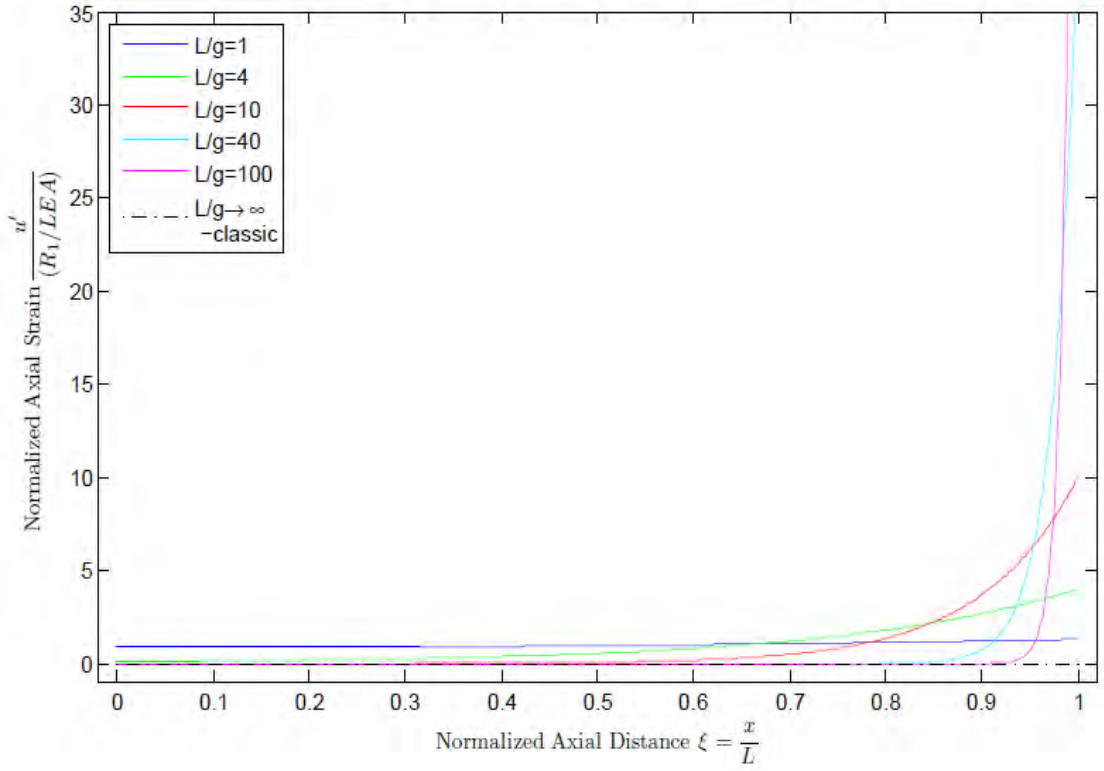

Fig. 106 Normalized axial strain $u'/(R_1/LEA)$ **versus normalized axial distance** $\xi = x/L$ **of a Fixed-free bar. The classical BCs are** $u(\xi = 0) = 0$, $P(\xi = 1) = 0$, **and the non classical ones** $R(\xi = 0) = 0$, $R(\xi = 1) = R_1$

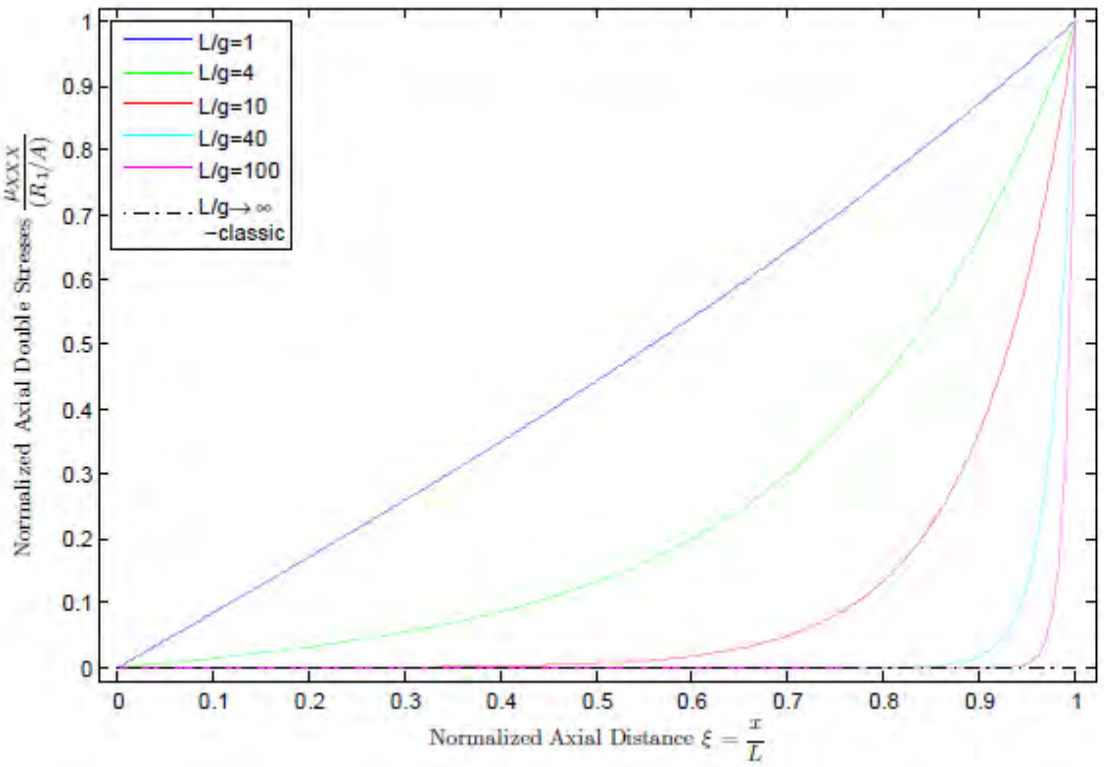

Fig. 107 Normalized axial double stresses $\mu_{xxx}/(R_1/A)$ **versus normalized axial distance** $\xi = x/L$ **of a Fixed-free bar. The classical BCs are** $u(\xi = 0) = 0$, $P(\xi = 1) = 0$, **and the non classical ones** $R(\xi = 0) = 0$, $R(\xi = 1) = R_1$

In the case of non zero surface strain energy λ≠0, the displacement field is $u = u_{\lambda=0} + u_{\lambda}$, where $u_{\lambda=0}$ is the displacement field of a bar with λ=0 described above and the u_{λ} field is given below.

$$u_{\lambda=0}(\xi) = U_0 + \frac{P_1 L}{EA}\xi + \frac{R_0}{EA}\left[\frac{\sinh(c\xi^*)}{\sinh(c)} - 1\right] + \frac{R_1}{EA}\left[\frac{\sinh(c\xi)}{\sinh(c)}\right]$$

$$u_{\lambda}(\xi) = \frac{P_1 L}{EA}\left\{\frac{\lambda^2}{1-\lambda^2}\left[\frac{\coth(c)}{c}\left(1 - \frac{1+\cosh(c\xi^*)-\cosh(c\xi)}{\cosh(c)}\right)\right] + \frac{\lambda}{1-\lambda^2}\left[\frac{1}{c}\left(1 - \frac{\cosh\left(\frac{c}{2}(1-2\xi)\right)}{\cosh(c/2)}\right)\right]\right\}$$

$$+ \frac{R_0}{EA}\left\{\frac{\lambda^2}{1-\lambda^2}\left[\frac{\sinh(c\xi^*)}{\sinh(c)} - 1\right] + \frac{\lambda}{1-\lambda^2}\left[-\coth(c)\left(1 - \frac{\cosh(c\xi^*)}{\cosh(c)}\right)\right]\right\}$$

$$+ \frac{R_1}{EA}\left\{\frac{\lambda^2}{1-\lambda^2}\left[\frac{\sinh(c\xi)}{\sinh(c)}\right] + \frac{\lambda}{1-\lambda^2}\left[-\frac{\sinh(c\xi)}{\sinh(c)}\tanh\left(\frac{c}{2}(1-2\xi)\right)\right]\right\}$$

Due to the many parameters in this problem the effect of the l parameter is displayed in the case where c=L/g=4

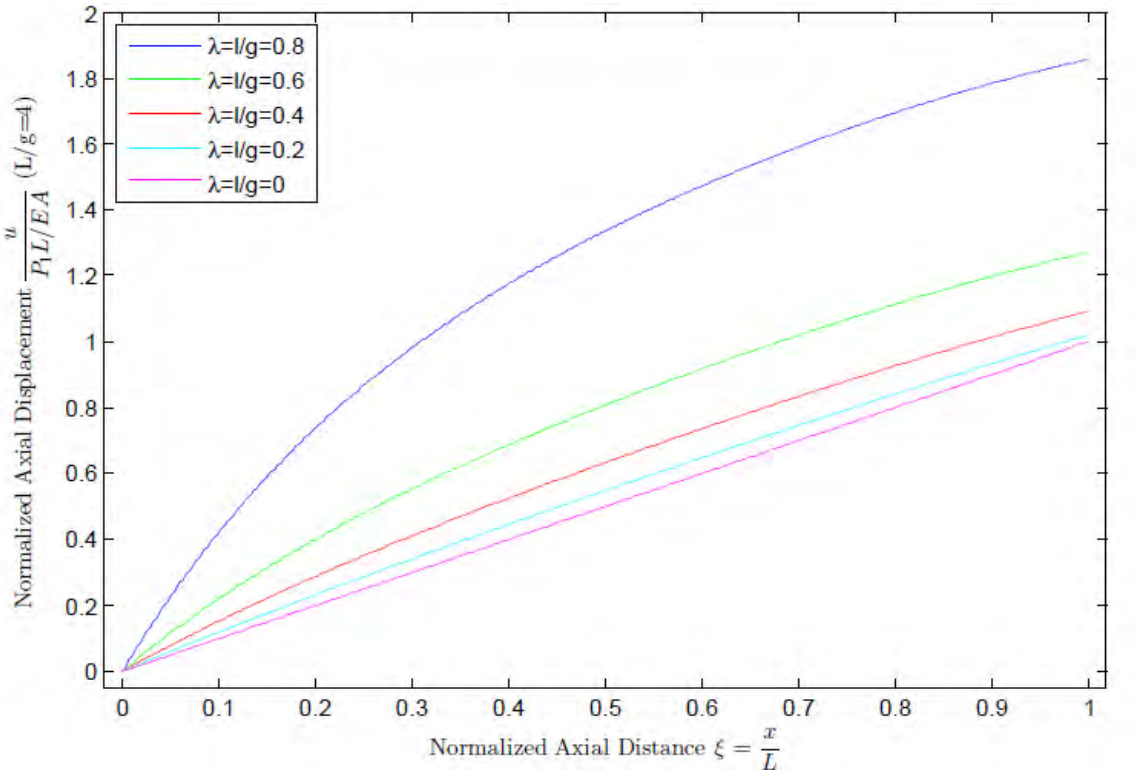

Fig. 108 Normalized axial displacement $u/(P_1 L/EA)$ **versus normalized axial distance** $\xi = x/L$ **of a Fixed-Fixed bar, for c=L/g=4 and various λ values. The classical BCs are** $u(\xi=0)=0$, $P(\xi=1)=P_1$, **and the non classical ones** $R(\xi=0)=0$, $R(\xi=1)=0$

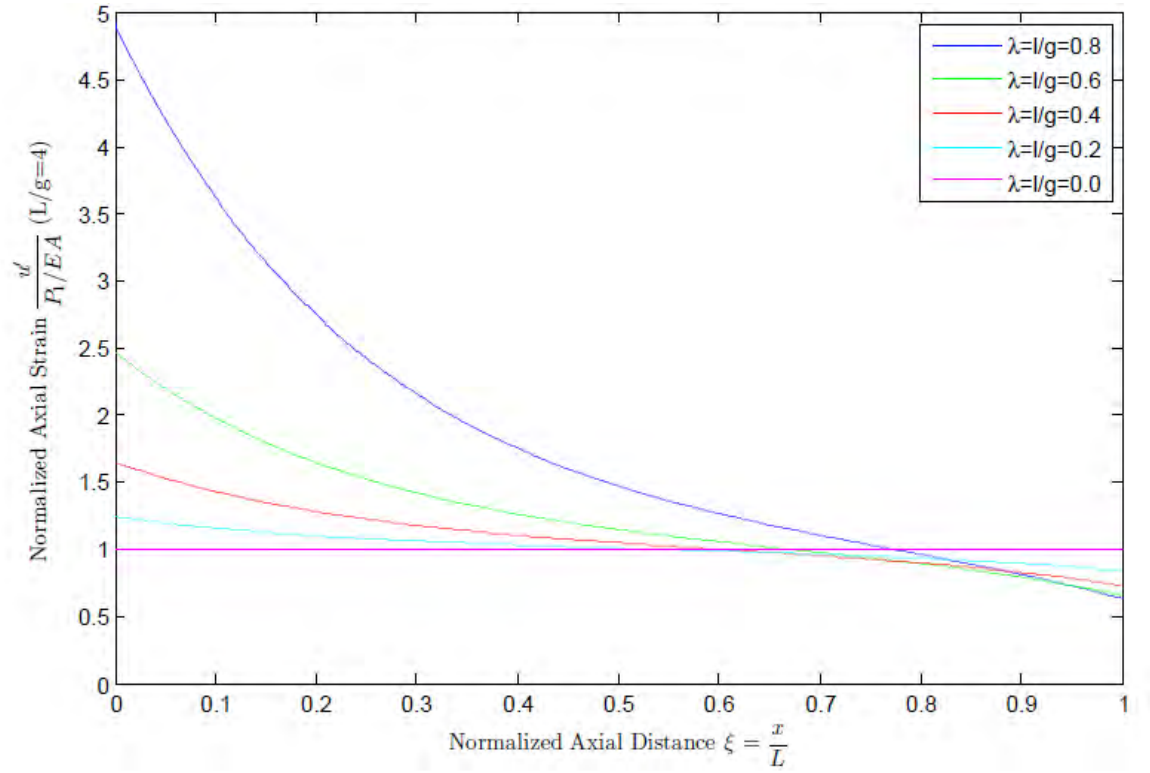

Fig. 109 Normalized axial strain $u'/(P_1/EA)$ **versus normalized axial distance** $\xi = x/L$ **of a Fixed-Fixed bar, for c=L/g=4 and various λ values. The classical BCs are** $u(\xi=0)=0$, $P(\xi=1)=P_1$, **and the non classical ones** $R(\xi=0)=0$, $R(\xi=1)=0$

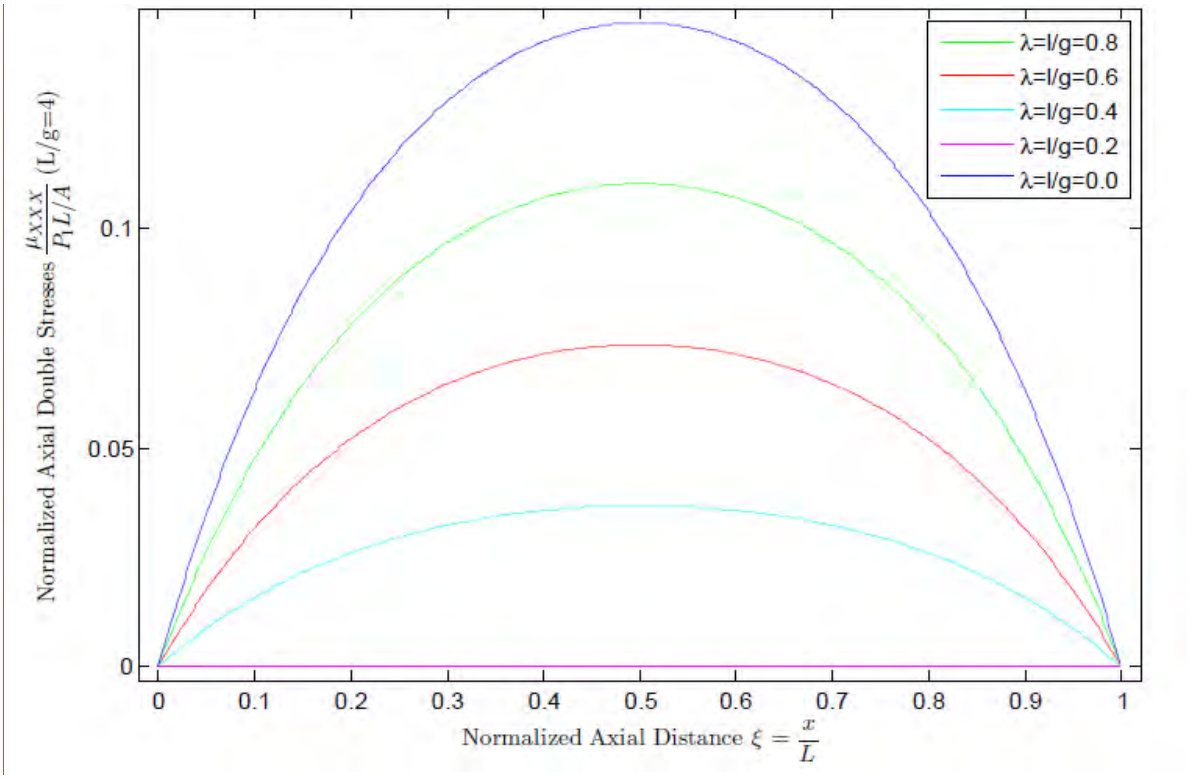

Fig. 110 Normalized axial double stresses $\mu_{xxx}/(P_1L/A)$ **versus normalized axial distance** $\xi = x/L$ **of a Fixed-Fixed bar, for c=L/g=4 and various λ values. The classical BCs are** $u(\xi=0)=0$, $P(\xi=1)=P_1$, **and the non classical ones** $R(\xi=0)=0$, $R(\xi=1)=0$

As in the case of the fixed fixed bar with double forces applied to its ends, the surface energy results to non uniform / non classical behavior from the bar even when only classical BCs are applied. Notice that greater displacements and strains appear throughout the bar and also double stresses appear, even though double forces are not applied at the bars ends.

In the following figures the effect of double forces at a bar's ends is presented, when $\lambda \neq 0$. When applying double forces to the fixed end of the bar, the bar is shortened, and the greater the λ parameter, the more the bar is shortened. When applying double forces to the free end of the bar, it elongates. In contrast with the fixed end, for greater λ values, the bar elongates less. Thus the λ parameter in any case contributes in a way that reduces the bar's length.

It is noted that double forces on either end, create a unique double stress field for all λ values, no matter their different effect on the displacement and strain fields.

The next figures present the effect of double stresses to the fixed free bars behavior. In is shown that the application of double forces triggers the l length, in a way that it attempts to minimize the bar's length. And for greater λ values the more the bar is shortened by the application of the double forces.

Also, it is noted that the double stress field in this problem is independent of the l parameter. So only the displacement and strain fields are affected

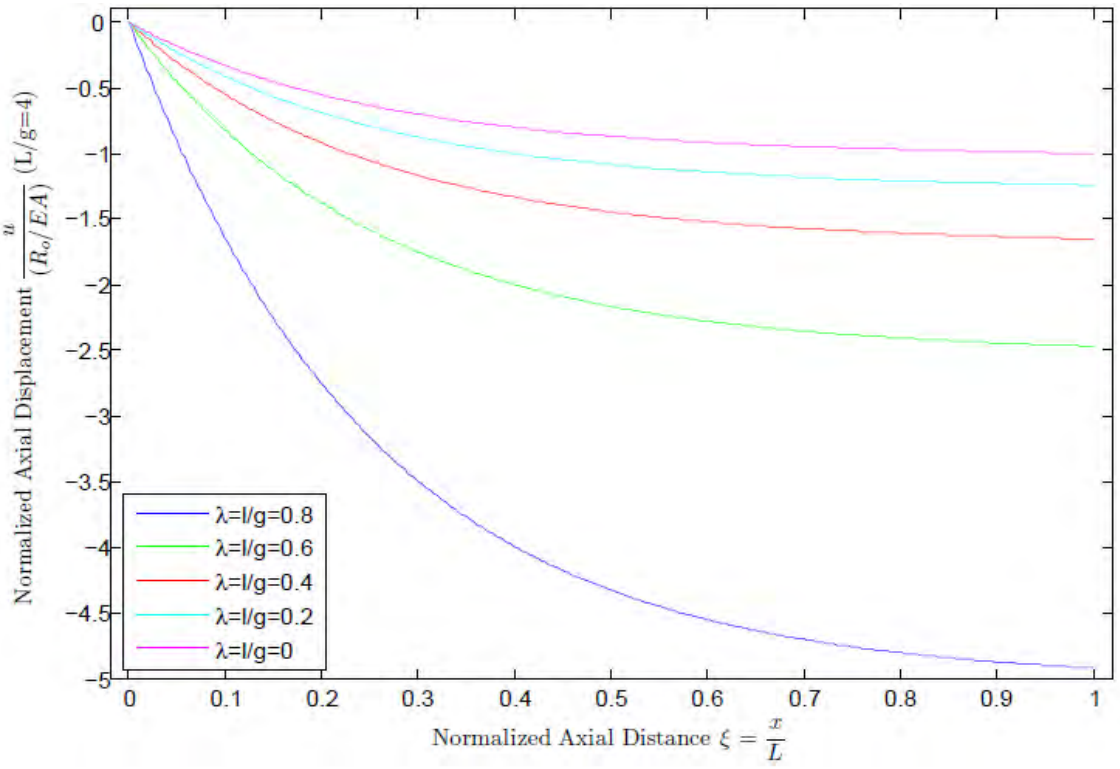

Fig. 111 Normalized axial displacement $u/(R_0/EA)$ **versus normalized axial distance** $\xi = x/L$ **of a Fixed-Fixed bar, for c=L/g=4 and various λ values. The classical BCs are** $u(\xi = 0) = 0$, $P(\xi = 1) = 0$ **and the non classical ones** $R(\xi = 0) = R_0$, $R(\xi = 1) = 0$

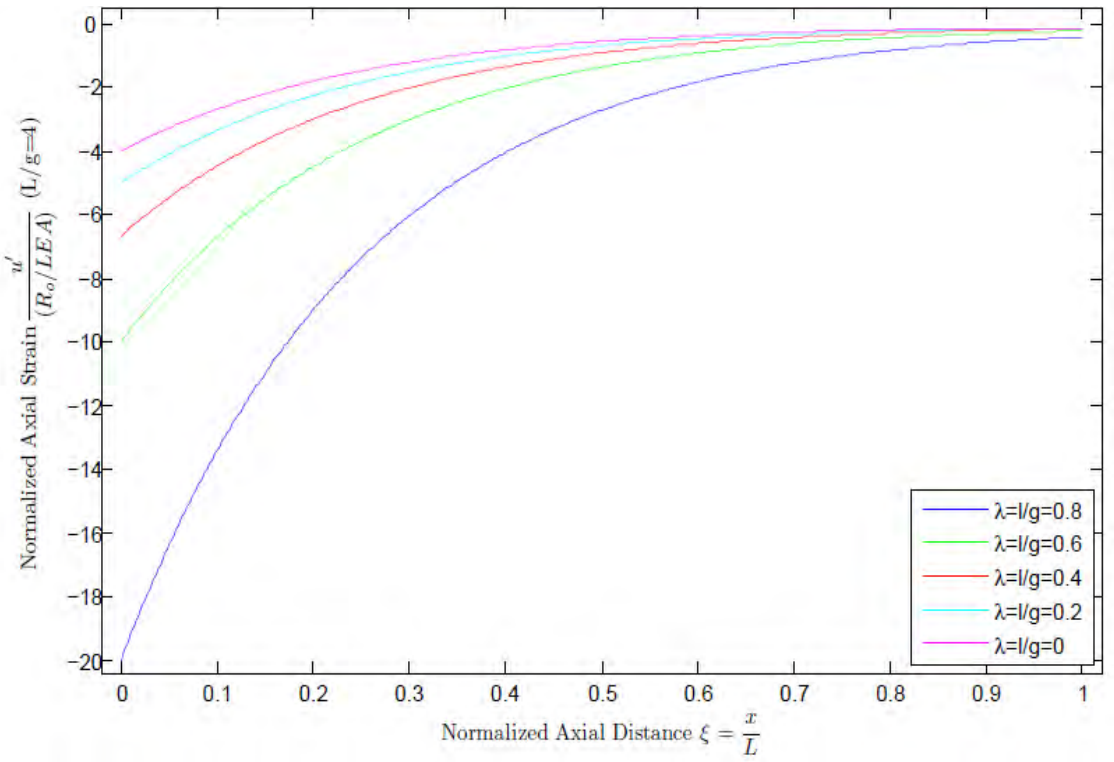

Fig. 112 Normalized axial strain $u'/(R_0/EAL)$ **versus normalized axial distance** $\xi = x/L$ **of a Fixed-Fixed bar, for c=L/g=4 and various λ values. The classical BCs are** $u(\xi = 0) = 0$, $P(\xi = 1) = 0$ **and the non classical ones** $R(\xi = 0) = R_0$, $R(\xi = 1) = 0$

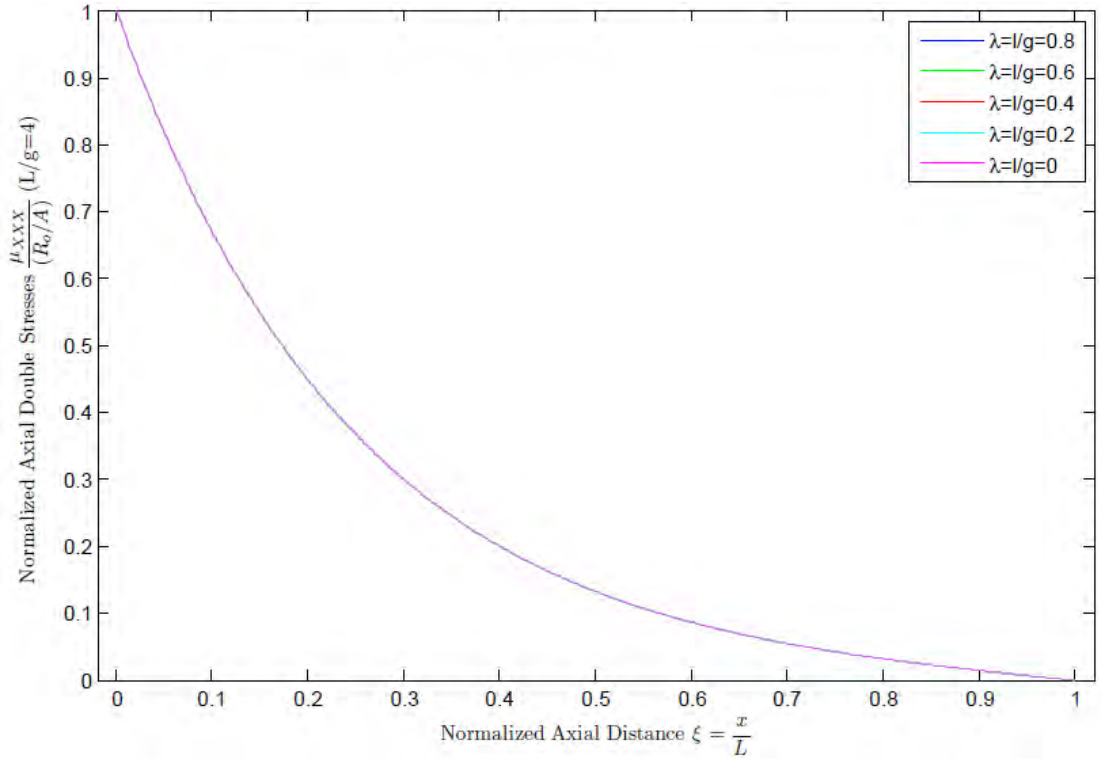

Fig. 113 Normalized axial double stresses $\mu_{xxx}/(R_0/A)$ versus normalized axial distance $\xi = x/L$ of a Fixed-Fixed bar, for c=L/g=4 and various λ values. The classical BCs are $u(\xi=0)=0$, $P(\xi=1)=0$ and the non classical ones $R(\xi=0)=R_0$, $R(\xi=1)=0$

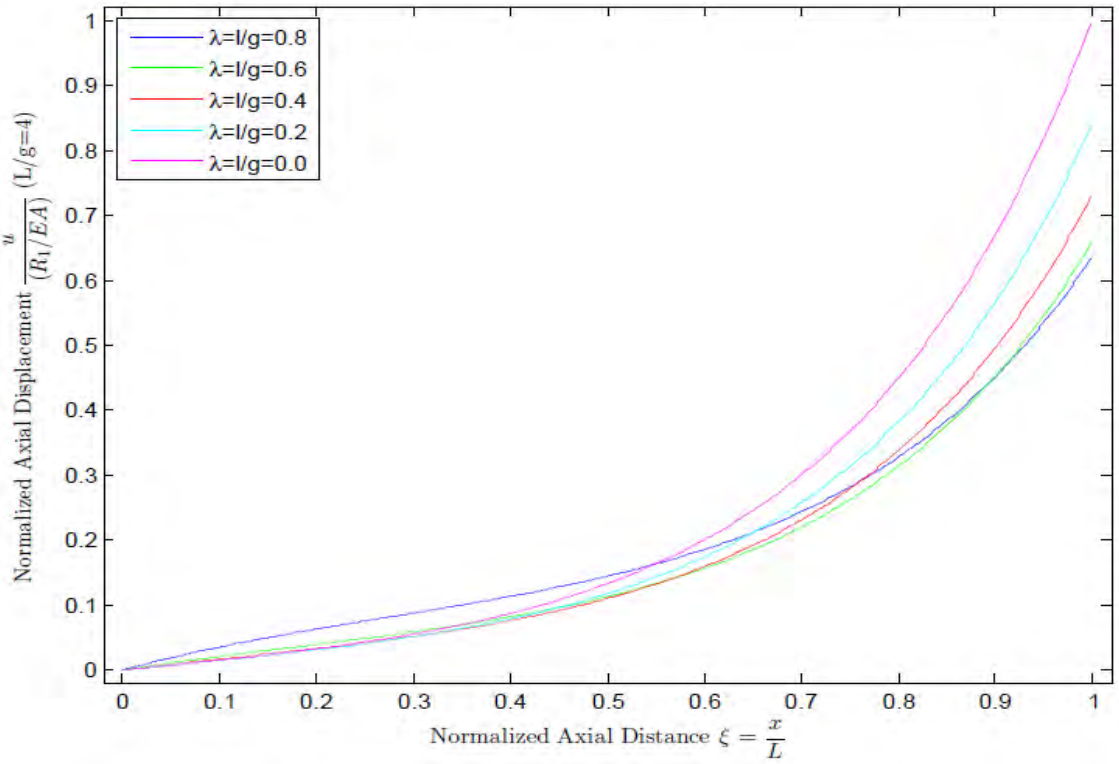

Fig. 114 Normalized axial displacement $u/(R_1/EA)$ versus normalized axial distance $\xi = x/L$ of a Fixed-Fixed bar, for c=L/g=4 and various λ values. The classical BCs are $u(\xi=0)=0$, $P(\xi=1)=0$ and the non classical ones $R(\xi=0)=0$, $R(\xi=1)=R_1$

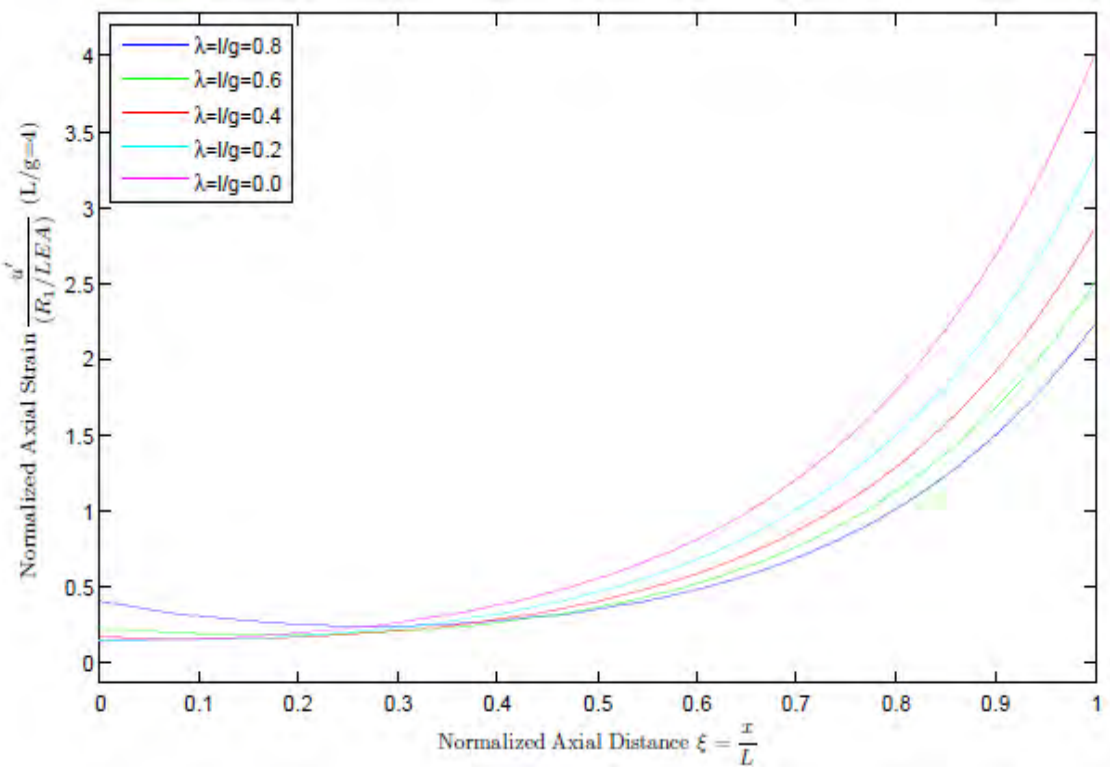

Fig. 115 Normalized axial strain $u'/(R_1/EAL)$ **versus normalized axial distance** $\xi = x/L$ **of a Fixed-Fixed bar, for c=L/g=4 and various λ values. The classical BCs are** $u(\xi=0)=0$, $P(\xi=1)=0$ **and the non classical ones** $R(\xi=0)=0$, $R(\xi=1)=R_1$

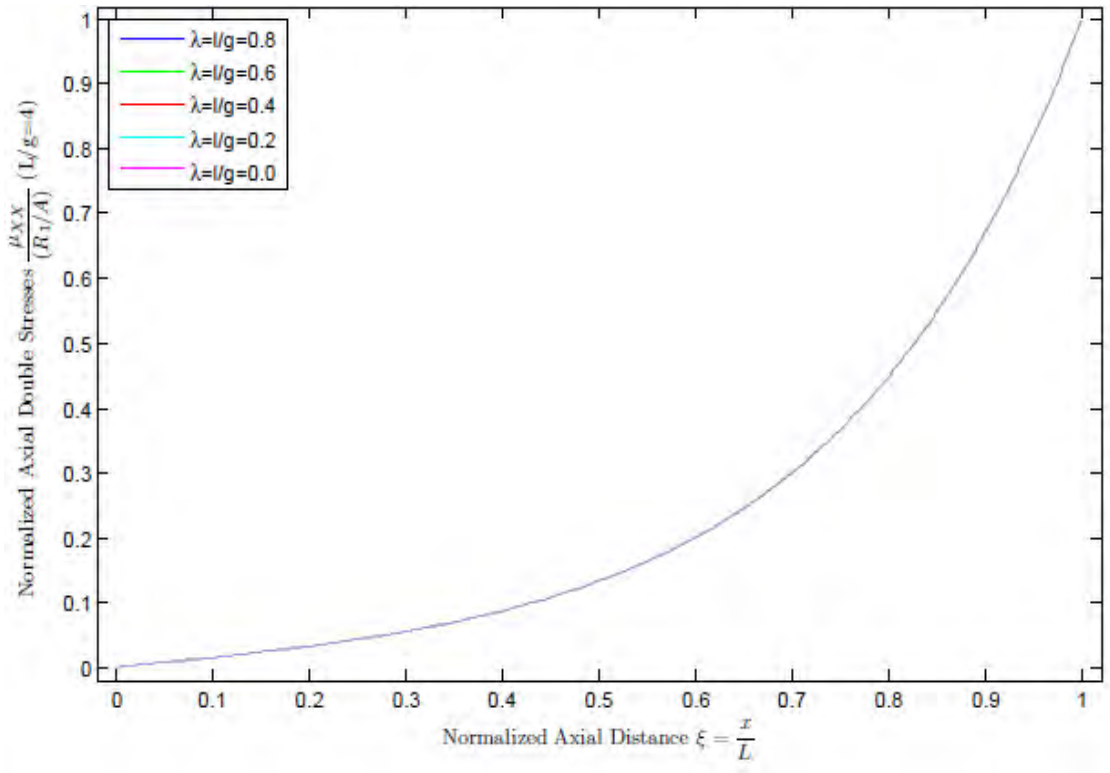

Fig. 116 Normalized axial double stresses $\mu_{xxx}/(R_1/A)$ **versus normalized axial distance** $\xi = x/L$ **of a Fixed-Fixed bar, for c=L/g=4 and various λ values. The classical BCs are** $u(\xi=0)=0$, $P(\xi=1)=0$ **and the non classical ones** $R(\xi=0)=0$, $R(\xi=1)=R_1$

4.II.2.iii. Conclusions

The following general conclusions can be drawn about the bars behavior.

- Prescribing the bars degrees of freedom generally results to non classical non uniform behaviors from the bar.
- Restraining the bar's ends strains does increase the bars stiffness, especially for small L/g ratios
- The bars behavior when instead of strain BCs, zero double forces BCs are applied is the same as the respective classical one, no matter L/g ratio.
- The l parameter affects the bar in a way that minimizes its length, by reducing its elongation, when in tension, and by additionally shortening the bar, when in compression.
- Any BC problem solution can be reduced to a classical one, when appropriate BC combinations are applied.
- The bar's behavior, under most loading cases, for great c=L/g values is reduced to the respective classical behavior

4.II.3 1-D composite bar structures

4.II.3.i. Node function in composite 1D structures

Before addressing any specific problem, independent of the loading applied, in a composite structure first one must investigate how a truss node would function in the framework of the gradient elasticity theory.

The classical elasticity node is considered to be a rigid point body that maintains the continuity of the bars' ends displacement, while it allows them to rotate independently. The node as a body only has displacement degrees of freedom and no rotational ones and also needs to satisfy the Newton's first law of motion (ΣF=0). In the case of two collinear bars joined with a node, the conditions above can be translated to

$$u_- = u_+ \quad \text{and} \quad P_- + P_+ + P^{\text{external}} = 0$$

In the classical elasticity framework one BC needs to be determined at each end of a bar. The node joins two bars thus the above BCs at the node are sufficient for a well posed problem.

This is not the case in the gradient elasticity framework, where two BCs need to be determined at each bars end, thus at the gradient node joining two collinear bars four BCs need to be determined, for a well posed problem. The classical conditions easily can be chosen to be the two BCs. The choice of the two extra – non classical conditions is not as obvious and needs to be discussed, since their effect to each bars behavior is crucial. Polizzoto (Polizzotto, 2003) considered the node as an interface between the bars. This is a fairly reasonable assumption and will be followed in the greatest part of the present work. Polizzoto demanded that besides the classical BCs, the strain and the curvature of the bars' displacement to be equal at the interface, i.e.

$$u'_- = u'_+ \quad \text{and} \quad u''_- = u''_+$$

Dealing with gradient elasticity and higher order differential equations, it is sure to use higher order BCs at nodes-interfaces as the ones discussed. A reasonable choice thought needs to be made so that they represent the real loading of the bar structure and provide the real bars behavior.

Demanding that the strain of both bars at the interface is equal is a very strict condition itself. However strain manipulation is one of the abilities given by the variation principle and it is an acceptable BC, although questions arise regarding the ability of the node's body/interface's to impose such a behavior.

On the other hand, demanding that both bars have the same curvature at the interface as a BC is not as reasonable. It does not have any physical support, and seems even more extreme than the one above. In the case of dividing a bar in multiple bar elements and applying any BCs, using these non classical BCs at the created interfaces, a continuous displacement field is obtained that coincides with the displacement field of the original bar. In other cases though where not all the bars are of the same material, the same Young's modulus and the same cross sectional area, it is expected that discontinuities will appear in the composite bodies displacement derivatives, which isn't the case with these interface conditions. Thus, demanding equal curvatures is not considered to be a functional BC and other interface conditions are seeked after.

Instead of the curvature condition, demanding that the double forces R at the interface are equal is considered more reasonable as the fourth BC. This is not an arbitrary condition since it is obtained through the variation principle. However, the double forces μ_{xxx} do not contribute neither to the force nor the moment equilibrium of a body, and it should not be necessary to make such a demand, based on classical elasticity concepts. However, an assumption of a gradient version of Newton's 3^{rd} law, together with the assumption of an elastic interface between the bars, not a body-node, justifies this BC in the sense that the two materials alone interact with their boundaries, and the double forces are applied from one another. This is the BC proposed in other interface elasticity problems, as wave transmition by Yueqiu Li (Li, et al., 2015).

Following the Kordolemis' (Kordolemis, et al., 2013) analog of the pretwisted beam, it is observed that at an interface that no extra axial stress is applied, both the axial force and the bimoment should be equal, thus the respective R term should be equal too. This is the case of an interface of two similar in geometry and properties structural parts. However, besides the loading, the R term presented depends on several

material and cross sectional parameters of the body thus the assumption of the R equality should not be generalized. It should be noted, though, that the analogy is not perfect since in this case there are exactly four degrees of freedom, while, the pretwisted beam has six, and assumptions are made for each of them.

A direct answer to this search is obtained by Weitzman in the field of couple-stress theories. He notes that assuming an elastic interface, the energy due to the couple-stresses ($E=\mu_r\omega_{r\theta}$ in his case) should be fully transmitted across the two bodies interface and thus the BCs chosen are $\mu_{r+}=\mu_{r-}$ and $\omega_{r\theta-}=\omega_{r\theta+}$ in his study. This note is translated in the present study, in gradient elasticity, as $\mu_{xxx-}=\mu_{xxx+}$ and $u'_-=u'_+ \rightarrow R_-=R_+$ and $u'_-=u'_+$, in the case of identical cross sections that are being joined. This, though, is considered to be the BC and in the case of an interface between two different cross sections. As noted before, this does not come fully in agreement with the conclusion obtained through the pretwisted beam analogy. But that can be attributed to the imperfection of the analogy.

It is also noted by Weitzman that it is equally reasonable to assume that no gradient strain energy is submitted through the interface, thus the BCs can be any of the following combinations

$u'_- = 0$ and $u'_+ = 0$

$R_- = 0$ and $u'_+ = 0$

$u'_- = 0$ and $R_+ = 0$

$R_- = 0$ and $R_+ = 0$

The last one, Weitzman notes, is the physically most possible and, as shown earlier, is a case that the bars behaves classically independent of the microstructure. Since the behavior of trusses with such nodes is the classical, which is known and no size effect is predicted, this case will not be studied.

There seems to be no reason that the node's - interface's BCs are not symmetrical thus the second and third BC combinations seem not to have some practical application and they will not be used.

The first BC combination is the one most commonly met in the literature, and as noted before is considered to be a very ‘intrusive’ BC, that induces very non-uniform stiffer than classical behavior of the bar. It so also noted that this BC implies that the double stresses at the two different adjoining bodies take different values, which, however, are linear functions of the axial forces applied or the displacements applies at each bars ends, $R_0 = -R_1 = \tanh(c/2)\, PL/c = g \tanh(L/2g)\, P$ or $R_0 = -R_1 = EA \dfrac{\tanh(c/2)}{c - 2\tanh(c/2)} (u_1 - u_0)$, in the case l=0.

The node that restrains the strains of the connected bars is hereupon referred a rigid node.

4.II.3.ii. 1-D Stiffness Matrix

Next step to solving multiple bar problems is obtaining the bar element stiffness and flexibility matrices of a gradient elastic bar element.

First, the stiffness matrix will be acquired. The stiffness matrix calculates the forces applied to the bar in order to accomplish certain displacements in the framework of the classical elasticity theory.

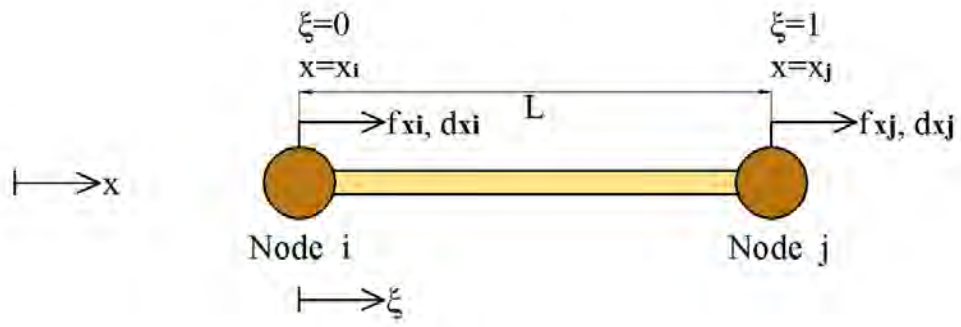

There are several ways to construct the stiffness matrix. Here the analytical solutions combined with the force equilibrium are used. The displacement field in the case of prescribed nodal displacements dxi and dxj is u= dxi+(dxj- dxi) ξ

while fxj=Pj=EAu'=EA/L(dxj- dxi)=k(dxj- dxi)

and the force equilibrium demands that fxi+ fxj=0-> fx-=- fxj=- k(dxj- dxi)

thus the local coordinate system stiffness matrix is

$$\begin{bmatrix} f_{xi} \\ f_{xj} \end{bmatrix} = \begin{bmatrix} k & -k \\ -k & k \end{bmatrix} \cdot \begin{bmatrix} d_{xi} \\ d_{xj} \end{bmatrix}$$

In the gradient elasticity framework, there are two more degrees of freedom – the stains at the bar's ends - the respective work conjugates R_0 and R_1

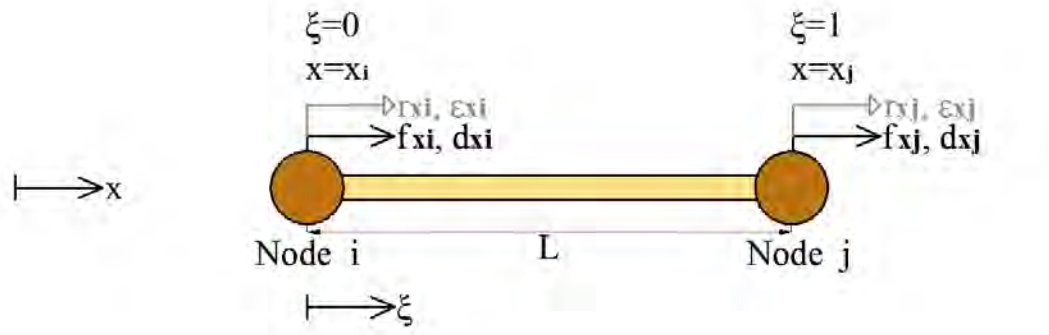

The displacement field of a bar with prescribed nodal displacements and strains is know, thus the f_{xk} ans r_{xk} generalized forces can be found. Once again the stiffness matrix satisfies the equation $f_i = K_{ij} d_j \rightarrow \mathbf{f} = \tilde{\mathbf{K}} \cdot \mathbf{d}$, in which case

$$\mathbf{f} = [fxi \quad rxi \quad fxj \quad rxj]^T = [-P_{(\xi=0)} \quad R_{(\xi=0)} \quad P_{(\xi=1)} \quad R_{(\xi=1)}]^T$$

$$\mathbf{d} = [dxi \quad \varepsilon xi \quad dxj \quad \varepsilon xj]^T = [dxi \quad -qxi \quad dxj \quad qxj]^T$$

The choice above for the $\mathbf{f}$ and $\mathbf{d}$ vector components is made based on the assumption that the 2D – 3D gradient theory by (Polyzos, et al., 2003) can be simplified and used to 1-D problems. Thus, the bars non classical degrees of freedom are $\mathbf{q} = \partial \mathbf{u} / \partial \hat{\mathbf{n}}$ at the ends and their work conjugates $\mathbf{R} = \hat{\mathbf{n}} \cdot \tilde{\boldsymbol{\mu}} \cdot \hat{\mathbf{n}}$, $\mathbf{u}$ being the displacement vector, $\hat{\mathbf{n}}$ the unit normal vector on the bodies surface, i.e. the bars ends, and $\tilde{\boldsymbol{\mu}}$ being the double stress tensor. In 1D problems they are simplified to:

$$\left.\frac{\partial \mathbf{u}}{\partial \hat{\mathbf{n}}}\right|_{\xi=0} = u'_{(\xi=0)} \hat{\mathbf{n}}_{(\xi=0)} = -u'_{(\xi=0)} \hat{\mathbf{x}} = -\varepsilon_{(\xi=0)} \hat{\mathbf{x}} \qquad \text{and} \qquad \mathbf{R}|_{\xi=0} = R_{(\xi=0)} \hat{\mathbf{x}}$$

$$\left.\frac{\partial \mathbf{u}}{\partial \hat{\mathbf{n}}}\right|_{\xi=1} = u'_{(\xi=1)} \hat{\mathbf{n}}_{(\xi=1)} = u'_{(\xi=1)} \hat{\mathbf{x}} = \varepsilon_{(\xi=1)} \hat{\mathbf{x}} \qquad \text{and} \qquad \mathbf{R}|_{\xi=1} = R_{(\xi=1)} \hat{\mathbf{x}}$$

The relations above show that no matter which end of the bar is considered, the double forces R positive direction is the same as the longitudinal axis' direction, while, the "strain" degree of freedom, depending on the cross section has a different positive direction.

After some simplifications the local coordinate system stiffness matrix is found to be the following

$$\tilde{\mathbf{K}} = \begin{bmatrix} K_{11} & K_{12} & K_{13} & K_{14} \\ & K_{22} & K_{23} & K_{24} \\ & & K_{33} & K_{34} \\ \text{symm} & & & K_{44} \end{bmatrix} =$$

$$= \frac{EA}{L - 2g\tanh(L/2g)} \begin{bmatrix} 1 & g\tanh(L/2g) & -1 & g\tanh(L/2g) \\ & \left\{ \begin{matrix} -g^2 - Ll + Lg/\tanh(L/g) \\ +2lg\tanh(L/2g) \end{matrix} \right\} & -g\tanh(L/2g) & +g^2 - Lg/\sinh(L/g) \\ & & 1 & -g\tanh(L/2g) \\ \text{symm} & & & \left\{ \begin{matrix} -g^2 + Ll + Lg/\tanh(L/g) \\ -2lg\tanh(L/2g) \end{matrix} \right\} \end{bmatrix}$$

$$= \frac{EA}{c - 2\tanh(c/2)} \begin{bmatrix} \frac{c}{L} & \tanh(c/2) & -\frac{c}{L} & \tanh(c/2) \\ & L\left\{ \begin{matrix} -\frac{1}{c} + \frac{1}{\tanh(c)} \\ -\lambda + 2\frac{\lambda}{c}\tanh(c/2) \end{matrix} \right\} & -g\tanh(L/2g) & \frac{L}{c} - \frac{L}{\sinh(c)} \\ & & \frac{c}{L} & -\tanh(c/2) \\ \text{symm} & & & L\left\{ \begin{matrix} -\frac{1}{c} + \frac{1}{\tanh(c)} \\ +\lambda - 2\frac{\lambda}{c}\tanh(c/2) \end{matrix} \right\} \end{bmatrix}$$

where ‘symm’ refers to the symmetric nature of the stiffness matrix. In the case that $\lambda=0$ the stiffness matrix is simplified:

$$\tilde{\mathbf{K}} = \frac{EA}{L - 2g\tanh(L/2g)} \begin{bmatrix} 1 & g\tanh(L/2g) & -1 & g\tanh(L/2g) \\ & -g^2 + Lg/\tanh(L/g) & -g\tanh(L/2g) & +g^2 - Lg/\sinh(L/g) \\ & & 1 & -g\tanh(L/2g) \\ \text{symm} & & & -g^2 l + Lg/\tanh(L/g) \end{bmatrix}$$

$$= \frac{EA}{c - 2\tanh(c/2)} \begin{bmatrix} c/L & \tanh(c/2) & -c/L & \tanh(c/2) \\ & -L/c + L/\tanh(c) & -\tanh(c/2) & L/c - L/\sinh(c) \\ & & c/L & -\tanh(c/2) \\ \text{symm} & & & -L/c + L/\tanh(c) \end{bmatrix}$$

The stiffness matrices of the present work are exact, so one finite element per physical member can be assigned and the exact solution still be obtained. Of course, the expressions of the stiffness coefficients here are more complicated than the ones in classical elasticity but they are in closed form and hence the additional computational effort is relatively small.

4.II.3.iii. 1-D Applications

Several examples are presented that indicate how the bar elements can be employed for solving problems of more complex loading than the simple bar with end forces and double forces, without using complex distributed force functions and with perfect agreement with the behavior predicted by the theory.

The majority of the numerical values used for the different parameters of the problem in the following examples are obtained by (Kahrobaiyan, et al., 2013) while some geometrical parameters were chosen properly.

First, the elements' response to a fundamental already known problem is tested. Assume a bar of made of gradient elastic material with internal length parameter g=11.01 μm, l=0μm, Young's modulus E=1.44 GPa, cross section area = 78.54μm^2, fixed at one end at x=0, while an axial force P=10^4 μN is applied at its free end and the strains at both ends are restrained and equal to zero, i.e. $u(\xi=0)=0,\ u'(\xi=0)=0,\ u'(\xi=1)=0,$ $P(\xi=1)=10^4\,\mu N$

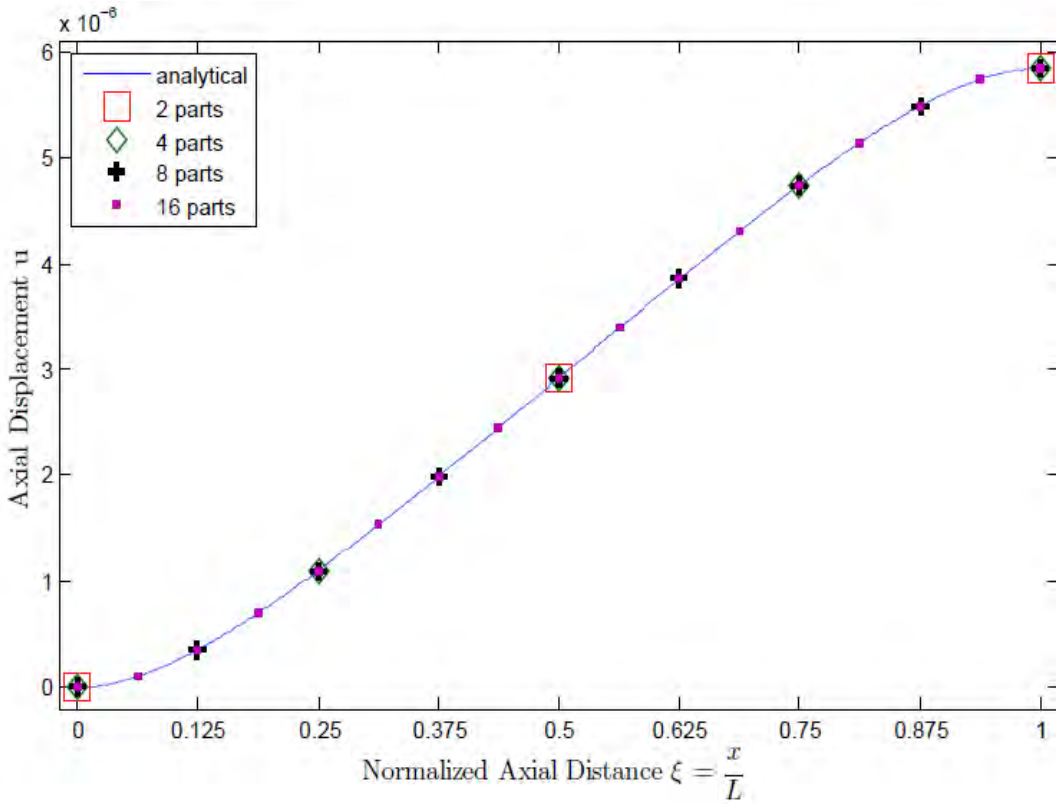

Fig. 117 FEM and analytical solutions of the axial displacement u **of a bar in tension with restrained end strains versus normalized axial distance** $\xi = x/L$**. The classical BCs are** $u(\xi=0)=0$**,** $P(\xi=1)=P_1$**, and the non classical ones** $u'(\xi=0)=0$**,** $u'(\xi=1)=0$

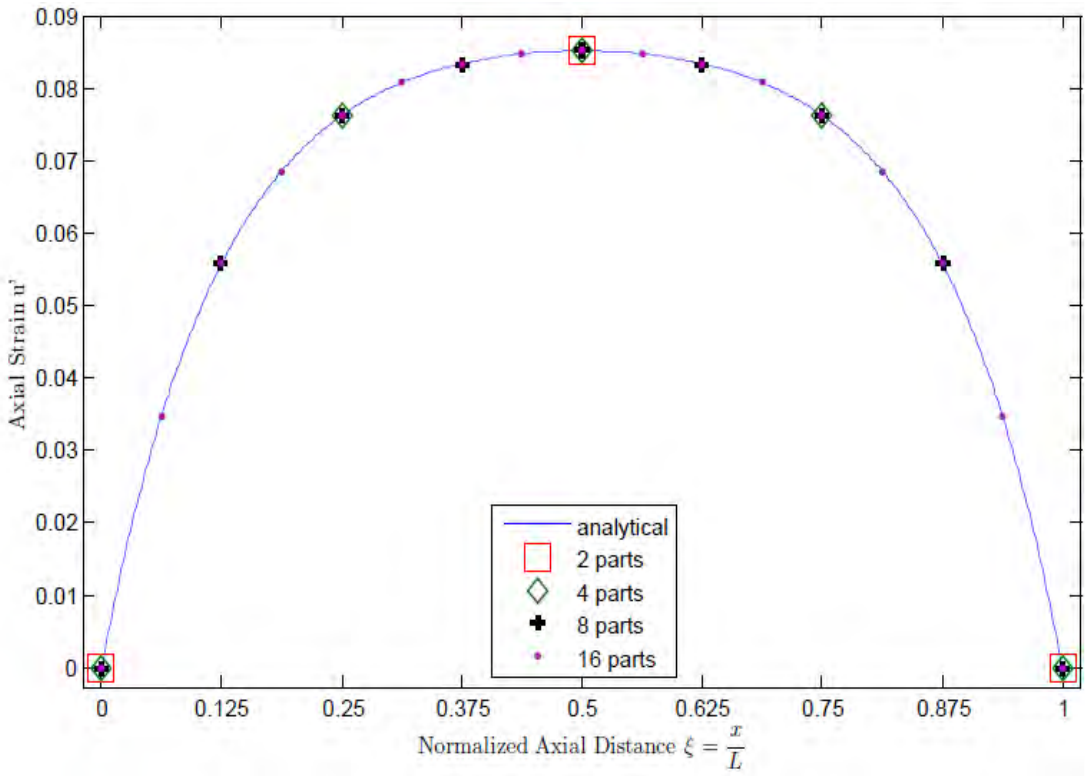

Fig. 118 FEM and analytical solutions of the axial strain u' of a bar in tension with restrained end strains versus normalized axial distance $\xi = x/L$. The classical BCs are $u(\xi = 0) = 0$, $P(\xi = 1) = P_1$, and the non classical ones $u'(\xi = 0) = 0$, $u'(\xi = 1) = 0$

In the figures above, the bars displacement and strain fields are presented as obtain by dividing it into 2, 4, 8, 16 parts and using the same number of bar elements connected by elastic nodes to model it. The FEM solutions describe perfectly the bars displacement and strain fields, no matter how big or small each element is chosen (the discretization). This is a very basic gradient elastic loading case, and the results are extremely satisfactory. Next, a less simple loading case puts these bar elements to the test.

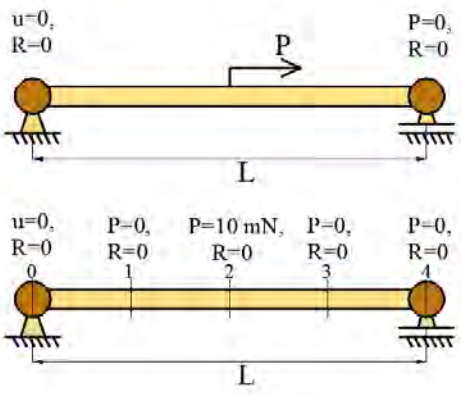

Fig. 119 Schematic representation of the second problem, and the four part discretization used.

In this, second, problem the same bar is studied, subjected to a different load. This time the concentrated force P is applied at the bars middle instead of its free end while no double forces are applied at its ends. The analytical solution was obtained using the distributed load function $q(x) = \delta(x - L/2)P$, δ being the dirac function and P the concentrated load, and

the BCs are $u(\xi=0)=0,\ R(\xi=0)=0,\ R(\xi=1)=0,\ P(\xi=1)=0$

The analytical solution obtained is:

$$u(\xi)=\frac{PL}{EA}\left\{\xi-\frac{\sinh(c/2)}{c}\frac{\sinh(c\xi)}{\sinh(c)}+\left\langle\xi-\frac{1}{2}\right\rangle\left(\xi-\frac{1}{2}+\frac{1}{c}\sinh\left(\frac{c}{2}(1-2\xi)\right)\right)\right\}$$

Where $\langle\bullet\rangle$ denotes the Heaviside step function, $\xi=x/L$ and $c=L/g$.

In the following figures is shown that, in this non standard case too, the bar elements can describe perfectly both the bars longitudinal displacement and strain, even when the discretization chosen is quite big, i.e. the length of the elements is half the bars length.

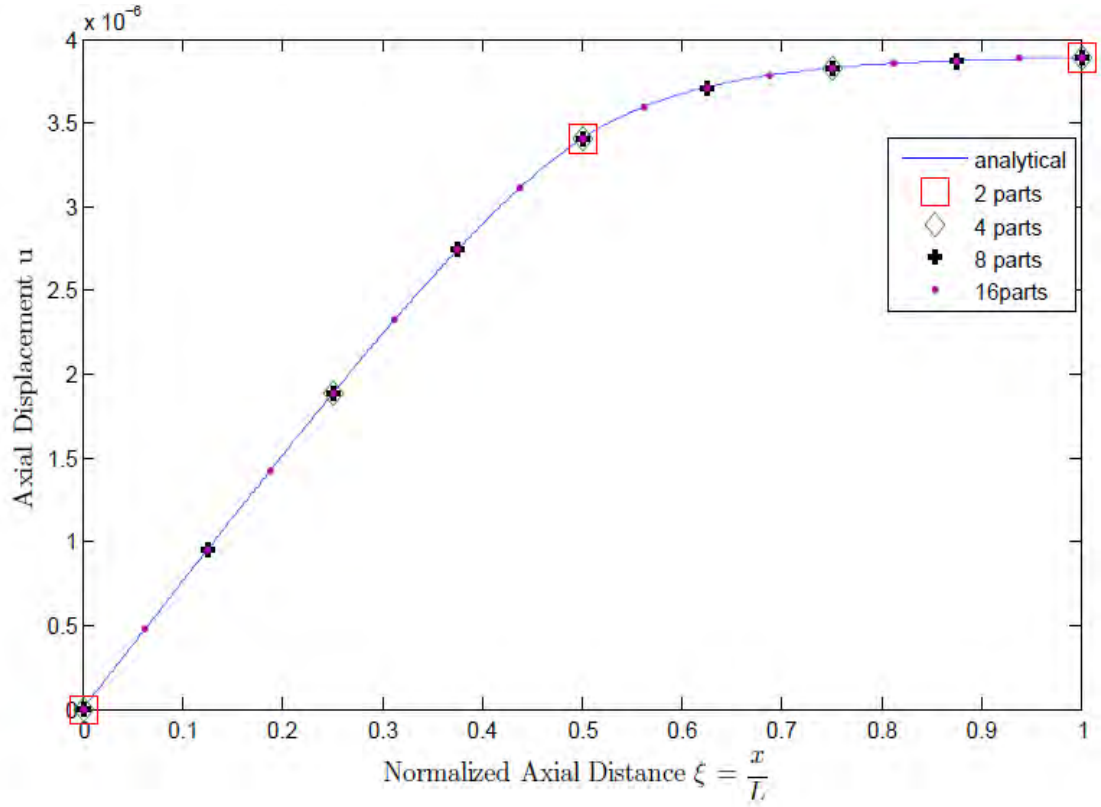

Fig. 120 FEM and analytical solutions of the axial displacement u of a bar with a force P applied at its middle versus normalized axial distance $\xi = x/L$. The classical BCs are $u(\xi=0)=0$, $P(\xi=1)=0$, and the non classical ones $R(\xi=0)=0$, $R(\xi=1)=0$

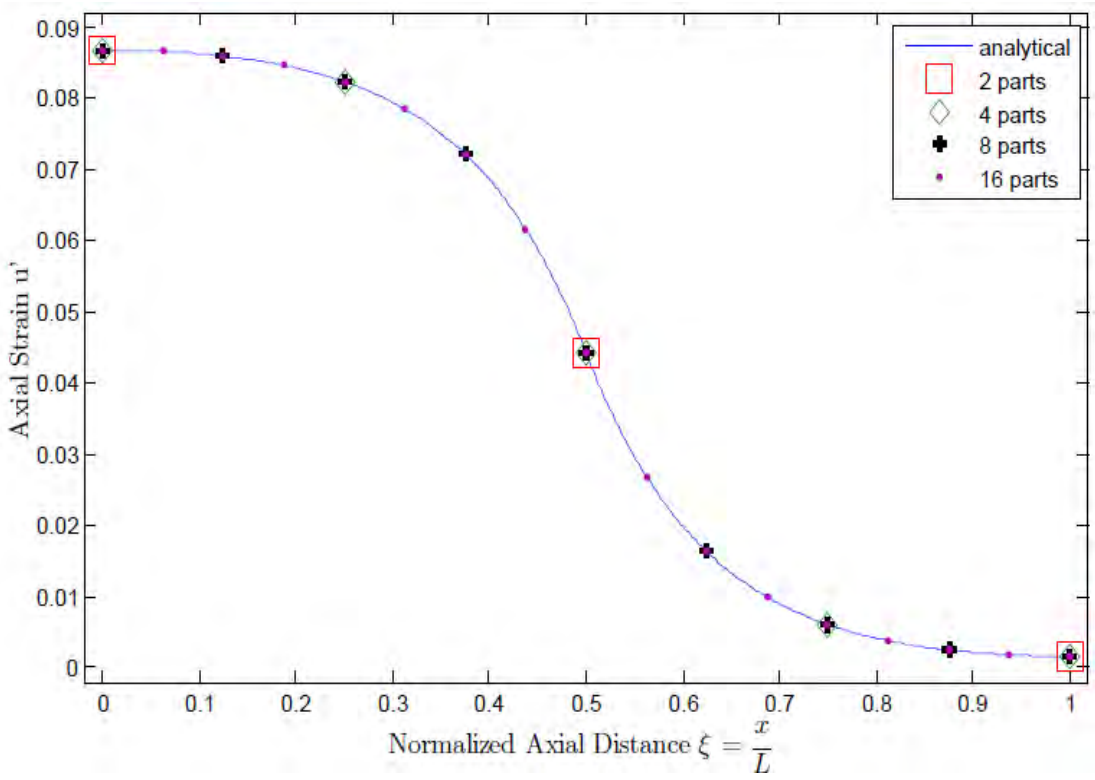

Fig. 121 FEM and analytical solutions of the strain u' of a bar with a force P applied at its middle versus normalized axial distance $\xi = x / L$. The classical BCs are $u(\xi = 0) = 0$, $P(\xi = 1) = 0,$ and the non classical ones $R(\xi = 0) = 0$, $R(\xi = 1) = 0$

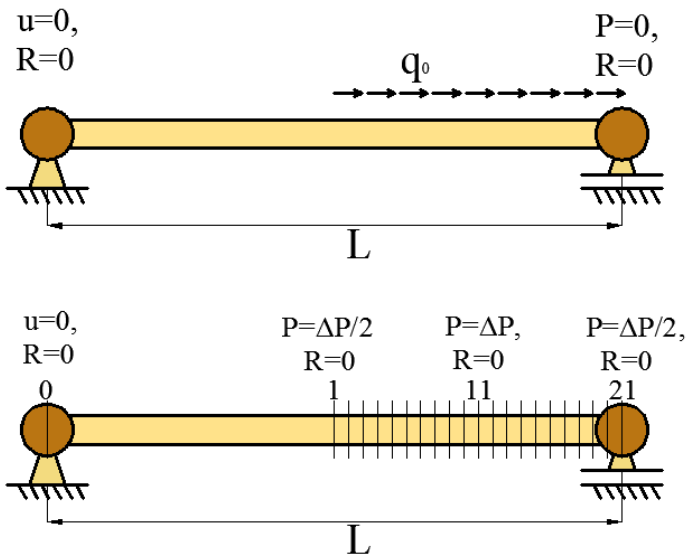

Fig. 122 Schematic representation of the third problem, and the 21 part discretization used.

Third, it is shown that these elements can be used to model cases of distributed axial load. In this example, the second half of the aforementioned bar is loaded with a distributed axial tensile load, while no double forces are applied at it's ends. The analytical solution was obtained using the distributed load function $q(x) = < x - L/2 > q_0$, $< \bullet >$ being the Heaviside step function and q_0=100μN/μm the distributed load. The BCs read $u(\xi = 0) = 0,\ R(\xi = 0) = 0,\ R(\xi = 1) = 0,\ P(\xi = 1) = 0$

The analytical solution obtained is

$$u(\xi)=\frac{q_0 L^2}{EA}\left\{\frac{\xi}{2}-\frac{2\sinh^2(c/4)}{c^2}\frac{\sinh(c\xi)}{\sinh(c)}+<\xi-\frac{1}{2}>\left(-\frac{\xi^2}{2}+\frac{\xi}{2}-1+\frac{2}{c^2}\sinh^2\left(\frac{c}{2}\left(\xi-\frac{1}{2}\right)\right)\right)\right\}$$

Where $\langle\bullet\rangle$ denotes the Heaviside step function, $\xi=\frac{x}{L}$ and $c=\frac{L}{g}$.

In order to model this loading there were used 21 bar elements, one for the first half of the bar, since as noted before, they describe the bars behavior perfectly, even when big elements are used, and twenty bar elements of the same length ΔL=L/40 to model the second half of the bar. The load was modeled as twenty one concentrated forces $\Delta P=q_0\Delta L$ applied an the nodes of the bar, except for the nodes 1 ans 21, to which half this force is applied (ΔP/2).

As show below, the FEM results for both the bars displacement and the strain are in perfect agreement with the analytical solution, even in this approximation of the external load.

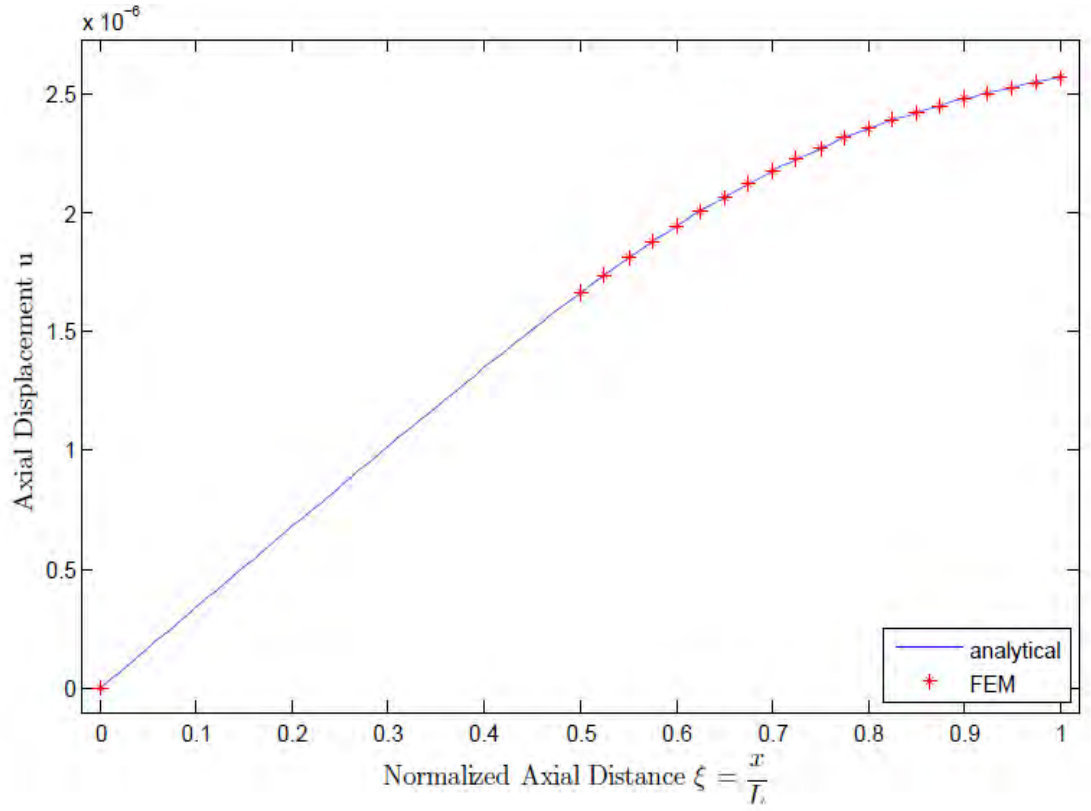

Fig. 123 FEM and analytical solutions of the axial displacement u of a bar with with distributed axial load at half its length versus normalized axial distance $\xi = x/L$. The classical BCs are $u(\xi=0)=0$, $P(\xi=1)=0$, and the non classical ones $R(\xi=0)=0$, $R(\xi=1)=0$

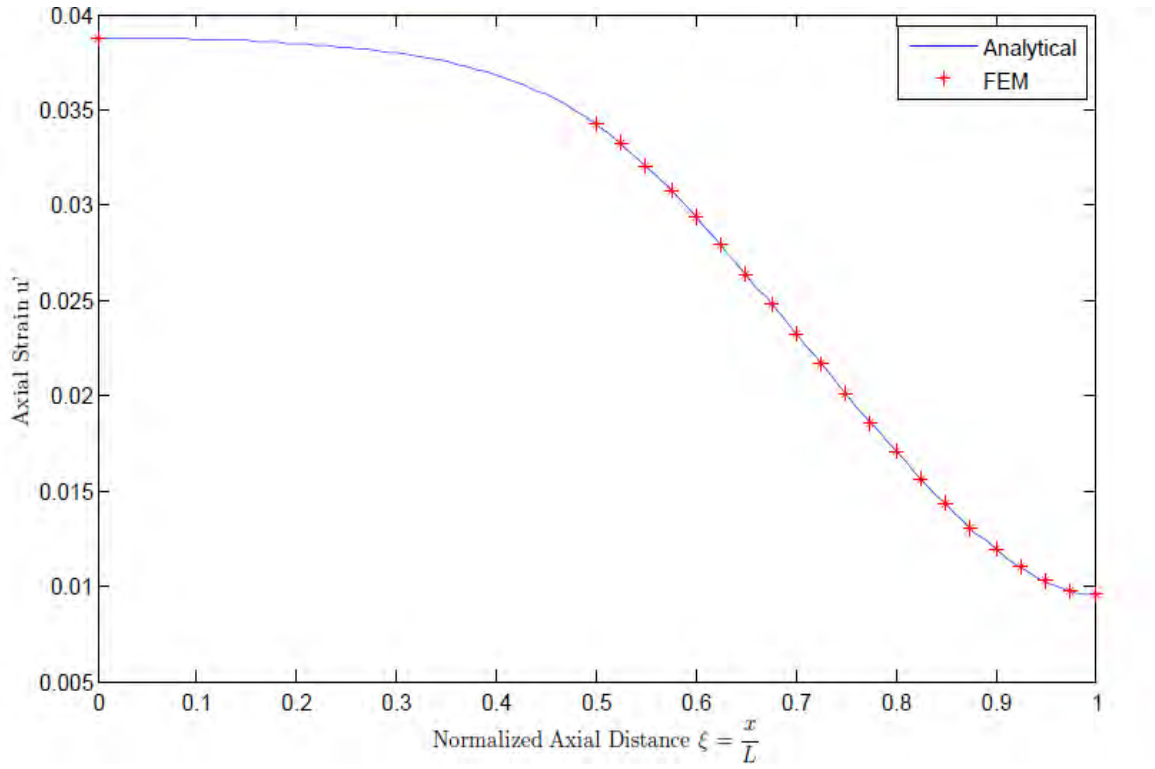

Fig. 124 FEM and analytical solutions of the axial strain u' of a bar with with distributed axial load at half its length versus normalized axial distance $\xi = x / L$. The classical BCs are $u(\xi = 0) = 0$, $P(\xi = 1) = 0,$ and the non classical ones $R(\xi = 0) = 0$, $R(\xi = 1) = 0$

A this point it must be noted that using the developed bar elements allows the application of double force loads at any point of the bar, even, practically, distributed double forces. This is not, though, a type of load that is directly supported by the analytical theory.

All the examples above were cases that could be addressed by the theory using jump and other functions. That, however, results to difficult and time consuming integrations, which sometimes may even not have closed form integrals, so the FEM provide an alternative route to address such problems.

The fourth and last example is one that cannot be addressed by the theory as developed earlier due the greater complexity of its geometry, but aspires to be solved nonetheless. It is inspired and also addressed by Kahrobayan (Kahrobaiyan, et al., 2013) and represents the longitudinal behavior of a micro drill subjected to an axial load.

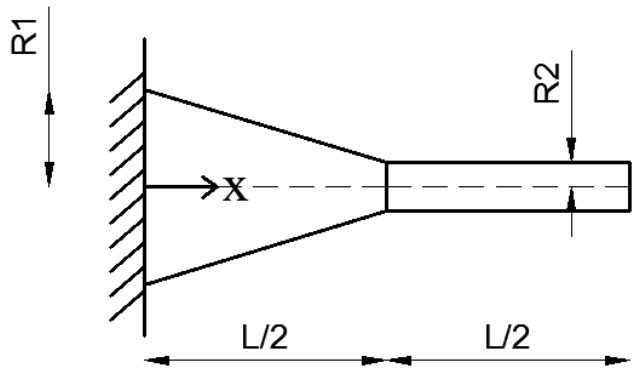

Fig. 125 Schematic representation of the third problem(microdrill).

The drill is assumed to be of length L=132,12μm, material length parameters g=11.01μm, l=0μm, Young's modulus E=600GPa and circular cross sections $R_1=4R_2, R_2=L/20$. An axial force $P=10^4$ μm is applied and no external double stresses.

It is modeled using bar elements of the same characteristics except cross sectional area, which depends on each elements position in this composite structure, as indicated from the geometry. It is modeled by dividing it to 20, 40 and 80 parts and the same number of bar elements. The figure below presents the drills behavior as obtained using both classical (red color) and gradient (blue color) FEMS.

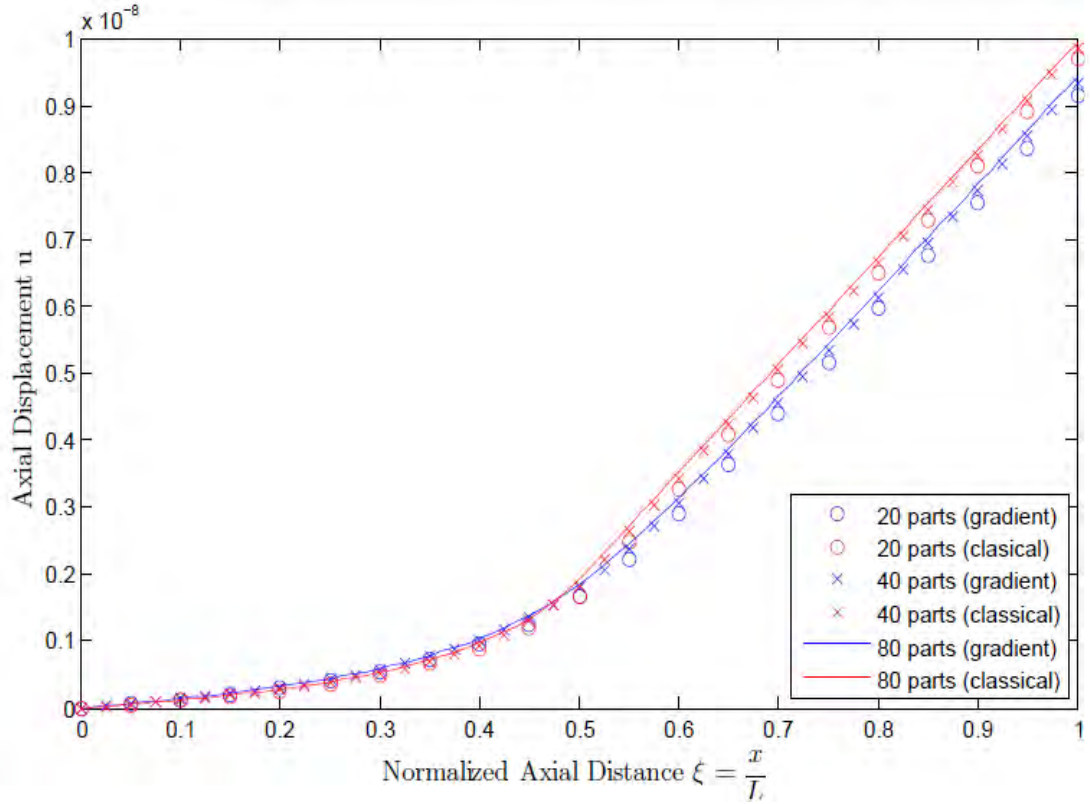

Fig. 126 FEM and analytical solutions of the axial displacement u **of the microdrill versus normalized axial distance** $\xi = x / L$**. The classical BCs are** $u(\xi = 0) = 0$**,** $P(\xi = 1) = 0$**, and the non classical ones** $R(\xi = 0) = 0$**,** $R(\xi = 1) = 0$

Note that resulting displacements depend on the number of elements used, which is to be expected, since an approximation of the true geometry is chosen, and the more elements are used, the geometrical modeling changes significantly and gets more exact. The solution with the most elements is considered to be the most accurate. In every case, though, the displacement calculated using the gradient FEMs is smaller than the one obtained using classical FEMS.

The stiffness matrices used to solve the problems above are to be used only when it is assumed that the elements interface is fully elastic. In the case that rigid nodes are assumed instead of interfaces, thus the strain at each elements ends is assumed to be zero, the stiffness matrix above can be simplified to a 2 by 2 matrix

$$\tilde{\mathbf{K}} = \frac{EA}{L - 2g\tanh(L/2g)}\begin{bmatrix} 1 & -1 \\ -1 & 1 \end{bmatrix}$$

$$\mathbf{f} = \begin{bmatrix} fxi & fxj \end{bmatrix}^T = \begin{bmatrix} -P_{(\xi=0)} & P_{(\xi=1)} \end{bmatrix}^T$$

$$\mathbf{d} = \begin{bmatrix} dxi & dxj \end{bmatrix}^T$$

In this case the strains at the end are a priori known and the double forces R applied by the node at each bar are different and not of great interest since they also are not aggregated in this node model. Note that the double forces R can easily be calculated as:

$$\frac{R_0}{EA} = -\frac{R_1}{EA} = \frac{\tanh(c/2)}{c - 2\tanh(c/2)}\frac{PL}{EA} = \frac{1}{c - 2\tanh(c/2)}\frac{\Delta u}{L},\ \Delta u = u_1 - u_0$$

This stiffness matrix is very similar to the classical elasticity one and when the g length is small compared to the length L is simplified to the classical one, but when the L/g parameter is not very high then this matrix denotes a much stiffer behavior of bar element. Dividing a gradient bar is several elements joined by these nodes, this composite body's behavior will be much stiffer than the one given by the analytical solution, since the smaller an elements length gets, the stiffer it gets, since the material parameter g is constant and each elements ends strain is assumed zero. The reason for such a result is that in this case is that this is not an equivalent problem to the one of the whole bar. The strain at several points throughout its length is determined and assumed zero, jumps of the double stresses and curvatures are applied, which are not present in the

original problem. A simple example of a bar that confirms the observation above is the following, which compares the behavior of a bar with zero end strains under axial tension.

i.e. the BCs are intended to be $u'(\xi=0)=u'(\xi=1)=0$, $u(\xi=0)=0$, $P(\xi=1)=P_1$

The numerical values used for the different parameters of the problem in the following example were obtained by Kahrobaiyan (Kahrobaiyan, et al., 2013) in their majority and some were chosen properly. it is assumed that E=1.44 GPa and g=11.01 μm, $P_1=10^4$ μN, c=L/g=8, l=0, A=

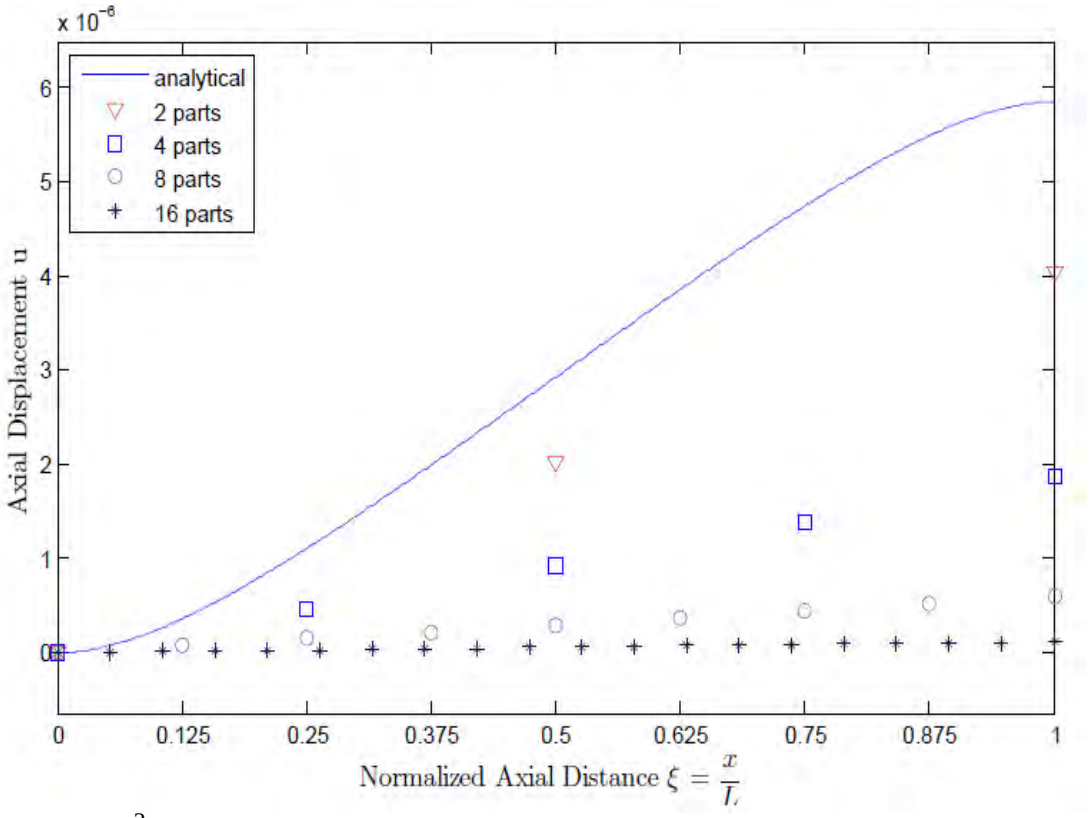

$78.54\mu m^2$

Fig. 127 FEM and analytical solutions of the axial displacement u of a bar in tension with restrained end strains versus normalized axial distance $\xi = x/L$ using rigid nodes. The classical BCs are $u(\xi=0)=0$, $P(\xi=1)=P_1$, and the non classical ones $u'(\xi=0)=0$, $u'(\xi=1)=0$

Although, these nodes are not to be used as finite elements to model bars, it does not mean they cannot be used in truss modeling problems.

4.II.4. 2-D Bar Structures - Trusses

4.II.4.i. Node function in composite 2D structures

In the framework of classical elasticity, 2D trusses are made by joining bars using nodes. These nodes are considered to be rigid bodies and their role is maintaining the continuity of the displacements while allowing the relative rotation of the bars. The node itself, as a point body has no rotation degrees of freedom, and only forces can be applied to it, no moments. Truss structures are loaded solely via their nodes, thus, no moments can be applied to the bars, which, this way, are loaded only axially.

However, studying the way that the bars are connected to the node in real trusses, one will see that usually, each bar is pinned to the node using more than one bolt. This type of connection allows moments to applied, since the bolts' distance can function as cantilever for forces couples. So it needs to be investigated whether the believed to be truss functions as a total of bars pinned together using nodes or as a total of beams fixed together at different angles. This problem is addressed in Appendix 1 in its most simple form, i.e. the case of two bar truss.

The following conclusion is drawn by that study: the bars' moments can be ignored, and the joint can be considered as a node, in the case that the bars' lengths are significantly greater than their other dimensions. Always, in trusses, slender bars are used; therefore, the assumption of no moments is acceptable.

As pointed out earlier, the node is a point body. Thus, Newton's law of motion it needs to be satisfied, besides the continuity of the displacements at it. In the case of i bars pinned together to a node, the following relations should be satisfied:

$$u_{x_i} = \bar{u}_x \,,\; u_{y_i} = \bar{u}_y \text{ for and } \sum P_{x_i} + P_{x\,\text{external}} = 0,\; \sum P_{y_i} + P_{y\,\text{external}} = 0$$

Any problem, either statically determinate or indeterminate, can be solved if the bars' properties and either the displacement or the external force in the direction of each axis is known each node. The unknown displacements can be found using the stiffness method.

In the case of a gradient elastic truss, knowing these relations does not suffice in order to find the trusses behavior. In contrast with the classical bars which have two degrees of freedom, the gradient bars have four, so at its of their ends two BCs need to be determined.

The choice of the non classical BCs depends on the kind of node that is used. The easiest node to assume is the rigid node, who restrains the strains of the bars' ends, the extra BCs are already known and very simple. The problem can be solved using a modified form of the stiffness method, using the gradient bars' stiffness matrix, which is presented in the next section. This type of node has been used by (Olufemi, 2011), who, however, did not use the stiffness method they way it is presented here, in order to obtain the nodal displacements. As expected, stiffer than classical behaviors were obtained for the structures considered when the microstructure parameter g was not insignificant.

Another kind of node should be considered, one that does not restrain the bars' strains, but allows the application of external double forces to the bars, following a gradient type generalization of action-reaction law. Also, as in the case of the 1D, the strain tensor of all connected to the node bars should be the same at the node, and its form should be the following

$$\begin{bmatrix} \varepsilon xx & 0 \\ 0 & \varepsilon yy \end{bmatrix}$$

since, the two deformations that can be considered in this model are the εxx and εyy because no shear loads can be applied to the bars and no equilibrium equation of the bars involves either shear stresses or strains. These demands are based on the assumption, that the node problem can be addressed as a plane problem of a continuous body.

Bars are 1D objects so the assumption can be made that the 1D boundary conditions should be satisfied. Thus, the condition $\partial \mathbf{u} / \mathrm{d}\hat{\mathbf{n}} = \varepsilon \hat{\mathbf{n}}$ should be satisfied for all bars joined to the node, no matter the angle they form. Due to the form of the displacement fields, $\partial \mathbf{u} / \mathrm{d}\hat{\mathbf{n}} = (\nabla \otimes \mathbf{u}) \cdot \hat{\mathbf{n}} = \tilde{\mathbf{e}} \cdot \hat{\mathbf{n}}$, which means that for any angle that the bars might be joined $\tilde{\mathbf{e}} \cdot \hat{\mathbf{n}} = \varepsilon \hat{\mathbf{n}}$. Hence, the strain tensor $\tilde{\mathbf{e}}$ must be the unit tensor multiplied by a constant.

4.II.4.ii. 2-D stiffness matrix

All the problems addressed to this point were one dimensional, so the stiffness matrix already presented was sufficient for their solution. However, two dimensional composite bar structures (trusses) are widely used in real time applications. In order to solve these problems it is needed to obtain the global stiffness matrix of a gradient elastic bar.

First, the 2-D stiffness matrix of a classical bar element is obtained, and next, the gradient bar element 2D stiffness matrix is presented.

Fig. 128 Forces and displacement vectors expressed in the local coordinate system of a classical bar

The force and displacement components of the classical bar element are linked by the member stiffness relations $f_i = K_{ij} d_j \rightarrow \mathbf{f} = \tilde{\mathbf{K}} \cdot \mathbf{d}$ which is written out in full is:

$$\begin{bmatrix} f_{xi} \\ f_{yi} \\ f_{xj} \\ f_{yj} \end{bmatrix} = \begin{bmatrix} K_{11} & K_{12} & K_{13} & K_{14} \\ K_{21} & K_{22} & K_{23} & K_{24} \\ K_{31} & K_{32} & K_{33} & K_{34} \\ K_{41} & K_{42} & K_{43} & K_{44} \end{bmatrix} \cdot \begin{bmatrix} d_{xi} \\ d_{yi} \\ d_{xj} \\ d_{yj} \end{bmatrix}$$

The element supports only axial loads, so no perpendicular to the axis of the bar forces are to be applied and any perpendicular displacements do not raise the stress of the bar, so, this relation is simplified to:

$$\begin{bmatrix} -P \\ 0 \\ P \\ 0 \end{bmatrix} = \frac{EA}{L} \begin{bmatrix} 1 & 0 & -1 & 0 \\ 0 & 0 & 0 & 0 \\ -1 & 0 & 1 & 0 \\ 0 & 0 & 0 & 0 \end{bmatrix} \cdot \begin{bmatrix} d_{xi} \\ d_{yi} \\ d_{xj} \\ d_{yj} \end{bmatrix}$$

These are the node force and node displacement vectors and the member stiffness matrix in local coordinate system x,y. In order to assemble bars that are not collinear the forces, displacements and the stiffness matrix should be expressed in the global coordinate system X,Y (capital letters).

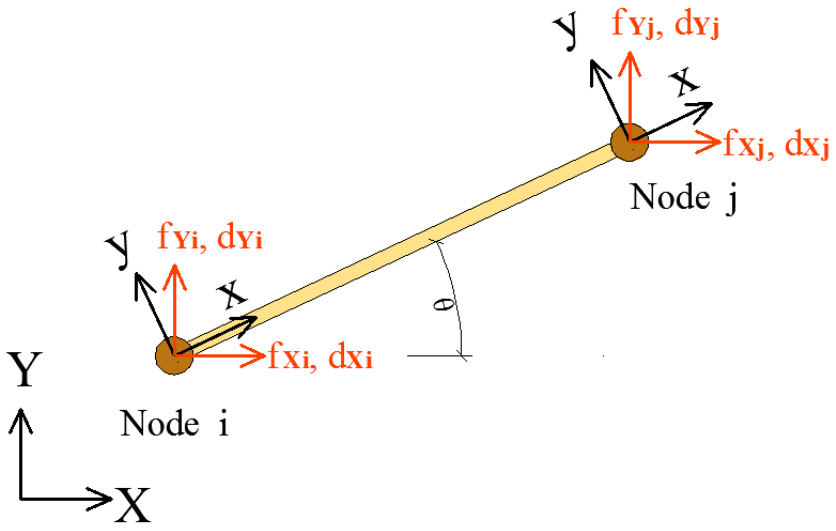

Fig. 129 Forces and displacement vectors expressed in the blobal coordinate system X,Y

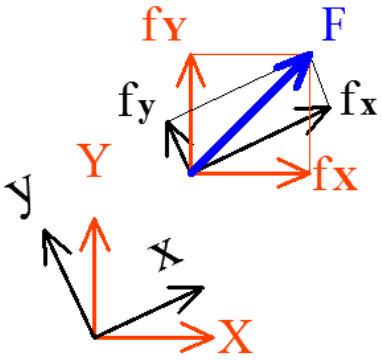

Fig. 130 vector analyzed in two coordinate systems x,y and X,Y

It is well known that a vector F when expressed in the two coordinate systems x,y and X,Y, it's components follow the relationship

$$\begin{bmatrix} F_X \\ F_Y \end{bmatrix} = \begin{bmatrix} \cos(\theta) & -\sin(\theta) \\ \sin(\theta) & \cos(\theta) \end{bmatrix} \cdot \begin{bmatrix} F_x \\ F_y \end{bmatrix}$$

$$\Leftrightarrow \mathbf{F}_G = \tilde{\mathbf{T}} \cdot \mathbf{F}_L, \quad \tilde{\mathbf{T}} = \begin{bmatrix} \cos(\theta) & -\sin(\theta) \\ \sin(\theta) & \cos(\theta) \end{bmatrix},$$

$$\tilde{\mathbf{T}}^{-1} = \tilde{\mathbf{T}}^{T} = \begin{bmatrix} \cos(\theta) & \sin(\theta) \\ -\sin(\theta) & \cos(\theta) \end{bmatrix},$$

where the subscripts G and L denote that the vector are expressed with respect to the global (X,Y) and the local (x,y) coordinate system respectively.

Using this identity the relation of the node displacements and forces in the local and global coordinate systems is

$$\mathbf{f}_G = \begin{bmatrix} \tilde{\mathbf{T}} & \tilde{\mathbf{O}} \\ \tilde{\mathbf{O}} & \tilde{\mathbf{T}} \end{bmatrix} \cdot \mathbf{f}_L \text{ and } \mathbf{d}_G = \begin{bmatrix} \tilde{\mathbf{T}} & \tilde{\mathbf{O}} \\ \tilde{\mathbf{O}} & \tilde{\mathbf{T}} \end{bmatrix} \cdot \mathbf{d}_L, \ \tilde{\mathbf{O}} = \begin{bmatrix} 0 & 0 \\ 0 & 0 \end{bmatrix}$$

The member stiffness relation is transformed as follows.

$$\mathbf{f}_L = \tilde{\mathbf{K}}_L \cdot \mathbf{d}_L \Leftrightarrow \begin{bmatrix} \tilde{\mathbf{T}} & \tilde{\mathbf{O}} \\ \tilde{\mathbf{O}} & \tilde{\mathbf{T}} \end{bmatrix} \cdot \mathbf{f}_L = \begin{bmatrix} \tilde{\mathbf{T}} & \tilde{\mathbf{O}} \\ \tilde{\mathbf{O}} & \tilde{\mathbf{T}} \end{bmatrix} \cdot \tilde{\mathbf{K}}_L \cdot \mathbf{d}_L \Leftrightarrow \mathbf{f}_G = \begin{bmatrix} \tilde{\mathbf{T}} & \tilde{\mathbf{O}} \\ \tilde{\mathbf{O}} & \tilde{\mathbf{T}} \end{bmatrix} \cdot \tilde{\mathbf{K}}_L \cdot \begin{bmatrix} \tilde{\mathbf{T}}^T & \tilde{\mathbf{O}} \\ \tilde{\mathbf{O}} & \tilde{\mathbf{T}}^T \end{bmatrix} \cdot \mathbf{d}_G$$

$$\Leftrightarrow \mathbf{f}_G = \tilde{\mathbf{K}}_G \cdot \mathbf{d}_G, \qquad \tilde{\mathbf{K}}_G = \begin{bmatrix} \tilde{\mathbf{T}} & \tilde{\mathbf{O}} \\ \tilde{\mathbf{O}} & \tilde{\mathbf{T}} \end{bmatrix} \cdot \tilde{\mathbf{K}}_L \cdot \begin{bmatrix} \tilde{\mathbf{T}}^T & \tilde{\mathbf{O}} \\ \tilde{\mathbf{O}} & \tilde{\mathbf{T}}^T \end{bmatrix}, \text{ which is the global stiffness matrix}$$

Gradient global stiffness matrix

Following the same steps, first the local and the global stiffness matrix of a gradient elastic bar is found.

$$\mathbf{f} = [fxi \quad fyi \quad rxi \quad ryi \quad fxj \quad fyj \quad rxj \quad ryj]^T = [-Pi \quad 0 \quad Ri \quad 0 \quad Pj \quad 0 \quad Rj \quad 0]^T$$

$$\mathbf{d} = [dxi \quad dyi \quad \varepsilon xi \quad \varepsilon yi \quad dxj \quad dyj \quad \varepsilon xj \quad \varepsilon yj]^T$$

$$\tilde{\mathbf{K}}_L = \begin{bmatrix} K_{11} & K_{12} & K_{13} & K_{14} & K_{15} & K_{16} & K_{17} & K_{18} \\ K_{21} & K_{22} & K_{23} & K_{24} & K_{25} & K_{26} & K_{27} & K_{28} \\ K_{31} & K_{32} & K_{33} & K_{34} & K_{35} & K_{36} & K_{37} & K_{38} \\ K_{41} & K_{42} & K_{43} & K_{44} & K_{45} & K_{46} & K_{47} & K_{48} \\ K_{51} & K_{52} & K_{53} & K_{54} & K_{55} & K_{56} & K_{57} & K_{58} \\ K_{61} & K_{62} & K_{63} & K_{64} & K_{65} & K_{66} & K_{67} & K_{68} \\ K_{71} & K_{72} & K_{73} & K_{74} & K_{75} & K_{76} & K_{77} & K_{78} \\ K_{81} & K_{82} & K_{83} & K_{84} & K_{85} & K_{86} & K_{87} & K_{88} \end{bmatrix}$$

However, no perpendicular to the bars axis force, double force, displacement or strain does not affect the bar, so the elements of the 2rd, 4th , 6th and 8th row and column are all zero. So it is simplified to

$$\tilde{\mathbf{K}}_L = \begin{bmatrix} K_{11} & 0 & K_{13} & 0 & K_{15} & 0 & K_{17} & 0 \\ 0 & 0 & 0 & 0 & 0 & 0 & 0 & 0 \\ K_{31} & 0 & K_{33} & 0 & K_{35} & 0 & K_{37} & 0 \\ 0 & 0 & 0 & 0 & 0 & 0 & 0 & 0 \\ K_{51} & 0 & K_{53} & 0 & K_{55} & 0 & K_{57} & 0 \\ 0 & 0 & 0 & 0 & 0 & 0 & 0 & 0 \\ K_{71} & 0 & K_{73} & 0 & K_{75} & 0 & K_{77} & 0 \\ 0 & 0 & 0 & 0 & 0 & 0 & 0 & 0 \end{bmatrix}$$

The non zero elements of the matrix are the same as the ones of the 1D element stiffness matrix and in the same order, i.e. this matrix can be obtained by adding a zero row and column after each row and column respectively to the 1d stiffness matrix.

The global stiffness matrix takes the following form

$$\tilde{\mathbf{K}}_G = \begin{bmatrix} \tilde{\mathbf{T}} & \tilde{\mathbf{O}} & \tilde{\mathbf{O}} & \tilde{\mathbf{O}} \\ \tilde{\mathbf{O}} & \tilde{\mathbf{T}} & \tilde{\mathbf{O}} & \tilde{\mathbf{O}} \\ \tilde{\mathbf{O}} & \tilde{\mathbf{O}} & \tilde{\mathbf{T}} & \tilde{\mathbf{O}} \\ \tilde{\mathbf{O}} & \tilde{\mathbf{O}} & \tilde{\mathbf{O}} & \tilde{\mathbf{T}} \end{bmatrix} \cdot \tilde{\mathbf{K}}_L \cdot \begin{bmatrix} \tilde{\mathbf{T}}^T & \tilde{\mathbf{O}} & \tilde{\mathbf{O}} & \tilde{\mathbf{O}} \\ \tilde{\mathbf{O}} & \tilde{\mathbf{T}}^T & \tilde{\mathbf{O}} & \tilde{\mathbf{O}} \\ \tilde{\mathbf{O}} & \tilde{\mathbf{O}} & \tilde{\mathbf{T}}^T & \tilde{\mathbf{O}} \\ \tilde{\mathbf{O}} & \tilde{\mathbf{O}} & \tilde{\mathbf{O}} & \tilde{\mathbf{T}}^T \end{bmatrix}$$

4.II.4.iii. 2-D Applications

Two truss problems will be addressed for each node. One problem that is statically determinate, in its classical meaning, and one statically indeterminate.

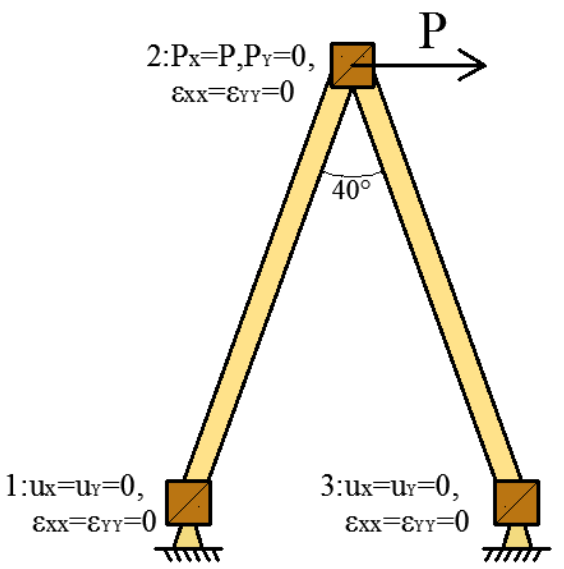

Fig. 131 the 2D truss of the first problem adressed

In the first problem considered, a two bar plane truss is loaded with a horizontal force $P=10^4\mu N$ at its top node. The bars are pinned rigid nodes, and they form an angle of 40^o. Each bar is of length $L=55\mu m$, Young's modulus $E=1.44$ GPa and of cross sectional area $A=78.54\ \mu m^2$. For the material length parameter g, four values are considered, g/L=0.5, 0.25, 0.125, 0.05, while l parameter is assumed to be zero. The trusses response, to this loading for each material length is calculated using a generalized stiffness method which is outlined further on.

There are three nodes, thus the structures degrees of freedom are 3x4=12.

The generalized force and displacement vectors are:

$$\mathbf{f}=\left[fx_1 \quad fy_1 \quad rx_1 \quad ry_1 \quad fx_2 \quad fy_2 \quad rx_2 \quad ry_2 \quad fx_3 \quad fy_3 \quad rx_3 \quad ry_3\right]^T$$

$$\mathbf{d}=\left[dx_1 \quad dy_1 \quad \varepsilon xx_1 \quad \varepsilon yy_1 \quad dx_2 \quad dy_2 \quad \varepsilon xx_2 \quad \varepsilon yy_2 \quad dx_3 \quad dy_3 \quad \varepsilon xx_3 \quad \varepsilon yy_3\right]^T$$

In order to facilitate the assembly of the total stiffness matrix, the elements global stiffness matrix is divided into 16 2 by 2 matrices as shown below.

$$\tilde{\mathbf{K}}_G=\begin{bmatrix} \tilde{\mathbf{K}}_{11} & \tilde{\mathbf{K}}_{12} & \tilde{\mathbf{K}}_{13} & \tilde{\mathbf{K}}_{14} \\ \tilde{\mathbf{K}}_{21} & \tilde{\mathbf{K}}_{22} & \tilde{\mathbf{K}}_{23} & \tilde{\mathbf{K}}_{24} \\ \tilde{\mathbf{K}}_{31} & \tilde{\mathbf{K}}_{32} & \tilde{\mathbf{K}}_{33} & \tilde{\mathbf{K}}_{34} \\ \tilde{\mathbf{K}}_{41} & \tilde{\mathbf{K}}_{42} & \tilde{\mathbf{K}}_{43} & \tilde{\mathbf{K}}_{44} \end{bmatrix},$$

$$\tilde{\mathbf{K}}_{ij} = K_{2i-1,\,2j-1} \cdot \tilde{\mathbf{T}} \cdot \begin{bmatrix} 1 & 0 \\ 0 & 0 \end{bmatrix} \cdot \tilde{\mathbf{T}}^{T} = K_{2i-1,\,2j-1} \cdot \begin{bmatrix} (1+\cos 2\theta)/2 & \sin 2\theta/2 \\ \sin 2\theta/2 & (1-\cos 2\theta)/2 \end{bmatrix}$$

The global stiffness matrix of the bar with ends at the nodes k,l is referred to as $\tilde{\mathbf{K}}_G{}^{k,l}$, and the k,l superscripts are also added to the $\tilde{\mathbf{K}}_{ij}$ matrices that form the global matrix, i.e. $\tilde{\mathbf{K}}_{ij}{}^{k,l}$.

Now, the assembly of the structure's stiffness matrix can be done exactly as the classical theory indicates.

$$\begin{bmatrix} fx1;fy1 \\ rx1;ry1 \\ fx2;fy2 \\ rx2;ry2 \\ fx3;fy3 \\ rx3;ry3 \end{bmatrix} = \begin{bmatrix} \tilde{\mathbf{K}}_{11}^{1,2} & \tilde{\mathbf{K}}_{12}^{1,2} & \tilde{\mathbf{K}}_{13}^{1,2} & \tilde{\mathbf{K}}_{14}^{1,2} & & \\ \tilde{\mathbf{K}}_{21}^{1,2} & \tilde{\mathbf{K}}_{22}^{1,2} & \tilde{\mathbf{K}}_{23}^{1,2} & \tilde{\mathbf{K}}_{24}^{1,2} & & \\ \tilde{\mathbf{K}}_{31}^{1,2} & \tilde{\mathbf{K}}_{32}^{1,2} & \tilde{\mathbf{K}}_{33}^{1,2}+\tilde{\mathbf{K}}_{11}^{2,3} & \tilde{\mathbf{K}}_{34}^{1,2}+\tilde{\mathbf{K}}_{12}^{2,3} & \tilde{\mathbf{K}}_{13}^{2,3} & \tilde{\mathbf{K}}_{14}^{2,3} \\ \tilde{\mathbf{K}}_{41}^{1,2} & \tilde{\mathbf{K}}_{42}^{1,2} & \tilde{\mathbf{K}}_{43}^{1,2}+\tilde{\mathbf{K}}_{21}^{2,3} & \tilde{\mathbf{K}}_{44}^{1,2}+\tilde{\mathbf{K}}_{22}^{2,3} & \tilde{\mathbf{K}}_{23}^{2,3} & \tilde{\mathbf{K}}_{24}^{2,3} \\ & & \tilde{\mathbf{K}}_{31}^{2,3} & \tilde{\mathbf{K}}_{32}^{2,3} & \tilde{\mathbf{K}}_{33}^{2,3} & \tilde{\mathbf{K}}_{34}^{2,3} \\ & & \tilde{\mathbf{K}}_{41}^{2,3} & \tilde{\mathbf{K}}_{42}^{2,3} & \tilde{\mathbf{K}}_{43}^{2,3} & \tilde{\mathbf{K}}_{44}^{2,3} \end{bmatrix} \cdot \begin{bmatrix} dx1;dy1 \\ \varepsilon xx1;\varepsilon yy1 \\ dx2;dy2 \\ \varepsilon xx2;\varepsilon yy2 \\ dx3;dy3 \\ \varepsilon xx2;\varepsilon yy2 \end{bmatrix}$$

From the displacement vector, only the terms $dx2;dy2$ are unknown and all the other terms are zero. To find the unknowns, the order of the equations and the unknowns is changed so that all the known forces, double forces and the unknown displacements and strains are placed as the first terms of the respective vectors. This way a new matrix is created.

$$\begin{bmatrix} fx1;fy1 \\ rx1;ry1 \\ P;0 \\ rx2;ry2 \\ fx3;fy3 \\ rx3;ry3 \end{bmatrix} = \begin{bmatrix} \tilde{\mathbf{K}}_{11}^{1,2} & \tilde{\mathbf{K}}_{12}^{1,2} & \tilde{\mathbf{K}}_{13}^{1,2} & \tilde{\mathbf{K}}_{14}^{1,2} & & \\ \tilde{\mathbf{K}}_{21}^{1,2} & \tilde{\mathbf{K}}_{22}^{1,2} & \tilde{\mathbf{K}}_{23}^{1,2} & \tilde{\mathbf{K}}_{24}^{1,2} & & \\ \tilde{\mathbf{K}}_{31}^{1,2} & \tilde{\mathbf{K}}_{32}^{1,2} & \tilde{\mathbf{K}}_{33}^{1,2}+\tilde{\mathbf{K}}_{11}^{2,3} & \tilde{\mathbf{K}}_{34}^{1,2}+\tilde{\mathbf{K}}_{12}^{2,3} & \tilde{\mathbf{K}}_{13}^{2,3} & \tilde{\mathbf{K}}_{14}^{2,3} \\ \tilde{\mathbf{K}}_{41}^{1,2} & \tilde{\mathbf{K}}_{42}^{1,2} & \tilde{\mathbf{K}}_{43}^{1,2}+\tilde{\mathbf{K}}_{21}^{2,3} & \tilde{\mathbf{K}}_{44}^{1,2}+\tilde{\mathbf{K}}_{22}^{2,3} & \tilde{\mathbf{K}}_{23}^{2,3} & \tilde{\mathbf{K}}_{24}^{2,3} \\ & & \tilde{\mathbf{K}}_{31}^{2,3} & \tilde{\mathbf{K}}_{32}^{2,3} & \tilde{\mathbf{K}}_{33}^{2,3} & \tilde{\mathbf{K}}_{34}^{2,3} \\ & & \tilde{\mathbf{K}}_{41}^{2,3} & \tilde{\mathbf{K}}_{42}^{2,3} & \tilde{\mathbf{K}}_{43}^{2,3} & \tilde{\mathbf{K}}_{44}^{2,3} \end{bmatrix} \cdot \begin{bmatrix} 0;0 \\ 0;0 \\ dx2;dy2 \\ 0;0 \\ 0;0 \\ 0;0 \end{bmatrix} \Rightarrow$$

$$\begin{bmatrix} P;0 \\ fx1;fy1 \\ rx1;ry1 \\ rx2;ry2 \\ fx3;fy3 \\ rx3;ry3 \end{bmatrix} = \begin{bmatrix} \tilde{\mathbf{K}}_{33}^{1,2}+\tilde{\mathbf{K}}_{11}^{2,3} & \tilde{\mathbf{K}}_{31}^{1,2} & \tilde{\mathbf{K}}_{32}^{1,2} & \tilde{\mathbf{K}}_{34}^{1,2}+\tilde{\mathbf{K}}_{12}^{2,3} & \tilde{\mathbf{K}}_{13}^{2,3} & \tilde{\mathbf{K}}_{14}^{2,3} \\ \tilde{\mathbf{K}}_{13}^{1,2} & \tilde{\mathbf{K}}_{11}^{1,2} & \tilde{\mathbf{K}}_{12}^{1,2} & \tilde{\mathbf{K}}_{14}^{1,2} & & \\ \tilde{\mathbf{K}}_{23}^{1,2} & \tilde{\mathbf{K}}_{21}^{1,2} & \tilde{\mathbf{K}}_{22}^{1,2} & \tilde{\mathbf{K}}_{24}^{1,2} & & \\ \tilde{\mathbf{K}}_{43}^{1,2}+\tilde{\mathbf{K}}_{21}^{2,3} & \tilde{\mathbf{K}}_{41}^{1,2} & \tilde{\mathbf{K}}_{42}^{1,2} & \tilde{\mathbf{K}}_{44}^{1,2}+\tilde{\mathbf{K}}_{22}^{2,3} & \tilde{\mathbf{K}}_{23}^{2,3} & \tilde{\mathbf{K}}_{24}^{2,3} \\ \tilde{\mathbf{K}}_{31}^{2,3} & & & \tilde{\mathbf{K}}_{32}^{2,3} & \tilde{\mathbf{K}}_{33}^{2,3} & \tilde{\mathbf{K}}_{34}^{2,3} \\ \tilde{\mathbf{K}}_{41}^{2,3} & & & \tilde{\mathbf{K}}_{42}^{2,3} & \tilde{\mathbf{K}}_{43}^{2,3} & \tilde{\mathbf{K}}_{44}^{2,3} \end{bmatrix} \cdot \begin{bmatrix} dx2;dy2 \\ 0;0 \\ 0;0 \\ 0;0 \\ 0;0 \\ 0;0 \end{bmatrix}$$

$\mathbf{L_{11}}$ $\mathbf{L_{12}}$ $\mathbf{L_{21}}$ $\mathbf{L_{22}}$

The new matrix is divided in four parts and the unknowns are easily found using the following relations, (in this specific problem)

$$[dx2\ dy2] = \tilde{\mathbf{L}}_{11}^{-1} \cdot [P\ 0] + \tilde{\mathbf{L}}_{12}^{-1} \cdot [0\,0 \quad 0\,0 \quad 0\,0 \quad 0\,0 \quad 0\,0]^T$$

$$[fx1\ fy1 \quad rx1\ ry1 \quad rx2\ ry2 \quad fx3\ fy3 \quad rx3\ ry3]^T = \tilde{\mathbf{L}}_{21} \cdot [dx2\ dy2] + \tilde{\mathbf{L}}_{22} \cdot [0\,0 \quad 0\,0 \quad 0\,0 \quad 0\,0 \quad 0\,0]^T$$

The following matrices present the displacement of the top node of the truss, as well as the external forces and double forces applied to the truss by the nodes, for each case of the g length that was considered.

	g/L=0.5	g/L=0.25	g/L=0.125	g/L=0.05	g/L→0-classical
dx2(10^{-4}m)	0.0496	0.1077	0.1559	0.1871	0.2079
dy2(10^{-4}m)	0	0	0	0	0

	g/a=0.5	g/a=0.25	g/a=0.125	g/a=0.05	g/a→0-classical
fx1(N)	-0.0050	-0.0050	-0.0050	-0.0050	-0.0050
fy1(N)	-0.0137	-0.0137	-0.0137	-0.0137	-0.0137
fx2(N)	0.0100	0.0100	0.0100	0.0100	0.0100
fy2(N)	0	0	0	0	0
fx3(N)	-0.0050	-0.0050	-0.0050	-0.0050	-0.0050
fy3(N)	0.0137	0.0137	0.0137	0.0137	0.0137

	g/a=0.5	g/a=0.25	g/a=0.125	g/a=0.05	g/a→0-classical
rx1(10^{-6}Nm)	-0.1047	-0.0663	-0.0344	-0.0137	0
ry1(10^{-6}Nm)	-0.2877	-0.1821	-0.0944	-0.0378	0
rx2(10^{-6}Nm)	0	0	0	0	0
ry2(10^{-6}Nm)	-0.5754	-0.3642	-0.1888	-0.0756	0
rx3(10^{-6}Nm)	0.1047	0.0663	0.0344	0.0137	0
ry3(10^{-6}Nm)	-0.2877	-0.1821	-0.0944	-0.0378	0

As expected, the use of the rigid node results to smaller displacements, especially when the microstructure is significant. Also, no matter the microstructure, each bar bears the same axial load, which was to be expected, since it is determinate truss. The double forces needed to restrain the bars' strain are smaller for smaller microstructure lengths g.

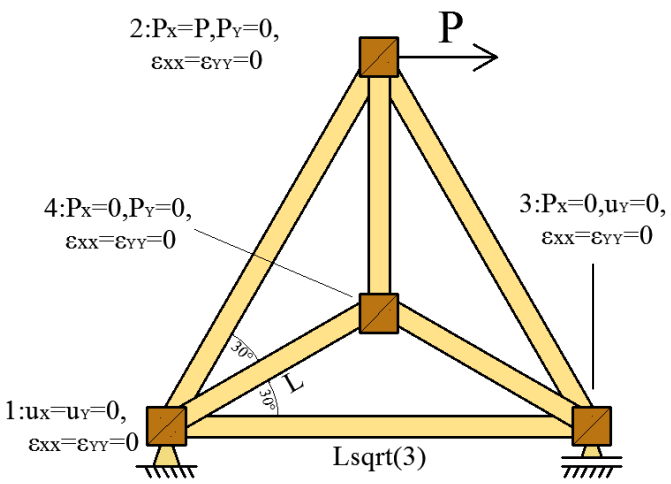

Fig. 131 2D indeterminate truss of the second problem addressed

The second problem addressed is the case of the statically indeterminate truss in figure 132. The bars are assumed to be of length L=5mm, Young's modulus E and cross sectional area A. The material parameter l is assumed zero and six values are assumed for the g length, g/a= 0.5, 0.25, 0.125, 0.005, 0.0001, 0.000001.

In the following matrices, the normalized displacement of the nodes 2, 3 and 4 are given for the different g values that were considered. Also the external forces and double forces applied to the bars by the nodes are given.

	g/L=0,5	g/L=0,25	g/L=0,125	g/L=0,005	g/L=0,0001	g/L=0,000001
d2x/(P/EA) (m)	0,008745	0,013644	0,016428	0,019110	0,019219	0,019221
d2y/(P/EA) (m)	-0,000873	-0,001284	-0,001494	-0,001699	-0,001707	-0,001708
d3x/(P/EA) (m)	0,001635	0,002628	0,003215	0,003778	0,003801	0,003802
d4x/(P/EA) (m)	0,000817	0,001314	0,001607	0,001889	0,001901	0,001901
d4y/(P/EA) (m)	-0,001054	-0,001614	-0,001924	-0,002223	-0,002236	-0,002236

	g/L=0,5	g/L=0,25	g/L=0,125	g/L=0,005	g/L=0,0001	g/L=0,000001
P1x/P	-1,000000	-1,000000	-1,000000	-1,000000	-1,000000	-1,000000
P1y/P	-0,866025	-0,866025	-0,866025	-0,866025	-0,866025	-0,866025
P3y/P	0,866025	0,866025	0,866025	0,866025	0,866025	0,866025

	g/L=0,5	g/L=0,25	g/L=0,125	g/L=0,005	g/L=0,0001	g/L=0,000001
R1x/P (m)	-2,2899E-03	-1,2429E-03	-6,2496E-04	-2,5000E-05	-5,0000E-07	-5,0000E-09
R1y/P (m)	-1,9999E-03	-1,0777E-03	-5,4124E-04	-2,1651E-05	-4,3301E-07	-4,3301E-09
R2x/P (m)	2,0575E-04	9,1991E-05	4,1360E-05	1,5292E-06	3,0504E-08	3,0502E-10
R2y/P (m)	-3,7783E-03	-2,0069E-03	-1,0109E-03	-4,0653E-05	-8,1319E-07	-8,1319E-09
R3x/P (m)	5,5886E-04	2,7127E-04	1,2404E-04	4,5877E-06	9,1511E-08	9,1506E-10
R3y/P (m)	-2,3563E-03	-1,2370E-03	-6,1288E-04	-2,4299E-05	-4,8585E-07	-4,8584E-09
R4x/P (m)	-1,0307E-19	-1,5441E-19	-1,9620E-20	-2,3816E-21	-1,3692E-23	-5,5050E-25
R4y/P (m)	-4,3368E-19	2,1684E-19	5,4210E-20	3,3881E-21	-5,2940E-23	4,1359E-25

In this case too, using the classical theory, bigger displacements are calculated. Also, when the microstructure to length ratio is big (g/L=0.5) the smallest displacements are calculated, half of the classical ones. However, the smaller this ratio is, the greater double stresses that the nodes need to apply. The way the forces are distributed to the nodes is not affected by the microstructure.

If not interested in the double forces, then instead of using the full stiffness matrix, one may use the global transformation of the simplified 2x2 stiffness matrix for the bar with restrained end, given in last problem of section 4.II.3.iii. . In other words, the classical stiffness method theory may be used, using the gradient element stiffness matrix that the non classical degrees of freedom and the non classical 'forces' are eliminated.

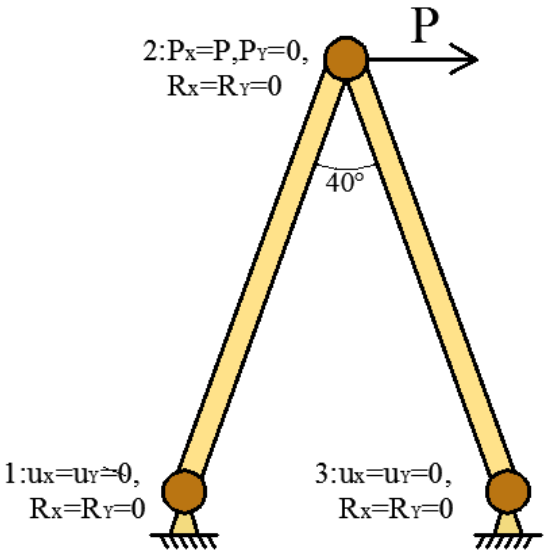

When attempting to address the respective two problems using the 'elastic' node instead of the rigid one with no extra double forces applied to the nodes, the equation matrix becomes singular. Thus, they are not well posed and it is not possible to

assume such a node. The reason for this conclusion will be explained next.

The classical properties of a node are attributed to the gradient node too, and two non classical properties have been attributed to it:

- One, it is assumed that external double forces can be applied to it and then be distributed to the bars.
- Two, it is assumed that the strain tensor at the bars' ends connected to the node is the same: $\begin{bmatrix} \varepsilon xx & 0 \\ 0 & \varepsilon yy \end{bmatrix}$

In any determinate problem the double forces R can be analyzed and the R BCs of each bar can be determined, thus their displacement fields can be found since the forces, too, in determinate trusses are easily found. However, the strain fields that are this way calculated at the ends of the connected bars are not of the form assumed so it is to be expected that this method crushes. Thus, this node model is not acceptable.

Problems of determinate trusses where nodal double forces are assumed to be applied can be solved following the next steps:

- The axial double forces applied to each bar member can be found using the assumed generalized action-reaction law.
- These double forces elongate the bar by a length $\Delta L=(R_j+R_i)/EA$, where i and j are the end points of the bar, and the positive direction for both R vectors is away from the bar's main body.
- This extra length can be integrated in the classical methods the same way that elongation due thermal strains is considered.

For indeterminate trusses to be solved this way, it first is needed to describe how the double forces will be distributed to the connected members, and then the same steps may be followed.

Finally it is noted that anothe types of nodes could be considered. For example a node that the applied double forces and the axial force follow a linear relation. This might be the result of the way that the connection of the bodies is actualized.

Truss problems with this type of nodes be solved by using a similar to the classical stiffness 2x2 matrix, that is be obtained through gradient elasticity, by substituting the relation of the double forces with the axial force to the respective gradient problem solution. This way, the new force displacement relation is obtained and it can be used in order to construct the member stiffness matrix as in the classical case. The case of the rigid node can be considered as a special case of this type of node, in which the relation of the forces and the double forces applied at the bars' ends is the following:

$$R_i = -R_1 = \left(\frac{\tanh(c/2)}{c - 2\tanh(c/2)} L \right) P = kP, \quad k = \text{constant}$$

4.II.5. Conclusions

The following conclusions can be drawn about the composite bar structures:

- Two types of 1D nodes were considered, the rigid and the elastic node.
- The rigid node restrains the joined elements ends strains and the structure is stiffer than one using elastic nodes
- The elastic node functions as an interface and demands that the strain of all joined member is the same and the double forces at the interface follow a generalized action reaction law.
- The elastic node can be used in modeling continuous 1D structures under any loading with very satisfactory results
- The 1D and 2 D stiffness matrices of a gradient bar were obtained
- A generalized stiffness method for gradient elastic for 2D and 1D problem was outlined
- In 2D structures there was not found a generalized form of an elastic node
- Determinate and indeterminate structures with rigid nodes, under simple loading were solved using the stiffness method
- Another type of non holonomic 2D node was proposed.

5.Appendices

5.I. Appendix I: Classical truss node function investigation

In this appendix, is tested the assumption that the bars of a truss when connected to a node are subjected only to axial loads. This means that no transverse loads or bending moments are significant, so they can be ignored.

It is noted that in real trusses more than one bolts are used to connect each bar a node. This connection in general may allow the development of bending moments. For this reason, the truss with the node is modeled as a lambda beam. A lambda beam is a continuous beam consisting of two beams pined at one end and fixed together at an angle at the other.

Practically, by substituting the truss by a continuous beam, the worst case scenario is being taken into account, which assumes that the choice of a node connection is incorrect, both moments and transverse forces are applied to the bar, which in reality are beams, and the degree of freedom of the relative rotation of the beams is restrained.

The material and geometrical properties of each beam are assumed to be different in the general case, and are given in the following matrix.

Property	Beam 1	Beam 2
Length	l_1	l_2
Young's Modulus	E_1	E_2
Shear Modulus	G_1	G_2
Area Moment of Inertia	J_1	J_2
Cross Sectional Area	A_1	A_2
Shear Area	A'_1	A'_2

The loading cases examined are the ones that can be applied to the original truss, i.e. only forces are applied to the top of the lambda beam, i.e. the point of the two beams connection.

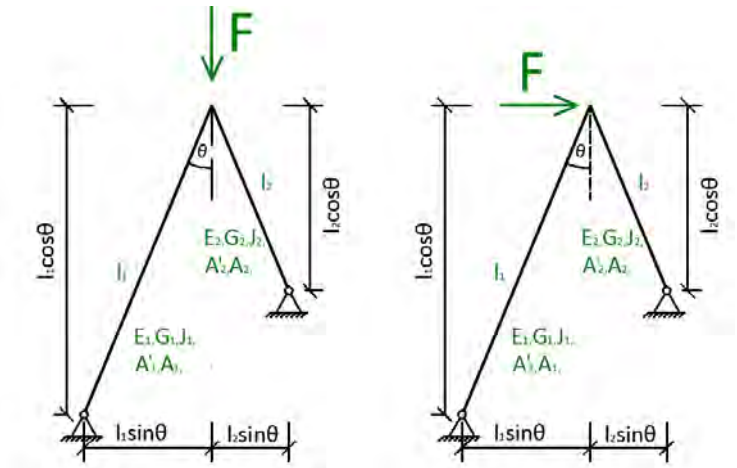

The problem of the Lambda beam is a statically indeterminate one, so the flexibility method is used in order to calculate the support reactions.

In this method, the restrained degree of freedom of the relative rotation of the beams is freed and two moments of equal magnitude X_1 are applied so that this DOF will be indirectly restrained. In order to find the X_1 value, the relative rotation of the released bars, due to the external loading (δ_{1q}) and to a unit two moments loading (δ_{11}) is calculated, and the X_1 unknown is found using the next equation that models the no restrain of the relative rotation of the beams

$$\delta_{1q} + \delta_{11} \cdot X_1 = 0$$

δ_{1q} and δ_{11} are found using the unit force theory, which can be summarized in the following equation, for classical beam structures:

$$\delta_{ij} = \int M_{,i}\, \kappa_{,j}\, ds + \int Q_{,i}\, \gamma_{,j}\, ds + \int N_{,i}\, \varepsilon_{,j}\, ds \rightarrow$$

$$\delta_{ij} = \int M_{,i}\, M_{,j} \frac{ds}{EJ} + \int Q_{,i}\, Q_{,j} \frac{ds}{GA'} + \int N_{,i}\, \varepsilon_{,j} \frac{ds}{EA}$$

, δ_{ij}: the generalized displacement that is work conjugate to the i^{th} generalized unit load applied, due to the application of the j^{th} generalized load.(generalized loads might be moment, shear of axial forces, two moments, constraints and other)

, $(\bullet),j$: the $(\bullet)$ field of the bar resulting from the application of the generalized j^{th} generalized load.

s: an axial coordinate of the whole structure

M,Q,N the moment, shear and axial stress fields of the structure respectively

κ,γ,ε the curvature, shear strain and axial strain fields of the structure respectively.

The following figures present the M,Q,N fields of the released structure, due to the external load and the unit moments. Then δ_{1q} and δ_{11} are found.

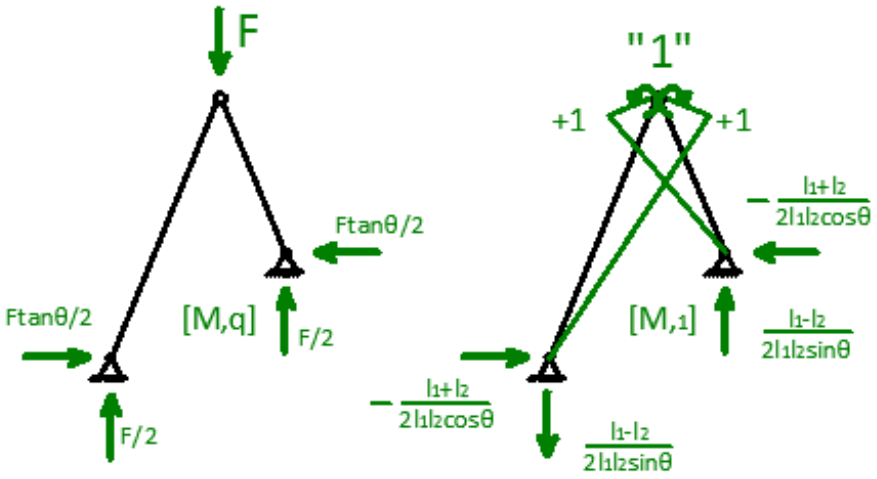

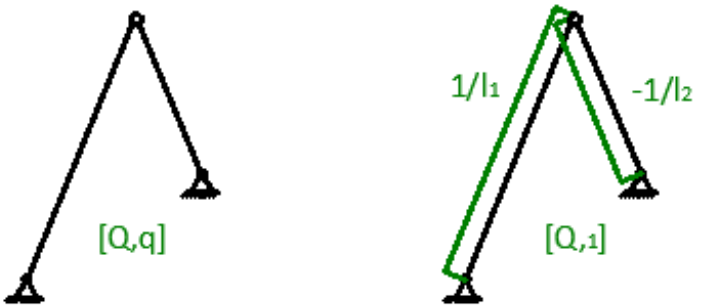

$$a=\frac{l_1+l_2}{2l_1l_2}\tan\theta+\frac{l_1-l_2}{2l_1l_2}\cot\theta$$

$$b=\frac{l_1+l_2}{2l_1l_2}\tan\theta-\frac{l_1-l_2}{2l_1l_2}\cot\theta$$

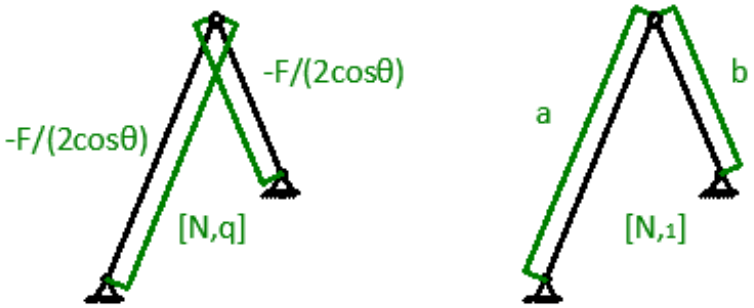

$$\delta_{1q}=0+0-\frac{F}{2\cos\theta}\left(\frac{l_1}{E_1A_1}a+\frac{l_2}{E_2A_2}b\right)$$

$$=-\frac{F}{2\cos\theta}\left(\frac{l_1}{E_1A_1}\left[\frac{l_1+l_2}{2l_1l_2}\tan\theta+\frac{l_1-l_2}{2l_1l_2}\cot\theta\right]+\frac{l_2}{E_2A_2}\left[\frac{l_1+l_2}{2l_1l_2}\tan\theta-\frac{l_1-l_2}{2l_1l_2}\cot\theta\right]\right)$$

$$\delta_{11}=\frac{l_1}{3E_1J_1}+\frac{l_2}{3E_2J_2}+\frac{1}{G_1A'_1l_1}+\frac{1}{G_2A'_2l_2}+\left(\frac{l_1}{E_1A_1}a^2+\frac{l_2}{E_2A_2}b^2\right)$$

So the X_1 moments are obtained:

$$X_1 = -\frac{\delta_{1q}}{\delta_{11}} = \frac{Fl_1}{2\cos\theta} \frac{al_1\left(1+\frac{l_2/E_2A_2}{l_1/E_1A_1}\frac{b}{a}\right)}{\frac{A_1{l_1}^2}{3J_1}\left(1+\frac{l_2/E_2J_2}{l_1/E_1J_1}\right)+\frac{E_1}{G_1}\frac{A_1}{A'_1}\left(1+\frac{G_1A'_1}{G_2A'_2}\right)+a^2{l_1}^2\left(1+\frac{l_2/E_2A_2}{l_1/E_1A_1}\left(\frac{b}{a}\right)^2\right)}$$

$$al_1 = \frac{1}{2}\left(\frac{l_1}{l_2}\right)\cdot\left(\left(1+\frac{l_1}{l_2}\right)\tan\theta+\left(1-\frac{l_1}{l_2}\right)\cot\theta\right), \qquad \frac{b}{a} = \frac{\tan^2\theta-\left(\frac{l_1/l_2-1}{l_1/l_2+1}\right)}{\tan^2\theta+\left(\frac{l_1/l_2-1}{l_1/l_2+1}\right)}$$

The moments X_1 become insignificant as their magnitude is small. The equation above indicates that for any given geometry of the problem, the magnitude of the moments is determined by the $A_1{l_1}^2/(3J_1)$ term, since the other terms can be assumed approximately equal to unity for any structure whose members are not made of very different materials and their cross sections do not differ dramatically. For great ratio values, the moment's magnitude is decreased.

For any given common cross section this A/J ratio is of order of magnitude of 10-10^2. This ratio is also multiplied with the bars length. Thus, when the Lambda beam consists of beams of great lengths, the moments' at their connection magnitude is small, and they can be ignored, so the fixed bars can be modeled as not fixed together, but as connected by a node, i.e. as a truss. Note that in trusses the bars used are slender, i.e. their length is greater than their other dimensions, so this condition is satisfied, and ignoring the moments is justified.

It should be noted that the $A_1{l_1}^2/J_1$ ratio also denotes how vulnerable a beam is to buckling. In this model no buckling effects are assumed.

In order to fully address this problem, it is needed to also investigate the case of a horizontal nodal loading. The same method is followed, and similar results are obtained, and the same conclusions can be drawn.

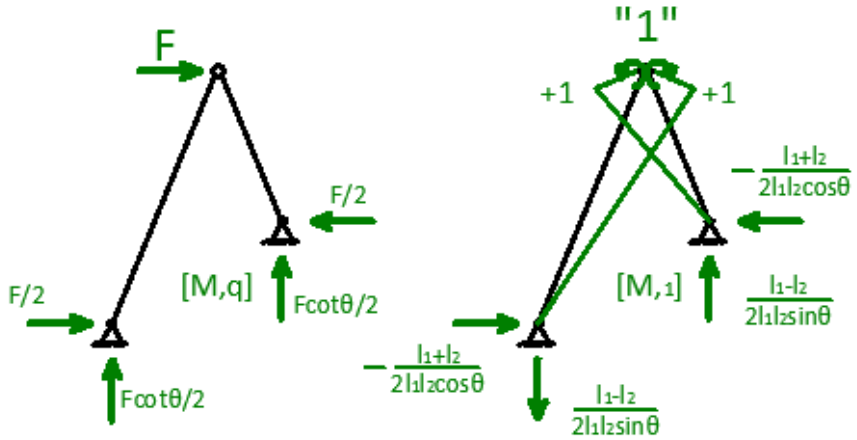

$$a=\frac{l_1+l_2}{2l_1l_2}\tan\theta+\frac{l_1-l_2}{2l_1l_2}\cot\theta$$

$$b=\frac{l_1+l_2}{2l_1l_2}\tan\theta-\frac{l_1-l_2}{2l_1l_2}\cot\theta$$

$$\delta_{1q}=0+0+\frac{F}{2\sin\theta}\left(\frac{l_1}{E_1A_1}a+\frac{l_2}{E_2A_2}b\right)$$

$$\delta_{11}=\frac{l_1}{3E_1J_1}+\frac{l_2}{3E_2J_2}+\frac{1}{G_1A'_1l_1}+\frac{1}{G_2A'_2l_2}+\left(\frac{l_1}{E_1A_1}a^2+\frac{l_2}{E_2A_2}b^2\right)$$

$$X_1=-\frac{\delta_{1q}}{\delta_{11}}=-\frac{Fl_1}{2\sin\theta}\frac{al_1\left(1+\frac{l_2/E_2A_2}{l_1/E_1A_1}\frac{b}{a}\right)}{\frac{A_1l_1^2}{3J_1}\left(1+\frac{l_2/E_2J_2}{l_1/E_1J_1}\right)+\frac{E_1}{G_1}\frac{A_1}{A'_1}\left(1+\frac{G_1A'_1}{G_2A'_2}\right)+a^2l_1^2\left(1+\frac{l_2/E_2A_2}{l_1/E_1A_1}\left(\frac{b}{a}\right)^2\right)}$$

5.II. Appendix II: Basic Spherical Coordinate System Identities

In the first part of this work problems of spherical symmetry, in spherical coordinate system were addressed. The transformation from Cartesian to spherical coordinates, as well as various identities and operator transformations concerning the spherical coordinate system are provided in this appendix.

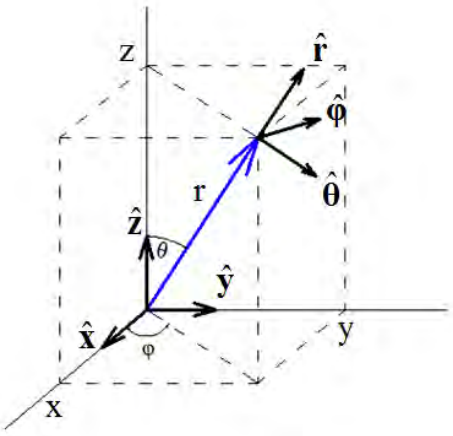

$$r = \sqrt{x^2 + y^2 + z^2} \qquad x = r\sin\theta\cos\phi$$

$$\theta = \tan^{-1}\left(\sqrt{x^2 + y^2}\,/\,z\right) \qquad y = r\sin\theta\sin\phi$$

$$\phi = \tan^{-1}(y/x) \qquad z = r\cos\theta$$

$$\hat{\mathbf{r}} = \frac{\mathbf{r}}{r} = \frac{x\,\hat{\mathbf{x}} + y\,\hat{\mathbf{y}} + z\,\hat{\mathbf{z}}}{r} = \sin\theta\cos\phi\ \hat{\mathbf{x}} + \sin\theta\sin\phi\ \hat{\mathbf{y}} + \cos\theta\ \hat{\mathbf{z}}$$

$$\hat{\boldsymbol{\varphi}} = \frac{\hat{\mathbf{z}}\times\mathbf{r}}{\sin\theta} = \frac{x\,\hat{\mathbf{x}} + y\,\hat{\mathbf{y}} + z\,\hat{\mathbf{z}}}{r} = -\sin\phi\ \hat{\mathbf{x}} + \cos\phi\ \hat{\mathbf{y}} + 0\,\hat{\mathbf{z}}$$

$$\hat{\boldsymbol{\theta}} = \hat{\boldsymbol{\varphi}}\times\hat{\mathbf{r}} = -\cos\theta\cos\phi\ \hat{\mathbf{x}} + \cos\theta\sin\phi\ \hat{\mathbf{y}} - \sin\theta\,\hat{\mathbf{z}}$$

The derivation of the spherical coordinate base vectors in respect with the coordinates themselves, i.e. the radius r, the polar φ and azimuth θ angle does not result to zero vectors, as it happens with the Cartesian coordinate base vectors.

	$\hat{\mathbf{r}}$	$\hat{\boldsymbol{\theta}}$	$\hat{\boldsymbol{\varphi}}$
$\partial/\partial r$	$\mathbf{0}$	$\mathbf{0}$	$\mathbf{0}$
$\partial/\partial\theta$	$\hat{\boldsymbol{\theta}}$	$-\hat{\mathbf{r}}$	$\mathbf{0}$
$\partial/\partial\phi$	$\hat{\boldsymbol{\varphi}}\sin\theta$	$\hat{\boldsymbol{\varphi}}\cos\theta$	$-\left[\hat{\mathbf{r}}\sin\theta + \hat{\boldsymbol{\theta}}\cos\theta\right]$

- $$d\mathbf{r} = d(r\,\hat{\mathbf{r}}) = d(r)\hat{\mathbf{r}} + r\,d(\hat{\mathbf{r}}) = dr\,\hat{\mathbf{r}} + r\left(\frac{\partial\hat{\mathbf{r}}}{\partial r}dr + \frac{\partial\hat{\mathbf{r}}}{\partial\theta}d\theta + \frac{\partial\hat{\mathbf{r}}}{\partial\phi}d\phi\right)$$
$$= dr\,\hat{\mathbf{r}} + r d\theta\,\hat{\boldsymbol{\theta}} + r\sin\theta d\phi\,\hat{\boldsymbol{\varphi}}$$

- $$\nabla u = \hat{\mathbf{r}}\frac{\partial u}{\partial r} + \frac{\hat{\boldsymbol{\theta}}}{r}\frac{\partial u}{\partial \theta} + \frac{\hat{\boldsymbol{\varphi}}}{r\sin\theta}\frac{\partial u}{\partial \phi}$$
- $$du = \nabla u \cdot d\hat{\mathbf{r}} = \frac{\partial u}{\partial r}dr + \frac{\partial u}{\partial \theta}d\theta + \frac{\partial u}{\partial \phi}d\phi$$
- $$\nabla \cdot \mathbf{v} = \frac{1}{r^2}\frac{\partial}{\partial r}\left(r^2 v_r\right) + \frac{1}{r\sin\theta}\frac{\partial}{\partial \theta}\left(\sin\theta\, v_\theta\right) + \frac{1}{r\sin\theta}\frac{\partial}{\partial \phi}\left(v_\phi\right)$$
- $$\nabla \times \mathbf{v} = \frac{\hat{\mathbf{r}}}{r\sin\theta}\left[\frac{\partial}{\partial \theta}\left(\sin\theta\, v_\phi\right) - \frac{\partial}{\partial \phi}\left(v_\theta\right)\right] + \frac{\hat{\boldsymbol{\theta}}}{r\sin\theta}\left[\frac{\partial}{\partial \phi}\left(v_r\right) - \sin\theta\frac{\partial}{\partial r}\left(r\, v_\phi\right)\right] + \frac{\hat{\boldsymbol{\varphi}}}{r}\left[\frac{\partial}{\partial \theta}\left(r\, v_\theta\right) - \frac{\partial}{\partial \theta}\left(v_r\right)\right]$$
- $$\Delta = \nabla^2 = \frac{1}{r^2}\frac{\partial}{\partial r}\left(r^2\frac{\partial}{\partial r}\right) + \frac{1}{r^2\sin\theta}\frac{\partial}{\partial \theta}\left(\sin\theta\frac{\partial}{\partial \theta}\right) + \frac{1}{r^2\sin^2\theta}\frac{\partial^2}{\partial \phi^2}$$
$$= \frac{2}{r}\frac{\partial}{\partial r} + \frac{\partial^2}{\partial r^2} + \frac{1}{r^2\tan\theta}\frac{\partial}{\partial \theta} + \frac{1}{r^2}\frac{\partial^2}{\partial \theta^2} + \frac{1}{r^2\sin^2\theta}\frac{\partial^2}{\partial \phi^2}$$

5.III. Appendix III: Hyperbolic Function Identities

Throughout this work many simplification have been made in order to obtain manageable forms of the mathematical solutions. Since, the non classical solutions of the differential equations are exponential ones and hyperbolic sins and cosines many hyperbolic trigonometric identities were used in extend. The ones used most often are presented in the present appendix.

$$\cosh x = \left(e^{x} + e^{-x}\right)/2$$

$$\sinh x = \left(e^{x} - e^{-x}\right)/2$$

$$\cosh^2 x - \sinh^2 x = 1$$

$$1 - \tanh^2 x = \operatorname{sech}^2 x, \qquad \coth^2 x - 1 = \operatorname{cosech}^2 x$$

$$\sinh(x \pm y) = \sinh x \cosh y \pm \sinh y \cosh x$$

$$\cosh(x \pm y) = \cosh x \cosh y + \sinh x \sinh y$$

$$\tanh(x \pm y) = \frac{\tanh x \pm \tanh y}{1 \pm \tanh x \tanh y}$$

$$\tanh(2x) = \frac{2\tanh x}{1 \pm \tanh^2 x}, \qquad \tanh(x) = \frac{2\tanh(x/2)}{1 \pm \tanh^2(x/2)}$$

$$\sinh^2(x/2) = \frac{\cosh(x) - 1}{2}$$

$$\cosh^2(x/2) = \frac{\cosh(x) + 1}{2}$$

$$\tanh(x/2) = \frac{\cosh x - 1}{\sinh x}, \qquad \coth(x/2) = \frac{\cosh x + 1}{\sinh x}$$

$$1-\frac{\cosh\{c(1-2x)\}}{\cosh c}=\sinh(2cx)\tanh c\left\{1-\frac{\tanh(cx)}{\tanh c}\right\}=1-\frac{\sinh(c(1-x))+\sinh(cx)}{\sinh c}$$

5.IV. Appendix IV: The pretwisted beam analogy by Kordolemis

This analogy has been the inspiration for a big part of the work presented in this thesis and is quoted several times when trying to better understand the gradient elastic problem of a bar in tension. This is the reason that the main points that were used are summarized below, in order to facilitate the reader. It should be noted that a different coordinate system is used than the one introduced in the original work by (Giannakopoulos, et al., 2013) and (Kordolemis, et al., 2013). This choise was made in order to use the same symbolism coordinate system that were used in the second part of this thesis for the gradient elastic bar.

The body considered is a cylindrical beam of length L, constant cross section of area A, Young's Modulus E and shear modulus G. A Cartesian coordinate system Oxyz is introduced, whose x axis coincides with the longitudinal axis of the beam and parallel to its generators. The beams bases are taken to lie in the Oyz plane, at x=0 (ξ=0 using the normalized coordinate system) and x=L (ξ=1). The origin is located at the center of the cross section at x=0, i.e. the x axis passes through the center of each cross section. The beam is pretwisted around the x axis by a constant amount of a0 per unit length of the beam, so that the rotation about the x axis of each cross section is $\phi_0(x) = a_0 x$. A local coordinate system η-ζ is introduced at each cross section by rotating the global y-z axes around the x axis by an angle $\phi_0(x) = a_0 x$, thus

$$\begin{bmatrix} \eta(x,y,z) \\ \zeta(x,y,z) \end{bmatrix} = \begin{bmatrix} \cos\phi_0 & \sin\phi_0 \\ -\sin\phi_0 & \cos\phi_0 \end{bmatrix} \cdot \begin{bmatrix} y \\ z \end{bmatrix} \quad , \phi_0 = a_0 x$$

The displacement field for the non-uniform torsion ('restrained warping') takes the following form

$$\mathbf{u}(x,y,z) = \begin{bmatrix} u_x(x,y,z) \\ u_y(x,y,z) \\ u_z(x,y,z) \end{bmatrix} = \begin{bmatrix} w_1(x) + \varphi'(x) \cdot \Psi(\eta(x,y,z), \zeta(x,y,z)) \\ -\varphi'(x)\, xz \\ \varphi'(x)\, xy \end{bmatrix}$$

where $\phi(x)$ is the infinitesimal rotation of the cross section around x axis, $w_1(x)$ a displacement component in the longitudinal (x-) direction, and

$\Psi(\eta,\zeta)$ is the Saint-Venant warping function of a similar beam without pretwist, normalized so that $\int_A \Psi(\eta,\zeta)\, d\eta d\zeta = 0$

Using the variation principle, the variation of external works is found

$$\delta W = \int_0^L (p_x\, \delta w_1 + m_x\, \delta\phi)\, dz + \left[N\, \delta w_1\right]_0^L + \left[T\, \delta\phi\right]_0^L + \left[-B\, \delta\phi'\right]_0^L,$$

where N is the axial load, T is the torque, $B = -\int_A \sigma_{xx} \Psi\, dA$ is the "Bimoment" applied at the ends and $p_x = -dN/dx$ and $m_x = -dT/dx$ are respectively the distributed axial load and tortional moment per unit length of the beam. The resulting governing equations and BCs are (giannakopoylos!!!)

$$\frac{d^2 w_1}{dx^2} + \frac{a_0 S}{A}\frac{d^2\phi}{dx^2} = -\frac{p_x}{EA}$$

$$-l_0{}^2 \frac{d^4\phi}{dx^4} + \left(1 + \frac{a_0{}^2 K}{J}\frac{E}{G}\right)\frac{d^2\phi}{dx^2} + \frac{a_0 S}{J}\frac{E}{G}\frac{d^2 w_1}{dx^2} = -\frac{m_x}{GJ}$$

An at the ends of the beam the BCs are:

i. Either the axial displacement is known $w_1 = \overline{w}_1$
   or the axial force is known $\left[\frac{dw_1}{dx} + \frac{a_0 S}{A}\frac{d\phi}{dx}\right] = \frac{\overline{N}}{EA}$

ii. Either the twist is known $\phi = \overline{\phi}$
   or the torque is known $\left[-l_0{}^2 \frac{d^3\phi}{dx^3} + \left(1 + \frac{a_0{}^2 K}{J}\frac{E}{G}\right)\frac{d\phi}{dx} + \frac{a_0 S}{J}\frac{E}{G}\frac{dw_1}{dx}\right] = \frac{\overline{T}}{GJ}$

iii. Either the rate of twist is known $\phi' = \overline{\phi}'$
   or the bimoment is known $\left[-l_0{}^2 \frac{d^2\phi}{dx^2} - l_1 \frac{d\phi}{dx}\right] = \frac{\overline{B}}{GJ}$

The superscript bars e.g. $\overline{\phi}$ denote prescribed values and following the definition of the extra parameters used is provided:

$$J = \int_A \left(\zeta^2 + \eta^2 + \eta\frac{\partial\Psi}{\partial\zeta} - \zeta\frac{\partial\Psi}{\partial\eta}\right) d\zeta d\eta = \int_A \left[\left(\frac{\partial\Psi}{\partial\zeta} + \eta\right)^2 + \left(\frac{\partial\Psi}{\partial\eta} - \zeta\right)^2\right] d\zeta d\eta > 0,$$

which is the usual Saint-Venant torsional constant of the cross section

$$J_{\omega} = \int_A \Psi^2(\eta,\zeta)\, d\zeta d\eta \geq 0,$$

$l_0 = \sqrt{\frac{E}{G}\frac{J_{\omega}}{J}} \geq 0$, $\quad l_1 = \frac{a_0 R}{J}\frac{E}{G}$, length scales that depend on the cross section and the material (E/G ratio)

$$K = \frac{1}{a_0^{\,2}}\int_A \left(\frac{\partial \Psi}{\partial x}\right)^2 d\zeta d\eta = \int_A \left[\left(\zeta\frac{\partial \Psi}{\partial \eta} - \eta\frac{\partial \Psi}{\partial \zeta}\right)^2\right] d\zeta d\eta \geq 0$$

$$R = \frac{1}{a_0}\int_A \Psi\frac{\partial \Psi}{\partial x} d\zeta d\eta = \int_A \Psi\left[\left(\frac{\partial \Psi}{\partial \eta}\right)^2 + \left(\frac{\partial \Psi}{\partial \zeta}\right)^2\right] d\zeta d\eta$$

$$S = \frac{1}{a_0}\int_A \frac{\partial \Psi}{\partial x} d\zeta d\eta = \int_A \left[\left(\frac{\partial \Psi}{\partial \eta}\right)^2 + \left(\frac{\partial \Psi}{\partial \zeta}\right)^2\right] d\zeta d\eta \geq 0$$

Giannakopoulos (Giannakopoulos, et al., 2013) combined the governing equation above in order to eliminate the $w_1(x)$ function and obtain a closed form solution for the twist field φ.

Kordolemis (Kordolemis, et al., 2013) then combined the governing equations in order to eliminate the φ(x) function and obtained the governing equation of the axial displacement field $w_1(x)$ of the beam.

$$\left(\frac{l_0^{\,2}}{c^2}\frac{d^2}{dx^2} - 1\right)\frac{d^2 w_1}{dx^2} = \frac{q(x)}{EA},$$

$$q(x) = \frac{1}{c^2}\left\{\left(1 - l_0^{\,2}\frac{d^2}{dx^2}\right)p_x(x) + \frac{E}{G}\left(\frac{a_0^{\,2}K}{J}p_x(x) - \frac{a_0 S}{J}m_x(x)\right)\right\},$$

$$c(a_0) = \sqrt{1 + \frac{a_0^{\,2}}{J}\frac{E}{G}\left(K - \frac{S^2}{A}\right)} >= 1$$

And at the ends of the beam the BCs are:

i. $w_1 = \overline{w}_1$ or $\left[\frac{dw_1}{dx} - \frac{l_0^{\,2}}{c^2}\frac{d^3 w_1}{dx^3}\right] = \frac{\overline{P}}{EA}$

ii. $w_1' = \overline{w}_1'$ or $\left[\frac{l_0^{\,2}}{c^2}\frac{d^2 w_1}{dx^2} + \frac{l_1^{\,2}}{c^2}\frac{dw_1}{dx}\right] = \frac{\overline{Y}}{EA}$ where,

$$\overline{P} = \frac{1}{c^2}\left\{\overline{N} + {l_0}^2 \frac{dp_x}{dx} + \frac{E}{G}\left(\frac{{a_0}^2 K}{J}\overline{N} - \frac{a_0 S}{J}\overline{T}\right)\right\}$$

$$\overline{Y} = \frac{1}{c^2}\left\{-{l_0}^2 \frac{dp_x}{dx} + l_1\overline{N} + \frac{a_0 S}{J}\frac{E}{G}\overline{B}\right\} \quad \overline{w}_1' = \frac{\overline{N}}{EA} - \frac{a_0 S}{J}\phi'$$

Note that N, T, B, p_x, m_x are the classical loads, while P and Y are the generalized loads that depend on the classical loads and are defined using the variation principle.

Kordolemis proposed the following analogy

variable	Pretwisted beam	1-D gradient elastic bar
Axial displacement field	$w_1(x)$	$u(x)$
Volume material length	$l_0 = \sqrt{\frac{E}{G}\frac{J_\omega}{J}} \geq 0$	$g = \frac{l_0}{c}$
Surface material length	$l_1 = \frac{a_0 R}{J}\frac{E}{G}$	$l = \frac{l_1}{c^2}$
Body force	$\frac{1}{c^2}\left\{\left(1 - {l_0}^2\frac{d^2}{dx^2}\right)p_x(x) + \frac{E}{G}\left(\frac{{a_0}^2 K}{J}p_x(x) - \frac{a_0 S}{J}m_x(x)\right)\right\}$	$q(x)$
Traction like boundary force	$\frac{1}{c^2}\left\{\overline{N} + {l_0}^2 p_x(x) + \frac{E}{G}\left(\frac{{a_0}^2 K}{J}\overline{N} - \frac{a_0 S}{J}\overline{T}\right)\right\}$	$\overline{P}$
Couple like boundary force	$\frac{1}{c^2}\left\{-{l_0}^2 p_x(x) + l_1\overline{N} + \frac{a_0 S}{J}\frac{E}{G}\overline{B}\right\}$	$\overline{Y}$

Using the gradient elastic bar analogy terminology, the solution takes the following more familiar to this thesis form.

$$\left(g^2\frac{d^2}{dx^2} - 1\right)\frac{d^2 w_1}{dx^2} = \frac{q(x)}{EA},$$

$$q(x) = \frac{1}{c^2}\left\{\left(1 - g^2\frac{d^2}{dx^2}\right)p_x(x) + g^2\frac{a_0 S}{J_\omega}\left(\frac{a_0 S}{A}p_x(x) - m_x(x)\right)\right\},$$

And at the ends of the beam the BCs are:

i. $w_1 = \overline{w}_1$ or $\left[w_1' - g^2 w_1'''\right] = \dfrac{\overline{P}}{EA}$, $\quad \overline{P} = \left(1 - \dfrac{d^2}{dx^2}\right)\overline{N} + g^2 \dfrac{a_0 S}{J_\omega}\left(\dfrac{a_0 S}{A}\overline{N} - \overline{T}\right)$

ii. $w_1' = \overline{w}_1'$ or $\left[g^2 w_1'' + l\, w_1'\right] = \dfrac{\overline{Y}}{EA}$, $\quad \overline{Y} = -g^2 \dfrac{dp_x}{dx} + l\,\overline{N} + g^2 \dfrac{a_0 S}{J_\omega}\overline{B}$

6.References

Aifantis, E., 1992. On the role of gradients in the localization of deformation and fracture. *International Journal of Engineering Science,* 30(10), pp. 1279-1299.

Aifantis, E., 2003. Update on a class of of gradient theories. *Mechanics of Materials*, Volume 35, pp. 259-280.

Altan, B., Evensen, H. & Aifantis, E., 1996. Logitudinal vibrations of a beam: a gradient elesticity aproach. *Mechanics Research Comunications*, pp. 35-40.

Altan, S. & Aifantis, E., 1992. On the structure of the mode III crack-tip in gradient elasticity,. *Scripta Metallurgica et Materialia,* 26(2), pp. 319-324.

Aravas, N. & Giannakopoulos, A., 2009. Plane asymptotic crack-tip solutions in gradient elasticity. *International Lournal of Solids and Structures*, pp. 4478-4503.

Benvenuti, E. & Simone, A., 2013. One-dimensional nonlocal and gradient elasticity: Closed-form solution and size effect. *Mechanics Research Communications*, pp. 45-51.

Bleustein, J. L., 1967. ANote on the boundary contitions of Toupin's strain-gradient theory. *International Journal of Solids and Structures*, pp. 1053-1057.

Exadaktylos, G. & Vardoulakis, I., 2001. Microstructure in linear elasticity and scale effects:a reconsideration of basic rock mechanics and rock fracture mechanics. *Technophysics*, 335(1-2), pp. 81-109.

Giannakopoulos, A., Amanatidou, E. & Aravas, N., 2006. A reciprocity theorem in linear gradient elasticity and the corresponding Saint-Venant principle. *International Journal of Solids and Structures*, pp. 3875-3894.

Giannakopoulos, A., Aravas, N., Papageorgopoulou, A. & Vardoulakis, I., 2013. A structural gradient theory of tortion, the effects of pretwist, and the tension of pre-twisted DNA. *International Journal of Solids and Structures*, pp. 3922-3933.

Glynos, E. & Koutsos, V., 2009. Nanomechanics of Biocompatible Hollow Thin-Shell Polymer Microspheres. *Langmuir*, 25(13), pp. 7514-7522.

Kahrobaiyan, M., Asgahari, M. & Ahmadian, M., 2013. Longitudinal behavior of strain gradient bars. *International Journal of Engineering Science*, pp. 44-59.

Kordolemis, A., Aravas, N. & Giannakopoulos, A., 2013. *Pretwisted beams in axial tension and torsion: An analogy with dipolar gradient elasticity and applications to textile materials.* Chania,Crete, s.n.

Kröner, E., 1963. On the physical reality of torque stresses in continuum mechanics. *International Journal of Engineering Science,* 1(2), pp. 261-278.

Li, Y., Wei, P. & Tang, Q., 2015. Reflection and transmission of elastic waves at the interface between two gradient-elastic solids with surface energy. *European Journal of Mechanics A/Solids*, Issue 52, pp. 54-71.

Mindlin, R., 1964. Microstrusture in linear elasticity. *Archive for Rational Mechanics and Analysis*, pp. 52-59.

Mindlin, R. D., 1965. Second gradient of strain and surface-tension in linear elasticity. *International Journal of Solids and Structures*, Volume 1, pp. 417-438.

Mindlin, R. & Eshel, N., 1968. On first strain-gradient theories in linear elasticity. *International Journal of Solids and Structures*, Volume 4, pp. 109-124.

Mindlin, R. & Tiersen, H., 1964. Micro-structure in linear elasticity. *Archive of Rational Mechanics and Analysis*, pp. 61-78.

Mindlin, R. & Tiersten, H., 1962. Effects of couple-stresses in linear elasticity. *Archive of Rational Mechanics and Analysis*, pp. 415-448.

Mustapha, K. & Ruan, D., 2015. Size-dependent axial dynamics of magnetitically-sensitive strain gradient microbars with and attachments. *Mechanical Scienses*.

Olufemi, A. T., 2011. *Analytical And Nymercal Stydy of the Mechanical Behavior Of Materials and Structures in the Theory of Grdient Elasticity,* Thesaloniki: s.n.

Pisano, A. A. & Fuschi, P., 2003. Closed form solution for a nonlocal elastic bar in tension. *International Journal of Solids and Structures*, pp. 13-23.

Polizzotto, C., 2003. Gradient elasticity and nonstandard bountary contitions. *International Journal of Solids and Structures*, pp. 7399-7423.

Polyzos, D., Tsepoura, K., Tsinopoulos, S. & Beskos, D., 2003. A boundary element method for solving 2-D and 3-D static gradient elastic problems Part I:Integral formulation. *Computer Methods in Applied Mechanics and Engineering*, 192(26-27), pp. 2845-2873.

Polyzos, D., Tsepoura, K., Tsinopoulos, S. & Beskos, D., 2003. A boundary element method for solving 2-D and 3-D static gradient elastic problems Part II:Numerical Implementation. *Computer Methods in Applied Mechanics and Engineering*, 192(26-27), pp. 2875-2907.

Ru, C. & Aifantis, E., 1993. A simple approach to solve boundary value problems in gradient elasticity. *Acta Mechanica*, 101(1-4), pp. 59-68.

Tsepoura, K., Papargyri-Beskou, S., Polyzos, D. & Beskos, D., 2002. Static and dynamic analysis of a gradient- elastic bar in tension. *Archive of Applied Mechanics*, pp. 483-497.

Tsepoura, K., Papargyri-Beskou, S., Polyzos, D. & Beskos, D., 2002. Static and dynamic analysis of a gradient-elastic bar in tension. *Archive of Applied Mechanics*, Volume 72, pp. 483-497.

Weitsman, Y., 1965. Couple-Stress Effects on Stress Concentration Around a Cylindrical Inclusion in a Field of Unaxial Tension. *ASME*, June, pp. 424-428.

Zibaei, I., Rahnama, H., Taheri-Behrooz, F. & Shokrieh, M., 2014. First strain gradient elasticity solution for nanotube-reinforced matrix. *Composite Structures*, Volume 112, p. 273–282.